The Nottingham Trent University

Department of Electrical and Electronic Engineering

Interactive Electromagnetic Circuits for Synchronous Machines

William J. Hudson BSc (Hons) MSc MBA MIEE CEng

A thesis submitted in partial fulfilment of the requirements of the Nottingham Trent University for the degree of Master of Philosophy

July 1997

This research programme was carried out in collaboration with The GEC Alsthom Engineering Research Centre, Stafford

This piece of work is dedicated to our two daughters Victoria Elizabeth and Lavinia Alexandra born on the eighth day of October 1991.

Abstract

The work presented in this thesis describes the development of new equivalent circuit modelling techniques for representing a synchronous machine during transient conditions. The models make use of the similarities between magnetic and electric field quantities by representing magnetic flux with electric flux within the equivalent circuit model. This representation permits the development of equivalent circuit models, the topology of which is consistent with the topology of the magnetic circuit they represented. The method of development is, therefore, general and is by no means limited to the development of models for the synchronous machine.

A brief description of the historical development of equivalent circuit models in general is presented. Alternative equivalent techniques proposed by a number of authors are identified and reviewed. A detailed investigation and evaluation of an equivalent circuit technique in which the rate of change of magnetic flux is represented by electric current is performed. This analogy is developed and it is suggested that magnetic flux may be more appropriately described as being analogous to electric flux. The use of single dimensional permeance components within two dimensional space is also discussed.

An original technique is developed to represent complex interlinking magnetic and electric circuits using equivalent circuit methods. The technique is developed specifically to allow a detailed representation of the eddy current and damper circuits within the synchronous machine's rotor but may also be applied more generally. The representation enables eddy current and damper circuits to be represented implicitly within a simplified equivalent circuit model of the magnetic circuit. A generalised matrix, termed the "dampance matrix", emerges from this work which significantly simplifies the implementation of equivalent circuit models.

Successful simulations are performed for flux decay and frequency response tests on three typical synchronous machines. Limited success is also achieved with the simulation of the sudden short circuit test. A comprehensive range of quantities are obtained from the test simulations. These include both terminal quantities and less accessible electrical quantities present within the machine's rotor. The results obtained from the equivalent circuit simulations compare well with both actual test data and finite element simulation results.

Acknowledgments

I would like to express my gratitude to a number of people and organizations for their kind assistance throughout the research described within this thesis.

First and foremost I would like to acknowledge the unfailing support and encouragement supplied by my dear wife Michele.

I would also like to acknowledge the initial assistance of Prof. L. Haydock and the continued assistance provided by my academic supervisors Prof. P.G. Holmes and more recently Mr M. Kansara. The help and advice provided during numerous technical discussions throughout the course of this research has proven to be invaluable.

The assistance of the staff of GEC Alsthom Engineering Research Centre, Stafford must also be acknowledged. In particular I would like to thank Dr T. Preston and Dr J. Sturgess for providing unrivalled assistance and technical support.

The two facilities I have made most use of at the University are the Computing Services Department and the Library. I wish to thank the people within these departments for their assistance with the more mundane activities associated with this research. More generally I would like to thank the staff of the Department of Electrical and Electronic Engineering for all the help I have received from them during my stay at The Nottingham Trent University.

I would also like to thank both the S.E.R.C. and GEC Alsthom for the financial support they have provided for myself and my family for the duration of this research.

Finally, I would like to acknowledge the assistance of my father during the preparation of this thesis. More generally, however, I would also like to thank my parents and parents-in-law together with their families for the quiet support and encouragement they have provided over the past few years.

Table of Contents

Page

Nomenclature

Uppercase

A	Magnetic vector potential; Current measuring device; Area
B	Magnetic flux density
C	Constant; Capacitance
D	Electric flux density; Direct axis; Dual; Dampance
E	Electric field strength
F	Magnetomotive force
H	Magnetic field strength; Current controlled voltage source
I	Current
J	Current density
K	Constant; Damper
L	Inductance
M	Mutual
N	Number of turns; Constant
O	Open circuit
P	Power
Q	Quantity of charge; Quadrature axis
R	Resistance
S	Reluctance
T	Time constant
U	Voltage in per unit (Canay)
V	Voltage
W	Energy; Wedge
Y	Admittance
Z	Impedance

Lowercase

c	constant
d	direct axis
e	exponential; induced voltage
f	frequency; field; fundamental
g	gap length
h	height
i	current
j	complex number
k	damper
l	leakage; length
m	maximum; magnetic
n	neutral; constant
o	open circuit
p	d/dt; instantaneous power
q	instantaneous charge; quadrature axis
r	resistance
s	seconds
t	time
v	voltage; velocity
w	wedge
x	reactance

Superscripts

'	Transient value
''	Subtransient value
'''	Sub subtransient value

Subscripts

a	armature; stator
d	direct
eff	effective
f	field
g	air gap
h	height
k	damper
kd	damper; direct axis
kq	damper; quadrature axis
l	leakage
l-l	line to line voltage
m	magnetic
n	number
o	open circuit
p	pole
ph	phase; line to neutral voltage
q	quadrature
rc	Canay reactance
w	wedge

Greek

$\propto$	proportional to
δ	skin depth
ξ	electric permitivity
π	pi = 3.1415927
θ	angle
μ	magnetic permeability
ρ	resistivity
Σ	summation of
σ	conductivity
Φ	electric flux; magnetic flux
ω	angular velocity

Abbreviations

( )	Function of
[ ]	Matrix
$\int$	Integral
AC	Alternating current
d/dt	Differential coefficient with respect to time
CPU	Central processing unit
DC	Direct current
e.m.f.	Electromotive force
m.m.f.	Magnetomotive force
pf	Power factor
pu	Per unit
r.m.s.	Root mean square
RC	A seris resistor capacitor network
SPICE	Simulation program for integrated circuits and electronics
$\delta\theta$	A small increment of θ

Chapter One
The field of study and outline of thesis

1.1 Historical perspective

The electromagnetic field has kept scientists occupied since Charles Augustin de Coulomb (1736-1806) investigated the forces between electrically charged objects in the late eighteenth century. During the early development of electromagnetic field theory scientists thought of the electric and magnetic forces in terms of an "action at a distance" concept (1). It is, however, the discoveries in the early part of the nineteenth century and particularly the thoughts of Michael Faraday (1791-1867) (2,3) which have formed the concept of the electromagnetic field as we know it today.

An early application of the electromagnetic field was in the creation of continuous motion. The first electromagnetic engines and subsequently the electric current generators were designed on a purely empirical basis with little regard for efficiency. The electromechanical devices developed throughout the nineteenth century from a scientific curiosity into public electricity supply schemes providing electrical street lighting. The first of these schemes was in Godalming, Surrey, around 1882, which provided both street lighting and lighting for private homes (2), a load of about 4.5kW.

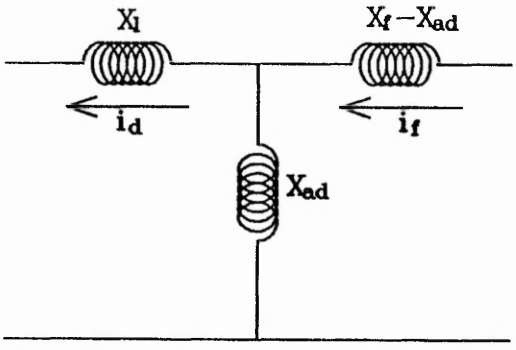

Figure 1.1 Early direct axis equivalent circuit for a typical synchronous machine developed by Park

The need to predict the behaviour of these machines was soon recognised. The first general purpose models for electrical machines were based on electrical circuits containing self and mutual inductances to represent the windings. A typical two axis model of a synchronous machine developed in the early part of this century (4,5) is given in figure 1.1. More recently the digital computer, by enabling rapid solution of numerical problems, has led to the development of more detailed models to represent electromagnetic systems. There are, in general, two techniques which are applied to the detailed investigation of the electromagnetic field. They are a finite element approach (6) and an equivalent circuit approach. The work contained within this thesis describes, investigates and develops an equivalent circuit method for representing a magnetic circuit which can be applied to a wide variety of electrical machines (7,8). The method is then applied to the prediction of the behaviour of synchronous machines under transient load conditions.

1.2 The modelling of magnetic circuits

The first mathematical relationship using the field theory concept was developed in the first half of the nineteenth century by Karl Friedrich Gauss (1777-1855). The formulation related the lines of force leaving an enclosed region with the total charge enclosed, now known as Gauss's Law. It was, however, James Clerk Maxwell (1831-1879)(9) who developed a comprehensive mathematical model to describe the behaviour of the electromagnetic field. This was in the form of a number of partial differential equations known collectively as Maxwell's Equations. Although this mathematical model could in theory be applied to any electromagnetic system, a solution for all but the simplest of problems was impossible because of the lack of computational facilities at the time.

The application of the finite element approach involves the discretisation of the region of interest into a large number of triangular elements. The resulting mesh may then be represented in matrix form to enable a numerical solution to be obtained for a partial differential equation describing the energy within the system. Its increase in popularity in recent years can be attributed to the quantum leap forward in computing technology.

The concept of a magnetic circuit has been used to predict the behaviour of an electromagnetic field for some time (10). The electromagnetic field is assumed to exist within physically well defined reluctance paths or flux tubes so that the field is constrained in much the same way as an electrical conductor constrains an electric current. The subdivision of the magnetic circuit allows the reluctance value for each part of the magnetic circuit to be calculated directly from the physical dimensions and material bulk constants of the region. The level of discretisation of the magnetic circuit will depend on the complexity

of the topology and the level of detail required by the model. The physical topology of the magnetic circuit is therefore very similar to the topology of the magnetic equivalent circuit.

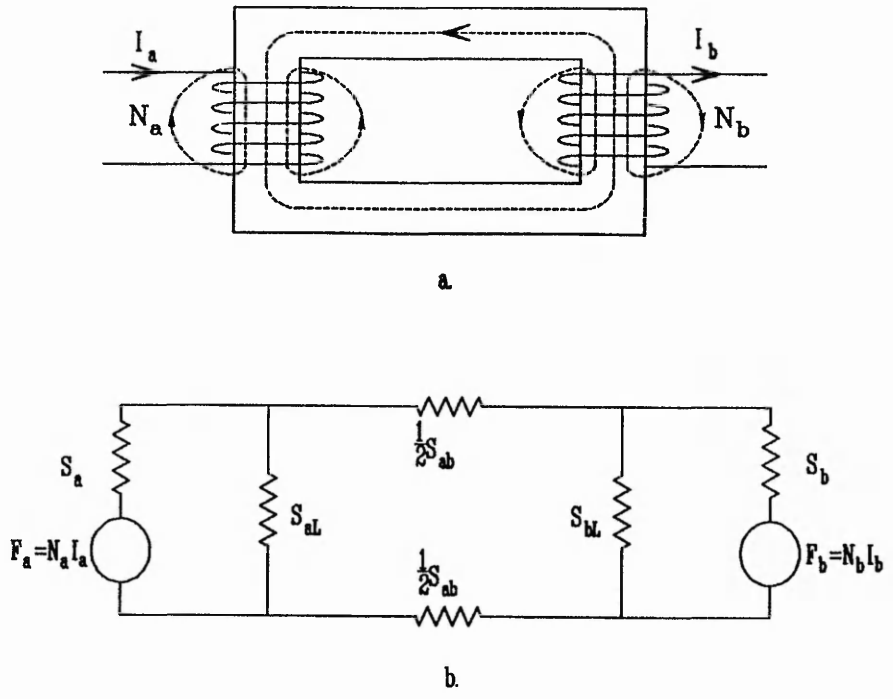

Figure 1.2 A typical magnetic circuit for a single phase transformer

Figure 1.2 shows a simple magnetic equivalent circuit and compares its topology to the physical magnetic circuit. The transformer's coils are represented as m.m.f. sources, F_a and F_b, the value of which is determined by their respective electrical currents. Reluctance, S, is represented as circuit devices, the position of which is consistent with their position in the physical system they represent. There are, in principle, two analogies which have been used to represent the magnetic quantities within a magnetic equivalent circuit.

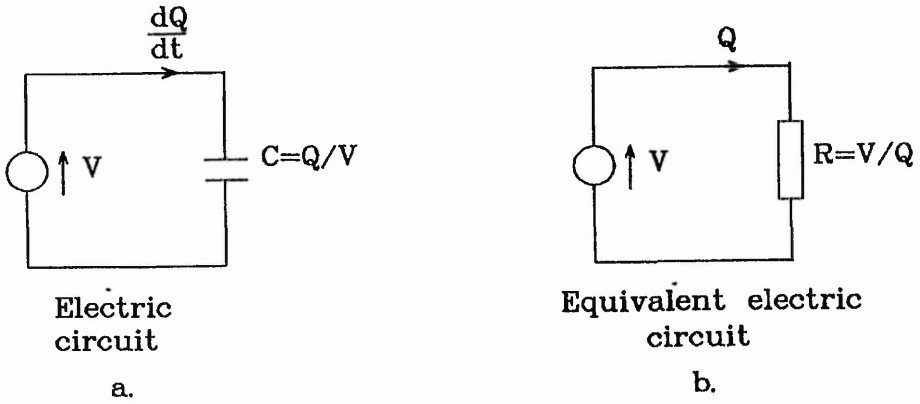

Figure 1.3 An electric circuit equivalent model

Initially the analogous quantities were based on the similarities between the equation for magnetic reluctance (equation 1.1) and electrical resistance (equation 1.2).

$$S = \frac{F}{\Phi} \qquad \text{....1.1}$$

$$R_e = \frac{V}{I} \qquad \text{....1.2}$$

This analogy between quantities in a magnetic circuit and quantities in the magnetic equivalent circuit has been used throughout this century (10,11,12,13,14) to predict the behaviour of electrical machines. Although this approach correctly represents the mathematical relationship between flux and m.m.f. under steady state or static conditions it fails to represent the magnetic circuit under transient conditions. Within a magnetic circuit the value of reluctance is inversely proportional to the rate of change of magnetic flux. This is inconsistent with the behaviour of electrical resistance, the value of which is independent of rate of change of electrical current.

More recently, Carpenter C.J. (15) has shown that the analogous quantities can be more consistently determined from the equations representing power flow across a surface in an electrical system compared with a magnetic system. Consider equations 1.3 and 1.4 which are used to describe the power flow across similar surfaces.

$$\text{Electrical power flow } P_e = vi \qquad \text{....1.3}$$

$$\text{Power transferred across a surface (E x H)} = F\frac{d\Phi}{dt} \qquad \text{....1.4}$$

To enable a direct comparison with equations 1.1 and 1.2 this analogy is presented here as equations 1.5 and 1.6.

$$S = \frac{F}{\Phi} \qquad \text{....1.5}$$

$$\frac{1}{C_e} = \frac{V}{Q} \qquad \text{....1.6}$$

Previous authors (15,16) have suggested that magnetic flux can, therefore, be represented by electric charge and rate of change of magnetic flux would be represented by a magnetic current in a magnetic equivalent circuit. However, in reality equivalent circuit components representing reluctance paths are not joined by interconnecting magnetic conductors in which a magnetic conduction current could flow. It is felt, therefore, that a more appropriate illustration of this analogy would be to describe electric flux as representing magnetic flux. Magnetic current, therefore, would be a displacement current. More generally, this clearly suggests that the use of such an analogy represents the use of an electric field to represent a magnetic field. Although this interpretation makes little difference to the development and solution of these magnetic equivalent circuits, it is an

important concept because it increases our understanding of the similarities between the electric and magnetic field. This concept is discussed fully in chapter three, and represents part of the fundamental work presented in this thesis.

An important advantage of representing a magnetic field in an equivalent circuit form is that a solution to the circuit may then be obtained using conventional circuit theory and, more recently, standard circuit solving computer programs. The package used throughout this work is SPICE version 2G6 (17) although it must be emphasised that the equivalent circuits developed using this approach may be solved using any electric circuit solver with the appropriate capacity.

1.3 The synchronous machine

The synchronous machine has formed the backbone of the electrical supply industry since the early part of this century when the first three phase alternators with a rotating field were being developed. The inherent high speed of the prime mover, the steam turbine, led to the development of the two pole rotor, initially with salient poles. The difficulties in adapting these rotors to a two pole field led to the evolution of the more familiar form of the round rotor used today. The very rapid early development of the turbogenerator is demonstrated by comparing a turbogenerator ordered from Parsons in 1912 having a rating of 25MW and the first commercial high speed AC generators of 75kW built only 23 years earlier (18).

The development of the turbogenerator has been characterised by enormous advances in size and performance in the absence of any significant technological breakthroughs (19). For example, in the 1950's the standard size of a generating set was 60MW, this figure rose

to 200MW in the 1960's and 660MW in the 1970's. This had been made possible by the continual refinement of existing materials, design techniques and methods of construction.

Perhaps the most significant development concerning the generator is the development of cooling techniques. To cool the 60MW units of the 1950's hydrogen was pumped through ducts outside the insulation wall. In more modern machines a common method of cooling the rotor conductors is to feed hydrogen into the base of the slots and allow it to filter up through the ducts in the rotor windings. The stator conductors are more usually cooled by passing hydrogen and, more recently, demineralized water along ducts within the conductors themselves.

Another major area of development is that of the materials used in the construction of the generator. The development of new insulation resins has enabled an increase in voltage ratings. Improved steels used in the construction of the rotor together with improved methods of stress analysis have enabled larger stresses to be present in the rotor. Figure 1.4 shows a cut away section of a rotor for a typical two pole synchronous machine.

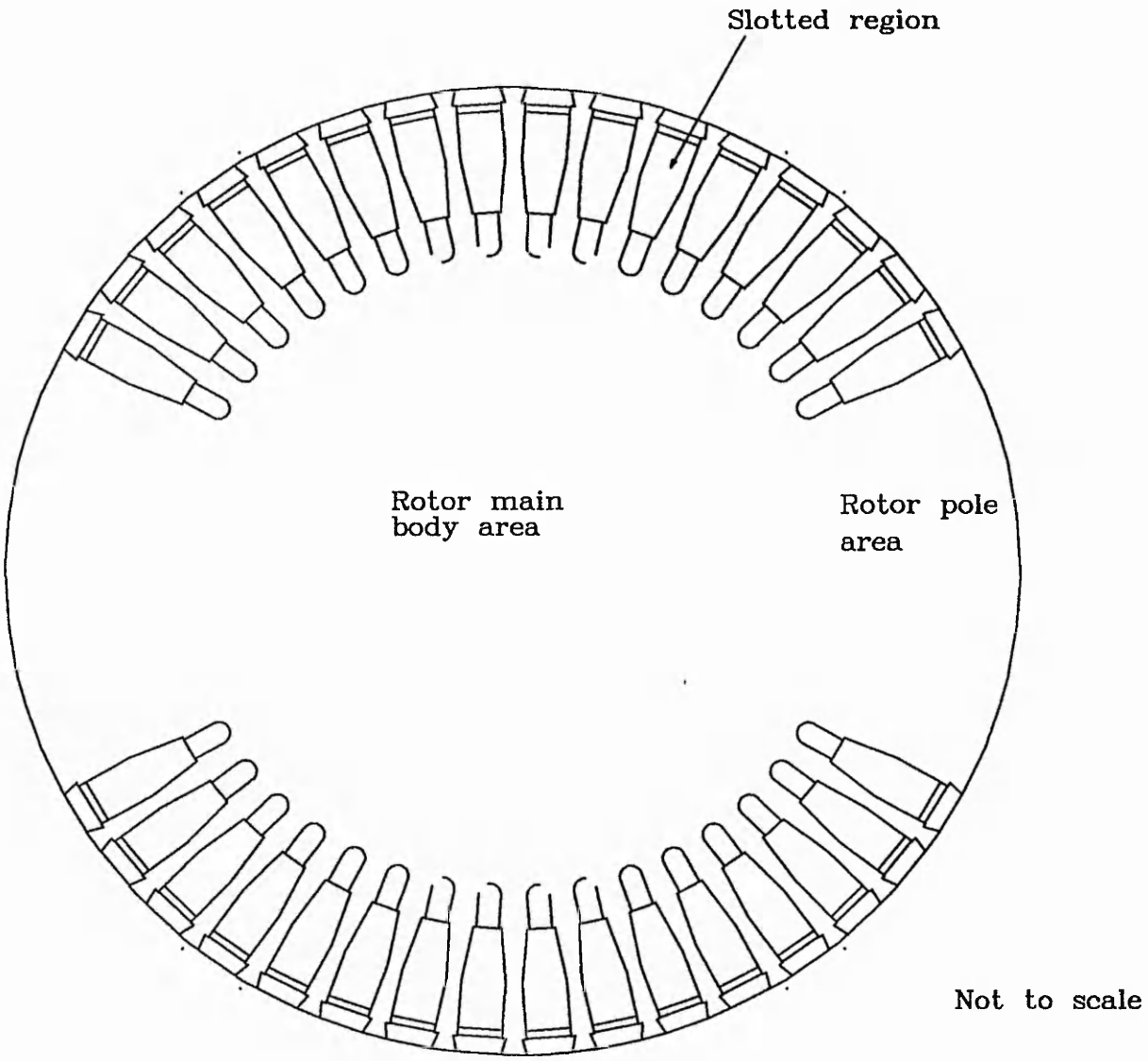

Figure 1.4 A typical rotor cross-section for a large two pole synchronous machine

A further significant factor which has contributed to the optimisation of turbogenerator performance is the increased understanding of their behaviour which has come about due to the development of computer aided design techniques. Although no significant increase in generator performance can be directly attributed to the introduction of computer aided techniques the benefits which have been gained from them are two fold. Firstly, the actual

process of generating the necessary computer programs has necessitated a reappraisal of basic design techniques and thus eliminated rule of thumb methods. Secondly, the ability to employ more sophisticated calculation processes has enabled engineers to better optimise the potential output per unit volume of material (18).

1.4 Synchronous machine models

The development of a model to represent the synchronous machine has progressed along a number of avenues over the past 90 or so years. The very fact that an accurate equivalent circuit model, able to predict the behaviour of such a machine over a wide range of operating conditions, is still not available gives an indication of the difficult nature of the problems encountered. A detailed review of the more significant equivalent circuit models is presented in chapter two of this thesis.

The difficulties that exist when modelling the synchronous machine over a wide range of operating conditions arise from the behaviour of the magnetic field within the machine. The magnetic field exists within the complex construction of the rotor and stator, the combination of the complex topology and differing materials, together with the effects of saturation within the magnetic circuit and complex eddy current circuits within the solid iron construction of the rotor, make it impossible to model the system without resorting to a complex model. Figure 1.5 shows a typical cross-section for a half pole pitch of a large synchronous machine.

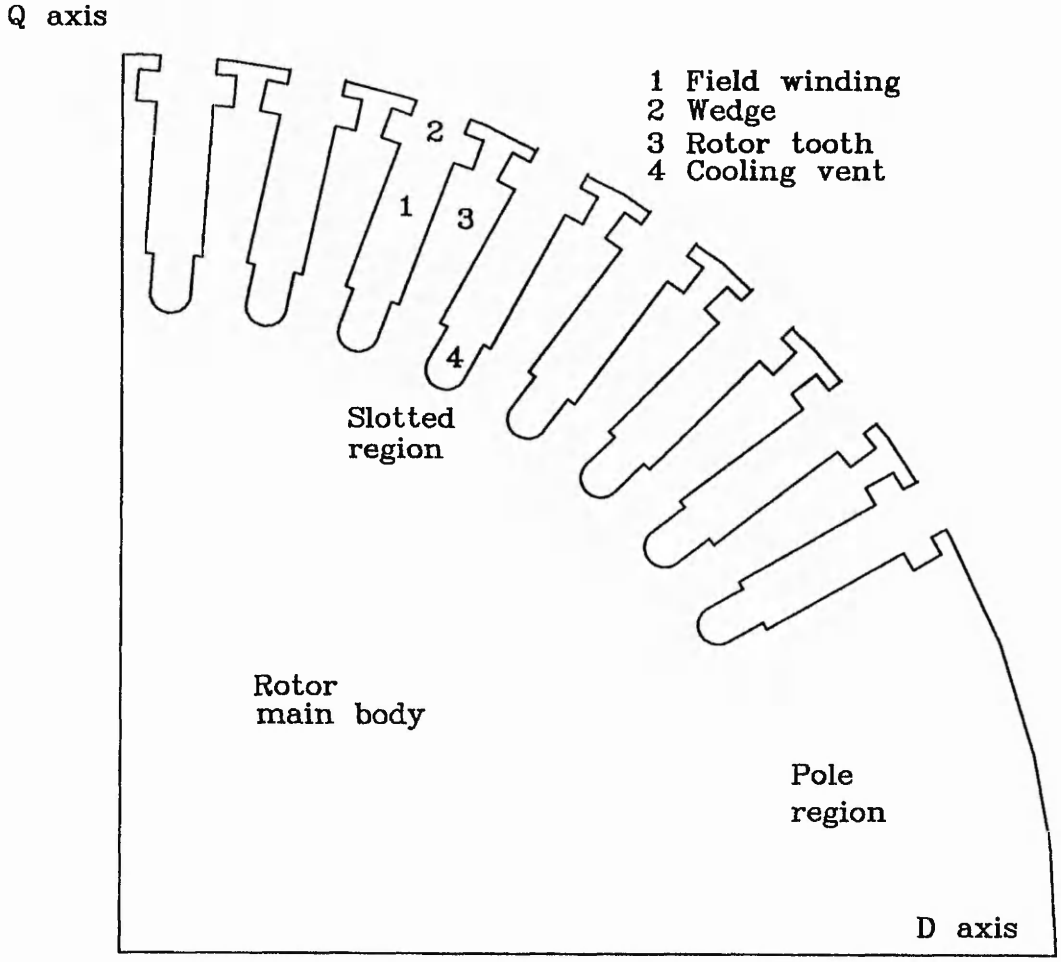

Figure 1.5 A typical half pole cross-section of a synchronous machine

The development of the synchronous machine has benefited considerably from the knowledge and understanding which has been gained from the process of developing models to represent it and from the results these models have provided. In general, models to predict the behaviour of the synchronous machine can be categorised into two main groups;

(i) During the design stage the prohibitively high cost of building a prototype machine means that detailed accurate information concerning the performance of each of the

components has to be obtained from a detailed model. This type of model is also able to assist in evaluating machine behaviour under fault conditions.

(ii) A model representing a machine connected to a supply network, however, is less complex and is typically used to represent a single machine within a larger power system model. This type of model tends to rely heavily on machine parameters which have been derived from machine test results or results provided from test simulations performed using a more detailed model.

To meet these modelling requirements three distinct approaches have been adopted.

The first models used to represent a machine were based on an equivalent circuit interpretation of the mathematical equations describing a set of mutually linked windings (4,5,20,21,22). These early simple equivalent circuit models were developed to represent the machine's behaviour within a power system, and have formed the basis for the synchronous machine model used in power system studies for a large part of this century (23,24,25,26). Continual improvements in the efficiency, and in particular the decrease in the mechanical time constants of the rotor coupled with an increase in the stator transient reactances, have had an adverse effect on system stability. There has, therefore, been a requirement to increase the accuracy of equivalent circuit models representing a modern synchronous machine which corresponded with the optimisation of machine design. The development of this type of equivalent circuit model in power system studies is briefly described in chapter two of this thesis.

The introduction of the digital computer and the ability to solve large numerical problems has led to the development of models representing magnetic fields using a finite element

approach (6,27). The approach involves sub dividing a region into small triangular shaped elements to form what is generally known as a finite element mesh. A potential function, usually magnetic vector potential, describing the magnetic field is then calculated at each vertex of each element, or node, using numerical techniques. An approximate value for the potential function between nodes is calculated using linear or quadratic interpolation methods. Flux and current densities are calculated as average values for each individual element. This approach is of particular use to a machine designer because it allows the conversion of the topology and material constants directly into the model from a design proposal. More recent developments in this field has led to the development of the method to enable three dimensional regions to be similarly represented (28). The development of user friendly pre and post processors to graphically represent the finite element mesh and simulation results respectively have considerably increased the usefulness of this method as a design tool.

Equivalent circuit models have also been developed from machine topology and material bulk constants (16,29,30). The fundamental difference between the finite element and the equivalent circuit approach is the simulation method. The equivalent circuit approach is essentially an analogue approach even though a solution is often obtained using numerical techniques. Analogue values within the equivalent circuit model represent the magnetic field. This greatly reduces the level of discretisation required to represent magnetically regular regions within a magnetic circuit when compared to finite element techniques. For example, consider figure 1.2a. Each limb of this transformer may be accurately represented using a single reluctance value because the field is constrained within the boundaries of the iron. However, if the same limb were to be represented using a finite element model it would be necessary to sub divide the limb into a number of triangular elements to obtain a

similar degree of accuracy from the model as a whole. It is envisaged, therefore, that the modelling techniques presented in this thesis could be applied to applications where two axis models are inadequate but finite element techniques too cumbersome. For example, Carpenter M.J. (29) adopts this equivalent circuit techniques to simulate the behaviour of a synchronous machine connected to a power electronic drive.

1.5 An outline of this thesis

1.5.1 Overview

The principal aim of this work was to develop an improved equivalent circuit technique for the representation of synchronous machines under a variety of transient load conditions. This work directly follows the work of Carpenter C.J. (15), Haydock (16) and Carpenter M.J. (29). Although work in this area has tended to concentrate on synchronous machines the equivalent circuit method is equally applicable to induction machines (7,8,31). Any electro-magnetic circuit may be represented using this approach.

During the early stages of this work it was discovered that the methods and analogies used to develop previous equivalent circuit models were not always consistent. The early part of this work (32) is therefore concerned with the development of a physically consistent approach from the existing approaches and analogies. This enhanced equivalent circuit technique is then applied to the development of a standard equivalent circuit topology which can be used to model the behaviour of large synchronous machines.

The resulting equivalent circuit models developed in this thesis are used for a number of synchronous machine test simulations. These include the flux decay test, frequency response test and sudden short circuit test. It soon became apparent, however, that the

developed equivalent circuit models were requiring an excessively long computation time to provide a solution. The topological complexity of these equivalent circuits is therefore reduced using dynamic circuit components to represent the diffusion of eddy currents into the rotor poles.

The contents of each of the chapters within this thesis is now described in more detail.

1.5.2 Chapter two

The work contained in chapter two is a critical appraisal of equivalent circuit modelling techniques relating to the magnetic field and, in particular, their application to the synchronous machine. The chapter describes, in detail, the techniques adopted by a number of authors with particular reference to the modelling analogies adopted. The reader's attention is drawn to any inconsistencies apparent in the principal approaches and how they may affect the validity of the proposed methods.

1.5.3 Chapter three

A consistent equivalent circuit approach is developed based on the work presented by Carpenter C.J. (15), Haydock (16), and Carpenter M.J. (29).

A detailed analysis and appraisal of the equivalent circuit analogy employed throughout this thesis is provided. The developed conceptual view presents the equivalent circuit analogy, introduced by Carpenter C.J. (15), in terms of quantities relating to the electric field rather than those based on an electrical circuit. This detailed appraisal has enabled the author to highlight short comings in previous models (15,29).

The present equivalent circuit analogy is extended to enable the effects of an electric current linking a number of defined reluctance paths to be represented completely. This method is then further extended to enable the representation of multiple electric conductors intersecting a number of defined reluctance paths. Finally, the representation of the effects of the eddy currents in a given region is developed so that a matrix may be employed to represent them. The identification of a pattern within this matrix is a significant aid for the construction of the standard equivalent circuit models presented in the further chapters. The development of the equivalent circuit analogy to represent multiple interlinking electric and magnetic circuits is believed to be original.

1.5.4 Chapter four

A basic generalised equivalent circuit topology is developed to model the behaviour of a large synchronous machine under various transient conditions. The equivalent circuit topology developed in this chapter makes use of the original techniques developed in chapter three to represent the effects of the field winding and damper circuits, allowing a variable level of discretisation. The general nature and flexibility of the equivalent circuit topology is discussed in terms of how it may be configured to represent the rotor to best effect. A brief description of how the numerical values for each of the circuit components are calculated is also presented. The various aspects of the general purpose topology and how they relate to the physical machine are discussed in detail. The configuration of the equivalent circuit is compared to the development of a finite element model which will be used in later chapters of this thesis. The general purpose, nature and construction of the equivalent circuit model developed in this chapter is believed to be original.

1.5.5 Chapter five

The general purpose equivalent circuit model developed in chapter four is used in simulations for three test conditions. A comparable finite element study is also presented to enable comparisons to be made between simulation results for quantities for which no test results are available. For example, eddy current values within closed damper circuits during test simulations. The three test conditions are, the flux decay test, the frequency response test and the sudden three phase short circuit test. A description of how the general purpose topology has been configured and linked to the stator winding to represent each of these test conditions is also presented.

1.5.6 Chapter six

The results from the test simulations performed in chapter five are presented and compared to actual test results or, if actual test results are unavailable, to the results obtained from the comparable finite element study. Results are presented for a number of internal and terminal quantities for the flux decay test and frequency response test. The quantities which are available from test simulations are dependent on the measuring capabilities of the equivalent circuit model. To demonstrate the ease with which quantities may be obtained from these equivalent circuits, values for the eddy currents in the damper circuits during the flux decay test are presented and compared to those from the finite element simulation. The effect of the different parts of the rotor is assessed by considering the contribution of varying equivalent circuit components to the characteristics of the results. The effects of the different parts of the rotor on the parameters determined from the different test conditions are discussed (16), in connection with the investigations using finite element simulations (6). The ability of the equivalent circuit model to provide such a range of

quantities from a single simulation represents a significant and original advance on previous equivalent circuit models (16,29).

1.5.7 Chapter seven

The equivalent circuit models developed in chapters four and five require a considerable amount of computing resources in terms of time and space. This type of equivalent circuit model is therefore unsuitable for use in power system studies. A less topologically complex model is therefore considered in this chapter. The concept of applying dynamic circuit components to represent the frequency dependence of the damper circuits that exist within the solid iron is discussed. This approach represents an attempt to transfer topological complexity to an equivalent circuit component. An initial prototype circuit is presented to represent a flux decay test on a turbogenerator.

1.5.8 Chapter eight

The work contained within this thesis is discussed with particular reference to its originality and the effect this may have on future developments of magnetic circuit representations. The ability of the present equivalent circuit modelling technique to represent two dimensional space at high levels of discretisation is discussed, and ideas for modified two or even three dimensional equivalent circuit devices are presented. Ideas and suggestions for further work that have arisen out of this thesis are also put forward.

Chapter Two
An appraisal of existing work

2.1 Introduction

The work presented in this chapter provides a critical appraisal of selected papers presented in the field of magnetic equivalent circuit modelling techniques and, in particular, their application to synchronous machine modelling. It is believed that the selected work provides a cross-section of the principal techniques which have been applied in this area. Although the work contained within this thesis is principally concerned with the development of the magnetic equivalent circuit approach, a brief overview of the traditional two axis representation for a synchronous machine is also included. The chapter is arranged in three sections.

Firstly, the development of the traditional two axis equivalent circuit approach for the synchronous machine is briefly discussed. A more comprehensive investigation of the two axis approach, and a demonstration of how traditional two axis equivalent circuits may be derived using magnetic equivalent circuit methods is presented by Haydock (16).

Secondly, the development of magnetic equivalent circuits derived directly from the physical topology and material bulk constants of a general magnetic circuit is discussed. This is a generalised technique which has been applied in a number of different ways to magnetic circuits of varying topologies. Induction machines (37) and transformers (31,41) are examples of previous alternative applications. However,

particular attention is given to their application to the prediction of synchronous machine behaviour.

Finally, the work presented by Carpenter C.J. (15), Haydock (15), and Carpenter M.J. (29) is discussed in detail. This work forms the basis from which the new and original equivalent circuit techniques described in this thesis have been developed.

2.2 Two axis models to represent the synchronous machine

2.2.1 The development of the traditional two axis model

The work presented by Park (4,5) in the late 1920's is usually considered to be the starting point for a discussion concerning the two axis or two reaction theory for synchronous machines. Prior to this time Alger (21) and Doherty and Nickle (20), to name but a few authors, have also been associated with the development of equivalent circuit models. The theory presented by Park and Robertson (4) defined what they considered to be the main "characteristic constants" for the definition of a synchronous machine. These parameters were used to describe machine in terms of reactive voltages and represent the machine for differing operating conditions. At the time this was considered to be a significant advance because machines of the day were typically represented with a single leakage reactance and armature reaction. The new machine characteristics were categorised into three main groups:-

- Distribution : Positive, negative, or zero phase sequences,
- Application in time : Sustained, transient or sub transient,
- Rotor axes : Direct or quadrature.

The various combinations of these types of armature reaction led to the definition of eight different armature reactances which could be used with the value of leakage reactance to represent the synchronous machine in the equivalent circuit form, presented in figure 1.1. It is perhaps interesting to note that the equivalent circuit topology was developed directly from a mathematical model linking flux generated by each of the assumed windings. The development of this equivalent circuit model is presented in appendix E of reference 20. It is acknowledged in this reference that to include additional rotor or damper circuits would be more difficult and, therefore, no attempt is made to include these within the equivalent circuit model at this stage.

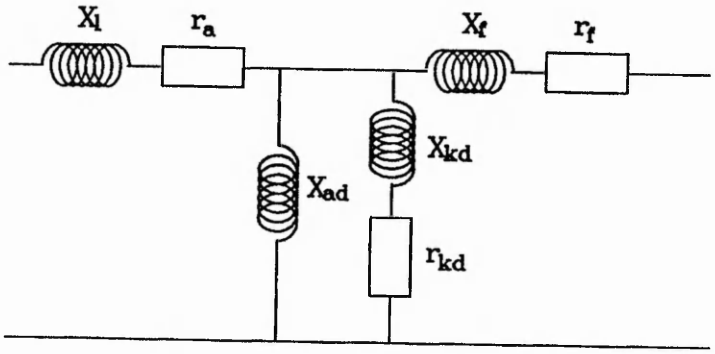

Figure 2.1 Traditionally accepted direct axis equivalent circuit model for a typical synchronous machine presented by Adkins

The two axis equivalent circuit model has subsequently been developed into what has been termed the traditional two axis equivalent circuit model, shown here in figure 2.1. The effects of the additional rotor circuits have been represented using an additional

branch consisting of X_{kd} and r_{kd} in series. The construction of this equivalent circuit model is perhaps best described by Adkins (42).

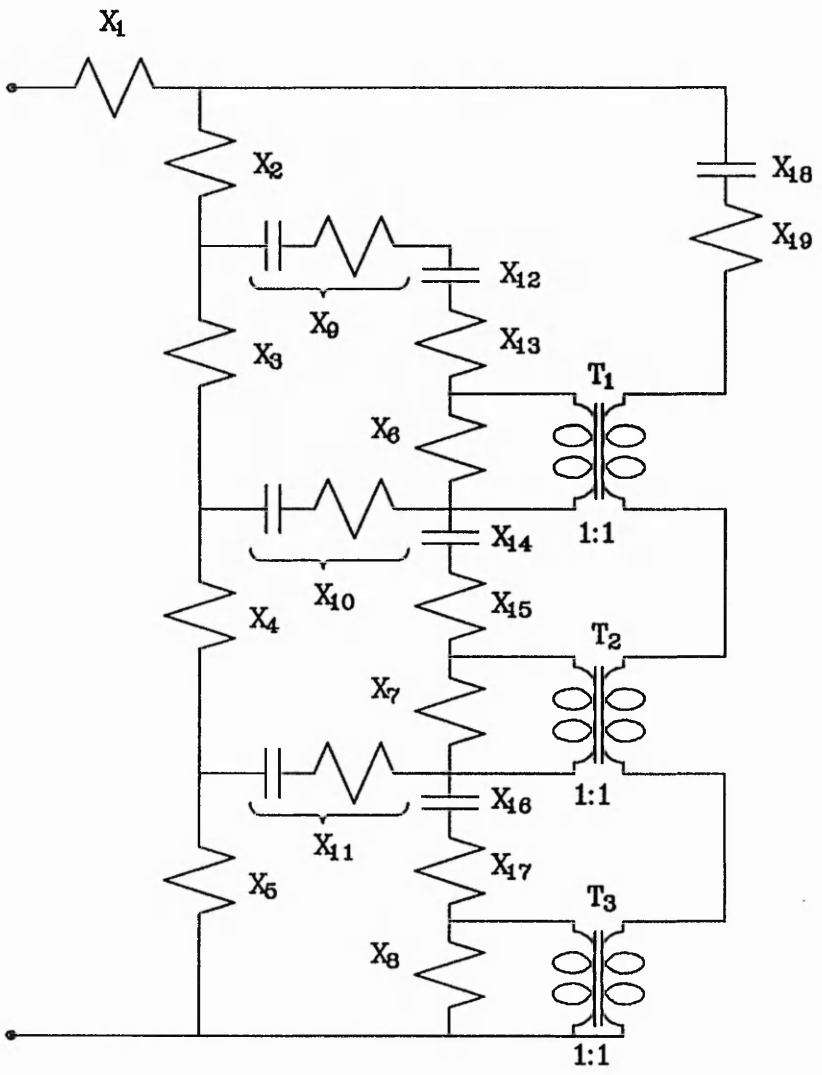

Figure 2.2 Rankin's direct axis equivalent circuit for five or six damper bars per pole

2.2.2 More advanced two axis models

The traditional two axis model was, in general, applied to synchronous machines using a single damper circuit representation on either the direct or quadrature axis so as to

represent the damping effect of the rotor. In the search for a more complete model for the synchronous machine Rankin (33,43) derived a more general set of equations to include an increased number of rotor circuits (43). A mathematical model could then be developed to model the effects of the individual closed rotor circuits within the machine. This model is realised in the form of an equivalent circuit model, shown here in figure 2.2, to provide a solution to the derived equations (33).

Rankin's work (33) is of particular interest because an equivalent circuit model has been generated from a more complete mathematical model. A combination of equations A1.1a... and A1.2a... presented here in appendix one is used to generate a set of simultaneous equations (equations A1.3a...) from which the equivalent circuit model has been generated. It is evident from the equivalent circuit model that electric current is used to represent ampere turns and the electric potential is used to represent flux linkage, although this is not stated in the text. To complete this analogy, resistance is used to represent reactance and capacitance is used to represent the effect of any linked windings or damper circuits. The equivalent circuit model also includes three transformers, T_1,T_2 and T_3. These transformers are used to model the transformer effect which links all the damper circuits and other windings of the machine together. They represent the effect described as mutual dampance in chapter three of this thesis. These have been shown necessary from the mutual terms in equations A1.3a.... Figure 2.2 shows the physical topology of the equivalent circuit the key to which is provided in appendix one. The calculation of the particular values for these equivalent circuit components is from the physical machine dimensions and

constants. The reader is referred to reference 33 for a detailed presentation of the calculations.

Although Rankin (33) was able to represent the machine with its damper circuits the resulting equivalent circuit model was unsuitable for use in power system studies because of its size and complexity. A simplified method of representing the damper circuits within an equivalent circuit model has been developed by Jackson and Winchester (34).

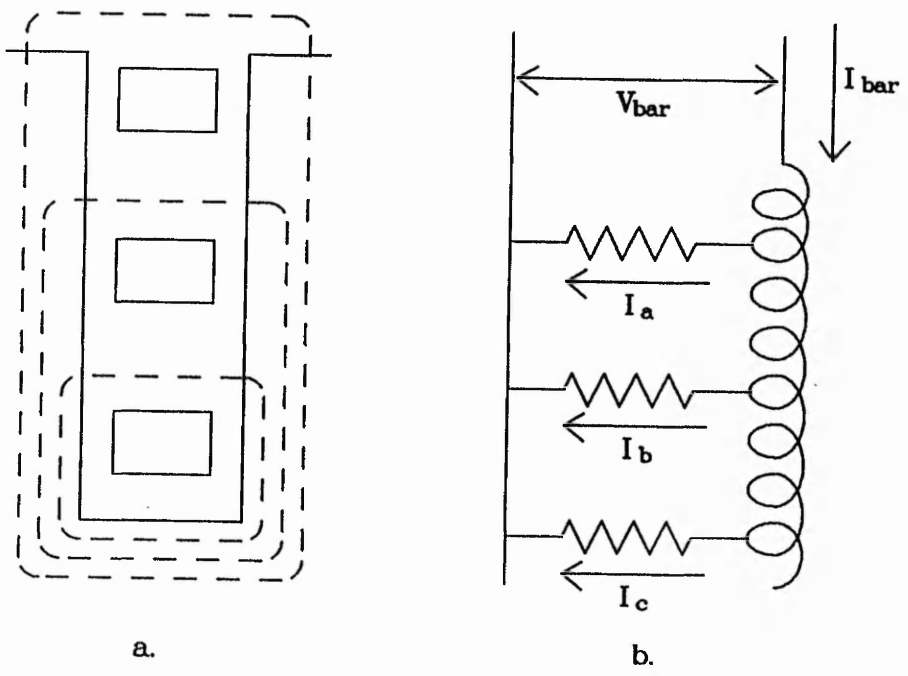

Figure 2.3 Babb and Williams conceptual view of a single slot

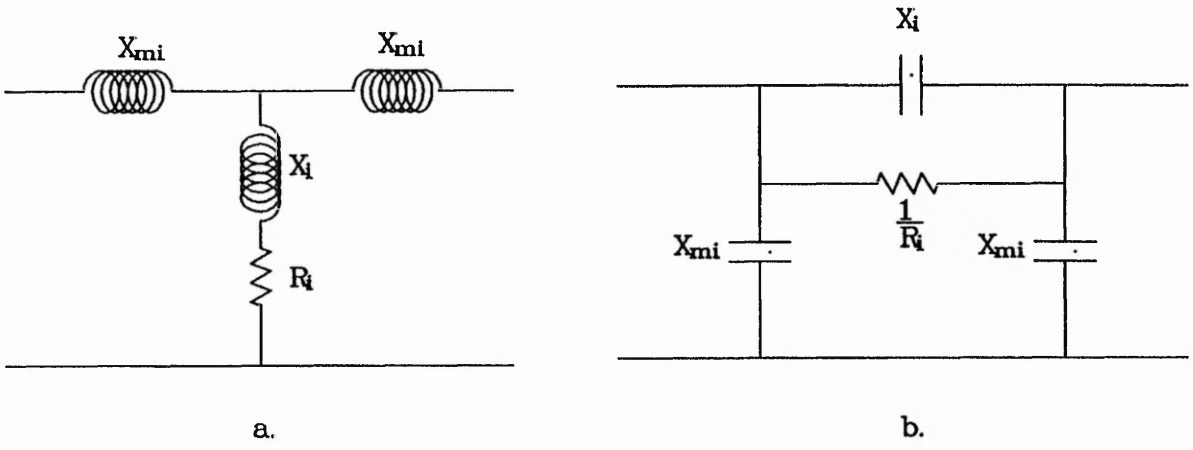

Figure 2.4 A Jackson and Winchester ladder type element and its dual

The AC impedances of machine conductors described by Babb and Williams (38) has been employed by Jackson and Winchester (34) to develop an equivalent circuit model for a synchronous machine. The method described by Babb and Williams (38) is based on a conceptual view of a single slot shown in figure 2.3a, using an inductor with a number of tappings shown in figure 2.3b. It can be seen from figure 2.3a that the self inductances of all but the deepest current paths have been ignored and the mutual flux linkage between a number of the current paths has also been ignored. The basic ladder type equivalent circuit employed by Jackson and Winchester (34) is therefore a very much simplified circuit and does not represent the flux around a slot pitch completely. This can be demonstrated by taking the dual of a typical T section presented in reference 34. Figure 2.4a shows a T section in the electric equivalent circuit form (this is indicated because the reluctances are represented as inductors). This T section is to represent one of a number of linked layers of rotor electrical currents flowing along the length of the rotor. If the T section is inverted (44), the resulting equivalent circuit,

shown here as figure 2.4b, is in the magnetic equivalent circuit form, which is similar to the topological arrangement of the magnetic circuit it represents. It now becomes apparent that when these pi sections are joined together to form a complete slot pitch there will not be any mutual coupling due to the linking damper circuits between the different layers of defined flux. It can therefore be concluded that the T-section equivalent circuit employed by Jackson and Winchester (34) is an approximation for the flux around the slot depth of the synchronous machine. The completed equivalent circuit models developed by Jackson and Winchester are a combination of two single rotor slot pitch type circuits in parallel. One is used to represent the slotted region of the rotor and the other the pole region.

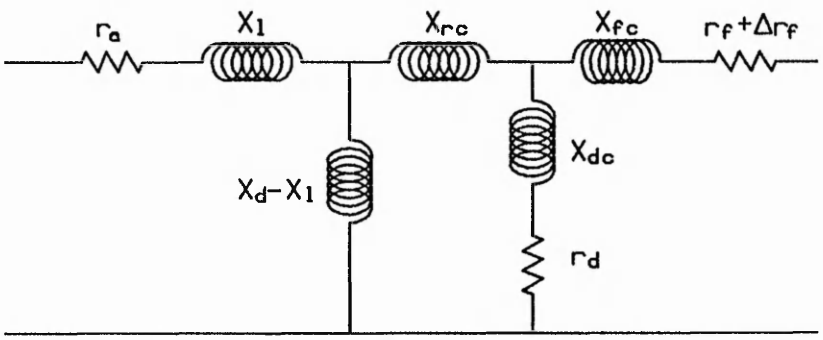

Figure 2.5 D-axis equivalent circuit model proposed by Canay

2.2.3 Improvements to the traditional two axis model

The traditional equivalent circuit (figure 2.1) which had been developed over the first half of this century, had proved itself to be a satisfactory tool to predict the terminal quantities for a synchronous machine. It became evident, however, that the predictions for the rotor quantities were not quite as accurate. The AC portion of the rotor

current for a three phase sudden short circuit amounts to approximately 23% of the calculated value (25). A considerable amount of Canay's work is directed towards determining a more accurate equivalent circuit model to represent the rotor of the synchronous machine (24,25). The proposed equivalent circuit (figure 2.5) contains an additional reactance (x_{rc}) which has been included to represent the mutual coupling of the field and damper circuits. The existence of this additional reactance is justified by the mathematical manipulation of the traditional two axis equations, shown in matrix form as equations 2.1.

$$\begin{bmatrix} e_d - u_d \\ u_f \\ 0 \end{bmatrix} = \begin{bmatrix} r_a+px_d & px_{df} & px_{dD} \\ px_{fd} & r_f+px_f & px_{fD} \\ px_{dD} & px_{Df} & r_D+px_D \end{bmatrix} \begin{bmatrix} i_d \\ i_f \\ i_D \end{bmatrix} \qquad \text{....2.1}$$

Haydock (16) has shown that it is possible to generate a similar equivalent circuit model starting from a topological view of a single slot model for a turbogenerator. Although this work may be used to confirm the topology of the equivalent circuit proposed by Canay (25) it also demonstrates the coarse lumping required to generate such a model. Takeda and Adkins (45) have developed the idea of a mutual reactance to link the field and damper circuits proposed by Canay (25) by improving the method of calculating the value for this reactance from short circuit oscillograms.

Canay has also suggested (25) using frequency dependent complex resistance to represent the damping effect of solid rotor iron. These would take the form of a single frequency dependent resistance to represent a solid pole region but a number of layers

of frequency dependent resistor/slot gap reactor combinations would be required to model the iron and cross field generated in the slotted region. This layering of the resistances in the slotted region is suggested because of the skin effect on the slot walls. This is different from the effect being modelled in chapter four using layers of fixed value resistances to represent the rotor. The work presented by Canay (24,25) is of particular interest because a mathematical model has been developed to represent one of the effects previously represented with a more complete model (25). Namely the effect of skin depth and associated damper resistance at different frequencies. This will enable a more accurate model of the machine to be developed for use in power system studies.

One of the initial assumptions made by early workers in this field (4,5,20,21,22) was to ignore the effect of magnetic saturation in the iron of the synchronous machine. As the synchronous machine was developed during the latter half of this century, more accurate models were required because lower inertia constants coupled with higher transient reactances meant that the modern generator is now more likely to become unstable under transient conditions (23). The approach adopted by Shackshaft (23,26) to improve the accuracy of the traditional two axis mathematical model (42) is to improve the way the model represented magnetic saturation. The mathematical model used by Shackshaft (23) to represent magnetic saturation is based on a function relating the currents in all the windings of the machine to the characteristic reactance. Using a non-linear function of m.m.f. the values of synchronous reactance (x_{ad}) are determined using equations 2.2a, 2.2b and 2.2c. Shackshaft later (26) goes on to improve on this representation by allowing for a sinusoidal variation in the mutual

reactances. This enables a value for the mutual reactance to be calculated for any rotor position. This work has enabled a more accurate model of the machine to be used in power system studies whilst maintaining a similar number of parameters to the more traditional approach (42).

$$x_{ad} = kx_{ad0} \quad \text{.... 2.2a}$$

$$x_{aq} = kx_{aq0} \quad \text{.... 2.2b}$$

where

$$k = f[x_{ad0}^2(i_{fd} + i_{kd} - i_d)^2 + x_{aq0}^2(i_{fq} - i_q)^2]^{1/2} \quad \text{.... 2.2c}$$

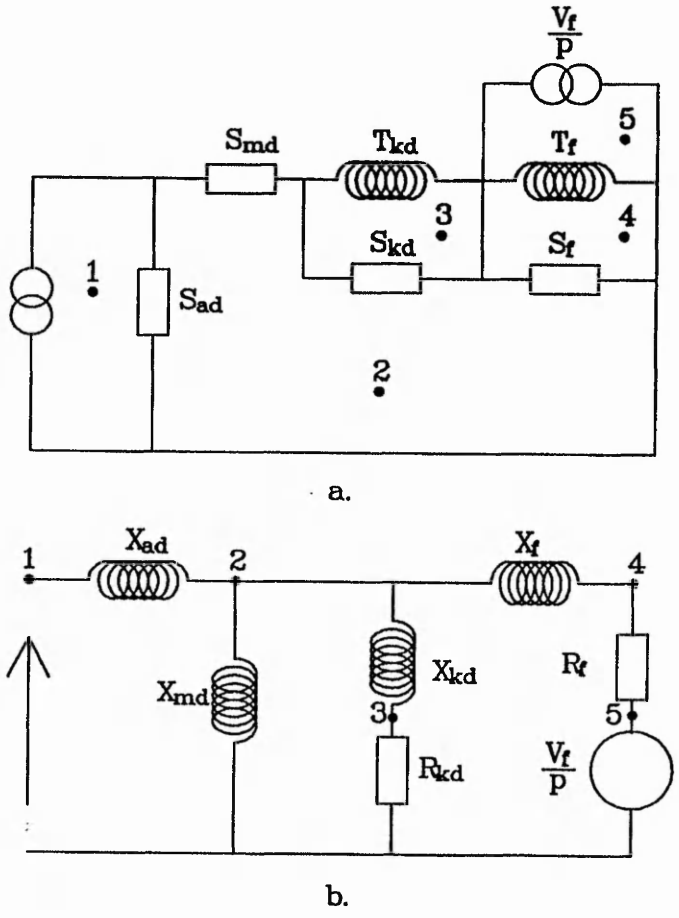

Figure 2.6 D-axis equivalent circuit proposed by Fiennes

2.2.4 A magnetic equivalent circuit approach to a two axis model

The topology of the traditional two axis model (42) can also be derived from the simplified topology of the magnetic circuit. The simplified magnetic circuit described by Fiennes (46) for the D-axis has been presented in the magnetic form based on work described by Laithwaite (12). In the magnetic equivalent circuit, presented here in figure 2.6a, current sources are used to represent the flux generated as a result of the field and D-axis windings, resistive devices being used to represent the main reluctance paths of the machine and inductive devices to represent the linked electric circuits as tranferences. The p (d/dt) operator has been introduced to represent transfer across an electric to magnetic linkage. The topology of the equivalent circuit derived by Adkins (42), presented here in figure 2.1, can be derived by taking the dual of the magnetic circuit in figure 2.6a. The dual circuit is presented in figure 2.6b. It is necessary to multiply throughout by the operator p (d/dt) to ensure that the applied voltage is defined as rate of change of flux. This peculiarity has arisen because of the persistent belief that reluctance should be represented with resistive devices.

The mathematical model defined by Park (5) in the late 1920's has formed the basis for a general equivalent circuit model for the larger part of this century. Although there have been many successful attempts to improve on it, the basic form of the model is still very much apparent. The main constraint when developing such a model is to ensure sufficient simplicity to enable a number of such models to be joined together to form a model for a complete power system. The use of dynamic equivalent circuit parameters as suggested by both Canay (25) and Shackshaft (23,26) is therefore

essential if the required accuracy of such models is to be achieved, whilst allowing such models to be used in power system studies. The use of frequency dependent components is discussed in more detail in chapter seven of this thesis.

2.3 The development of topological equivalent circuit models

2.3.1 The differing approaches to magnetic equivalent circuits

The equivalent circuits described in this section are models which have generally been developed from the physical topology of the magnetic circuit they represent. Equivalent circuits may be presented in a magnetic or electric form, one being the dual of the other. Within equivalent circuits presented in the magnetic form two analogies have been adopted, the flux/current and the flux/charge analogies. Magnetic flux is therefore represented using an electric current or electric charge. The topology of an equivalent circuit in the magnetic form is similar to the topology of the magnetic circuit it represents. Within an equivalent circuit in the electrical form the potential quantity may be representing rate of change of flux or flux linkage and the flow quantity may be representing m.m.f. or electric current. The exact configuration is dependent on how the model represents the respective windings. This approach has led to almost as many equivalent circuit topologies and methods as there has been authors, all of which are equally valid. This type of equivalent circuit does not generally require the use of test data for its development because the device values used in the circuit can be derived directly from the machines' material constants and physical dimensions. This type of equivalent circuit is, therefore, usually of more use to the machine designer because the models can be developed with variable levels of detail.

2.3.2 The traditional approach to magnetic circuits

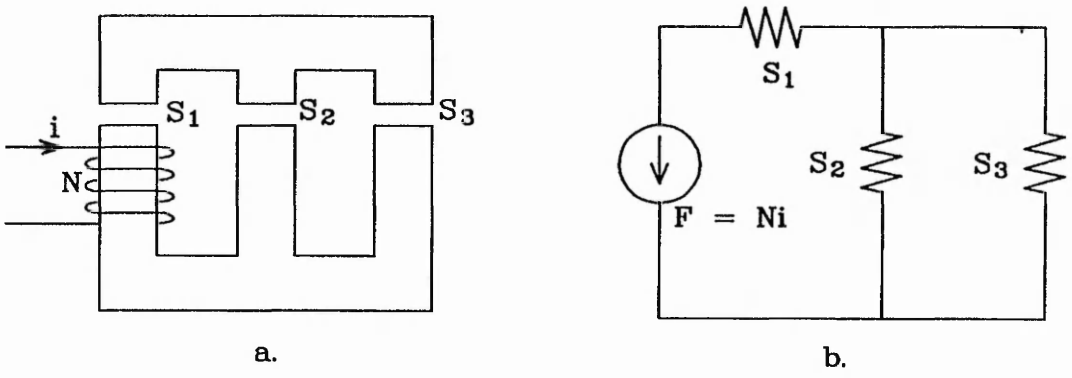

Figure 2.7 A simple magnetic circuit

The concept of a magnetic circuit is perhaps best introduced by Karaptoff (10). Karaptoff presents the magnetic circuit not as an electric equivalent circuit but as a circuit concept of its own. M.m.f. and flux are described as the potential and flow quantities within the circuit. These quantities are related to each other by way of a reluctance as described by equation 2.3.

$$F = S\Phi \qquad \text{.... 2.3}$$

Reluctances may be combined as follows:
In series combinations

$$S_t = \sum_n s_n \qquad \text{.... 2.4}$$

In parallel combinations

$$P_t = \sum_n P_n \qquad \text{.... 2.5}$$

where P = permeance = $\frac{1}{S}$

The similarities between voltage, current and resistance in an electric circuit are obvious. Figure 2.7a shows a relatively simple magnetic circuit. It is a straight forward exercise to generate a magnetic equivalent circuit from the topological picture

of this magnetic circuit (figure 2.7b). This magnetic circuit may be solved in an identical manner to an electric circuit because the rules determining the behaviour of the magnetic circuit are identical to those of an electric circuit. The main disadvantage of representing the magnetic circuit in this manner is that there is no known magnetic insulator to constrain the flux, which leads to calculations that are less accurate than in a comparable electric circuit.

2.3.3 The duality between electric equivalent and magnetic equivalent circuit models

If the magnetic circuit is to be included in an electrical network, an electric equivalent circuit model of the magnetic circuit is required. This is because an equivalent circuit in the electric form may be developed such that the current and potential values are numerically equal to the values of current and voltage at the windings' terminals. This has effectively been achieved by the two axis equivalent circuit model representing a synchronous machine described earlier in this chapter although the method used to develop the models was somewhat different. Cherry (44) describes a method of determining such an electric equivalent circuit from a magnetic equivalent circuit, derived from the physical topology of the magnetic circuit.

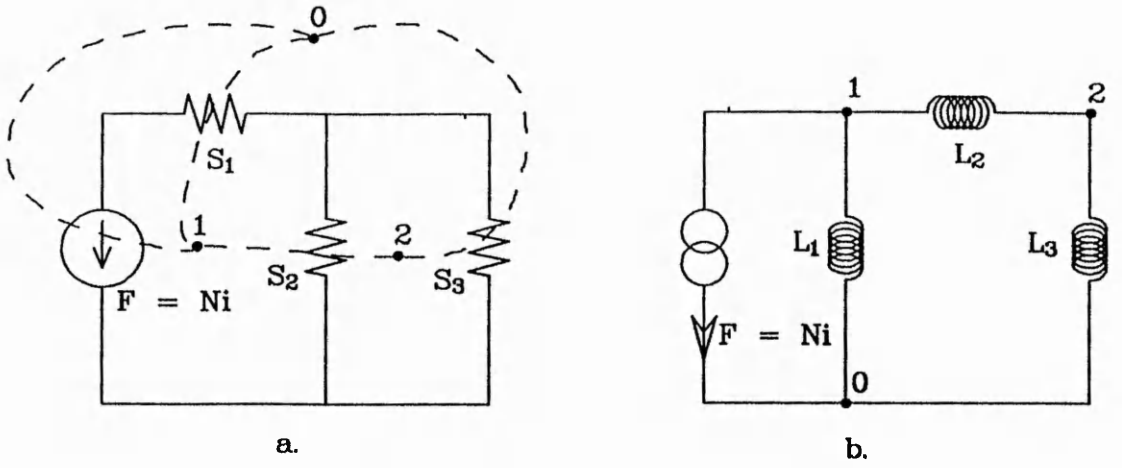

Figure 2.8 Dual equivalent circuits

Cherry (44) observed that the relationship between the magnetic circuit of a transformer and its electric equivalent circuit was identical to an electric circuit and its inverse or dual. The generation of an inverse or dual circuit, in principle, involves the interchanging of the potential and flow quantities within the circuit. As a result, there is also a geometrical change in the circuit topology in so much as nodes become meshes and meshes become nodes, and there is also a reciprocal relationship between the impedances within the original and dual circuits. The process of obtaining the dual of a circuit is demonstrated in figure 2.8.

This approach allows, in principle, the generation of an electric equivalent circuit topology from the physical topology of the magnetic system being modelled. Each component in the equivalent circuit may thus be attributed to a specific part of the machine's magnetic circuit. In practice, however, this process becomes progressively more and more difficult as the magnetic circuit being modelled becomes more complex.

In describing the dual quantities for the magnetic and electric equivalent circuits, Cherry (44) defines the potential and flow quantities as voltage and current in the

electric circuit and m.m.f and rate of change of flux in the magnetic or dual circuit. This implies, although it is not stated, that current in the magnetic equivalent circuit represents rate of change of flux and not flux. This differs from the traditional view that current is used to represent flux. Cherry then goes on to suggest that the dual of the reluctance must be inductance. However, he also states that the dual of inductance was capacitance, and so this would imply that reluctance was the magnetic equivalent of capacitance. In more recent times (15,16) it has been shown that the dual, and therefore the magnetic equivalent of, inductance is in fact capacitance, which corresponds to the reciprocal of reluctance or permeance.

2.3.4 The magnetic equivalent circuit approach using the flux/current analogy

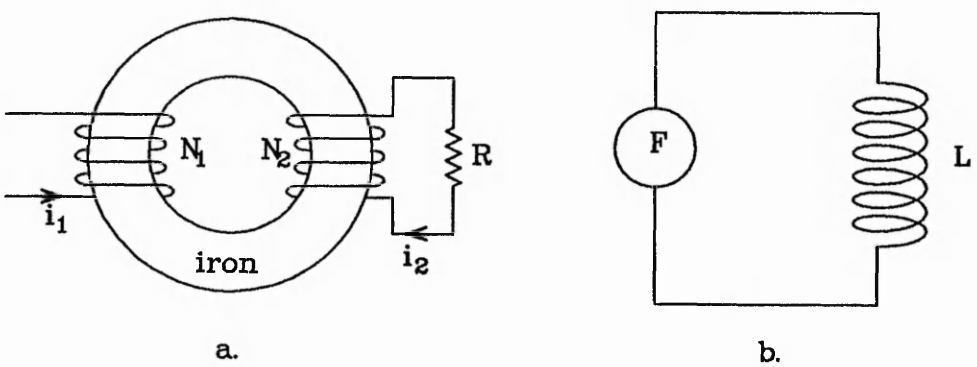

Figure 2.9 Magnetic equivalent circuits described by Laithwaite

The description of an equivalent magnetic circuit in which electric current is used to represent magnetic flux is, perhaps, best summarised in a paper by Laithwaite (12). The work described in this paper deals exclusively with the modelling of magnetic circuits in their magnetic, or reluctance, form. The paper clearly sets out how differing

linked electric circuits (inductance, capacitance and resistance) can be correctly represented in the magnetic equivalent circuit model. A resistive component connected to a winding which links a magnetic circuit becomes what is called a transference when it is referred across a linkage into the magnetic circuit. Transference is shown to be the magnetic equivalent of inductance (figure 2.9a and b). An inductance connected to a winding which links the magnetic circuit is shown to become equivalent to a reluctance when referred into the magnetic circuit. A reluctance, therefore, is modelled identically regardless of whether it is situated within the magnetic circuit itself or in a magnetic circuit which is linked to it by an electric circuit. In the latter case the number of linking turns present is used to scale the remote reluctance value.

Later in this chapter it is shown how Slemon (30) described linked resistive circuits, for example eddy current paths, as the equivalent to capacitors in equivalent circuit models used to model synchronous machines. This can be explained by considering the form of the equivalent circuits. The circuits described by Slemon (30) are shown in their electric equivalent circuit form which is the dual or inverse of the circuits described by Laithwaite (12). What appears as an inductance in one will therefore appear as a capacitance in the dual circuit (44). This confirms that the two methods are consistent.

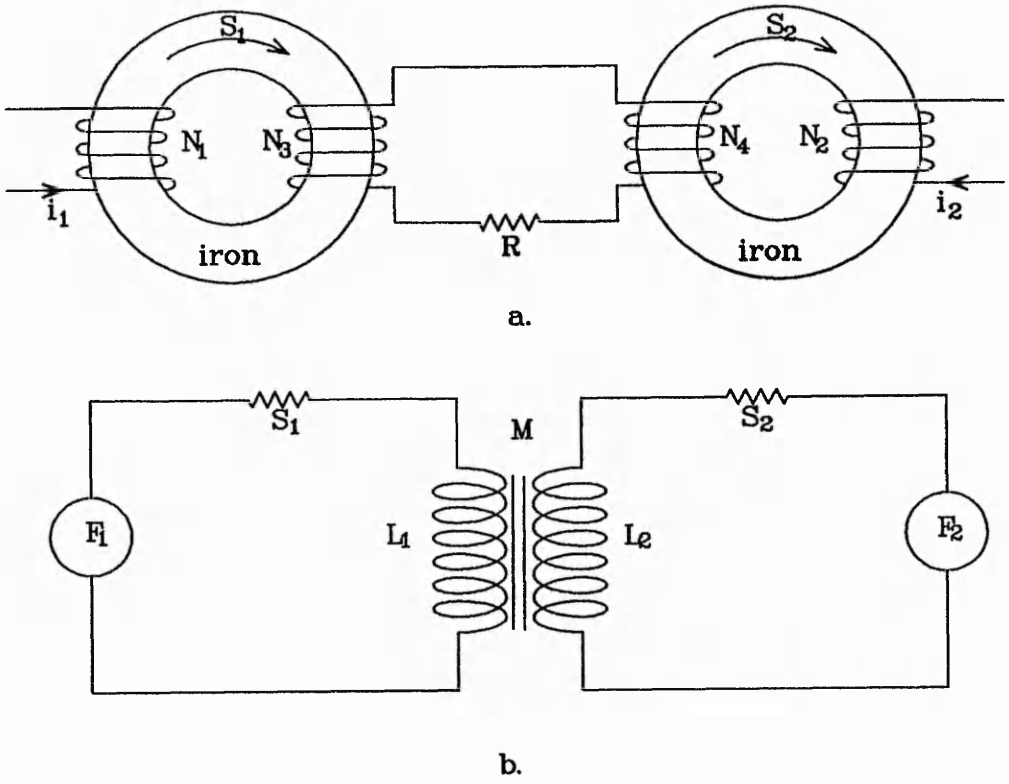

Figure 2.10 The concept of magnetic mutual inductance presented by Laithwaite

The paper (12) goes on to describe how more complex magnetic circuits may be represented. A method for representing two magnetic circuits linked by a mutual electric circuit is shown to be analogous to the concept of mutual inductance. Figure 2.10a and b show how the concept of magnetic mutual inductance is implemented. This method of representing the mutual linking effect of electric circuits is consistent with transformers T_1, T_2 and T_3 used by Rankin shown in figure 2.2. The following equations, 2.6 and 2.7, have been deduced to verify this analogy.

$$F_1 = L_1 \frac{d\Phi_1}{dt} + M \frac{d\Phi_2}{dt} + \Phi_1 R_1 \quad \text{.... 2.6}$$

$$F_2 = L_2 \frac{d\Phi_2}{dt} + M \frac{d\Phi_1}{dt} + \Phi_2 R_2 \quad \text{.... 2.7}$$

2.3.5 An application of the flux/current analogy

The relationship between magnetic and electric equivalent circuits described by Cherry (44) formed the basis for the equivalent circuits developed by Slemon (11,30) to model various electrical machines including transformers, induction machines and synchronous machines. An electric equivalent circuit is initially developed (11) for the magnetic circuit within a simple transformer, ideal transformers are then appropriately situated to link the equivalent circuit to the electrical network connected to the windings. The development of this circuit is described in figures 2.11a to e. There are two ways to view the equivalent circuit between the two ideal transformers in figure 2.11e. The electric equivalent circuit may be described as a representation of the magnetic circuit within the system which has been generated by a succession of geometrical transformations. This interpretation is, of course, entirely valid because it is an exact description of the method used to generate the circuit. However, the electric equivalent circuit between the two ideal transformers may also be described as a per turn or normalised electric equivalent circuit. The function of the two ideal transformers in figure 2.11e is to numerically scale the voltages and currents so that they are representative of the flux and m.m.f. respectively.

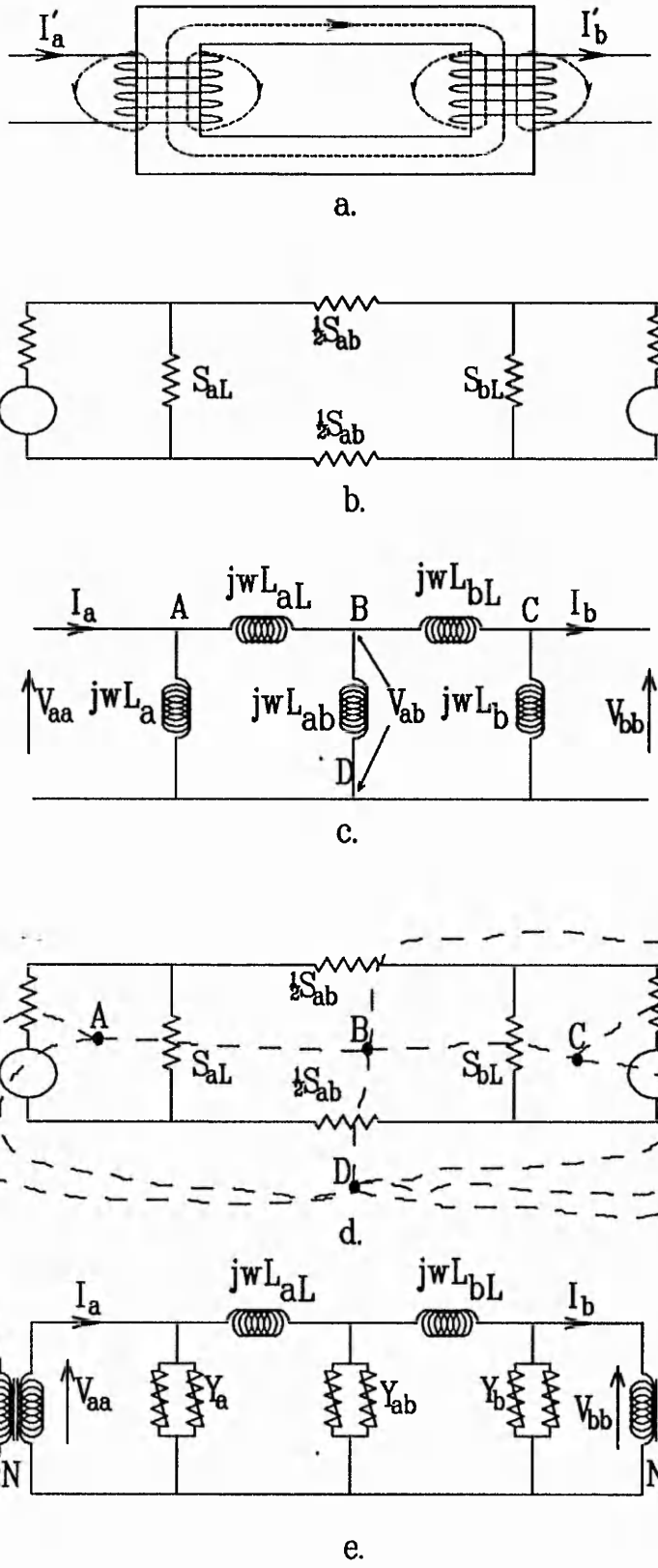

Figure 2.11 Equivalent circuit to represent a transformer developed by Slemon

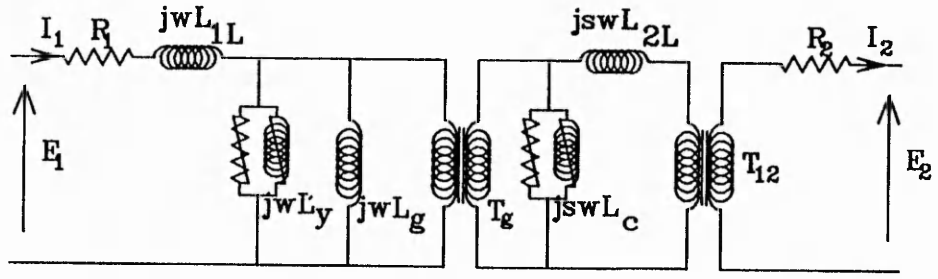

Figure 2.12 Equivalent circuit to represent an induction machine developed by Slemon

Slemon (11) also describes an equivalent circuit which could be used to model rotating machines. These circuits are developed in an identical manner to those used to model the transformer, described previously. To illustrate the method Slemon uses an induction machine, figure 2.12, a per turn equivalent circuit is generated by transforming the magnetic circuit to form its dual. The effect of the number of turns per winding or damper circuit is then modelled using ideal transformers. A further special transformer T_g is introduced to model the effect of rotor motion. This special transformer, called an ideal induction machine, has a current ratio of 1:1 and a voltage ratio of 1:slip. The current ratio is 1:1 because the current through the transformer on the stator side (numerically equal to the m.m.f.) is equal to the current on the rotor side of the air gap. This is because the current (m.m.f.) for the air gap flows through a reactance jwL_g, representing the air gap. The remaining current through the transformer being, therefore, the current (m.m.f.) on the rotor side. The voltage ratio is 1:slip because the slip represents the difference in angular velocity between the flux and the rotor winding. The induced voltage per turn is therefore the rate of change of

flux due to this difference in the angular velocities. A more complete explanation and derivation of this ideal induction motor is provided in reference 9.

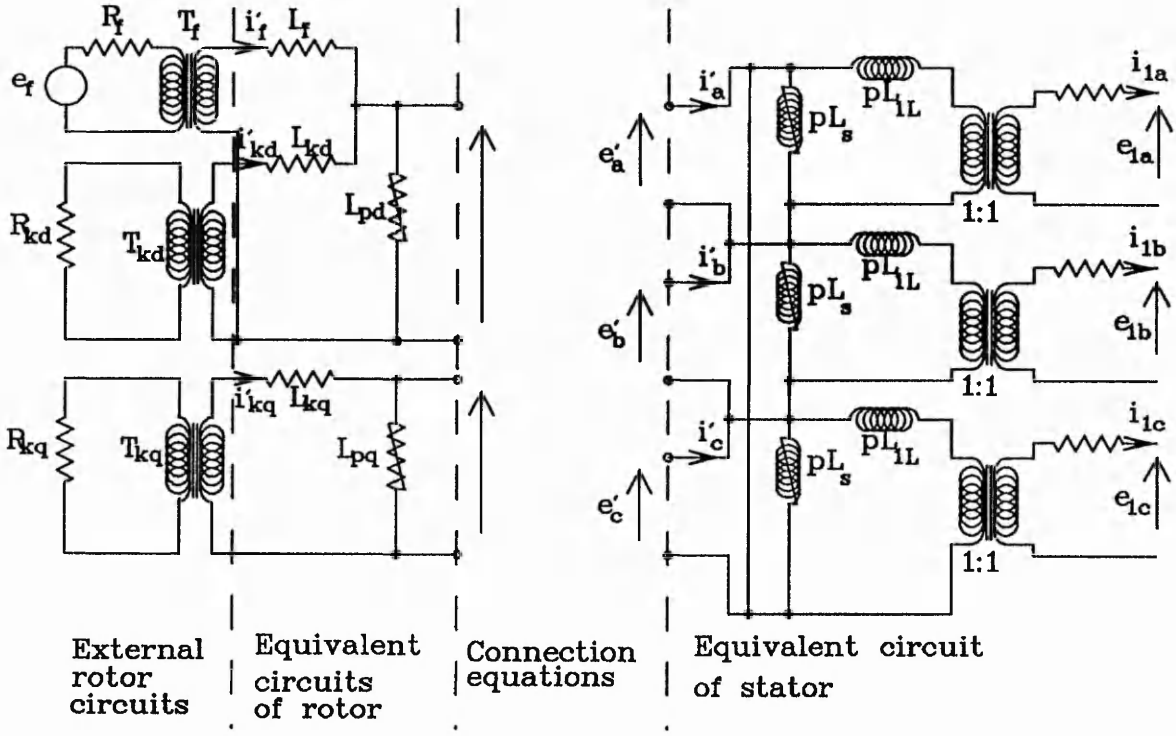

Figure 2.13 Equivalent circuit to represent a synchronous machine developed by Slemon

To obtain an equivalent circuit for a synchronous machine under transient conditions (figure 2.13) Slemon (11) replaces the special transformer with a box of connection equations. On the stator side of the air gap the equivalent circuit has been generated as before using the dual transformation of the magnetic circuit. On the rotor side of the air gap, however, there are two equivalent circuits, representing the direct and quadrature axis, their forms being those of the dual of the respective magnetic circuits. Slemon then uses a mathematical transformation to ensure that the total flux linkage appears as a voltage across the air gap. In performing this transformation the air gap inductance L_g is represented by a conductance of value $1/L_g$. The connection

equations used by Slemon are similar in form to those described by Adkins (42) and used as the method of transforming from the theoretical D and Q axis windings of a synchronous machine to the three phase bands. This is surprising because the induced e.m.f. in the hypothetical D and Q windings is directly proportional to the rate of change of flux linkage.

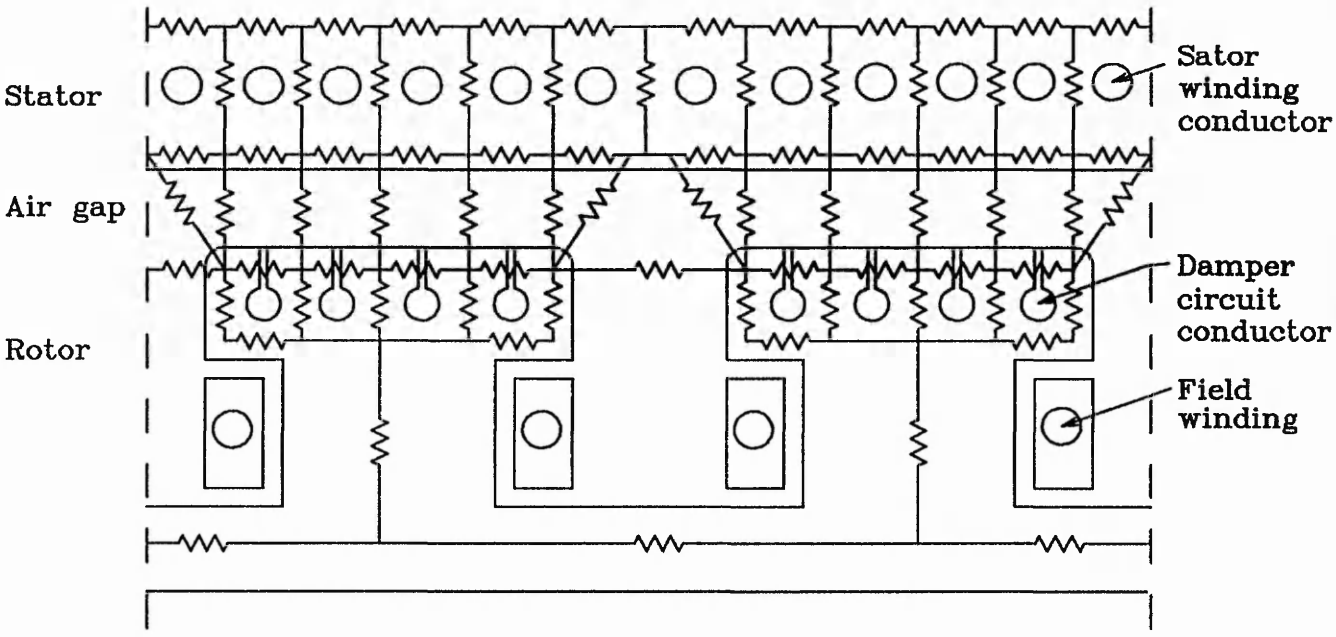

Figure 2.14 Detailed equivalent circuit to represent a synchronous machine developed by Slemon

In later work, Slemon (30) uses a similar method to generate a detailed equivalent circuit for a salient pole synchronous machine, the initial approach being very similar to his previous work. The magnetic circuit is divided up into discrete reluctance paths and the dual taken to form an electric equivalent circuit model. The topology of the magnetic equivalent circuit is shown in figure 2.14. In the magnetic circuit Slemon has assumed the potential quantity to be ampere turns and the flow quantity to be flux.

These are then inverted as the circuit is inverted such that in the equivalent circuit the potential quantity is flux linkage and the flow quantity is m.m.f. per turn. Because the electric current in the windings or damper circuits flows in meshes in the magnetic circuit they can be represented as current sources flowing into and out of nodes in the dual circuit. The induced e.m.f. in any winding or eddy current path is proportional to the rate of change of flux linkage. These linked electric circuits are therefore represented as capacitors, the value of which depends on their electrical resistance and the number of turns. To represent the stator, currents are injected into and extracted out of the appropriate nodes within the dual circuit so as to correctly distribute the stator m.m.f. The concept of injecting a current into a single node to represent the effect of a current flowing in a slot of the stator implies that the current only has a local effect. In reality, however, a current flowing in a conductor has an effect on every closed magnetic mesh which surrounds it and not just the most local one. This concept is discussed in more detail in chapter three of this thesis.

The approach adopted by Slemon (11,30) relies heavily on the inverse relationship between a magnetic circuit and its electric equivalent circuit described by Cherry (44). Even though Cherry states that the dual of current is rate of change of flux, Slemon has used the more traditional approach that current should represent flux in the electric equivalent circuit. This has tended to make the transformation and therefore equivalent circuit more obscure than it need be. However, this does not make the equivalent circuit any less valid, with energy being stored in the electric circuits of the equivalent circuit model rather than in the magnetic. Although this is not physically accurate the representation is mathematically valid.

An approach using a similar equivalent circuit analogy has been applied and developed by Ostovic (14). To represent relative motion between the rotor and stator, Ostovic describes a method using dynamic air gap reluctances. The stator and rotor surfaces are divided up into a number of long thin elements running the full length of the machine. Each element on the stator is connected to each element of the rotor using a reluctance with a variable value. The effects of rotor skew and eccentricity have also been taken into account by modifying the value of air gap reluctance between the respective elements.

The work by Ostovic provides a very good introduction to the field of magnetic circuit modelling, and in particular the calculation of values of reluctance for different physical topologies. The work tends to concentrate on the magnetic circuit with little attention to any linked electric circuits. It is assumed that any electric current may be represented by a m.m.f source in the magnetic circuit. Although this will be shown to be true for simple magnetic circuit topologies, a little more detail is required to represent the more complex magnetic circuit. This will be more fully described in chapter three of this thesis. The approach uses a matrix representation throughout which, although in itself does not alter the overall approach, tends to improve the readability of the mathematical representation.

2.3.6 The use of tensors to represent the synchronous machine

The method of tensor analysis is particularly useful in the solution of problems with a large number of variables. It involves the geometric manipulation or transformation of

dimensionless matrices which have been used to describe a physical system. This method has, therefore, been applied to the investigation of electrical networks (47). The development of a final or suitable equivalent circuit model tends to always follow a similar pattern. Kron describes three postulates which have been used to form and transform the basic system matrices in order to generate this equivalent circuit model. These general rules or postulates are briefly described as follows:-

1. The n algebraic equations describing a physical system with n degrees of freedom may be replaced by a single equation having the same form as that of a single unit of the system, if the coefficient of each unknown is used as the corresponding element in an n x n dimensional matrix.

2. If the matrix equation of a particular physical system is known, the same equation is valid for a large number of physical systems of the same nature, provided that each n x n matrix in the equation becomes an appropriate tensor (geometric object), that is, if each n x n matrix becomes endowed with a definite law of transformations. This postulate is defined as the transformation of system equations between the different reference frames. It has been used by Kron (41) to enable the use of the same system matrix equations on similar machine types.

3. The equations describing the properties of n-dimensional Euclidean spaces become applicable to n-dimensional non-Euclidican spaces also, if all "ordinary" derivatives in the equations (such as dA/dt) become "absolute" (or covariant) derivatives derived from the former routine procedure. This postulate enables the ordinary derivative $di/dt = \pi$ for a stationary network to be replaced by the absolute derivative. This transformation is then used to model the relative motion between the stator and rotor by making use of the effective or absolute frequency that exists in the moving system.

All equivalent circuit models developed by Kron (41) are established without using a single performance equation. The starting point for the development of these equivalent circuit models is a primitive model of the system which is then developed using the postulates described above.

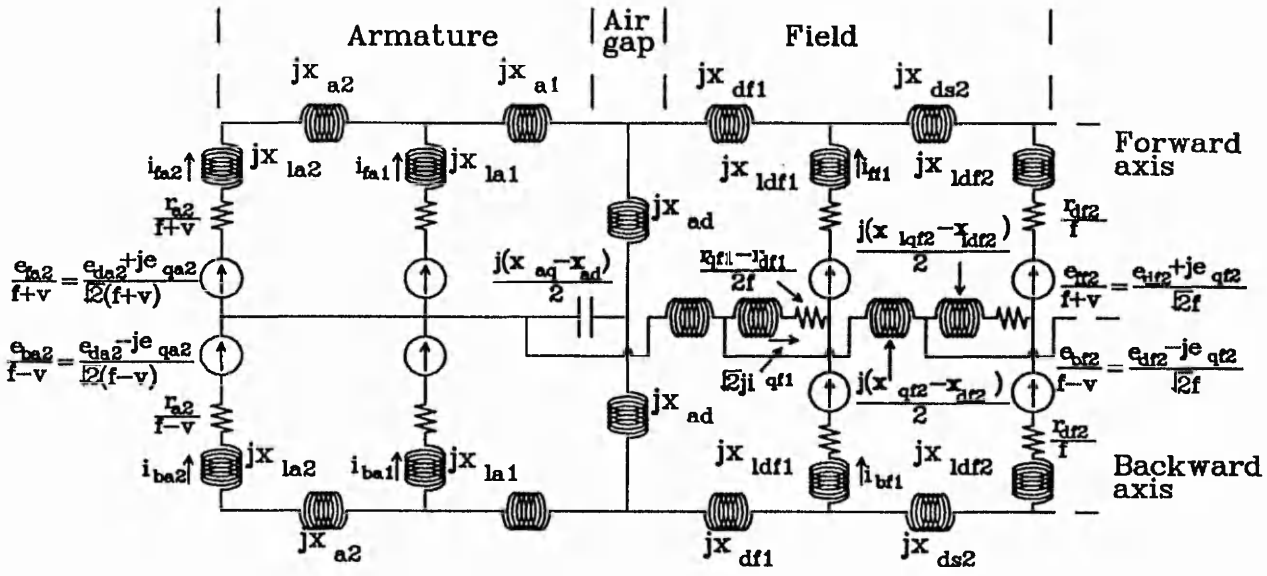

Figure 2.15 Equivalent circuit to represent an induction machine developed by Kron

An equivalent circuit for what is described as a primitive machine is initially generated by an inspection of the magnetic circuit when a rotating machine is at a standstill. The primitive machine given in figure 2.15 initially represents an induction machine at a standstill. This arrangement is assumed similar to a four winding transformer. In developing this equivalent circuit Kron (41) describes the reluctance equivalent circuit, which is based on the topology of the machine as the electric equivalent circuit and the dual of this as the magnetic equivalent circuit. This is opposite to the terminology adopted in this thesis. In the reluctance equivalent circuit Kron represents reluctance paths using resistances, which implies that the flux/current analogy has been adopted. In this particular case, however, the choice of analogy adopted does not effect the process of generating the final equivalent circuit because the resistive components are only required to assist in the topological transformations and are not used in any actual

calculations. The effect of rotor motion is modelled by modifying the value of the frequency used in the differing parts of the equivalent circuit to represent the absolute frequency experienced by the components. The absolute frequency is calculated as the arithmetic sum of the supply frequency, the angular velocity of the rotor and the angular velocity of the reference frame. The topology of the equivalent circuit (figure 2.15) remains unchanged.

The approach adopted by Kron (41,47) is based on a technique more usually applied to pure physics. It has been demonstrated that the technique may be successfully applied to the study of field problems (41). The modelling methodology has similarities with both the traditional approach using a mathematical model and the approach adopted in this thesis using the topology of the magnetic circuit. Initially, the model is based on a concept called a primitive machine which is not dissimilar to the concept of a two axis model. However, a particular advantage of this method is the standard approach to expanding the primitive model using postulates or transformations to increase the level of discretisation to that required by a particular application.

2.4 The magnetic equivalent circuit approach using the flux/charge analogy

2.4.1 The development of the flux/charge analogy

The concept of the magnetic circuit approach described by Cherry (44) and Laithwaite (12) is extended by Carpenter C.J. (15) initially with the aim of creating a magnetic equivalent circuit for systems with less well defined magnetic paths. However, as the technicalities of the paper unfold it becomes apparent to Carpenter that an equivalent

circuit in which electric charge is used to represent flux would more appropriately represent the magnetic circuit.

The paper commences by introducing the concept of magnetic terminals. Magnetic terminals are defined for a region enclosed by a surface chosen such that the magnetic field is tangential to it everywhere except over two or more regions at which the surface is intersected by the flux. These areas of intersection are called the magnetic terminals. The magnetic impedance between such terminals is defined in terms of flux at, and m.m.f. between, them. Care must be taken when defining such magnetic terminals so as to ensure that the terminal areas are equipotential surfaces. The reader is directed to reference 13 for a more complete description of the concept of magnetic terminals. In essence, provided they have been defined correctly, magnetic terminals can be assumed to have similar properties to electric terminals. The careful definition is required because there is no equivalent to an electrical insulator in a magnetic circuit.

$$e = \frac{d\lambda}{dt} \qquad \text{....2.8}$$

$$F = \gamma = \frac{dQ}{dt} \qquad \text{....2.9}$$

where λ = flux linkage
and γ = current linkage

The concept of both self and mutual transference (12), shown in figure 2.10a and b, is further investigated by Carpenter C.J. (15). Carpenter C.J. presents the e.m.f. induced at the terminals of an inductor using equation 2.8. The flux linkage, λ, represents the

magnetic flux multiplied by inductor turns, NΦ. Further, Carpenter C.J. compares this to the m.m.f. induced in a magnetic circuit by a time varying charge or electric current. Equation 2.9 describes this m.m.f. as a current linkage, γ, and is described as the charge linkage per unit flux with units of coulombs per weber.

Although Laithwaite's (12) method of representing a linked resistive electric circuit in terms of an inductance in the magnetic circuit has been shown to be valid mathematically (12,15), it does not portray a physically consistent picture of the system being modelled. It is expected that a resistive or energy dissipative electric circuit can be represented by an inductive component which, by definition, is an energy storage device. The same is true of reluctance. This is made possible because the equivalent circuit models are equivalent circuit representations of the mathematical equations describing the magnetic field. They are, of course, perfectly valid models, but they do not represent the physical behaviour of the system.

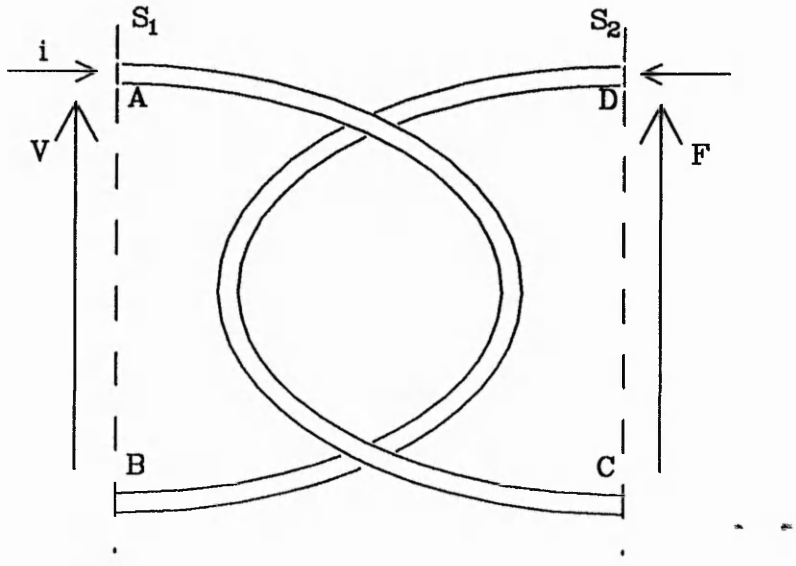

Figure 2.16 Power flow described by Carpenter C.J.

The most significant assertion by Carpenter (15), and in particular because it forms the basis for the work contained within this thesis, is the use of the equivalent circuit analogy that electric current should be used to represent rate of change of flux and not flux, as had been assumed since the early part of this century. This idea is developed by considering the power and energy flow across two similar surfaces, one in an electrical system and one in a magnetic system. Consider figure 2.16, the instantaneous power flow across the surface S_1 being given by equation 2.10.

$$P = vi \qquad \text{.... 2.10}$$

In a similar magnetic system where two magnetic terminals have been defined on a surface S_2 (figure 2.16), the power flow across the surface S_2 is given by integrating the poynting vector ExH giving equation 2.11.

$$P = \text{m.m.f.} \frac{d\Phi}{dt} \qquad \text{.... 2.11}$$

An alternative form of equivalent circuit is then presented in which current is used to represent rate of change of flux, capacitance is used to represent permeance (the reciprocal of reluctance) and linked electric resistive circuits are represented by a conductance. These equivalent circuit analogies are identical to the dual quantities stated by Cherry (44). The dual of the potential quantity in the electric circuit (voltage) is rate of change of flux, the dual of the electric flow quantity (current) is m.m.f., the dual of inductance is capacitance and the dual of resistance is conductance. In chapter three of this thesis this analogy will be investigated in detail and it will be

shown that a more physically consistent description of this analogy could be presented such that electric flux is used to represent magnetic flux.

2.4.2 The application of the flux/charge analogy to represent a synchronous machine.

The alternative equivalent circuit analogy described by Carpenter C.J. (15) in which electric charge is used to represent magnetic flux has more recently been adopted by Haydock (7,8,16,48).

The general approach adopted by Haydock is similar to that used by earlier authors (10,11,12,44) in that within a physical magnetic circuit a significant or dominant flux pattern is defined. This pattern is then used to determine the basic topology for the magnetic equivalent circuit. The reluctances representing discrete parts of the magnetic circuit are represented using what have been termed magnetic capacitors, these are magnetic devices which behave in an identical manner to an electric capacitance, their value being equal to the magnetic permeance of the discrete reluctance they represent. This differs from the more traditional analogy in which reluctance is represented using a resistive device.

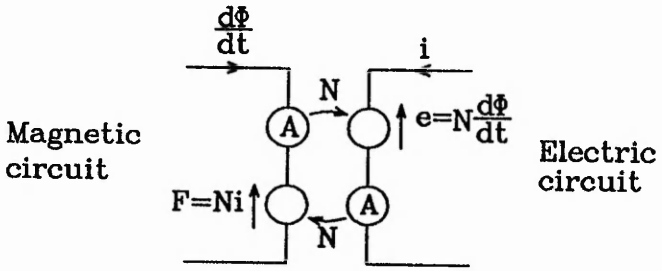

Figure 2.17 Equivalent circuit linkage described by Haydock

To determine the representation of windings and other electric current carrying conductors within the magnetic circuit model Haydock (16) describes the tearing principle. This principle is ensures that no flux mesh which completely encircles an electric current path will escape its effect because the electric conductor is torn from its present position towards its return path. The number of linking turns is, therefore, reduced to zero. This is similar to a method described by Kron (47). As the conductor tears through a defined flux path a linkage is inserted to model the effect of the conductor on that flux path. A linkage consists of a pair of flow controlled potential sources linked by a parameter representing the number of turns. The flow quantity in one circuit is measured, multiplied by the number of turns and induced in the other circuit as a potential quantity. This process is illustrated in figure 2.17.

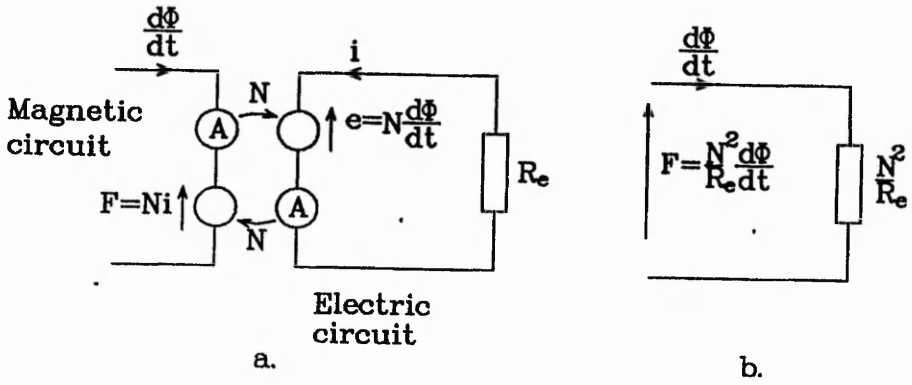

Figure 2.18 Equivalent circuit dampance described by Haydock

Laithwaite (12) describes the advantages to be gained from expressing the equivalent circuit in a wholly magnetic form. The concept of referring a purely resistive linked electric circuit across a linkage to reduce the topological complexity of the model,

described by Laithwaite (12), is applied by Haydock (16). In this case a purely resistive linked electric circuit may be referred across the linkage to form what Haydock has termed a dampance. This has been so termed because the effect of a closed electric circuit on a magnetic system is to damp magnetic circuit transients. The dampance is a resistive device, the value of which is dependent on the square of number of linked turns divided by the electrical resistance of the current path. This is demonstrated in figure 2.18.

The representing of linked electric current paths using single dampance elements in the wholly magnetic equivalent circuits presented by Haydock (16) clearly indicates that the magnetic transformer effect (12) between mutually linked magnetic circuits is ignored. This assumption is challenged by the author because the magnetic transformer has a significant affect on the damping of mutually linked magnetic circuits. Further, the author is unable to obtain an agreement between simulation and test results for equivalent circuit models presented in this thesis unless magnetic transformers are include in the equivalent circuit models. What is believed to be original work relating to the representation of magnetic transformers in equivalent circuit models is presented in chapter three of this thesis.

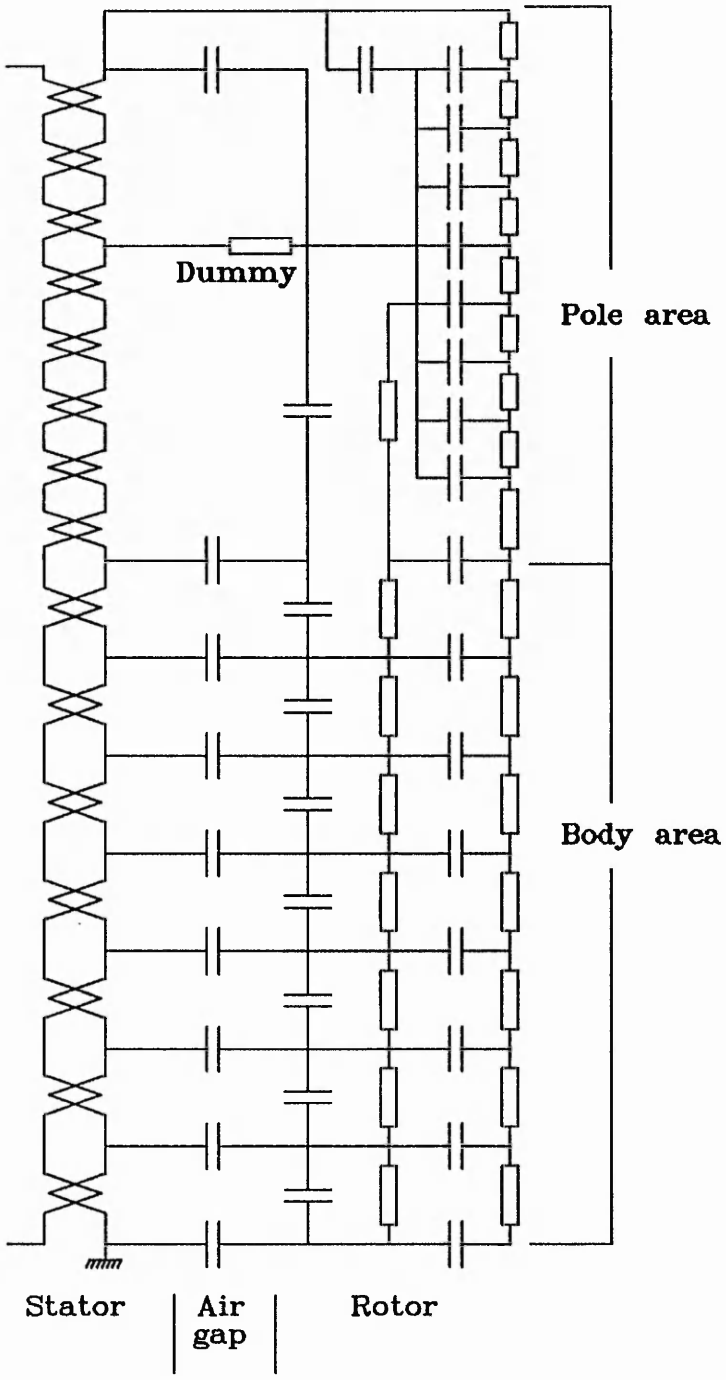

Figure 2.19 Q axis equivalent circuit for a synchronous machine developed by Haydock

Figure 2.19 shows a typical equivalent circuit topology developed by Haydock (16) which has been used to model a Q axis flux decay test on a large synchronous machine. The topology of the equivalent circuit was developed using the standard approach of lumping the magnetic circuit into the significant flux paths and then representing these using a network of permeances, modelled as magnetic capacitors. The position of the damping resistors shown have been determined after tearing the electrical conductors (field, wedges, damper circuits and rotor iron) towards the neuman boundary defined along the D axis. The electrical resistances of the damper circuits are then individually referred into the magnetic circuit using the method described by figure 2.18. The values for all the components have been calculated from the physical dimensions and material bulk constants of the machine and are constant for the duration of any one simulation. To simulate a flux decay test, an initial charge is placed sinusoidally on the air gap permeance to represent a sinusoidal distribution of flux and then allowed to decay. The stator voltage envelope is calculated directly from the magnetic charge stored within the air gap permeance as it decays. A similar equivalent circuit model has also been developed to represent the machine during a D axis flux decay test using an identical approach.

The results presented by Haydock (16) are in close agreement with actual test results obtained from the machine itself. However, it is noted that Haydock's results are limited to the initial four second period of a flux decay tests. The inability of Haydock's models to represent mutually linked magnetic circuits and insufficient descritisation, particularly at the rotor surface, is thought to be responsible for this limited set of results.

The equivalent circuit models developed by Haydock (16,48) are presented in a wholly magnetic form, and a solution to these models is obtained using the general purpose electric circuit solving software SPICE (17). One of the principal advantages of representing an equivalent circuit in this form is that it reduces the computational requirements of the model to a minimum. However, this approach also places a severe limitation on the quantities which are available from the model under investigation. The results presented by Haydock are limited to magnetic quantities that exist only within the confines of the magnetic circuit. This prohibits these equivalent circuit models from being linked into an electrical supply network.

Although, the equivalent circuits presented by Haydock (16,48) are considerably more discretised than the more traditional two axis approach (42), the D axis model's ability to represent the outer layers of the rotor surface is limited to a single slot leakage in parallel with a single dampance representing a slot pitch. However, it has been demonstrated using finite element methods (6) that the transient and in particular the sub transient behaviour of a synchronous machine is directly affected by the topology and material constants present in the outer regions of the rotor.

Since the work described in this thesis was undertaken by the author in 1991 (32) Haydock (35) has presented a matrix formulation to represent magnetic transformer effects within a wholly magnetic equivalent circuit model. Within the appendix to reference 35 two matrices are presented one as equation A3 and an unnumbered

equation immediately following equation A3, assumed here to be equation A4. Equation A4 is reproduced here as equation 2.12.

Equation 2.12

$$\begin{bmatrix} V_{m1} \\ V_{m2} \\ V_{m3} \\ \\ V_{mn} \end{bmatrix} \quad \begin{bmatrix} N_1^2/R_1 & N_1N_2/R_1 & N_1N_3/R_1 \ldots & N_1N_n/R_1 \\ N_2N_1/R_2 & N_2^2/R_2 & N_2N_3/R_2 \ldots & N_2N_n/R_2 \\ N_3N_1/R_1 & N_3N_2/R_3 & N_3^2/R_3 \ldots & N_3N_n/R_1 \\ \\ N_nN_1/R_1 & N_nN_2/R_1 & N_nN_3/R_1 \ldots & N_nN_m/R_n \end{bmatrix} \begin{bmatrix} i_{m1} \\ i_{m2} \\ i_{m3} \\ \\ i_{mn} \end{bmatrix}$$

Clearly, the similarities between the topology of matrix equation 2.12 and those developed by the author (32) and presented later in this thesis are a direct result of the similarities between the physical systems the equations are attempting represent. However, the equation presented by Haydock is seemingly inconsistent with the representation of multiple interlinked magnetic and electric circuits.

$$V_{m1} = N_1^2/R_1.i_{m1} + N_1N_2/R_1.i_{m2} + N_1N_3/R_1.i_{m3} \ldots + N_1N_n/R_1.i_{mn} \qquad \ldots. 2.13$$

Consider the expansion of the first row of equation 2.12 presented here as equation 2.13. The terms contained in equation 2.13 clearly indicate one electrical circuit of resistance R_1 linking n magnetic circuits carrying magnetic currents i_{m1}, i_{m2} ... i_{mn}. V_{m1}, therefore, represents the m.m.f. induced in the first magnetic circuit by the electric circuit R_1.

$$V_{m2} = N_2N_1/R_2.i_{m1} + N_2^2/R_2.i_{m2} + N_2N_3/R_2.i_{m3} \ldots N_2N_n/R_2.i_{mn} \quad \ldots. 2.14$$

Now consider the expansion of the second row of equation 2.12 presented here as equation 2.14. The terms contained in equation 2.14 clearly indicate one electrical circuit of resistance R_2 linking n magnetic circuits carrying magnetic currents i_{m1}, i_{m2} ... i_{mn}. V_{m2}, therefore, represents the m.m.f. induced in the second magnetic circuit by the electric circuit R_2.

Clearly, therefore, within the representation presented by Haydock there is no mechanism for the electrical circuit containing R_1 to induce an m.m.f. into any magnetic circuit other than the first. Further, there is no mechanism for the electrical circuit containing R_2 to induce an m.m.f. in any magnetic circuit other than the second, and so on. The limitations of the method and associated equations presented by Haydock (35) are, therefore, obvious.

Further one of the terms presented in equation 2.12 is clearly in error. The term written as N_nN_m/R_n should be written as N_n^2/R_n.

A matrix representation describing the effect of mutually linking electric circuits has been presented by the author (32). This work is described in detail in chapter three of this thesis. The original techniques developed in chapter three of this thesis precede the work presented by Haydock (35) and have enabled a significant increase in the level of discretisation obtainable using magnetic equivalent circuit methods. This has

enabled consistent results to be obtained for a wide range of internal and terminal quantities and test conditions. This work is fully described in later chapters of this thesis.

2.4.3 The development of time varying linkages to represent rotor motion

The traditional two axis models developed for synchronous machines (42) have been primarily developed to enable the machine and its supply network to be modelled simultaneously. However, this traditional approach is not suitable for modelling the behaviour of such a machine when it is connected to a power electronic drive circuit. This is because high frequency harmonics are generated in the electrical supply to the machine. An equivalent circuit model, based on the ideas developed by Carpenter C.J. (15) and Haydock (16) has recently been developed by Carpenter M.J. (29), which has successfully been applied to a detailed investigation of the effects of the magnetic circuit within a synchronous machine on the commutation of a three phase thyristor bridge.

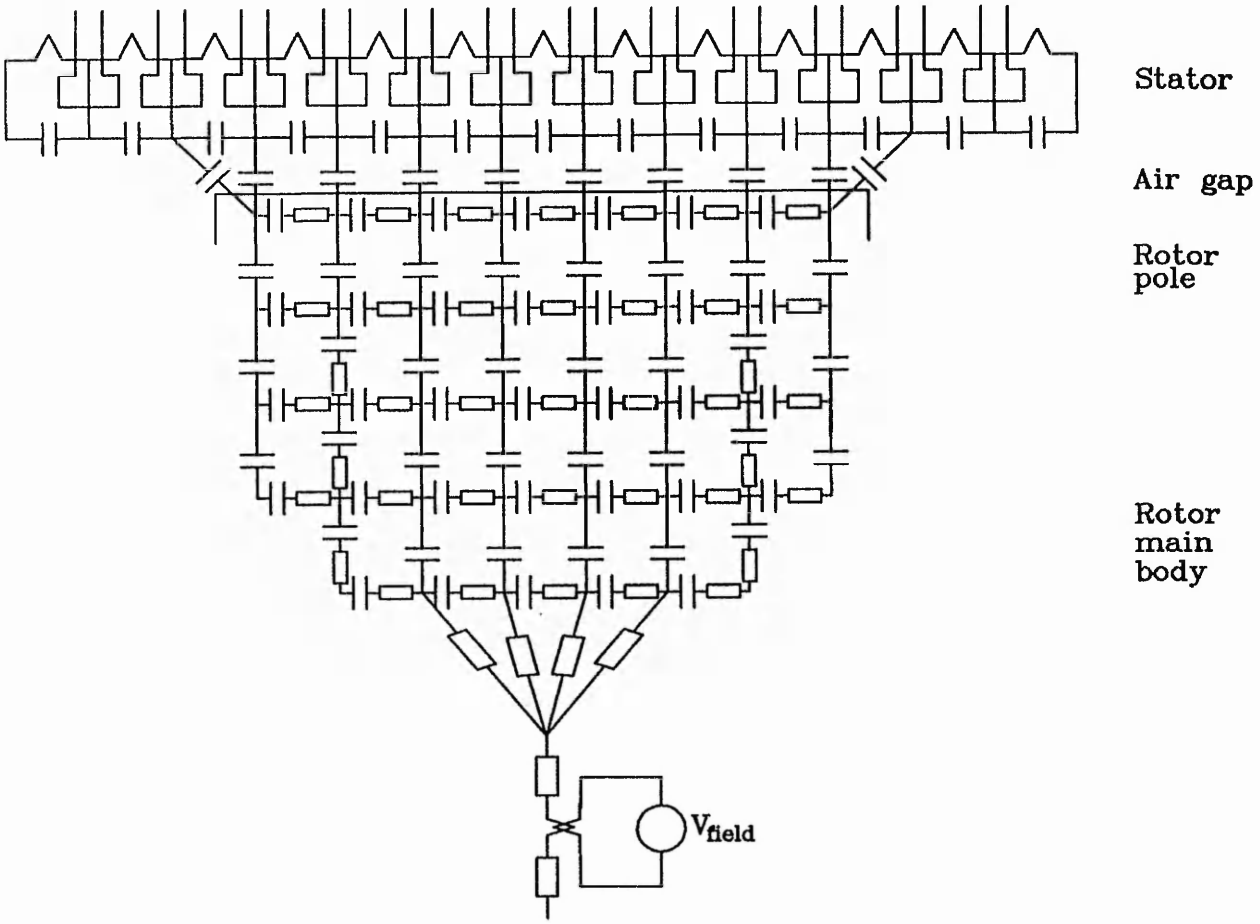

Figure 2.20 Equivalent circuit for a synchronous machine developed by Carpenter M.J.

The topology of the equivalent circuit model is based on the topology of the machine and, within the magnetic equivalent circuit, charge is used to represent magnetic flux. The equivalent circuit model can readily be divided into three sections, the rotor, the stator, and the thyristor bridge. Figure 2.20 shows a section of the equivalent circuit representing a single pole pitch of the machine.

The equivalent circuit representing the rotor is made up from the two solid pole regions around a linkage representing the field winding. The pole regions are discretised into a regular mesh, the radial dimension of the mesh increasing with an increasing rotor depth. Eddy currents are assumed to flow axially along the rotor within the boundaries defined by the permeance mesh. The damper circuits of the rotor have in general been torn towards the centre of the rotor. Magnetic resistance or dampance has been inserted into the permeance network to represent the electrical damper circuits referred across each linkage. However, this approach is incapable of representing the magnetic transformer effect of the linking damper circuits because it is identical to the method used by Haydock (16). The thyristor bridge is modelled in an innovative manner using current dependent voltage sources configured as a time dependent switch. A more detailed description of this part of the model is beyond the scope of this thesis. The interested reader is directed towards reference 29 for a more detailed description.

The representation of the air gap and stator windings is dependent on the method used to represent the relative motion between the stator and rotor. To represent this motion Carpenter M.J. (29) experimented with two methods. Initially considered were a network of permeance paths across the air gap such that each rotor tooth was connected to each stator tooth. The value of each permeances would then be a function of rotor position. For a constant angular velocity each permeance would, therefore, be time dependent. The constantly varying permeances will in themselves generate a back e.m.f. at the stator terminals. This method has been used successfully by Ostovic (13). In this particular example, however, the number of rotor and stator

teeth led to a prohibitively high number of time varying air gap permeances. The second method involves making the stator winding linkage position dependent. Again, if the rotor is rotating with a constant speed the linkage becomes time dependent. Each stator slot must therefore link with each of the three phase windings. This method ensures that the linkage is in the correct position to model the appropriate transformer effect. However, a variable linkage is incapable of inducing a rotationally induced e.m.f. at the stator terminals. For this purpose an e.m.f. is induced in each stator conductor which is calculated using the flux cutting rule. This method is equivalent to the movement of the stator conductors from slot to slot around the stator in a similar manner to that applied by Turner (6) in finite element studies.

A test rig consisting of a thyristor bridge and machine was set up and run so that a direct comparison could be made between actual and simulated results. A good agreement is obtained. The effect of magnetic transformers within the machine's rotor is thought to be less than those for the simulations presented by Haydock (16) because the simulation is performed under steady state conditions.

2.5 Conclusion

The discussion presented in this chapter highlights three types of equivalent circuit which have been used to model the behaviour of the synchronous machine. Two axis equivalent circuits, flux/current equivalent circuits and flux/charge equivalent circuits.

The two axis equivalent circuit is intended to be simple so that it can be easily incorporated into power system studies. Component values or parameters are

determined from test results. Equivalent circuit models developed using the flux/current or flux/charge analogy, however, are topologically more complex and their parameters are determined physically from the machine topology and material bulk constants.

Equivalent circuits developed using the flux/current analogy are considered valid, however, the behaviour of a model's components is not consistent with the behaviour of the sections of the physical system they represent. For example, in an equivalent circuit model reluctance is typically represented by resistance and capacitance is typically used to represent linked electric circuits. Within the model, therefore, energy is being dissipated by the components representing the magnetic circuit and stored in those representing the linked electric circuits of the windings, dampers and eddy current paths. Equivalent circuits developed using the flux/charge analogy, however, maintain a link between the functionality of the equivalent circuits components and the sections of the physical system they represent.

Although Haydock (16) presents equivalent circuit models for synchronous machine using the flux/charge analogy only limited results are presented. This is thought to be due to the inability of Haydock's models to represent the magnetic transformer effect between mutually linked magnetic circuits and insufficient descritisation, particularly at the rotor surface. The author is unable to achieve similar agreement between simulation and test results using these assumptions.

The remaining work contained within this thesis is principally concerned with the development of the flux/charge analogy previously described by Carpenter C.J. (15), Haydock (16) and Carpenter M.J. (29). Magnetic equivalent circuit models developed using this technique are developed directly from the topology of the magnetic circuit or in this particular case, the magnetic circuit within a synchronous machine. The magnetic equivalent circuit is linked to electric circuits to enable the windings and damper circuits to be represented. The linked magnetic and electric equivalent circuits that represent a complete machine are then modelled simultaneously. This approach means that no test results are required for the development of the equivalent circuit because component values are entirely dependent on machine dimensions and material bulk constants.

It is appreciated that such a short appraisal of selected works can in no way do justice to the respective authors. It has been the intention of the author to only discuss the general approach adopted by previous authors in the field which have influenced the work presented in the remaining chapters of this thesis. A considerable amount of technical detail has obviously been omitted.

Chapter Three
Magnetic Circuit Representation

3.1 Introduction

The concept of an equivalent circuit may be introduced in a number of ways. An equivalent circuit may be presented as an electric circuit made up of electric devices each of which behave in an identical manner to the sections of the magnetic circuit they represent. Alternatively, an equivalent circuit may be considered as a network of magnetic devices shown diagramatically and solved as an electrical network. In practice, however, the overriding reason for developing an equivalent circuit representation is to enable the relatively straightforward solution techniques associated with electrical networks to be used with magnetic circuits. An equivalent circuit, may, therefore, be described as a representation of the magnetic circuit which may then be solved as an electrical network.

The formation of a magnetic equivalent circuit model implies the use of an equivalent circuit analogy to enable quantities within an electrical network to represent quantities within a magnetic circuit. The type and value of the equivalent circuit devices are determined physically from the topology, dimensions and material bulk constants of the magnetic circuit they represent. This approach allows each equivalent circuit device to be related to a specific section of the magnetic circuit. This feature enables the effect of different parts of the magnetic circuit on the overall behaviour of the system to be evaluated.

The work contained within this chapter investigates and develops the equivalent circuit analogy described by Carpenter C.J. (15) and adopted by Haydock (16) and Carpenter M.J. (29). This work was first presented by the present author in reference 32.

Firstly, the flux/charge analogy described by Carpenter C.J. (15) is investigated in detail and an alternative conceptual view of this analogy is presented. In particular, the relationship between the electric field, the magnetic field and electric circuit is investigated and the concept of duality is used in an attempt to evaluate analogous quantities for magnetic potential, magnetic flux, magnetic flux density and magnetic current.

Secondly, the analogy and methodology presented by Haydock (16) is developed to include a technique for representing the mutual coupling effect of an electrical circuit linking multiple flux tubes. This is equivalent to representing magnetic transformers (12) in a wholly magnetic equivalent circuit model. The technique is presented as a general technique, the use of which is not limited to synchronous machine modelling. The technique enables a theoretically limitless level of discretisation within an equivalent circuit model to be achieved. However, in reality, the complexity of the developed equivalent circuit models is limited by the simulation software.

Three types of equivalent circuit are used to help illustrate the work presented in this chapter. The types of equivalent circuit are basically the same as the types presented in chapter two. However, a further brief description is also provided here.

A magnetic equivalent circuit. This equivalent circuit is a direct representation of the magnetic circuit. Within this circuit the flow quantity is rate of change of magnetic flux and the potential quantity is magneto-motive force. Reluctance is represented as a permeance using capacitive devices in an equivalent circuit model.

An electric equivalent circuit. This is the dual or inverse (44) of the magnetic equivalent circuit. Within this circuit the flow quantity is magneto-motive force and the potential quantity is rate of change of magnetic flux. Reluctance is represented by inductive devices, the value of which is the inverse of permeance.

$$L = \frac{N^2}{S} \qquad \text{....3.1}$$

An electric circuit. This circuit is not strictly an equivalent circuit but an actual electric circuit. The flow and potential quantities are ampere turns or electric current and electro-motive force. Inductors are used to represent the reluctance paths which exist within the magnetic circuit. An electrical circuit is identical in topology to the electrical equivalent circuit representing the same magnetic circuit, however, inductor values are related to magnetic permeance by equation 3.1.

An electric circuit may be linked to a magnetic equivalent circuit using linkages (figure 3.1) to represent the link between electrical conductors and the magnetic circuit, forming a linked electric and magnetic equivalent circuit (16). The ability to link

electric and magnetic circuits together in this manner enables the derived magnetic equivalent circuit models to be readily connected to their supply circuits.

3.2 The existing magnetic equivalent circuit analogy

Magnetic variables		Electric variables
Magnetic flux	⟺	Electric charge
Magneto motive force	⟺	Electro motive force
Rate of change of magnetic flux	⟺	Electric current
Magnetic permeance	⟺	Electric capacitance

The linkage.

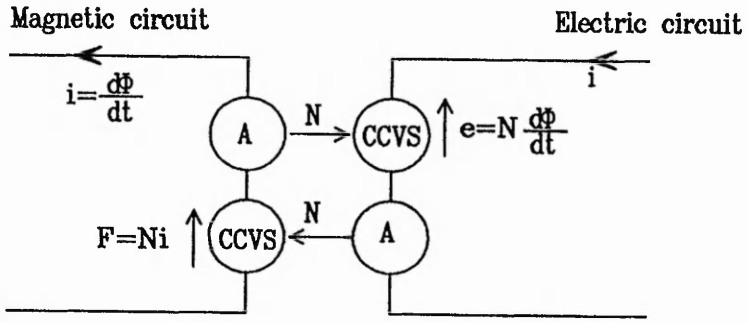

Figure 3.1 Existing equivalent circuit analogy

The development of an equivalent circuit to represent a magnetic circuit relies on an equivalent circuit analogy. An analogy relates quantities in the magnetic field to quantities within the equivalent circuit model. The equivalent circuit analogy used

throughout this thesis differs from the traditional flux/current analogy described by Laithwaite (12). The analogy has been developed by Carpenter C.J. (15) after considering the power flow in linked electric and magnetic circuits (figure 2.17). The two fundamental quantities within the magnetic field are regarded as m.m.f. and magnetic flux. In the magnetic equivalent circuit electric potential is used to represent m.m.f. and electric charge is used to represent magnetic flux.

The definitions of the potential and flow quantities leads directly to the definition of the rate of change of magnetic flux as being a magnetic current, which is analogous to electric current. Magnetic reluctances are described as permeances and represented using magnetic capacitors, the properties of which are identical to those of electrical capacitors.

The definition of these analogous quantities has led to the development of the equivalent circuit analogy described in figure 3.1. The effect of flow to potential inversion (electric current to m.m.f.) across a linkage is identical to the principle of inversion described by Cherry (44), provided the number of turns is unity.

Electric current carrying conductors linking lines of magnetic flux are linked to the magnetic equivalent circuit, forming a linked electric and magnetic equivalent circuit. This link is implemented using current controlled voltage sources (CCVS). These are used to convert the flow quantity on one side of the linkage to the potential quantity on the other. The operation of such a linkage is also presented in figure 3.1.

The traditional method of generating an equivalent circuit from the topology of a magnetic system has previously been described by a number of authors (12,15,16,29). The method relies heavily on the definition of flux tubes with magnetic terminals situated at each end. The flux tube and associated magnetic terminals have been defined (15) as a volume of space in which magnetic flux exists, the flux only being able to enter or leave the defined space via the magnetic terminals. This definition is intended to describe the flux tube in an identical manner to an electric conductor. Although the equivalent to an electric insulator for a magnetic field has yet to be discovered, the large relative permeability of iron means that the air surrounding it may be approximated to a magnetic insulator. The magnetic terminals of the flux tubes may, therefore, be connected together to form a network which is readily represented as a network of permeances. The mathematical relationship between flux and m.m.f. at the magnetic terminals of a flux tube is defined by equation 3.2. The definition of a magnetic capacitor or permeance is consistent with the definition for an electric capacitor shown here as equation 3.3.

$$C_m = \frac{\Phi}{F} = \frac{\mu_o \mu_r A}{l} \qquad \frac{Wb}{A\text{-}t} \qquad \text{....3.2}$$

$$C = \frac{Q}{V} = \frac{\xi_o \xi_r A}{l} \qquad \frac{C}{V} \qquad \text{....3.3}$$

$$R_m = \frac{N^2}{R_e} \qquad \text{ohms}^{-1} \qquad \text{....3.4}$$

The effect of a purely resistive electric circuit linking magnetic flux tubes is represented within the magnetic equivalent circuit as a single resistive device termed dampance (16). A closed electric circuit consisting of N turns and electrical resistance R_e is referred across the linkage into the magnetic circuit to form a magnetic resistance or dampance. The value of dampance is given by equation 3.4.

This value for R_m (equation 3.4) is only valid for an electric circuit which links a single flux tube. When an electric circuit is torn through multiple flux tubes there are mutual linkage terms which need also to be considered. The representation of the effect of mutual linkages forms part of the original content of this thesis and is developed later in this chapter.

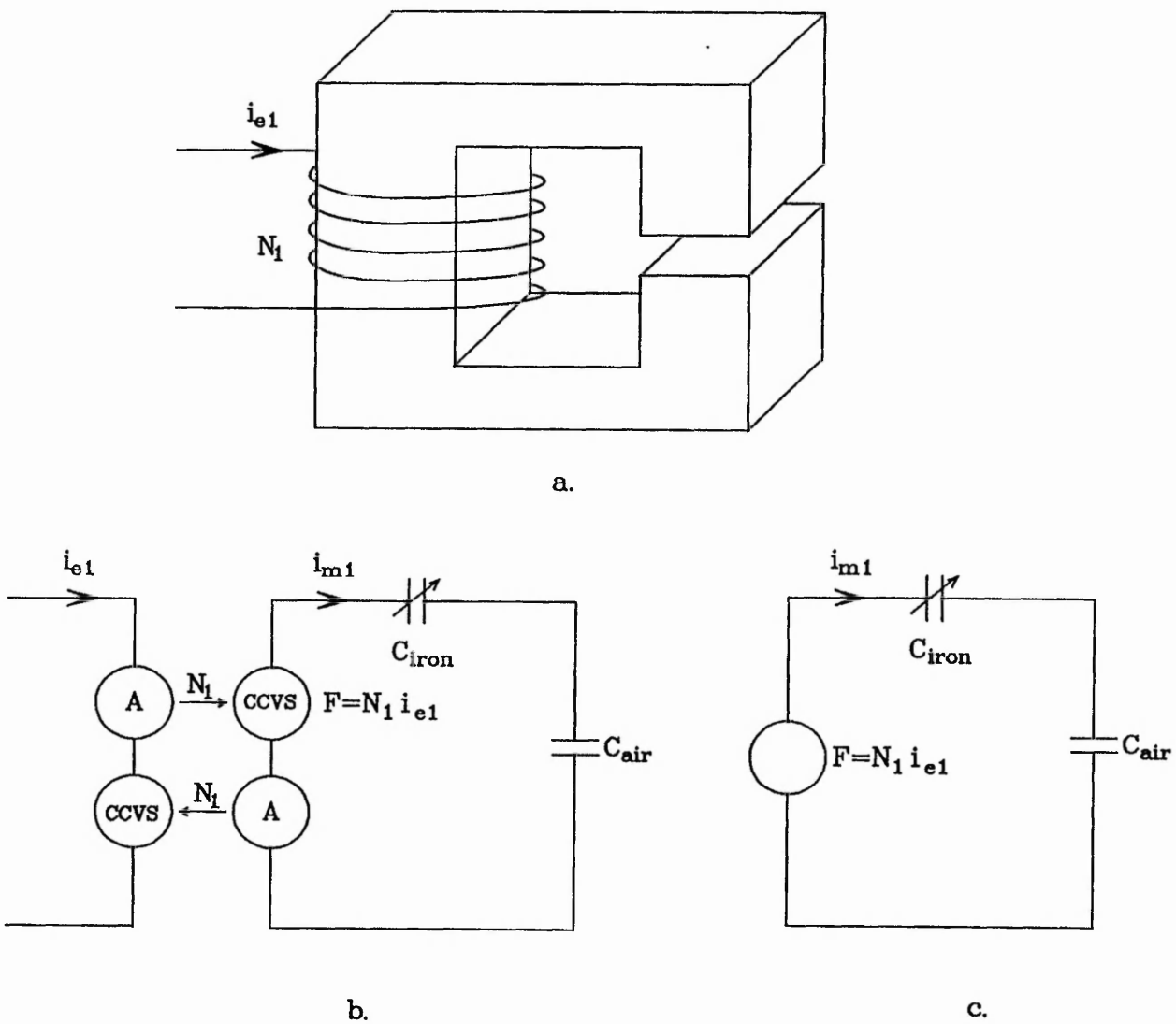

Figure 3.2 Typical C core and associated equivalent circuit

Figure 3.2 shows a typical example of a simple magnetic circuit (a), its linked electric and magnetic equivalent circuit (b) and its wholly magnetic equivalent circuit (c). The magnetic flux within the system is assumed to exist in a network of reluctances or flux tubes. The topology of the magnetic equivalent circuit is developed directly from the

topology of the circuit being modelled. The significant flux tubes are identified and connected together to form a network of permeances. In this example, the network has been lumped into two permeances representing the iron and the air. These have been represented as capacitive devices within the magnetic equivalent circuit. The value of permeance for the air gap is calculated using equation 3.2. The cross-sectional area for the air gap may be adjusted to allow for the fringing effect of the flux.

The winding has been represented as a linkage in figure 3.2b, the position of which is determined when the conductors of the winding were torn through the linked flux path in the iron to join the current's return conductor and thus reduce the number of linked turns to zero. The linked electric and magnetic equivalent circuit may be further simplified into a wholly magnetic equivalent circuit by referring the source present in the electric circuit across the linkage into the magnetic circuit and representing it as a m.m.f. source, shown here in figure 3.2c.

3.3 A detailed investigation of the flux/charge analogy

The concept of an equivalent circuit has been introduced in two ways. For the purpose of this discussion it is useful to regard the traditional magnetic equivalent circuit as consisting of a network of magnetic devices which have been defined so that they behave in an identical manner to their electrical equivalents. Consider figure 3.2, this shows a typical magnetic circuit used for demonstration purposes. The magnetic

capacitors C_{air} and C_{iron} are assumed to react to time varying magnetic voltages and currents in the same way as an electric capacitor reacts to time varying electric voltages and currents. However, voltages and currents within an electrical network are a result of the distribution and drift of charged electrons within electrical conductors. There are no such conductors in magnetic circuits. This section, therefore, attempts to reconcile this fundamental difference between magnetic and electric circuits with the concept of duality presented by Cherry (44).

The values for C_{air} and C_{iron} in figure 3.2 are determined by equation 3.2. An inspection of the calculation for the value of permeance (equation 3.2) indicates that the equivalent circuit component encompasses a rectangular volume of length l and cross-sectional area A, in which the magnetic field exists. If the complete magnetic circuit is to be represented, the magnetic terminals of the individual flux tubes will be effectively butted together. It, therefore, becomes evident that the "lengths of magnetic conductor" joining the magnetic terminals of C_{air} and C_{iron} are included in the equivalent circuit model for convenience only. They do not physically exist within the magnetic circuit. The magnetic current as defined by Carpenter C.J. (15) cannot, therefore, physically exist as a conduction current because there are no conductors within the magnetic circuit in which one could flow.

$$D = \xi E \qquad \text{....3.5}$$

$$B = \mu H \qquad \text{....3.6}$$

The equivalent circuit shown in figure 3.2c is clearly a number of rectangular shaped permeances connected together end to end or magnetic terminal to magnetic terminal.

The space in which the magnetic field exists may be regarded as being sub divided into flux tubes represented by discrete equivalent circuit devices each of which contain a magnetic field. These equivalent circuit devices are topologically identical to electrical capacitors and have indeed been termed magnetic capacitors. The arrangement is as if electric capacitors, containing an electric field, had been joined end to end with no interconnecting conductors. It is, therefore, proposed that the equivalent circuit analogy described by Carpenter C.J. (15) and used by Haydock (16) and Carpenter M.J. (29) is, in principle, an approach which makes use of the similarities in behaviour between the electric field and magnetic field. Electric potential being equivalent to magnetic potential and electric flux density being equivalent to magnetic flux density. The similarities in behaviour are illustrated by the similarities between equations 3.5 and 3.6. Hence, it is suggested that the magnetic equivalent circuit quantity representing magnetic flux is electric flux rather than electric charge as suggested by Carpenter (15).

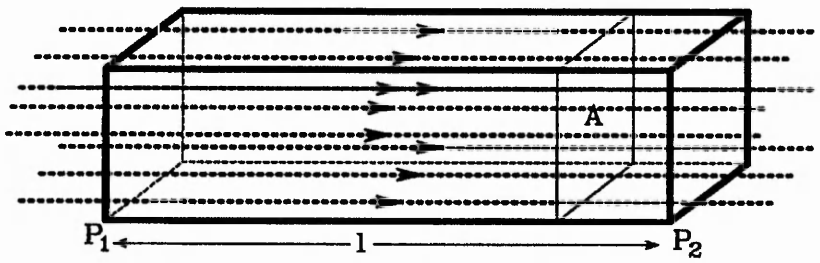

Figure 3.3 Rectangular shaped reluctance shown as a flux tube

Consider the rectangular shaped flux tube of cross-sectional area A and overall length l shown in figure 3.3. Within a magnetic equivalent circuit this flux tube or reluctance is represented as a parallel plate capacitive device. The device consists of two parallel plates P_1 and P_2 and a material of relative permeability μ_r between them. Whenever this arrangement is used to describe an electrical capacitor there exists an electric flux between the plates of the capacitor, the rate of change of which is described as a displacement current. It is, therefore, proposed that the corresponding quantity describing rate of change of magnetic flux within a magnetic permeance is a magnetic displacement current. This implies that the magnetic current present in the magnetic equivalent circuit described by Carpenter C.J. (15) would better be described as the rate of change of magnetic flux or a magnetic displacement current, shown here as equation 3.7.

$$\text{magnetic displacement current, } i_{dm} = \frac{d\Phi}{dt} \text{ volts} \qquad \ldots.3.7$$

It, therefore, follows that magnetic current density is given by equation 3.8.

$$\text{magnetic current density, } \qquad J_{dm} = \frac{dB}{dt} \quad \frac{V}{m^2} \qquad \ldots.3.8$$

The magnetic displacement current, i_{dm}, that exists within a magnetic equivalent circuit, translates to an e.m.f in windings which link with the changing magnetic flux. This can be compared to an electric system in which the displacement current within a capacitor translates to a conduction current at its electrical terminals. The magnetic displacement current in the magnetic equivalent circuit may, therefore, be described as

a displacement e.m.f., e_d, because it translates to a conduction e.m.f., e_c, in linked electrical circuits.

$$v = \frac{Q}{C} \text{ volts} \qquad \text{....3.9}$$

$$i = \frac{dQ}{dt} \text{ amps} \qquad \text{....3.10}$$

The principle of duality described by Cherry (44) is associated with the inversion of electrical networks. When an electrical network is inverted the potential and flow quantities are interchanged, capacitive and inductive devices are interchanged and current loops are interchanged with potential nodes. This phenomenon can be thought of in terms of the relationship between the electric and magnetic fields and charged electrons within electrical conductors. The fundamental quantity responsible for voltages and currents within an electric circuit is the charged electron. Consider equations 3.9 and 3.10. Within an electric circuit it is obvious that the instantaneous voltage across a capacitor is proportional to charge and that the instantaneous electric current is proportional to rate of change of charge. Given that the charge of an electron is constant, voltage is, therefore, dependant on the distribution of electrons and current their drift velocity.

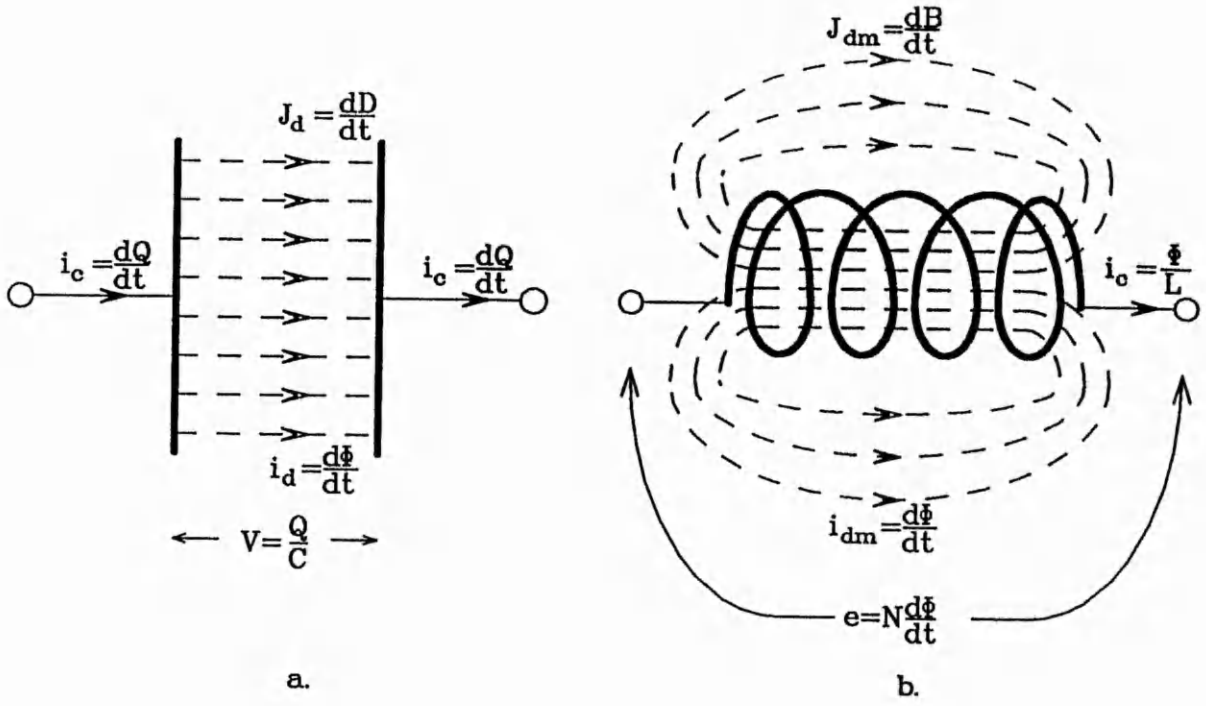

Figure 3.4 The duality between electric and magnetic fields

Consider the terminal quantities of a capacitor. The potential difference between its terminals' is the sum of the applied potential difference and the potential difference induced by the electro static forces on charged electrons. Electrons are repelled from the negatively charged plate and attracted to the positively charged plate by the electric field that exists between them. The mechanism for the opposition to change to terminal potential difference, therefore, exists because the magnitude of the electric field, and the resulting electro static forces, within the capacitor are dependant on the its terminal potential difference. Clearly, as electrons are physically prevented from crossing between plates an electric current can only exist when there is a time-varying potential difference between them.

Now consider the terminal quantities of an inductor. The potential difference between its terminals is the sum of the applied potential difference and the potential or e.m.f. induced by the force on charged electrons exerted by the changing magnetic field within the coil. This force is the same force as that exerted on electrons when an electrical conductor is physically moved through a magnetic field cutting lines of flux. However, the magnetic field responsible for exerting this force is a result of electric current or the movement of charge within the conductor. This is different from the electric field which is dependant solely on the distribution of charge. The mechanism for the opposition to change of electric current in the winding of the inductor, therefore, exists because the magnetic field within the inductor is dependant on the electric current in its winding. Clearly, therefore, if the magnitude of the electric current in an inductor's winding is constant then no force due to a changing magnetic flux is exerted on the drifting electrons.

It has been demonstrated that to further the concept of duality proposed by Cherry (44) it is necessary to define additional quantities termed displacement e.m.f., e_d, and conduction e.m.f, e_c. The displacement e.m.f. has been defined as the rate of change of magnetic flux and the conduction e.m.f. as the energy gained by electrons due the force exerted on them by a time varying magnetic field. These are the dual of the displacement and conduction currents that exist at the terminals of a capacitor.

	Electric quantity	Magnetic or dual quantity
Flux	Electric Flux (Φ)	Magnetic Flux (Φ)
Flux density	B	D
Field potential	H	E
Rate of change of flux density	Displacement current	Displacement e.m.f.
Electric circuit variables	Conduction current	Conduction e.m.f. or potential difference

Figure 3.5 The duality between electric and magnetic circuits

Figure 3.5 shows a developed interpretation of the equivalent circuit analogy described by Carpenter C.J. (15). The similarities between the behaviour of the electric and magnetic field in space are obvious. However, in addition to this it is the mutual relationship between the respective field quantities and electric circuit quantities which is responsible for the duality phenomenon described by Cherry (44). In essence, electric charge generates an electric field, the rate of change of which induces an electric current. However, within a magnetic system the rate of change of charge or electric current generates a magnetic field the rate of change of which will induce an e.m.f.

3.4 The development of mutual dampance and the dampance matrix.

The development of an equivalent circuit for a magnetic system is by no means a new idea. The first equivalent circuits were developed at the beginning of this century (10) using the traditional flux/current analogy. It is believed that this analogy was originally used because the early magnetic equivalent circuits were developed directly from the

mathematical relationship between flux and m.m.f. In more recent times Carpenter C.J. (15) has described an analogy using electric current to represent rate of change of magnetic flux. This analogy has since been applied by Haydock (16) and Carpenter M.J. (29) to the modelling of synchronous machines with results presented by both authors.

However, the detailed examination of the equivalent circuits developed by Haydock and Carpenter M.J. (figures 2.20 and 2.21) performed in chapter two of this thesis reveals that a fundamental assumption is made. It is assumed that the effect of electrical circuits which mutually link multiple flux tubes can be ignored. In principle, this is equivalent to ignoring the effect a changing flux in one flux tube has on flux tubes linked by common electrical circuits.

The work contained within this section is intended to develop C.J. Carpenter's (15) equivalent circuit representation for magnetic circuits so that the effect of linked electrical circuits can be represented completely. The resulting representation is presented in a matrix form and thus termed the dampance matrix.

Further, an investigation is performed to quantify mutual linking components within the dampance matrix in terms of their overall damping effect on the magnetic circuit.

The dual of the multiple flux linkage equivalent circuit is also obtained from first principles. This is intended to enable the representation of multiple flux linkages or magnetic transformers in a wholly electric equivalent circuit form. The resulting

electric equivalent circuit uses voltage controlled current sources (VCCS) to represent the mutual damping effect of the linking winding. The absence of such mutual linkage components from the electric equivalent circuits presented by Slemon (11,30) implies that the assumption concerning the mutual coupling effect of an electric circuit used by Haydock (16) is also been made.

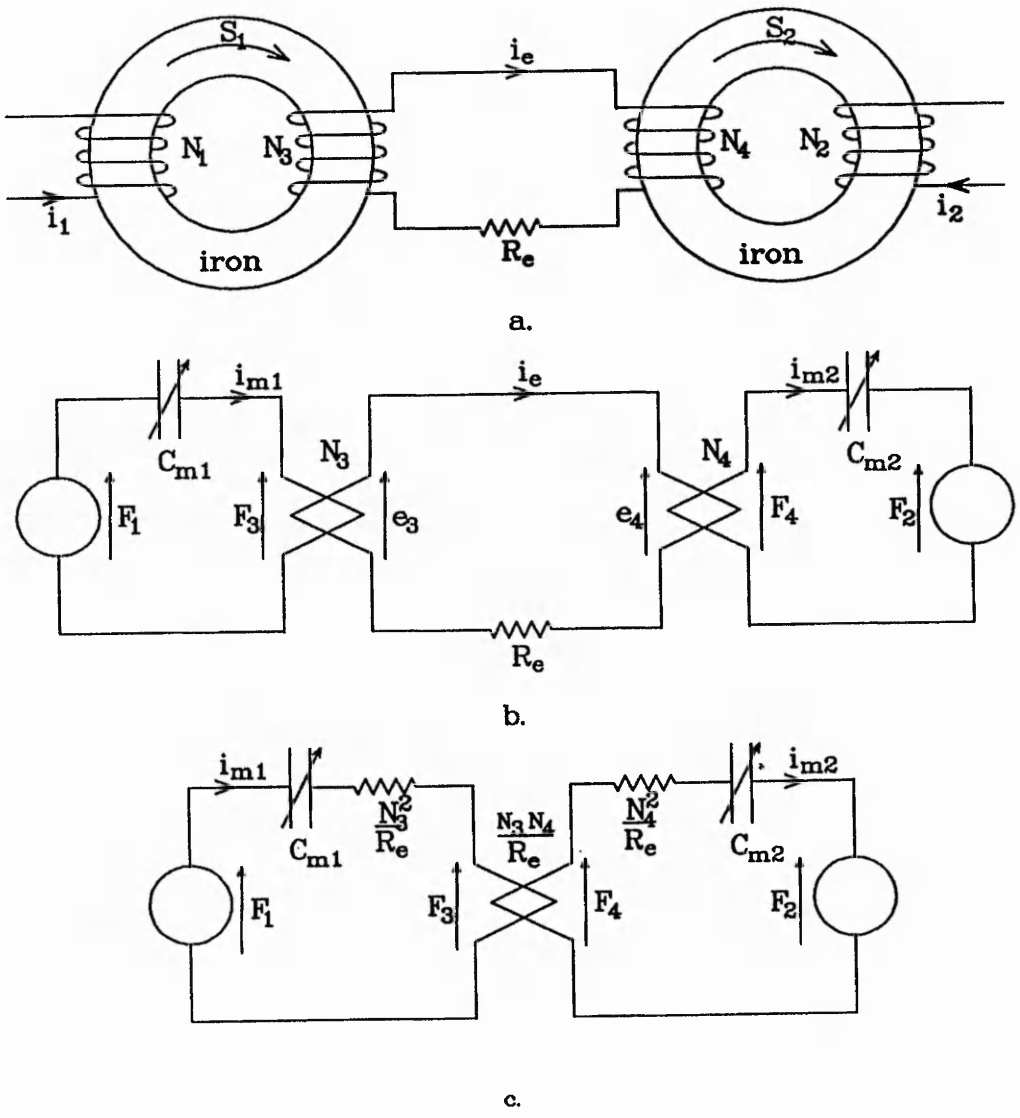

Figure 3.6 Magnetic equivalent circuit for Laithwaite's "magnetic transformer"

Laithwaite (12) describes a 'magnetic transformer' (figure 2.11) as consisting of two self transferences and a mutual transference. This arrangement is repeated here in figure 3.6a to enable a wholly magnetic equivalent circuit to be derived using the flux/charge analogy. The linked electric and magnetic equivalent circuit (figure 3.6b) is generated by representing magnetic reluctance as magnetic capacitors C_{m1} and C_{m2}, tearing the electrical conductors towards the centre creating linkages N_3 and N_4 and referring the linkages N_1 and N_2 into the magnetic circuit as m.m.f. sources F_1 and F_2.

The linked electric and magnetic equivalent circuit shown in figure 3.6b is translated into a wholly magnetic equivalent circuit by developing the mathematical relationship between the magnetic circuit flow and potential quantities. Consider the m.m.f. F_3 induced in left hand magnetic circuit by the linking electric circuit of resistance R_e and carrying a current i_e. The induced m.m.f. is given by equation 3.11.

$$F_3 = N_3 i_e \qquad \text{....3.11}$$

however

$$i_e = \frac{e_3 + e_4}{R_e} \qquad \text{....3.12}$$

therefore

$$F_3 = \frac{N_3 e_3 + N_3 e_4}{R_e} \qquad \text{....3.13}$$

however

$$e_3 = N_3 i_{m3} \qquad \text{....3.14}$$

and

$$e_4 = N_4 i_{m4} \qquad \text{....3.15}$$

therefore

$$F_3 = \frac{N_3^2 i_{m3}}{R_e} + \frac{N_3 N_4 i_{m4}}{R_e} \qquad \text{....3.16}$$

similarly

$$F_4 = \frac{N_3 N_4 i_{m3}}{R_c} + \frac{N_4^2 i_{m4}}{R_c} \qquad \text{....3.17}$$

The linking electric circuit can, therefore, be referred into the appropriate magnetic circuits, generating the wholly magnetic equivalent circuit representation presented in figure 3.6c. Further equations 3.16 and 3.17 may be rewritten as the matrix equation 3.18. This matrix equation contains a two by two matrix term which defines the damping effect of the linked electric circuit on all linked magnetic circuits. This matrix has, therefore, been termed the dampance matrix by the author.

$$\begin{bmatrix} F_3 \\ F_4 \end{bmatrix} = \begin{bmatrix} N_3^2/R & N_3N_4/R \\ N_4N_3/R & N_4^2/R \end{bmatrix} \begin{bmatrix} i_{m3} \\ i_{m4} \end{bmatrix} \qquad \text{....3.18}$$

$$\begin{bmatrix} e_1 \\ e_2 \end{bmatrix} = \begin{bmatrix} L_1 & M_{12} \\ M_{21} & L_2 \end{bmatrix} \begin{bmatrix} di_1/dt \\ di_2/dt \end{bmatrix} \qquad \text{....3.19}$$

The terms in equation 3.18 containing N_3^2 and N_4^2 can clearly be thought of as self dampance terms. They are equivalent to the dampance expressions used by Haydock (16) and Carpenter M.J. (29) in their wholly magnetic equivalent circuit models. The terms containing N_3N_4 and N_4N_3, however, are mutual dampance terms and represent the coupling of magnetic circuits by linking electric circuits. These mutual terms are similar to the mutual inductance terms M_{12} and M_{21} in equation 3.19 which represent the coupling of electric circuits by a linking magnetic circuit. However, the self and mutual terms in equations 3.18 are purely resistive whereas in equation 3.19 are inductive.

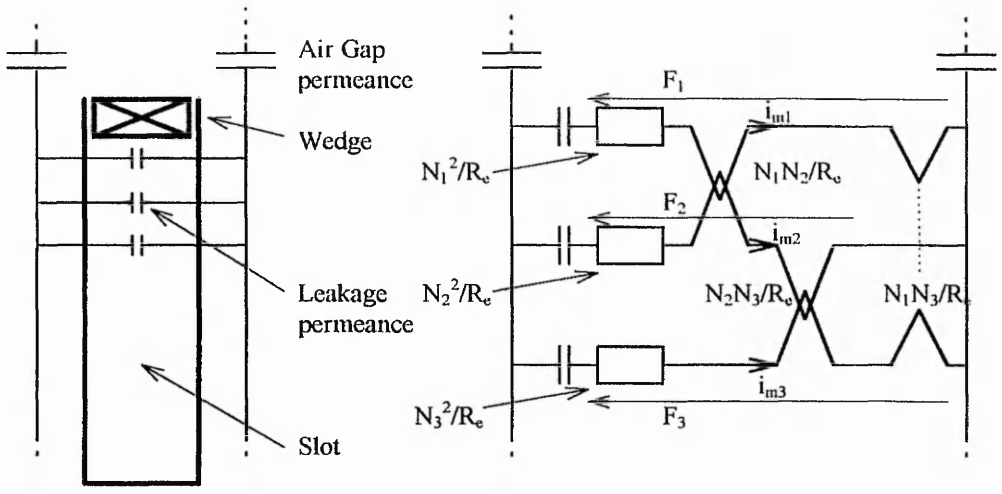

a. b.

Figure 3.7 The development of a wholly magnetic equivalent circuit for a single slot pitch of a synchronous machine.

Consider figure 3.7a, the diagram shows a magnetic circuit super-imposed on a simplified slot pitch of a synchronous machine. Leakage flux is assumed to be perpendicular to the slot walls which is typical within a synchronous machines under transient conditions. A single linked electric circuit is assumed to be made up from the slot wedge, a wedge on the diametrical opposite side of the rotor and the end bells. In chapter four this representation is extended to represent multiple slot pitches and all linking electric circuits and eddy current paths. Clearly, the effect of the resistance in the electric circuit will be to damp transients in the magnetic circuit.

Figure 3.7b shows the wholly magnetic equivalent circuit model for the system shown in figure 3.7a. The linkage terms N_1N_2/R_e, N_2N_3/R_e and N_1N_3/R_e represent the mutual damping effect of the wedge circuit. The terms include N_1, N_2 and N_3 to indicate that the electrical circuit may link individual magnetic circuits with differing number of turns. However in this example N_1, N_2 and N_3 are unity.

For the purposes of the dampance matrix derivation the configuration is considered as a magnetic transformer with three linked magnetic circuits. It is, therefore, possible to develop equations 3.16 and 3.17 so as to represent a three limb magnetic transformer.

$$F_1 = \frac{N_1^2 i_{m1}}{R_e} + \frac{N_1 N_2 i_{m2}}{R_e} + \frac{N_1 N_3 i_{m3}}{R_e} \quad \text{....3.20}$$

$$F_2 = \frac{N_2 N_1 i_{m1}}{R_e} + \frac{N_2^2 i_{m2}}{R_e} + \frac{N_2 N_3 i_{m3}}{R_e} \quad \text{....3.21}$$

$$F_3 = \frac{N_3 N_1 i_{m1}}{R_e} + \frac{N_3 N_2 i_{m2}}{R_e} + \frac{N_3^2 i_{m3}}{R_e} \quad \text{....3.22}$$

Consider equations 3.20, 3.21 and 3.22. These equations represent the m.m.f. induced in each of the leakage flux paths shown in figure 3.7 by the mutually linking electric circuit. They are derived by inspection from equations 3.16 and 3.17 describing a two winding magnetic transformer. Clearly, in this example the terms N_1, N_2 and N_3 are unity, however, they are maintained explicitly because they are required in the derivation of the dampance matrix to represent the mutli-turn field winding. Rewriting 3.20, 3.21 and 3.22 in a matrix form gives equation 3.23. This contains the three by three dampance matrix for the configuration presented in figure 3.7a.

$$\begin{bmatrix} F_1 \\ F_2 \\ F_3 \end{bmatrix} = \begin{bmatrix} N_1^2/R_e & N_1 N_2/R_e & N_1 N_3/R_e \\ N_2 N_1/R_e & N_2^2/R_e & N_2 N_3/R_e \\ N_3 N_1/R_e & N_3 N_2/R_e & N_3^2/R_e \end{bmatrix} \begin{bmatrix} i_{m1} \\ i_{m2} \\ i_{m3} \end{bmatrix} \quad \text{....3.23}$$

The derived dampance matrix in equation 3.23 is a three by three matrix made up of a clearly visible pattern of expressions containing N_x and R_e. Using this matrix as a template, therefore, it is possible to derive the dampance matrix for any number of

magnetic circuits linked by a common electric circuit. Indeed, this template is used throughout this thesis in the derivation of dampance matrices to represent the complex damping circuits within the synchronous machine.

3.5 An investigation of the mutual dampance components.

It has been clearly demonstrated both here and elsewhere (16) that the effect of a closed electric circuit linking magnetic flux tubes is to damp the rate of change of that flux. Within a straightforward example in which an electric circuit links a single magnetic flux tube the damping effect may easily be determined from equation 3.4. However, if the electric circuit links a number of flux tubes the mutual dampance components must also be considered. The work presented in this section is intended to quantify the proportion of magnetic circuit damping which occurs as a result of the mutual dampance terms in the dampance matrix.

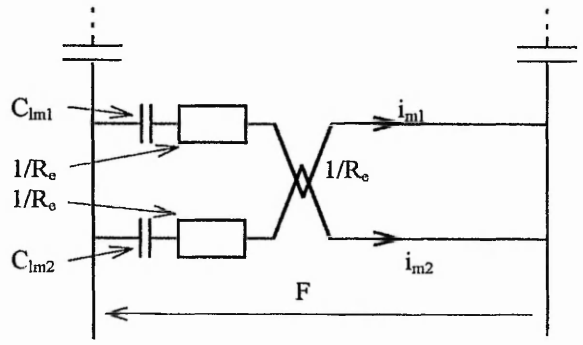

Figure 3.8 The wholly magnetic equivalent circuit for a simplified representation of a single slot pitch of a synchronous machine.

Consider the wholly magnetic equivalent circuit model of a simplified slot pitch presented in figure 3.8. This is derived from a configuration similar to that presented

in figure 3.7 with the exception that only two leakage flux paths are used to join the main flux in the rotor teeth and the number of linked turns is assumed to be unity. Equation 3.24 shows the dampance matrix, R_{dm}, for the electrical circuit, of resistance R_e, made up from the wedges and end bells.

$$R_{dm} = \begin{bmatrix} 1/R_e & 1/R_e \\ 1/R_e & 1/R_e \end{bmatrix} \qquad \text{....3.24}$$

The overall magnetic impedance of the two leakage flux tubes in parallel carrying sinusoidal magnetic currents i_{m1} and i_{m2} is given by equation 3.25. This is obtained by inspection assuming the two flux tubes have been represented as a single lumped leakage path within the model.

$$\frac{F}{i_{m1} + i_{m2}} = R_m + jX_m \qquad \text{.... 3.25}$$

where

$$R_m = \frac{1}{R_e} \qquad \text{.... 3.26}$$

and

$$X_m = \frac{1}{\omega(C_{lm1} + C_{lm2})} \qquad \text{.... 3.27}$$

By considering the equivalent circuit configuration shown in figure 3.8 and assuming $C_{lm1} = C_{lm2}$ it can be shown that the overall magnetic impedance of the two branches is given by equation 3.33.

$$F = (R_m + j2X_m).i_{m1} + R_m i_{m2} \qquad \text{.... 3.28}$$

$$F = R_m i_{m1} + (R_m + j2X_m).i_{m2} \qquad \text{.... 3.29}$$

$$i_{m1} = \frac{F - R_m i_{m2}}{(R_m + j2X_m)} \qquad \text{.... 3.30}$$

$$i_{m2} = \frac{F - R_m i_{m1}}{(R_m + j2X_m)} \quad \text{.... 3.31}$$

$$i_{m1} + i_{m2} = \frac{2F - R_m(i_{m1} + i_{m2})}{(R_m + j2X_m)} \quad \text{.... 3.32}$$

$$\frac{F}{i_{m1} + i_{m2}} = \frac{2R_m + j2X_m}{2} \quad \text{.... 3.33}$$

Equation 3.33 is identical to equation 3.25 thus validating the configuration used in figure 3.8 and in particular the application of the dampance matrix. To demonstrate the effect of the mutual terms within the dampance matrix it is possible to repeat a similar mathematical procedure to obtain an expression for the combined damping effect with the mutual terms omitted. This is given by equation 3.34.

$$\frac{F}{i_{m1} + i_{m2}} = \frac{R_m + j2X_m}{2} \quad \text{.... 3.34}$$

The arithmetic difference between equations 3.34 and 3.33 is equivalent to $R_m/2$ or 50% of the total damping resistance. The effect of this greatly reduced damping resistance is clearly demonstrated in chapter six of this thesis. Figure 6.5 shows a comparison between results obtained from a D axis flux decay test simulation with and without the effects of mutual dampance associated with the field winding. The stator voltage envelope for the D axis flux decay test simulation with the mutual dampance terms omitted, clearly decays more rapidly than the curve for the same quantity with the mutual dampance terms included. This provides a clear demonstration of the reduced damping effect of the field winding that is directly attributable to the omission of the mutual dampance terms equivalent to the mutual terms in equation 3.28 and

3.29. This clearly challenges the implied assumption made by Haydock (16) and Carpenter (29) that the mutual dampance terms associated with linking electrical circuits can be ignored.

3.6 The electric equivalent circuit representation for the dampance matrix

The transformation of an electrical network into its dual or inverse as described by Cherry (44) involves an interchanging of the potential and flow quantities. To enable a flow to be transformed into a potential, meshes must be transformed into nodes and vice versa. Capacitive devices must be interchanged with inductive devices because of the differing effects changing electric and magnetic fields have on an electric conductor.

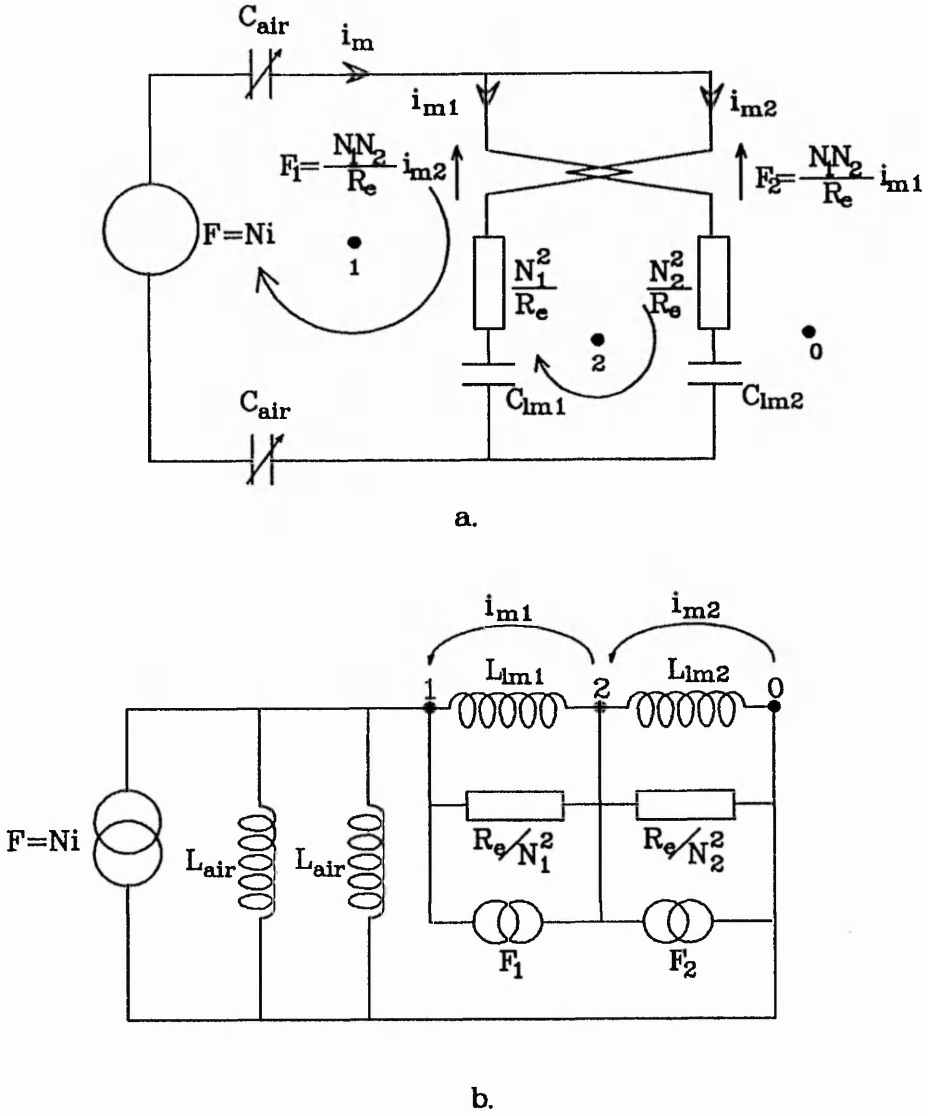

Figure 3.9 Dual of mutual linkage representation

Figure 3.9a is a wholly magnetic equivalent circuit representing a simplified slot pitch within a synchronous machine. This is derived from a configuration similar to that presented in figure 3.7 with the exception that only two leakage flux paths are used to join the main flux in the rotor teeth.

The transformation of this wholly magnetic equivalent circuit into the wholly electric equivalent circuit shown in figure 3.9b is performed in three stages.

Firstly, the inverse of each of the network devices is obtained. In this example the potential source F is transformed into a current source with the same numerical value. The capacitive devices C_{air1}, C_{air2}, C_{lm1} and C_{lm2} are transformed into inductive devices L_{air1}, L_{air2}, L_{lm1}, and L_{lm2}, again with the same numerical values. The resistive devices remain as resistive components the values of which are reciprocated by the transformation.

Secondly, the topology of the network is transformed using the principles described in figure 2.9. In this example meshes 1 and 2 in figure 3.9a become nodes 1 and 2 in figure 3.9b, and branches in 3.9a with devices in series are transformed into branches with transformed devices in parallel.

Finally, the mutual dampance linkage must be transformed. This is perhaps best achieved by considering the effect the mutual dampance linkage has on the potential and flow quantities within the network. The effect of the linkage is to induce a potential quantity into one branch dependent on the flow quantity in the linked branch. The form of the inverted linkage may therefore be assumed to be a current source the value of which is dependent on a potential elsewhere in the network. Consider the second limb. The potential F_2 is proportional to the flow in limb 1, i_{m1}. The potential F_2 is in series with the other components in the same branch so the potential source F_2

will be transformed into a current source in parallel with the components L_{lm2} and R_e/N_2^2. The quantity i_{m1} can be transformed into a potential quantity which exists between nodes 2 and 1 because the flow quantity i_{m1} exists as the difference between currents in meshes 2 and 1. A similar argument exists for the potential source F_1 being a current source in parallel with R_e/N_1^2 and L_{lm1} and depending on the potential between nodes 2 and 0.

3.7 Conclusion

The work contained within this chapter is intended to develop the subject of magnetic circuit modelling in two main areas. These are the basic conceptual ideas on which the flux/charge analogy is based and the application of these ideas to develop wholly magnetic equivalent circuit models for complex magnetic circuits. It is acknowledged that some work has already been done in this area. However, it is felt by the present author that previous work (16, 29) has been significantly limited by the absence of a magnetic representation for what has been termed mutual dampance. Indeed, this work directly challenges the validity of the equivalent circuit models presented by Haydock (16) and Carpenter (29) in which mutual dampance terms have been ignored.

The analysis of the flux/charge analogy has lead to the development of dual quantities for displacement and conduction currents. These have been presented as displacement and conduction potentials and represent the effect a time varying magnetic field has on linked electrical conductors. Further, it is also suggested that the flux/charge analogy presented by Carpenter C.J. (15) could be better described as the magnetic/electric flux

analogy because it is demonstrated that an electric field is effectively being used to represent a magnetic field.

Perhaps the most significant work presented in this chapter relates to the development of mutual dampance and the dampance matrix. The technique enables linked magnetic circuits to be correctly represented in wholly magnetic equivalent circuit models. The development and application of mutual dampance and the dampance matrix forms part of the original work presented in this thesis. The equivalent circuit models developed in later chapters of this thesis rely heavily on the dampance matrix to represent field, damper and eddy current circuits within the rotor of synchronous machines under transient test conditions.

Finally, the dual or inverse of the mutual dampance equivalent circuit representation is obtained.

Chapter Four
Equivalent circuits for the synchronous machine

4.1 Introduction

The development of modelling techniques to represent the complex magnetic circuits within a synchronous machine has been driven by the on going development of the machine itself described in chapter one. Three areas of research have been identified in this thesis.

The work presented by Canay (25) and Shackshaft (23,26) and described in chapter two is directed towards developing the traditional two axis models so as to provide improved equivalent circuit models for use in power system studies.

Developments within the area of finite element methods (6,28) are intended to provide improved models for use by machine designers. Finite element models are particularly suited to this application because they can provide a detailed insight into the behaviour of magnetic flux within a machine design. However, the large and cumbersome nature of these models means that they are unsuitable for applications requiring connection to, and simulation with, an electrical supply network.

The third area is that of an equivalent circuit model derived directly from the topology of a magnetic circuit and is the approach adopted throughout this thesis. The aim of the work presented in this chapter is to develop an equivalent circuit model topology to represent a general synchronous machine for a wide range of operating conditions. The developed equivalent circuit topology is intended to be of use to engineers

requiring machine models for simultaneous simulation with power electronic supply circuits. It may also be feasible for machine designers to use these techniques to assess machine designs more rapidly than the more complex finite element techniques.

A general purpose equivalent circuit model topology is developed directly from the physical topology of a half pole pitch of a typical two pole round rotor machine, the cross-section of which is shown in figure 4.1. A particular advantage of using this approach is the ease with which the relationship between the equivalent circuit topology and devices, and the magnetic circuit can be maintained. The topological framework is initially developed from the results obtained from a steady state finite element study. Although the finite element study has proved useful for obtaining the main flux distribution it is of limited use for identifying the leakage flux paths. A number of authors including Babb and Williams (38) and Levy et al (49) describe a method for representing a single slot as a magnetic equivalent circuit. This approach has been adapted, improved and superimposed on the main flux distribution identified from the results of the finite element study using the original methods described in chapter three of this thesis. The basic topological framework for this general purpose magnetic equivalent circuit model developed in this chapter is believed to be original.

Although the broad aim of the work in this chapter is to develop a general purpose magnetic equivalent circuit topology for a synchronous machine, for the purposes of this thesis it is intended to concentrate on representing a machine for three well known generator tests. These are the flux decay or stator decrement test, the frequency response test and the sudden short circuit test. The developed equivalent circuit

models are to be used to simulate tests on three typical round rotor synchronous machines, the 500MW machine at Eggborough, the 150MW machine at Uskmouth, and the 660MW machine at Torness. These three machines although of similar overall design differ in size and rotor cross-sectional detail, thus providing a basis for the initial trials of this general purpose model. The transient simulations using the magnetic equivalent circuit developed in this chapter are described in chapter five and the results from these simulations are presented and discussed in chapter six of this thesis.

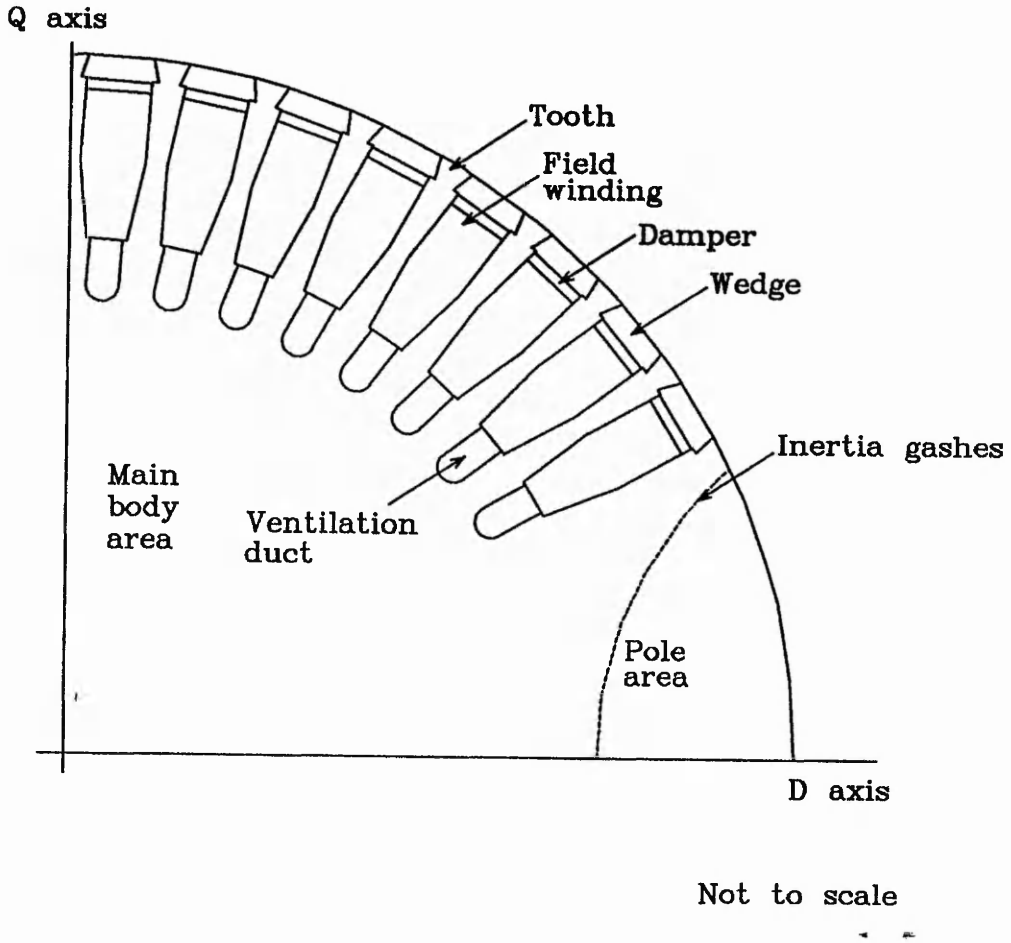

Figure 4.1 A typical half pole pitch of a synchronous machine

4.2 The application of the finite element study

A steady state finite element study is performed for the D axis of the Eggborough machine, this is a 500MW machine and is typical of the large two pole synchronous machines in use today. A further advantage of using this machine is that a considerable amount of design data, modelling information (6,16) and test results (50) are available.

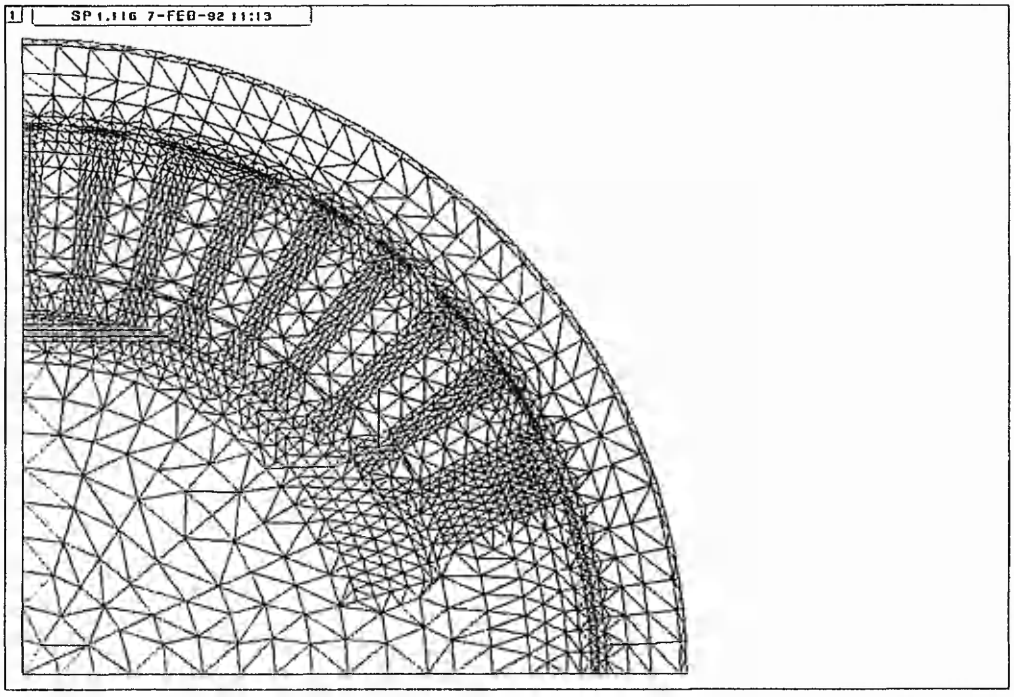

Figure 4.2 The finite element mesh representing a half pole pitch for the Eggborough machine

The steady state finite element study briefly described here uses a similar approach to the work described by Turner (6,51), using the same integrated finite element

computer software (28) running on an Apollo Domain 3500 workstation. The finite element mesh used to describe a half pole pitch consists of 3422 elements and 1776 nodes, and is shown in figure 4.2. This finite element mesh is also used in a transient finite element study described in chapter five of this thesis. The exciting operation of the stator windings is represented using a sinusoidally distributed current sheet situated on the outer periphery of the air gap. This approximation eliminates the need to represent the stator and the conductors contained within explicitly, and is validated by the results described here and in chapter six of this thesis.

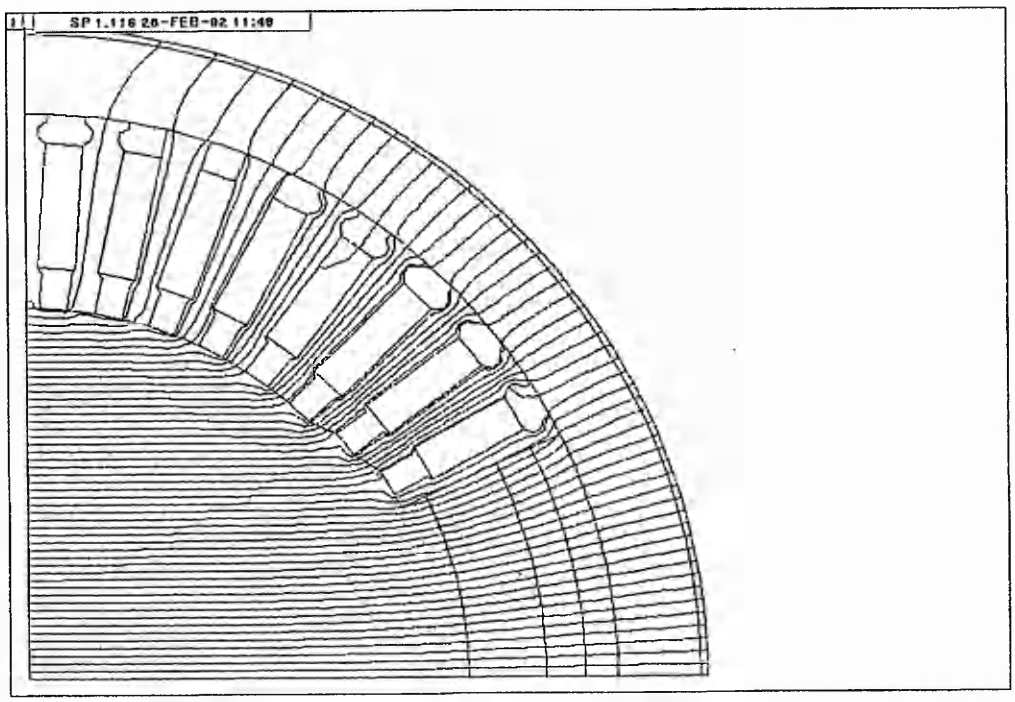

Figure 4.3 Results from a steady state finite element study showing lines of equal magnetic vector potential or flux

The results obtained from the steady state finite element study are presented in figure 4.3. The main flux distribution can be clearly identified from figure 4.3 and it is, therefore, relatively straightforward to determine a suitable topology for a magnetic equivalent circuit to represent this distribution. However, it is not as straightforward to identify the leakage flux distribution from a steady state finite element study. This is because the amount of leakage flux is relatively small during steady state conditions. However, the behaviour of leakage flux during transient conditions has a significant effect on the behaviour of the machine. To enable transient studies to be performed the work of Babb and Williams (38) and Levy et al (49) has been adopted and adapted as a method for representing the tooth to tooth leakage flux within a machine's rotor.

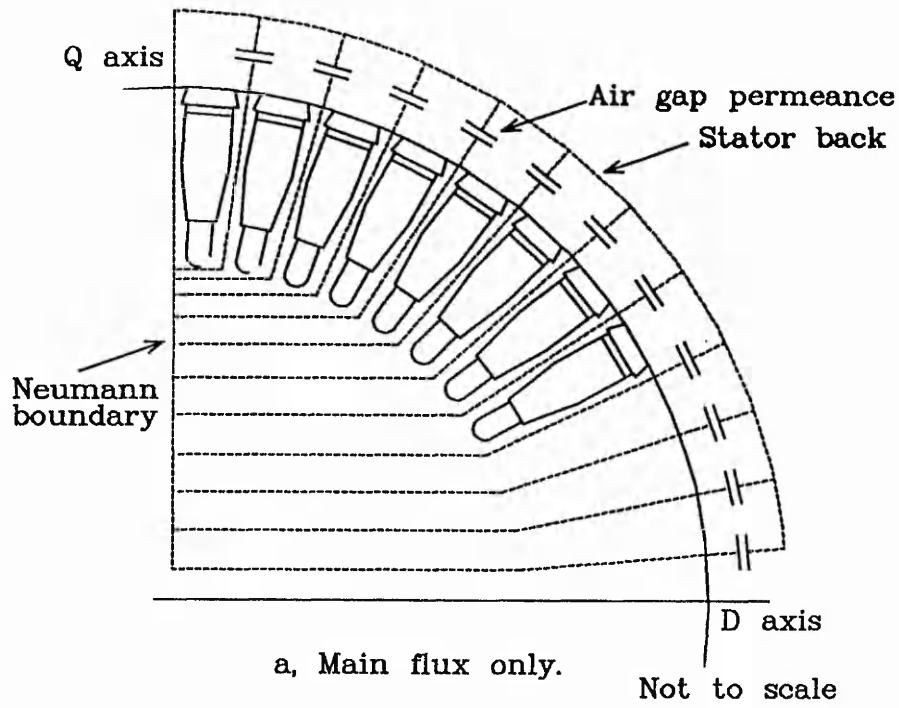

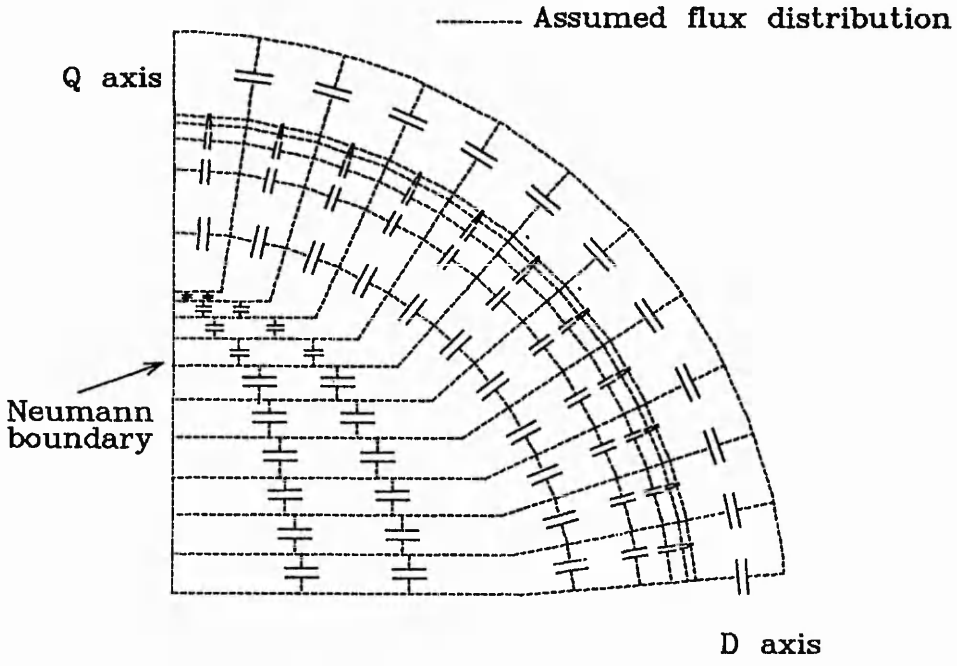

Figure 4.4 Equivalent circuit topology to represent (a), the main flux, and (b), the main and leakage flux within a typical rotor cross-section

4.3 The development of the topological framework

4.3.1 The representation of the main flux distribution

The results obtained from the finite element study, described previously, forms the basis for the topology of the permeances which support the main flux. An arrangement for a half pole pitch of a typical machine using a pitch of a single slot is shown here in figure 4.4a. This is very similar to the arrangement used by Haydock (16,48) to support the main air gap and rotor flux shown here in figure 2.20. The framework consists of four component parts, the stator, air gap, rotor and Neumann boundary. Previous work (6,16,29) has demonstrated that a good approximation for the behaviour of a machine during a flux decay test may be determined by considering the magnetic circuit within the air gap and rotor only. The Neumann boundary and stator are, therefore, represented as magnetic short circuits.

$$\text{Permeance} = \frac{\mu_o \mu_r A}{l} \quad \frac{\text{Wb}}{\text{A-t}} \qquad \ldots.4.1$$

The permeances or flux tubes which are to support the main flux within the rotor and air gap have initially been defined at intervals of a single slot pitch for flux decay and frequency response test simulations. Each flux tube has been defined to represent a single slot pitch and magnetically links the stator and Neumann boundary. The value of permeance for each slot pitch is determined from the modified dimensions of the air gap using equation 4.1. The modified value for air gap length is determined using Carter's coefficient, and allows for stator and rotor slotting. The length of the machine or air gap width is modified to allow for the effects of fringing. It is therefore assumed that the m.m.f. within each slot pitch is carried by the air gap permeance. A magnetic

conductor links the air gap magnetic terminal and the Neumann boundary. This assumption is justified by the relatively large permeability of the iron rotor.

To represent the effect of the stator and Neumann boundary the extended terminals of the air gap permeances are connected together. This represents the relatively high permeability of the stator iron and the magnetic short circuit of the Neumann boundary. To complete the representation of the main magnetic circuit the Neumann boundary is connected to the stator back, either on the D axis or the Q axis. Figure 4.4a shows the main permeance paths suitable to represent a steady state D axis flux superimposed on a typical rotor cross-section.

4.3.2 Representation of the leakage flux

A number of authors including Babb and Williams (38), Levy et al (49) and Carpenter M.J. (29), have represented leakage flux within an equivalent circuit model by introducing layers of leakage permeance into the slotted and pole regions. These layers effectively join adjacent defined main flux paths and, therefore, represent the permeance of material between them.

A characteristic of finite element meshes is that the size of the elements can be varied to enable a more detailed representation of regions with high flux density gradients. Within finite element studies of synchronous machines (6) the elements close to the rotor surface are typically made very much smaller than those closer to the rotor's centre. Transient conditions are, therefore, more accurately modelled because skin

effect, associated with the magnetic field, is better represented by this increased descritisation.

Carpenter M.J. (29) was able to increase equivalent circuit descritisation at the rotor surface using layers of leakage permeances at increasing depths to represent a rotor's pole region. The depth of the leakage permeance representing the outer most layer is half that of the next layer. This depth is half that of the next and so on. However, within M.J Carpenter's model the magnetic transformer effect between defined permeance layers mutually linked by eddy current paths is ignored. This assumption is more fully discussed in chapters two and three of this thesis.

The equivalent circuit framework developed in this chapter incorporates the concept of permeance layers used by Carpenter M.J. (29) to represent leakage flux. Increased descritisation at the rotor surface can, therefore, be achieved. The technique superimposes tooth to tooth and pole leakage permeance onto the defined main flux paths shown in figure 4.4a. The calculation to determine the value of each slot leakage permeance is based on equation 4.1 and is fully described in appendix two. The developed framework, shown here in figure 4.4b, is made up of a number of adjacent ladder networks each representing a single slot pitch or pole region segment. Using this approach the framework will be able to represent a rapidly changing flux at the surface without using a prohibitively large number of leakage permeance branches.

The concept of layering the leakage permeance paths is also applied in the main body of the rotor using two additional equally spaced permeances joining adjacent main flux

paths. Although these are shown diagramatically in figure 4.6 as being non linear the values of permeance used for these devices is frozen at pre test values. These were found to be necessary to correctly represent the longer time constants of the flux decay test and the low frequency response for the machine. Turner (6) has shown that, for a finite element flux decay test simulation, when the permeability of the solid iron rotor is "frozen" at its initial value the resulting parameters determined from the test results are in close agreement with the parameters determined from a simulation using non linear permeability. It is suggested that this is due to the effect of the residual circulating flux within the iron rotor as the flux decays (6).

The final layer of the equivalent circuit model represents the Neumann boundary and is modelled using a magnetic short circuit between the extended magnetic terminals attached to the air gap permeance. The arrangement is shown in figure 4.4b.

The term "leakage" has been adopted as a term to describe all the layers of permeance which join the magnetic conductors carrying the main flux. The number of layers may be selected to suit the level of discritisation required of the model. This approach to developing the equivalent circuit model, therefore, allows for a varying degree of discritisation in two dimensions.

4.3.3 The representation of the electric circuits within the rotor

The electric circuits within the rotor may be considered to exist in three areas, the wedges and damper circuits, the field winding, and the less well defined circuits which exist within the solid iron of the rotor. These are shown on the cross-section presented

in figure 4.1. For the purposes of an equivalent circuit model the currents flowing in all these areas are regarded in an identical manner to a current flowing in a conventional well defined conductor. The wedges, damper and field conductors are reasonably well defined and run axially along the full length of the machine. However, the eddy currents in the solid rotor are not constrained to well defined conductors. It is, therefore, necessary to assume that the eddy currents within the rotor iron do run axially along the full length of the machine because the equivalent circuit model does not allow for any cross-sectional variation of any variables along the length of the rotor. This assumption has also been made in previous finite element and equivalent circuit work (6,16,29) with good results being obtained.

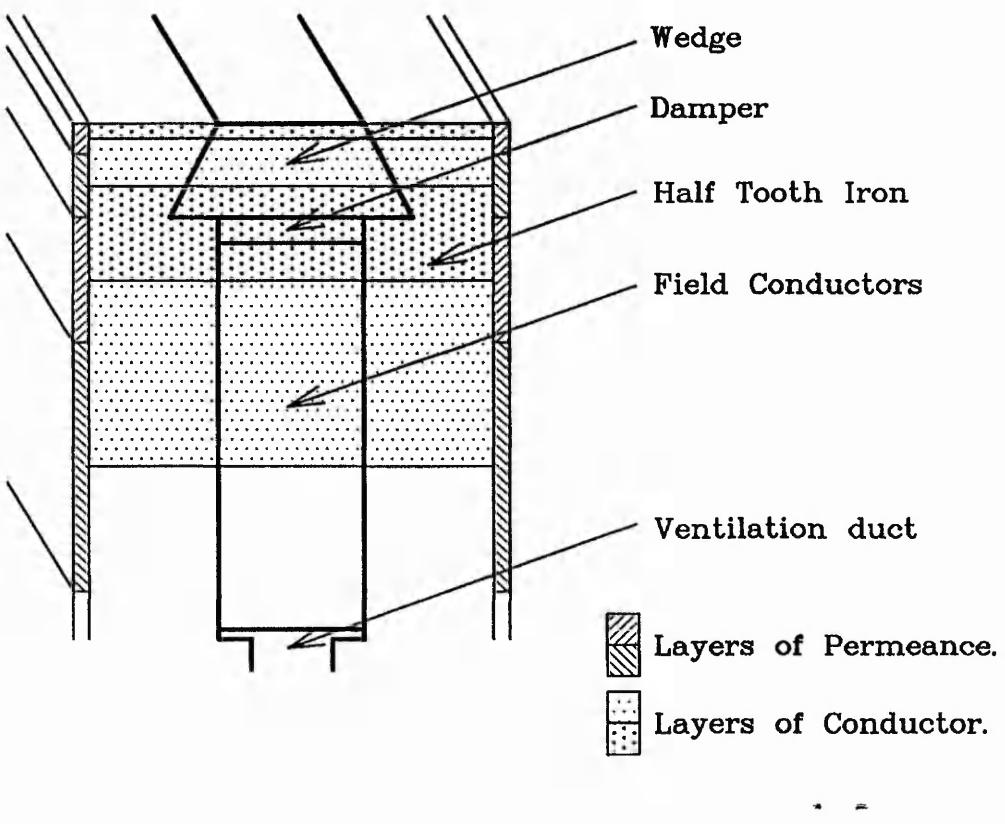

Figure 4.5 Relative positions of magnetic permeances and electrical conductors within a single slot pitch

The description of a permeance presented in chapter three of this thesis describes it as being a volume of space, defined by its width, height and depth, in which a magnetic flux is present. The eddy current conductors may also be described as volumes defined by a width, height, and depth perpendicular to the direction of the definition of the permeances. Figure 4.5 shows how the permeances physically interlock with the conductors in space.

In figure 4.4 the magnetic permeance can be likened to a number of parallel plate capacitors placed in line one on top of the other. The capacitor representing slot leakage permeance at the rotor surface has the smallest cross sectional area. The cross sectional area of the capacitor representing the second layer permeance is twice that of the surface layer because its radial height is doubled. This pattern is continued for capacitors representing deeper permeances. The arrangement of capacitors forms a corridor for each slot pitch which runs along the full effective length of the machine's rotor. This corridor is considered to be filled with slabs of electrical conductor the thickness of which increases with increasing depth.

Within an equivalent circuit representation a certain degree of lumping is required to obtain discrete equivalent circuit devices. The dimensions which have been used in the calculations for conductor resistance are determined from the mid points of the dimensions used for the permeance calculations and vice versa. For convenience when the permeances and conductors are displayed in a diagrammatic form, as shown in figure 4.6, the eddy current conductors are assumed to run axially within an area

effectively bounded by the magnetic conductors joining the magnetic terminals of the permeances. The calculation method used to determine the electrical resistance values of individual rotor sections is presented in appendix two.

4.3.3.1 The calculation for the damper resistance values

$$R_e = \frac{l}{\delta A} \qquad \text{.... 4.2}$$

The value of effective conductor length was determined by considering a complete damper coil including its return path. This amounted to twice the actual length of the rotor. The effect of the end bell is taken into account by modifying the bulk material conductivity. The values used in the calculations for the resistance of the damper circuits are derived directly from the physical dimensions of the conductor if the conductor is well defined. If the conductor is not well defined the dimensional values are derived from figure 4.5.

The value for the resistances of the electrical current paths used in the equivalent circuit model were also modified because only a half pole pitch of the machine is being represented. Consider a half pole D axis model which is being designed to represent a flux decay or frequency response test. There are two lines of symmetry, one on the Q axis and one on the D axis. The effect of dividing the rotor along the Q axis has no effect on the level of flux in the machine because, although there is only half the excitation from the stator current there is only half the rotor present for the flux to be distributed in. However, the field winding has been divided in two. This implies that

the induced voltage in the field winding will be halved. The effect of dividing the rotor along the D axis further subdivides the field winding, and therefore further reduces the induced voltage by a half, because there is only half the amount of flux present within the rotor. It is, therefore, necessary to reduce the value of the field winding resistance by a quarter to ensure that the correct value of current is induced into the field winding so that it can be fed back into the magnetic circuit as an induced m.m.f.

The D axis line of symmetry also has the effect of halving the induced voltage in the damper current paths of the wedges, dampers, and rotor iron. It is therefore necessary to halve the values of these resistances as well. This is effectively achieved by using the length of the rotor instead of the conductor or circuit length in the calculations for the electrical resistance (equation 4.2).

4.3.3.2 Creating the electric/magnetic circuit linkages

The electrical and magnetic circuits which exist within the rotor of a synchronous machine interact in a manner described by electromagnetic induction. This is a two way interaction, the flow quantity in the electric circuit inducing a potential in the magnetic circuit and vice versa. To represent this interaction within an equivalent circuit model linkages are introduced.

The tearing principle presented by Haydock (16) describes a method of tearing an electrical conductor through a magnetic conductor to create a linkage. If this method is applied to the single slot pitch shown in figure 4.6 which has been divided into eight

layers, 36 two way linkages would be required to represent a single slot pitch within the model. The representation of this system is considerably simplified using the dampance matrix described in chapter three.

The following paragraphs describe the application of the dampance matrix to the modelling of a single slot pitch shown in figure 4.6. The resulting equivalent circuit model is therefore believed to be original.

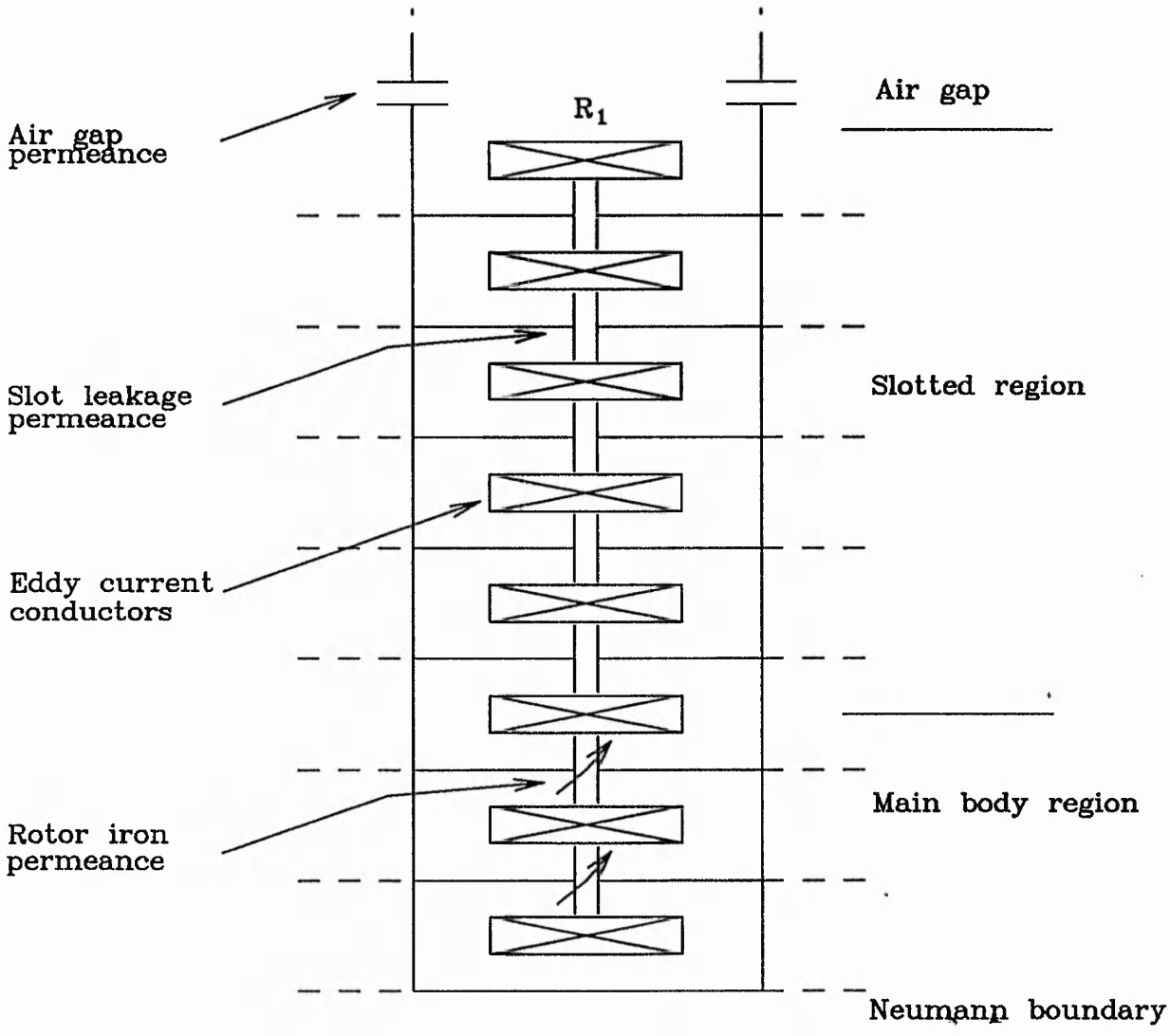

Figure 4.6 Equivalent circuit representation for a single slot pitch

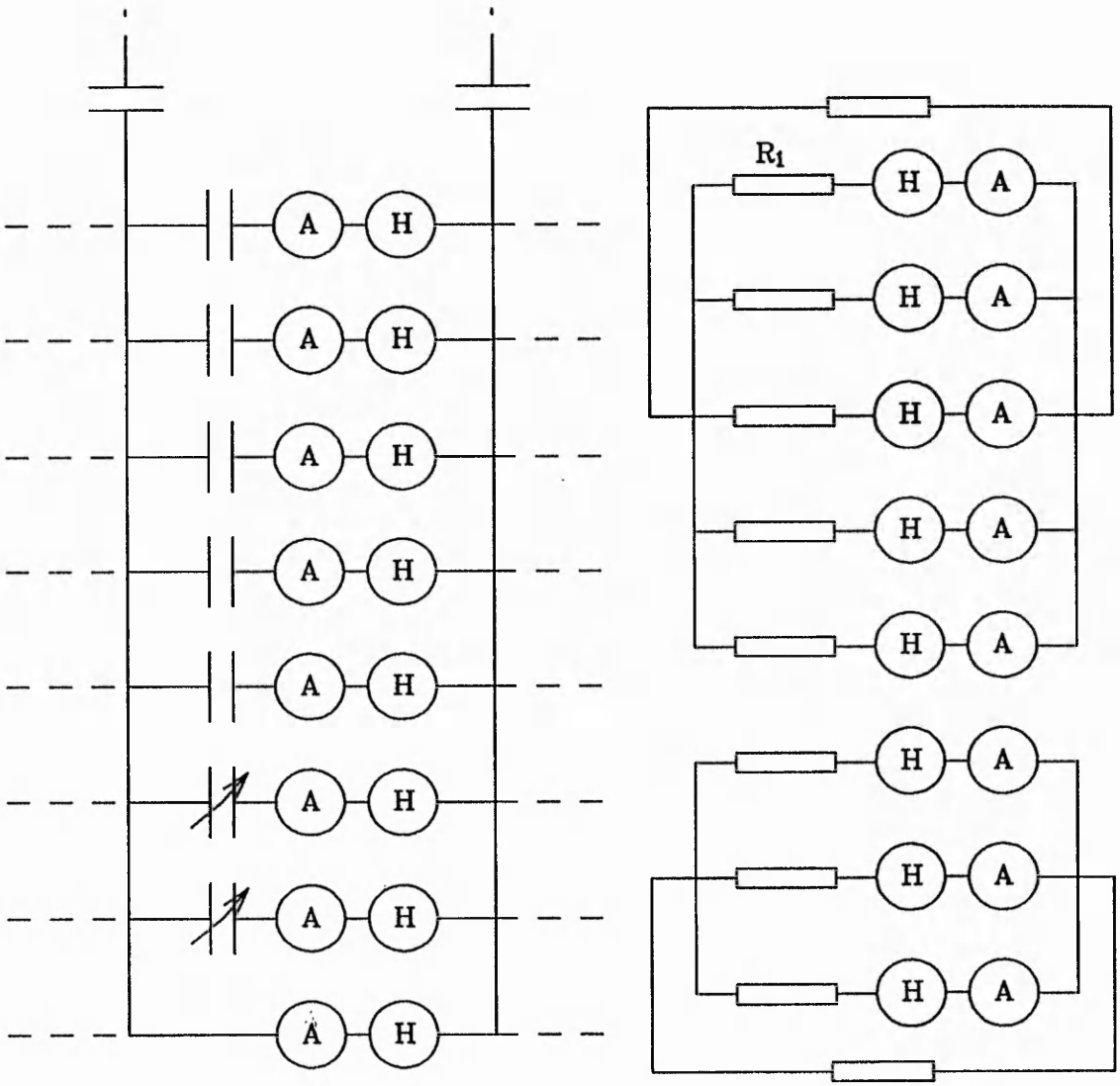

Figure 4.7 Linked electric and magnetic equivalent circuit representation for a single slot pitch in the pole region

Consider the outermost eddy current layer in figure 4.6. The resistance of this conductor path (R_1) is calculated as the resistance of the wedge top in parallel with the resistance of the tooth top, to a depth equal to half the width of the first permeance layer using equation 4.2. The effect on the magnetic circuit is determined by tearing

the defined conductor through the eight layers of the magnetic circuit. The conductor links all the defined leakage permeances and the Neumann boundary in the slot pitch. A rate of change of flux in any of the linked permeances will induce an e.m.f. into the first layer of eddy current conductor. Similarly any current in the first layer of eddy current conductor will induce a m.m.f. in all the linked permeance paths. It can therefore be concluded that any rate of change of magnetic flux in a particular slot will have an effect on the whole of the magnetic circuit within that slot via an induced current in the first eddy current layer.

This concept may be developed to include the effect the other layers of conductors have on the magnetic circuit. Deeper layers of conductor will only have an effect on the magnetic circuit with which they are linked. For example, the eddy current flowing in the second layer of conductor will have no effect on the first layer of permeance and a rate of change of flux in the first layer of permeance will have no effect on the current flowing in the second and deeper layers of conductor. Figure 4.7 shows the developed linked electric and magnetic equivalent circuit for a single slot pitch consisting of eight layers of conductor and seven layers of leakage permeance. Measuring the current in the appropriate branches of the equivalent circuit is achieved using current sensors, these are denoted by A in figure 4.7. In the magnetic portion of the circuit they measure rate of change of flux and in the electric portion of the circuit they measure electric current. The circuit components denoted by H in figure 4.7 may be described as flow dependent potential sources. The dependent voltage sources in the electrical conductor circuits sum the effects of all the rates of change of flux in all the layers of permeance linked by the conductors, and induce the appropriate e.m.f. in

the conductor. Similarly the dependent m.m.f. sources in the magnetic branches of the circuit sum the effects of all the linking currents and induce the appropriate m.m.f. into the leakage permeance.

4.3.4 The development of the wholly magnetic equivalent circuit model

A combination of linked electric and magnetic equivalent circuits describing a number of slot pitches similar to the circuit shown in figure 4.7, is both large and cumbersome to develop and implement as an equivalent circuit model. It is, therefore, a considerable advantage to be able to accurately represent the effects of the electric circuit from within the magnetic circuit. The advantage of such an approach is also described by Laithwaite (12) and has been achieved here by representing the linking electric circuits as a single dampance matrix.

For the complete representation of a machine's rotor a dampance matrix is required for each slot pitch. From the original work presented in chapter three of this thesis a standard dampance matrix is developed which may be applied to any enclosed ladder type magnetic circuit with interlinking electric circuits. However, it is important to minimise the requirement for these mutual linkages by carefully implementing the tearing principle. The implementation of a standard matrix format is consistent with the overall aim of this work to develop a standard general purpose equivalent circuit model to represent a synchronous machine.

Consider figure 3.7, showing the development of a wholly magnetic equivalent circuit model for a simplified slot pitch with a single damper circuit linking three layers of

leakage flux. The three by three dampance matrix, shown as equation 3.23, is developed to represent the linking wedge circuit within a wholly magnetic equivalent circuit model. Now consider figures 4.6 and 4.7. This is also an equivalent circuit representation for a single slot pitch. However, within this slot pitch representation are multiple damper circuits linking multiple layers of leakage permeance.

The dampance matrix for the representation of the single slot pitch presented in figures 4.6 and 4.7 is developed in two stages. Firstly, a dampance matrix is developed for a typical damper circuit in isolation. To represent the complete slot pitch would, therefore, require eight such matrices, one for each of the eight damper circuits. Secondly, these eight damper circuit matrices are summed. The result is a single dampance matrix representing all of the linking damper circuits. The implementation of such a dampance matrix within an equivalent circuit will enable a rotor's slot pitch to be represented as a wholly magnetic equivalent circuit model.

Initially consider the single turn damper circuit, R_1 in figure 4.7. This circuit links all eight of the defined leakage permeance paths. This is similar to the topology described in figure 3.7 and represented by equation 3.23. However, in figure 4.7, eight flux paths are linked rather than three. Expanding by inspection equation 3.23 to represent these eight flux paths yields an eight by eight dampance matrix. Such a matrix is presented as equations 4.3a. Equation 4.3a represents the dampance matrix for the single turn damper circuit, R_1, mutually linking the eight flux paths in figure 4.7. Each term within the matrix is none zero because R_1 links all of the eight flux paths. That is, there will be an induced m.m.f. in each of the linked flux paths which is dependant on

the rate of change of flux in all flux paths. Further, the value of each term within the matrix is the reciprocal of the circuits electrical resistance because the number of linking terms is one.

Equation 4.3a

$$\text{Dampance} = \begin{bmatrix} 1/R_1, & 1/R_1, & 1/R_1, & 1/R_1, & 1/R_1, & 1/R_1, & 1/R_1, & 1/R_1 \\ 1/R_1, & 1/R_1, & 1/R_1, & 1/R_1, & 1/R_1, & 1/R_1, & 1/R_1, & 1/R_1 \\ 1/R_1, & 1/R_1, & 1/R_1, & 1/R_1, & 1/R_1, & 1/R_1, & 1/R_1, & 1/R_1 \\ 1/R_1, & 1/R_1, & 1/R_1, & 1/R_1, & 1/R_1, & 1/R_1, & 1/R_1, & 1/R_1 \\ 1/R_1, & 1/R_1, & 1/R_1, & 1/R_1, & 1/R_1, & 1/R_1, & 1/R_1, & 1/R_1 \\ 1/R_1, & 1/R_1, & 1/R_1, & 1/R_1, & 1/R_1, & 1/R_1, & 1/R_1, & 1/R_1 \\ 1/R_1, & 1/R_1, & 1/R_1, & 1/R_1, & 1/R_1, & 1/R_1, & 1/R_1, & 1/R_1 \\ 1/R_1, & 1/R_1, & 1/R_1, & 1/R_1, & 1/R_1, & 1/R_1, & 1/R_1, & 1/R_1 \end{bmatrix}$$

Equation 4.3b

$$\text{Dampance} = \begin{bmatrix} 0, & 0, & 0, & 0, & 0, & 0, & 0, & 0 \\ 0, & 1/R_e, & 1/R_e, & 1/R_e, & 1/R_e, & 1/R_e, & 1/R_e, & 1/R_e \\ 0, & 1/R_e, & 1/R_e, & 1/R_e, & 1/R_e, & 1/R_e, & 1/R_e, & 1/R_e \\ 0, & 1/R_e, & 1/R_e, & 1/R_e, & 1/R_e, & 1/R_e, & 1/R_e, & 1/R_e \\ 0, & 1/R_e, & 1/R_e, & 1/R_e, & 1/R_e, & 1/R_e, & 1/R_e, & 1/R_e \\ 0, & 1/R_e, & 1/R_e, & 1/R_e, & 1/R_e, & 1/R_e, & 1/R_e, & 1/R_e \\ 0, & 1/R_e, & 1/R_e, & 1/R_e, & 1/R_e, & 1/R_e, & 1/R_e, & 1/R_e \\ 0, & 1/R_e, & 1/R_e, & 1/R_e, & 1/R_e, & 1/R_e, & 1/R_e, & 1/R_e \end{bmatrix}$$

Now consider the dampance matrix presented as equation 4.3b. This is an eight by eight matrix similar to equation 4.3a except that the first row and column contain zero. Each none zero value represents the dampance of a single turn damper circuit of resistance R_e. The pattern within the matrix indicates that no m.m.f. is induced in the outer most flux path by a rate of change of flux in any of the other flux paths and that a rate of change of flux in the outer flux path will not induce an m.m.f. in any of the remaining flux paths. The matrix presented as equation 4.3b, therefore, represents the dampance matrix for the second layer damper circuit which does not link with the

outer most flux path. Similarly, the matrix describing the effects of the third layer damper circuit yields a pattern in which the first two rows and first two columns contain zero. Finally, the eighth layer damper circuit yields a matrix containing a single non zero value in the bottom right hand position which represents the self damping effect of the deepest damper circuit only. This is because the deepest damper circuit only links a single flux path and, therefore, does not interact with any of the other flux paths.

The combined effect of all the conducting layers in any one slot pitch on the flux within the magnetic circuit, may be described by summing the effects of the individual conducting layers. The resulting dampance matrix is shown as equation 4.4. This matrix is symmetrical about the leading diagonal which demonstrates the reciprocal nature of potential and flow quantities within the magnetic and electric circuits.

Equation 4.4

$$\text{Dampance} = \begin{bmatrix} 1/R_1, & 1/R_1, & 1/R_1, & 1/R_1, & 1/R_1, & 1/R_1, & 1/R_1, & 1/R_1 \\ 1/R_1, & 1/R_2, & 1/R_2, & 1/R_2, & 1/R_2, & 1/R_2, & 1/R_2, & 1/R_2 \\ 1/R_1, & 1/R_2, & 1/R_3, & 1/R_3, & 1/R_3, & 1/R_3, & 1/R_3, & 1/R_3 \\ 1/R_1, & 1/R_2, & 1/R_3, & 1/R_4, & 1/R_4, & 1/R_4, & 1/R_4, & 1/R_4 \\ 1/R_1, & 1/R_2, & 1/R_3, & 1/R_4, & 1/R_5, & 1/R_5, & 1/R_5, & 1/R_5 \\ 1/R_1, & 1/R_2, & 1/R_3, & 1/R_4, & 1/R_5, & 1/R_6, & 1/R_6, & 1/R_6 \\ 1/R_1, & 1/R_2, & 1/R_3, & 1/R_4, & 1/R_5, & 1/R_6, & 1/R_7, & 1/R_7 \\ 1/R_1, & 1/R_2, & 1/R_3, & 1/R_4, & 1/R_5, & 1/R_6, & 1/R_7, & 1/R_8 \end{bmatrix}$$

Within equation 4.4, R_1 is the combined electric resistance of all the components (tooth top and wedge) within the conducting area of layer 1. These link only layer 1 flux paths. R_2 is the combined electric resistance of all the components (tooth top and wedge) within the conducting area of layers 1 AND 2. These link both layer 1 and 2

flux paths. R_3 is the combined electric resistance of all the components (tooth top, wedge and damper) within the conducting area of layers 1, 2 AND 3. These link layer 1, 2 and 3 flux paths. R_4, R_5, R_6, and R_7 are similarly defined. Finally, R_8 is the combined electric resistance of all the components (tooth top, wedge, damper and main body iron) within the area of the whole rotor depth defined by the appropriate slot pitch.

The purpose of the dampance matrix is to mathematically link the m.m.f. and rate of change of flux in each of the defined flux paths that result from linked electric circuits. The matrix equation 4.5 describes the induced m.m.f. in each of the flux paths defined in figures 4.6 and 4.7. It clearly represents a mathematical link between induced m.m.f. and rate of change of flux throughout the network which result from the linked electrical circuits in wholly magnetic terms. To implement this matrix equation in an equivalent circuit model, therefore, is to represent the magnetic circuit around a rotor's slot pitch by a wholly magnetic equivalent circuit model.

Equation 4.5 may be implemented directly in SPICE ver 2G6 (17) using multi dimensional current controlled voltage sources. These sources, denoted by F_1 ,F_2, ...,F_8 in figure 4.8, induce the appropriate m.m.f. into each layer of leakage permeance. The magnetic current, or rate of change of magnetic flux, is measured by the magnetic ammeters denoted by i_{m1},i_{m2},...,i_{m8}. The dampance matrix, therefore, may be described as the magnetic resistance of the linking electric circuits experienced from within the magnetic circuit.

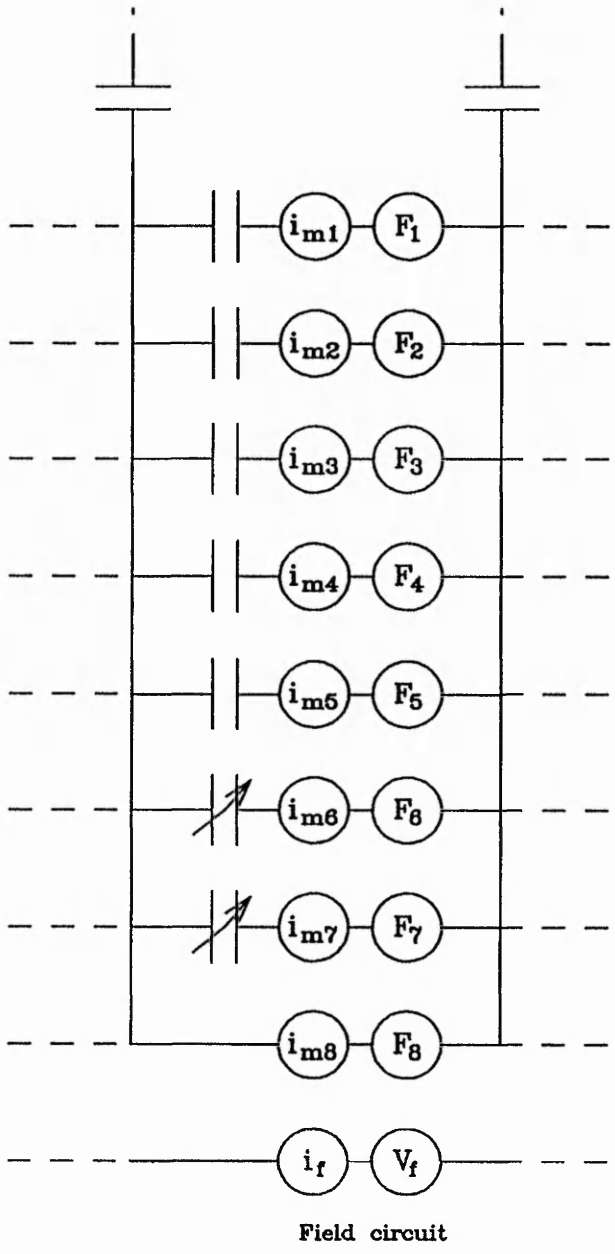

Figure 4.8 The magnetic equivalent circuit representing a single slot pitch of the slotted region within the rotor of a typical synchronous machine

Equation 4.5

$$\begin{bmatrix} F_1 \\ F_2 \\ F_3 \\ F_4 \\ F_5 \\ F_6 \\ F_7 \\ F_8 \\ V_f \end{bmatrix} = \begin{bmatrix} 1/R_1, 1/R_1, 1/R_1, 1/R_1, 1/R_1, 1/R_1, 1/R_1, 1/R_1, 0 \\ 1/R_1, 1/R_2, 1/R_2, 1/R_2, 1/R_2, 1/R_2, 1/R_2, 1/R_2, 0 \\ 1/R_1, 1/R_2, 1/R_3, 1/R_3, 1/R_3, 1/R_3, 1/R_3, 1/R_3, 0 \\ 1/R_1, 1/R_2, 1/R_3, 1/R_4, 1/R_4, 1/R_4, 1/R_4, 1/R_4, N_{f4} \\ 1/R_1, 1/R_2, 1/R_3, 1/R_4, 1/R_5, 1/R_5, 1/R_5, 1/R_5, N_{f5} \\ 1/R_1, 1/R_2, 1/R_3, 1/R_4, 1/R_5, 1/R_6, 1/R_6, 1/R_6, N_{f6} \\ 1/R_1, 1/R_2, 1/R_3, 1/R_4, 1/R_5, 1/R_6, 1/R_7, 1/R_7, N_{f7} \\ 1/R_1, 1/R_2, 1/R_3, 1/R_4, 1/R_5, 1/R_6, 1/R_7, 1/R_8, N_{f8} \\ 0 \ , \ 0 \ , \ 0 \ , N_{f4} \ , N_{f5} \ , N_{f6} \ , N_{f7} \ , N_{f8} \ , 0 \end{bmatrix} \begin{bmatrix} i_{m1} \\ i_{m2} \\ i_{m3} \\ i_{m4} \\ i_{m5} \\ i_{m6} \\ i_{m7} \\ i_{m8} \\ i_f \end{bmatrix}$$

This approach allows a considerable saving in the number of equivalent circuit components required to represent the rotor of a synchronous machine in an equivalent circuit model. The magnetic equivalent circuit topology is shown in figure 4.8. The linkages shown in the equivalent circuit of figure 4.8 may be described as the equivalent of a number of interlinking traditional transformers. Just as a traditional transformer may link two or more electrical networks together with a common magnetic circuit, in this equivalent circuit it is the magnetic networks which are being linked together by common electric circuits. However, it must be noted that the magnetic transformer effect is purely resistive, unlike the traditional transformer effect.

The representation of the field is a little more complex. Because it has been assumed that the eddy currents in the damper circuit flow axially along the full length of the machine, inter slot pitch effects due to eddy currents in these circuits have been ignored. However, the field links flux in two dimensions. The field links the flux which is present within the defined layers of any one slot pitch as well as in other slot pitches. To include these interactions in a wholly magnetic representation is possible but would increase and not decrease the complexity of the equivalent circuit model.

The field circuit is, therefore, represented in its electrical form and linked to the magnetic circuits. The linkage is implemented via the dampance matrix (equation 4.5) by introducing an additional row and column to represent the field winding. Within this additional row and column V_f represents the induced e.m.f. in the field winding, N_{f4}, N_{f5}, N_{f6}, N_{f7} and N_{f8} represent the actual number of turns linking the field winding with the associated layer of defined magnetic circuit and i_f represents the electrical current flowing in the field winding. The field winding resistance is reprented explicitly in the field circuit.

4.4 Conclusion

The general purpose equivalent circuit framework presented in this chapter is a combination of standard sub circuit topologies each of which represents a single slot pitch. The slot pitch sub circuit may be further sub divided into a combination of inter connecting layers. This ability to build up an equivalent circuit model by combining simple sub circuit branches is similar in some aspects to the finite element method. A finite element network of elements is a combination of triangular shaped elements of varying sizes. The pre-processing facilities which are now widely available for the generation of finite element meshes (28) are considerably more user friendly than the facilities available for equivalent circuit methods (17). The equivalent circuit approach adopted here using a combination of standard sub circuits could be incorporated into an equivalent circuit pre-processing package which would make the equivalent circuit more attractive from a the user view point.

The level of discritisation shown in figure 4.8 is used successfully for the equivalent circuit models which are used to simulate the frequency response and flux decay tests. The level of discritisation is variable in two dimensions although it is necessary to consider the available computing capacity if a more discritised model is required. This technique, therefore, represents a significant improvement on the level of detail represented using the traditional two axis models.

The different stator winding arrangements which are linked to the magnetic equivalent circuit developed in this chapter are described in the next chapter.

The equivalent circuit model developed in this chapter may be presented as a wholly magnetic equivalent circuit (figure 4.8), a linked electric and magnetic equivalent circuit (figure 4.7), or any combination of the two. This facility is particularly useful for investigating electric currents in specific areas of the machine's rotor. The model need only represent the electric circuits of interest explicitly as linked circuits. Similarly, if the model is required only to provide terminal quantities from a simulation, the damper circuits may be represented within the magnetic circuit implicitly, thus simplifying the model's topology. This ability to represent linked electric circuits in a flexible manner is a significant and original advance on the previous equivalent circuit models developed by Haydock (16) and Carpenter M.J. (29).

The work contained within this chapter represents an application of the original work described in chapter three to the solution of machine problems. The general purpose equivalent circuit framework which has been subsequently developed is a combination

of a number of different approaches which have been adopted and adapted in the light of the theory described in the previous chapter. However, the developed equivalent circuit framework is, in effect, two dimensional which will limit its ultimate accuracy. Further discussion on the accuracy and possible applications of the framework is contained in chapter eight of this thesis.

Chapter Five
Test simulations

5.1 Introduction

The testing of large synchronous machines is expensive, time consuming and potentially destructive. However, prior to the 1960's it used to be the principal method for obtaining information about their behaviour and performance. Machine parameters, determined from test results, are used as equivalent circuit parameters in simple two axis models (5,23,24) and power system studies. More recently, detailed finite element models have been used to reduce the need for expensive testing by simulating test conditions (6,51,52,53,54). Although the finite element models are capable of providing a detailed insight into the behaviour of the magnetic field within a synchronous machine and give excellent test results (6), they require a large amount of computing resources and are not suitable for the simultaneous simulation of a machine and an electrical supply network.

The work presented in this chapter describes the simulation of three common test conditions using the basic equivalent circuit topology presented in the previous chapter. The terminal quantities from these test simulations are available directly, if required, as actual voltages and currents from the simulation. The equivalent circuit approach is, therefore, ideal for machine models which require connection to, and simultaneous simulation with an electrical supply network. One such application has been demonstrated by Carpenter M.J. (29), who describes a simultaneous simulation of, a small synchronous machine and power electronic controller using a single equivalent circuit model.

A very common characteristic of models and simulations in general is the on going conflict between ease and speed of solution and required discretisation. Clearly, increased discretisation will typically yield improved results however, the quality of the results needs to be balanced with the available computational time and resources. The equivalent circuit and finite element approaches to modelling synchronous machines are no different in this respect. However, the equivalent circuit approach does appear to be sufficiently robust to withstand a considerable reduction in circuit discretisation whilst maintaining a reasonable degree of accuracy particularly if the range of operation is limited. A good example to demonstrate this are the equivalent circuits developed by Shackshaft (23) and Cannay (24). These are very simple equivalent circuit models consisting of a handful of circuit devices. By limiting the operating range, implied by the use of transient or sub transient parameters, adequate simulation results are obtained.

The new equivalent circuits described in this thesis are designed to provide accurate results over a much wider operating range than previous equivalent circuit models. However, the required level of discretisation remains relatively low when compared to an equivalent finite element study. These equivalent circuit models which are to be accurate over a wide range of operating conditions should, therefore, be suitable for obtaining machine parameters. The three simulations described in this chapter are designed to validate the general purpose nature of the equivalent circuit model developed in the previous chapter. Chapter six describes the results obtained from these simulations and compares them to the actual test results and results obtained

from finite element simulations.

The computer simulation software used throughout this work is SPICE version 2G6 (17). This package was developed in the early 1970's principally for the solution of electronic circuits. This software is used because it is the most widely used general purpose circuit simulation computer package.

5.2 The test conditions

The three test conditions which are to be modelled using the equivalent circuit techniques described in this thesis are the flux decay test, the frequency response test and the sudden short circuit test. These are referred to in the British Standards BS4296 (55) and more recently this has been superseded by BS4999 part 104 (56).

5.2.1 The flux decay test

The flux decay test is performed by running the machine at synchronous speed with the stator winding connected to a supply usually at or near to the stator rated voltage. The field winding may be open circuit, short circuit or a short circuit via a discharge resistor. At $t = 0$ the stator supply is disconnected and the decay of the stator voltage recorded for a period of time. The field current is also recorded if applicable. The voltage induced in the stator winding is directly proportional to the amount of flux linking the stator. This test is therefore a measure of the rate of decay of magnetic flux within the machine, which is determined by the ability of the rotor eddy current circuits to support the flux.

5.2.2 The frequency response test

The frequency response test is performed on a static machine. A variable frequency supply is connected on to a phase of the stator winding. The frequency is usually varied between 0.001 Hz and 1000 Hz and the rotor usually aligned with the D or Q axis. The magnitude of the excitation voltage is usually only a fraction of the rated stator voltage. The test has therefore been criticised because these conditions are not consistent with typical operating or fault conditions. Typical measurements taken from the test may be stator voltage and current, field voltage and/or current and the voltage and/or current in other stator windings. From this information it is possible to determine the impedance and therefore the inductance of the excited stator winding, and the transfer functions describing the linkage with the other windings. The test measures the ability of the eddy current paths in the rotor circuit to control the level of flux linking the various windings at different frequencies. The behaviour of the flux is therefore subtly different from in the flux decay test. This, together with the artificially low level of excitation, may be used to explain the difference between parameters obtained from the two tests (6). A further criticism of this test is the variation of the resistance of the damper circuits as a result of the mechanical effects on the damper circuits due to the rotation of the rotor.

5.2.3 The sudden short circuit test

The sudden short circuit test is performed by running the machine at synchronous speed with the rotor excited and the stator winding on open circuit. The field excitation is usually sufficient to induce 50% of the rated stator voltage. At $t = 0$ the stator terminals are simultaneously short circuited and to the neutral point. Because of

the large currents which flow in the stator windings and the resulting forces on them, this test is potentially destructive. The results obtained from the test usually describe the initial rise and settling of the stator currents. The test is favoured because the test conditions are relatively close to typical fault conditions. The test conditions are subtly different from those of the flux decay and frequency response tests. The test measures the ability of the rotor damper circuits to withstand a large rate of change of flux induced by the introduction of large currents in the stator. The current in the stator windings is induced as a result of the changing flux linking it, the behaviour of which is determined by the distribution of eddy current conductors within the rotor.

5.3 The flux decay test simulation

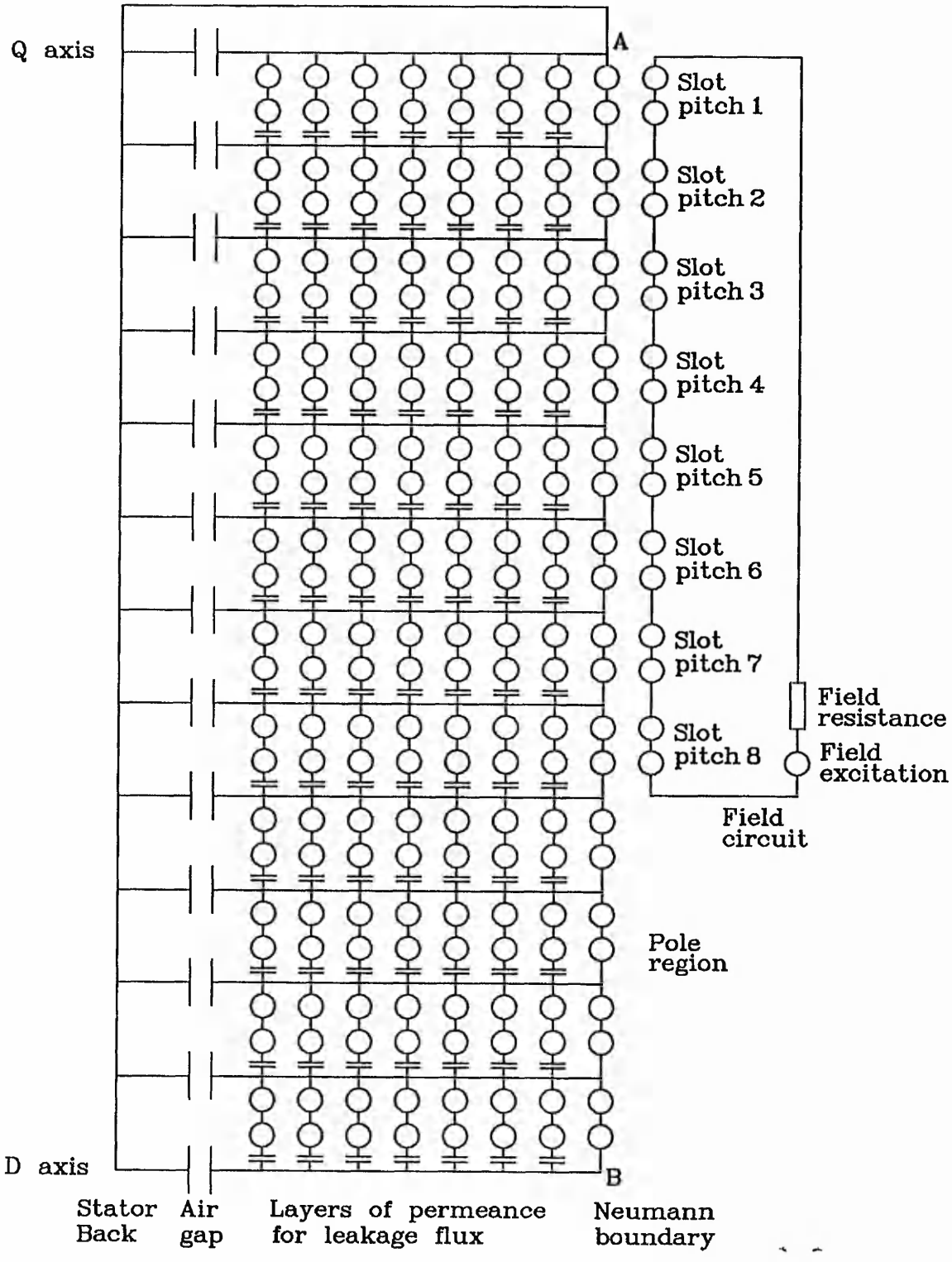

Figure 5.1 D axis linked electric and magnetic equivalent circuit model

The D axis flux decay test simulation is performed using the equivalent circuit presented in figure 5.1. The equivalent circuit model is constructed from a number of the standard slot pitch models presented in figure 4.8 connected together side by side.

The field winding is represented in an electrical form and linked to the magnetic equivalent circuit using current controlled voltage sources. The reasons for this are two fold. Firstly, it is possible to obtain values for field voltage and current directly from the simulation results. Secondly, to represent the field winding in this form is more straightforward than a wholly magnetic form. This is because the field winding links flux in multiple layers and slot pitches. To represent these linkages in a wholly magnetic form would increase the complexity of the model considerably.

The rotor damper circuits are referred into the magnetic circuit using the dampance matrix technique described in chapter four. Each flux leakage limb is, therefore, linked to every other limb in the same slot pitch using an array of multi dimensional current controlled voltage sources. This arrangement, therefore, represents the linking of slot leakage flux by eddy current paths at different rotor depths.

The topology of the equivalent circuit model used to represent a Q axis flux decay test is identical to this, with two exceptions. Firstly, the stator back is connected to the Neumann boundary at point B rather than point A (figure 5.1) and, secondly, a representation of the field circuit is not required because the Q axis flux does not effectively link with the field winding.

An additional simulation is also performed to test the relative significance of the mutual terms in the dampance matrix (equation 4.5). The damper and eddy current circuits are represented as single resistive devices, the values of which are determined by the self dampance terms in the dampance matrix. The significance of the mutual coupling effect associated with the field winding is also determined by referring the field resistance into the magnetic circuit as a self dampance only. The resulting equivalent circuit model, therefore, is based on the same assumptions as those adopted by Haydock (16) and Carpenter C.J. (15). The results from these investigations are presented in chapter six of this thesis.

The flux decay test is perhaps the most straight forward of the simulations to perform, for two reasons. Firstly, the flux remains locked to the rotor for the duration of the test. The flux distribution may therefore be considered as stationary with respect to the rotor reference frame. Secondly, the induced e.m.f. in the stator winding is directly proportional to the air gap m.m.f.. It is therefore possible to obtain a value for the magnitude of the stator voltage directly from the air gap m.m.f.. The need to represent the stator winding explicitly is therefore removed and an allowance is made for the stator leakage in the calculation for the initial air gap m.m.f.. Haydock (16) has shown that the initial rapid decay of the stator voltage during the test may be attributed to stator slot leakage. This assumption enables the effect of stator leakage to be subtracted from the air gap m.m.f.. prior to the simulation. An initial air gap m.m.f. is sinusoidally distributed on to the air gap permeances in such a way as to represent the D axis or Q axis flux. The equation showing how the initial air gap m.m.f. was

calculated for a typical machine is given in equation 5.1.

$$\text{pu air gap voltage} = 1 - (I_{ph} \,.\, X_l)\ \text{pu} \qquad \ldots. 5.1$$

The stator voltage envelope is determined directly from the air gap m.m.f. distribution. This is achieved using an identical method to that described by Turner (6). Equation 5.2 is used to determine the magnitude of the fundamental component of the air gap flux.

$$\text{fundamental flux, } \Phi_f = \frac{\sum_{i=1}^{n} \Phi_i \,.\sin\theta_i.\delta\theta_i}{\sum_{j=1}^{n} \delta\theta_j \,.\sin\theta_j} \qquad \ldots. 5.2$$

where $\Phi_i \,.\sin\theta_i$ = Flux on an individual air gap permeance.
$\delta\theta_i$ = Width of an air gap permeance.
n = Number of air gap permeances.
θ_i = Angle of permeance from D or Q axis.

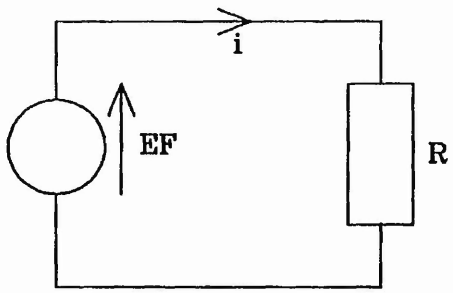

Figure 5.2 Electrical network used to determine the fundamental of the air gap flux

The electrical network used as an implementation of equation 5.2 is shown in figure 5.2. The resistance R is numerically equal to the denominator of equation 5.2. The source EF is a voltage controlled voltage source. EF sums the m.m.f.s' of the air gap permeances in the proportions described by equation 5.3.

$$V_{EF} = k_0 + k_1V_1 + k_2V_2 + k_3V_3 + k_4V_4 + \ldots + k_nV_n \qquad \ldots. 5.3$$

where k_0 = 0
k_i = angular width ($\delta\theta_i$) of permeance i.
V_i = m.m.f. across permeance i.
i = 1,2,3,4, ... n

The circuit current, therefore, represents the magnitude of the fundamental component of air gap flux. This value of flux is scaled by modifying the value of the circuit resistance so that the circuit current is numerically equal to the envelope of the stator voltage using equation 5.4.

$$V_{t\text{-}t} = 3.2.\pi.f.N_{eff}.\Phi_f \qquad \text{.... 5.4}$$

5.3.2 An alternative representation for selected damper circuits

The configuration of the equivalent circuit model presented in figure 5.1 is modified to represent selected damper circuits explicitly. This representation allows values for the eddy currents flowing in the damper circuits to be obtained directly from the simulation results. Consider figure 4.7. This shows a linked electric and magnetic equivalent circuit representing a single slot pitch. This configuration is used to represent a single slot pitch in the equivalent circuit shown in figure 5.1. The linkages used to link the magnetic circuit and the damper circuits are simple half transformer linkages, shown here in figure 3.1. The mutual linking effect of the damper circuits is performed by the electrical network of the damper circuits. The topology of the magnetic circuit is almost unchanged by the introduction of a linked electric circuit. Although the self dampance resistive elements are returned to the electric circuit the m.m.f. sources are still required to represent the link between magnetic and electric circuits. However, the parameters used to determine the induced m.m.f. are derived from the linked electric circuit and not the magnetic circuit.

The results for the eddy current values determined from this equivalent circuit representation are compared to the results of a comparable finite element study. The finite element study is, as far as is practicable, consistent with the equivalent circuit representation in terms of machine dimensions and material bulk constants, so that a direct comparison can be made of the results obtained using both methods.

The finite element mesh used for this study is identical to that described in the previous chapter as figure 4.2 and used to perform a steady state study. The time stepping program developed by Turner (6) is used to perform the flux decay test simulation. The output from this transient analysis program was in the form of magnetic vector potential (A) and its rate of change (dA/dt) at each node. The current densities for each triangular element were determined using equation 5.5.

$$\text{current density, } J_c = \frac{\sigma}{3}\left[\frac{dA_1}{dt} + \frac{dA_2}{dt} + \frac{dA_3}{dt}\right] \qquad \ldots. 5.5$$

Post processing software (28) is used to integrate the current density over a number of elements within defined areas equivalent to the definition of the conductors within the equivalent circuit model. The values of the electric currents within the damper circuits could then be compared directly with values obtained using the equivalent circuit technique.

The results from these simulations are presented and discussed in the next chapter. However, because the value for conductivity used in these simulations has been modified in certain regions of the rotor to allow for end effects and inertia gashes as described by Turner (6), the rate at which the eddy currents penetrate into the rotor iron will not be consistent with the physical test conditions. The results, therefore, are expected to differ from the actual machine behaviour. However, because the two representations have been developed using the same assumptions and material bulk constants, similar results are expected.

5.4 The frequency response test simulation

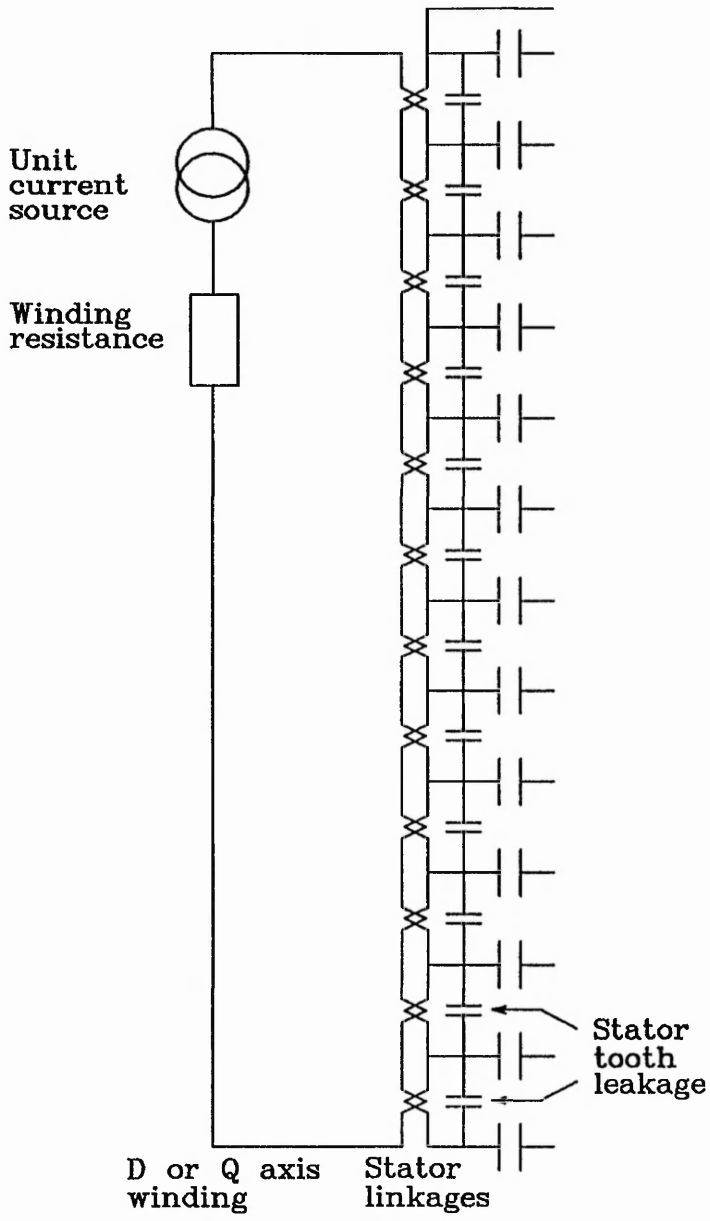

Figure 5.3 An equivalent D or Q axis winding used in the frequency response test simulation

The frequency response test simulation is performed using an identical equivalent circuit topology to represent the rotor to that used for the flux decay test simulation

described in figure 5.1. However, to present the results for the test in the more usual form as operational inductances described by Adkins (42), a sinusoidally distributed D or Q axis winding is linked to the stator of the existing equivalent circuit model.

The D and Q axis stator windings have been described by Adkins (42) as being stationary with respect to the rotor reference frame and give rise to the same m.m.f. per pole as the three phase windings. It is therefore possible to calculate the required turns per pole for a given stator winding current using the method described by Turner (6). A sinusoidally distributed air gap m.m.f. is obtained using a sinusoidally distributed stator current. To represent this effect the parameters representing the stator linkages are varied sinusoidally around the stator using equation 5.6.

$$\text{Turns per slot pitch} = \frac{6/\pi . N_{eff} . \sin\theta_i . \delta\theta_i}{\sum_{j=1}^{n} \delta\theta_j . \sin\theta_j} \qquad \ldots. 5.6$$

The representation of the stator D axis winding within the equivalent circuit model is shown in figure 5.3. The development of an equivalent circuit representation of the Q axis winding is identical with the exception that the angles used in the calculation for the value of the linkage are measured from the Q axis instead of the D axis. The equivalent circuit representation of the stator is identical to that used for the flux decay test simulation, with two exceptions. Firstly, a slot leakage permeance has been introduced, the value of this being calculated directly from the stator slot dimensions. Secondly, the linkages representing the winding are situated where the conductors

have been torn away from the machine centre through the stator back. The linkage is a standard transformer type because the rotor is stationary for the duration of the transient. The value of the linkage is dependent on its position with respect to the D or Q axis and has a value which is determined from equation 5.6. The representation of the winding consists of the series combination of a current source, a resistance equal to a quarter of the phase resistance and a linkage for each of the slot pitches in the magnetic circuit.

It is difficult to represent the stator winding within the magnetic circuit as a wholly magnetic equivalent circuit representing the stator back, because the stator conductors also mutually link the flux in all the other stator teeth. The stator winding circuit in these simulations has therefore been modelled in its electrical form. This representation is also most suited to providing the excitation and obtaining the operational impedance directly from the simulation results. A representation of the eddy current paths within the stator is not required because machines of this type use laminated stators.

The stator winding is excited from a unit current source, the frequency of which is varied from 0.001Hz to 1000Hz. The operational impedance is therefore numerically equal to the e.m.f. induced in the stator winding by the magnetic field within the machine. The operational inductance is obtained from equation 5.7a by rearranging and replacing d/dt with $j\omega$ for sinusoidal excitation. The operational inductance is therefore calculated using equation 5.7b.

$$\text{Induced e.m.f.,} \qquad e = L\frac{di}{dt} \qquad \text{.... 5.7a}$$

$$\text{Operational inductance,} \quad L(s) = \frac{e}{j\omega i} \qquad \text{.... 5.7b}$$

A simple computer program was written to automatically convert the SPICE output of voltage versus frequency to operational inductance versus frequency, by dividing the magnitude of the induced voltage by the frequency and subtracting 90 degrees from its phase angle.

The field transfer function is described as the ratio of field current to stator current. The transfer function is therefore numerically equal to the field current because a unit current source is used in the stator winding. This is obtained directly from the SPICE simulation results.

The results are compared to actual test results wherever possible. However, Turner (6) and Reece et al (54) have done a considerable amount of work on simulating the frequency response test for turbogenerators. This work is also used in chapter six to compare with the results obtained from the equivalent circuit method described here.

5.5 The sudden short circuit test simulation

The behaviour of the magnetic flux within a synchronous machine during a sustained short circuit test is different from the tests described previously, in that the magnetic field does not remain locked to the rotor for the duration of the transient. The

synchronous machine model must, therefore, be capable of representing not only the stator conductors but also the relative motion between the stator and rotor conductors.

Finite element studies (52) have shown that immediately after the short circuit has been applied, flux linking the stator conductors is trapped in an attempt to oppose the rapid rate of change of current in the phase windings. Because the phase windings are static, the decay of this flux is responsible for the d.c. component present in the current waveform, which is characteristic of this test. The rotating field continues to induce a sinusoidally varying current in the phase windings, which is superimposed on this d.c. component.

The basic concept which is adopted to derive the topology of the magnetic equivalent circuit representing the rotor, is identical to that which has been adopted to generate the equivalent circuits shown in figures 5.1. The rotor cross-section is sub divided into sectors and each sector is further sub divided into layers of varying depth. To represent the complex behaviour of the flux within the rotor it is necessary to represent the rotor as a 360 degree model. At the centre of this model is supposed a infinitesimally small cylinder along the full length of the machine to allow conductors torn towards the centre of the rotor to be united with their respective return paths and removed from the system. The north and south poles of the rotor circuit are created on the D axis by the m.m.f. induced by a field current. Particular attention needs to be paid to the polarity of the m.m.f. sources and rate of change of flux feedback sensors in the magnetic circuit, to ensure correct operation of the field circuit linkages. As with the half pole pitch model, it is impossible to include the field winding within the

magnetic circuit without increasing the complexity of the sectors' dampance matrices. This is because the field winding links a number of sectors as well the layers within each sector.

Early finite element simulations designed to represent the sustained short circuit test (53,57) used a half pole pitch representation for the machine. The simulations used the two axis approach to represent the phase bands and, although reasonable agreement with test results was obtained for the stator current, a similar agreement could not be obtained for the field quantities. Turner (52) has since successfully modelled the sustained short circuit test using finite element techniques. The finite element model represents a single pole pitch and uses a periodicity boundary situated on the D axis. This is possible because the solution to the finite element problem is obtained using bespoke software which is designed to incorporate such a boundary condition. No such boundary condition exists within the general electrical network solver SPICE.

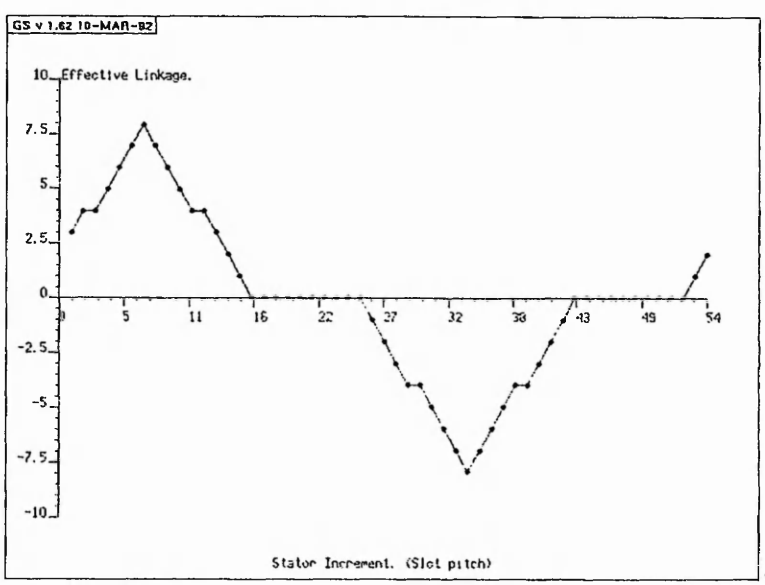

Figure 5.4 The variation of stator winding linkage with rotor position

The topology of the magnetic equivalent circuit representing the stator is similar to the topology used for the frequency response test simulation. The magnetic equivalent circuit for each sector consists of a slot leakage permeance and three position dependent linkages, linking the stator magnetic circuit with the three phase bands. Each phase band is linked to each sector of the magnetic circuit using a time varying linkage. The function of linkage versus time is presented in figure 5.4, each of the linkage variations being identical in shape but displaced in time, depending on the phase and sector being represented. These time dependent linkages may be interpreted as being position dependent because the rotor is rotating with a constant speed. The value of the linkage has been determined by rotating the rotor a slot pitch at a time and evaluating the linkage for each sector at each position with each winding. Linear interpolation has been used to determine a value for the linkage in the inter slot space. This method for representing the stator windings is identical to the method used successfully by Carpenter M.J. (29).

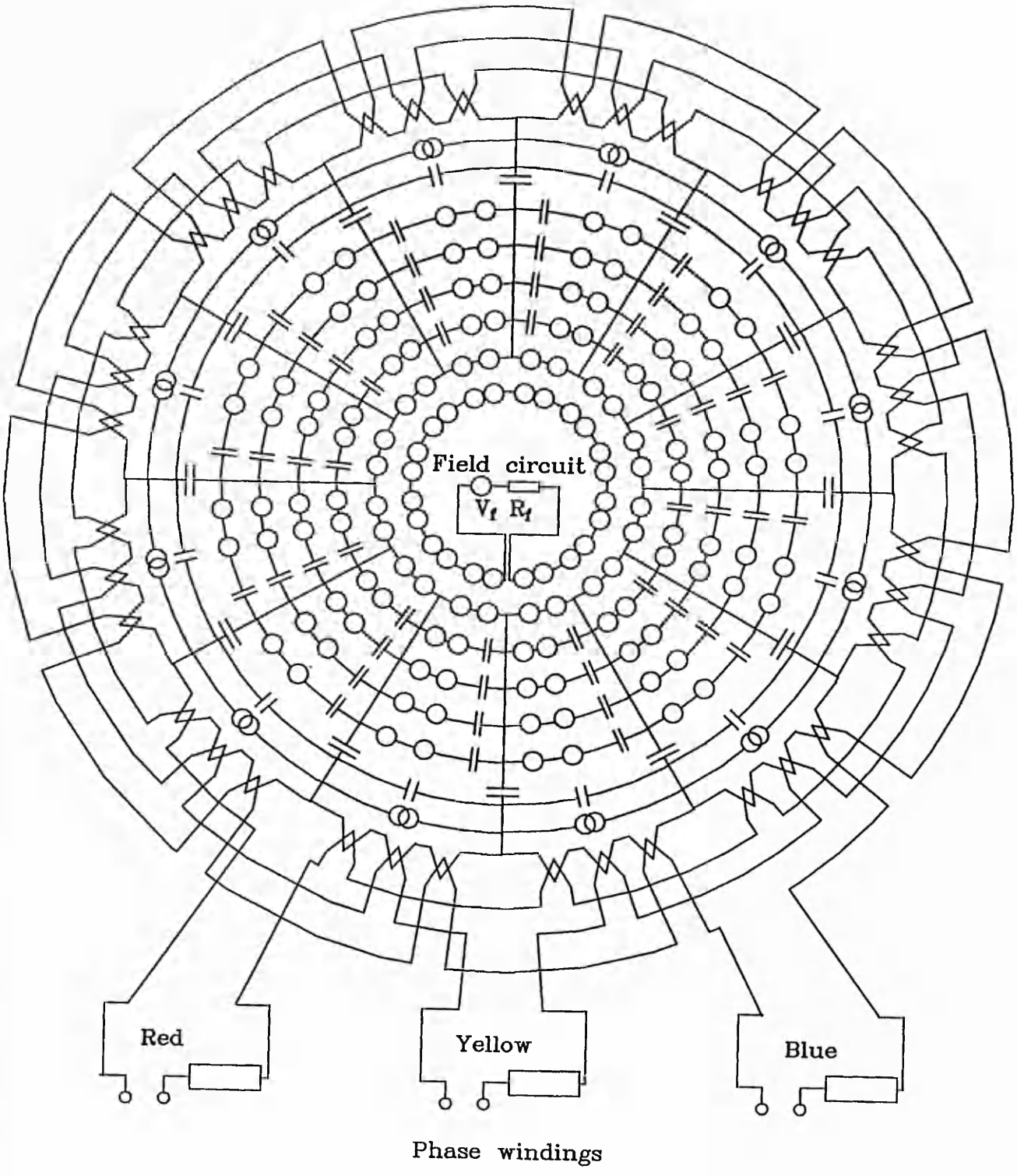

Figure 5.5 The equivalent circuit model used to represent a machine for the sudden short circuit test

The effect of saturation within the rotor iron during the sustained short circuit is modelled using the same method as has been used to represent saturation during the

flux decay test simulation. The level of saturation is fixed at its pre-test value for the duration of the transient. Finite element studies (52) have shown that this may be difficult to justify and have used a non linear approach for relative permeability to represent the effects of saturation. This approach is difficult and cumbersome to adopt in an equivalent circuit environment because the circuit solver SPICE ver 2G6 has a very limited ability in the area of non linear magnetic models. The introduction of any equivalent circuit representation to represent magnetic saturation would inevitably increase the complexity of the equivalent circuit model.

The linked electric and magnetic equivalent circuit model used to represent the synchronous machine is shown in figure 5.5. Although the linkage elements are not annotated in detail, the general pattern is identical to the arrangement described in figure 4.8. The discretisation of the circuit is considerably less than has been used to represent the previous transient conditions because of the limitations imposed by the circuit solver SPICE. Although results are presented in chapter six for a steady state simulation using this equivalent circuit model it has proven impossible to obtain results for a sustained short circuit test simulation. The possible reasons for this are discussed later in this chapter. The circuit presented in figure 5.5 must, therefore, be presented as a proposed circuit to represent a short circuit transient because of this inability to obtain a solution using SPICE.

5.6 Practical considerations

The equivalent circuits described in the present and previous chapters may be implemented on any electrical network solving computer software provided it has the

capacity to accommodate them. The comments in the next few paragraphs concern the implementation of the equivalent circuit models using SPICE ver 2G6 on a VAX 8700 at Nottingham Trent University.

The CPU times required for a solution to the equivalent circuits described previously are typically 30 to 40 minutes for a flux decay test simulation and 3 to 5 minutes for a frequency response test. The sustained short circuit test simulation was been left running on the computer for a periods of up to 30 days with converging onto a solution.

Capacitors and inductors in SPICE are considered to be ideal. This implies that capacitors have infinite resistance and inductors have zero resistance. SPICE imposes a limitation such that each node must have a d.c. current path to ground and the use of meshes with zero resistance is prohibited. This restriction is imposed because the computer can only perform calculations with finite numbers. Additional resistance components must therefore be included in the equivalent circuit model to satisfy this restriction. These additional dummy components are not shown in the equivalent circuits presented in this thesis because they do not contribute to an understanding of the circuits' operation.

SPICE has been developed as a general purpose electronic circuit solver (Simulation Package with Integrated Circuit Emphasis). It contains a number of solution optimisation routines. These routines have been shown to work well with a typical electronic network, however, the equivalent circuit models developed within this thesis

contain a large number of capacitive elements. The large rates of change of voltage and currents in the equivalent circuit under transient conditions causes the internal time step used in the transient analysis to continually be reduced. Eventually the time step becomes to small for computation to continue. It is possible to reduce the effect of this optimisation process, however, this has an adverse effect on the solution times.

5.7 Conclusion

The central part of the equivalent circuit model topology developed in the previous chapter has been included in equivalent circuit simulations for three common test conditions on synchronous machines. Successful simulations have been completed for two of the test simulations. However, the simulation of the sustained short circuit test has not been successful because of the inability of SPICE to converge onto a solution.

The equivalent circuit model for the sustained short circuit test was tested extensively. Indeed simulation results are presented using this model in a steady state simulation. It is thought that the very large rates of change of the voltages and currents together with large number of inter branch interactions within the equivalent circuit are responsible for the excessive solution times and the ultimate inability of SPICE to converge onto a solution.

The equivalent circuit techniques developed within this thesis, for the modelling of magnetic circuits, has obvious uses within the field of electrical machine modelling. However, it is felt by the present author that whilst the theoretical level of discretisation has now been shown to be without limit the practical level is limited by

the ability of the simulation software to provide a solution to the more complex models.

It has been demonstrated that using equivalent circuits to model the behaviour of the synchronous machine is not suitable if the user requires detailed information about the magnetic field within the machine. The representation of the magnetic field is limited by the definition of magnetic permeance and in particular its magnetic terminals within an equivalent circuit model. An alternative approach is to develop a special purpose computer package capable of solving equivalent circuit models containing special magnetic devices. However, the presence of finite element analysis software for essentially the same purpose is likely to limit the enthusiasm for such a major undertaking. This approach is more fully discussed in chapter eight of this thesis.

Equivalent circuit models are, however, suited to providing terminal quantities directly from simulation runs. They are also suitable for use in applications where simultaneous simulation of a machine and its supply network are required. The equivalent circuit models required for such simulations are ideally topologically simple and sufficiently accurate for a wide range of operating conditions. This is particularly relevant if a power electronic controller is contained within the supply circuit because of the effects of harmonics on the machine's performance. The complex physical attributes that determine the behaviour of a machine must, therefore, be represented either within the topology of the equivalent circuit model or within complex equivalent circuit devices. The latter approach would enable an equivalent circuit model with reduced topological complexity to represent the machine. This approach is further

discussed in chapter seven of this thesis.

Chapter Six
Test results

6.1 Introduction

The results presented in this chapter have been obtained from a number of simulations using the equivalent circuit models developed in the previous two chapters of this thesis. Simulation results are presented for three machines, the 500MW Eggborough machine, the 150MW Uskmouth machine and the 660MW Torness machine. Although simulations for three transient test conditions have been attempted, successful simulations were only completed for the flux decay or stator decrement test and the static frequency response test. However, results are presented for a steady state simulation using the sustained short circuit test equivalent circuit model. The difficulty associated with obtaining a solution for this equivalent circuit model under transient conditions is caused by the inability of the circuit solver SPICE to converge onto a solution. These difficulties are discussed in the previous chapter.

The results from each test simulation are, wherever possible, compared directly with actual test data (50,58) obtained from a machine test. Where this has proved impossible, use has been made of finite element software (28) to provide the necessary test data for comparison. Simulation and test results are limited to a graphical comparisons for two reasons. Firstly, it is felt that the derivation of machine parameters from simulation and test results has been dealt with sufficiently in previous work (6,16,23,59), and secondly, the direct comparison of test data is preferred rather than comparing the parameters derived from them.

The raw simulation results obtained from the test simulations are presented in appendix three. These have been translated into three forms. Firstly, results in the form of terminal quantities which may be compared directly with the terminal quantities obtained during a machine test. This form is used when comparing the simulation and test results for a flux decay test. Secondly, results in the form of terminal quantities which would exist in the D and Q windings described by Adkins (42). This form is used for comparing test and simulation results for frequency response tests. The form of these simulation results has been selected because it matches the traditional format of frequency response test data and not because of any limiting factor of the simulation technique. Finally, the simulation results may be in the form of quantities internal to the machine. This type of test data is unavailable from existing machine test data. It is, therefore, necessary to compare these results with an alternative simulation technique. The simulation results have therefore been compared with the results obtained from a comparable finite element simulation.

The equivalent circuits used to obtain the simulation results have been derived directly from the physical topology of the machine's cross-section and its material bulk constants. It is, therefore, conceivable that the technique may be used to derive machine parameters because no prior knowledge of the machine's behaviour is required for the simulations.

6.2 The flux decay test simulation results

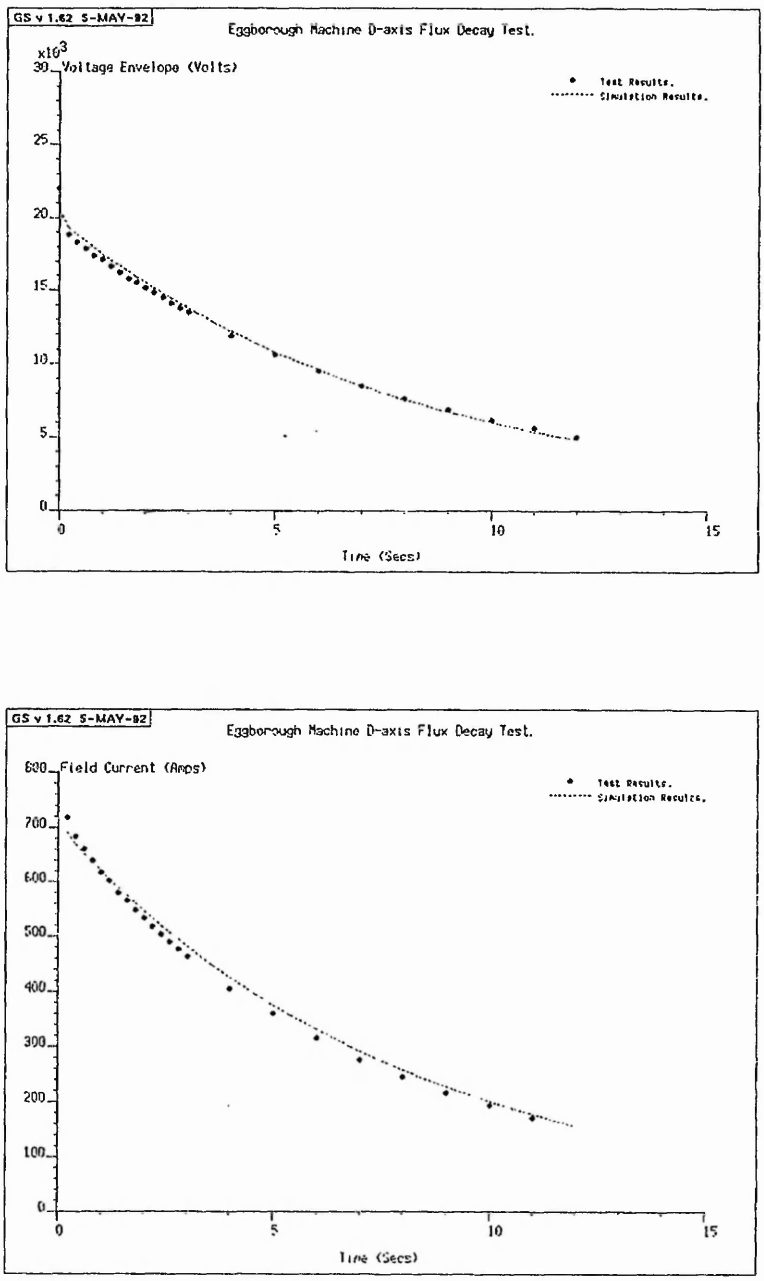

Figure 6.1, Eggborough machine D axis flux decay test

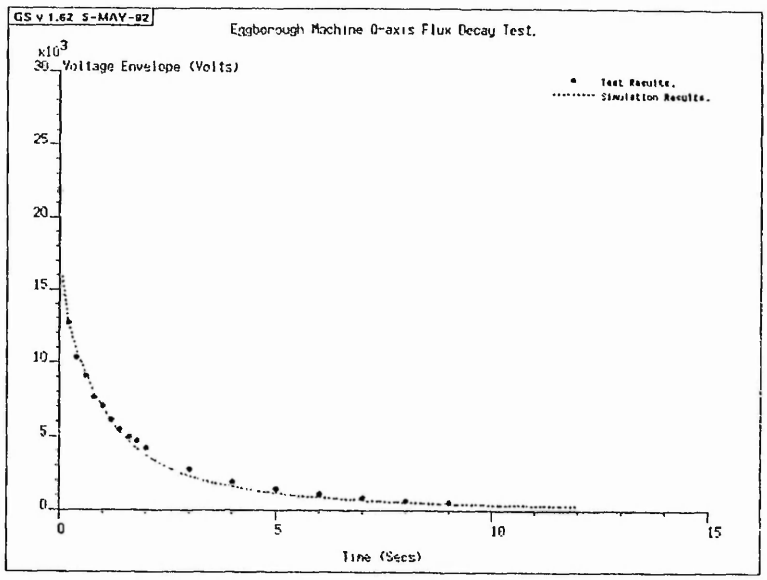

Figure 6.2, Eggborough machine Q axis flux decay test

6.2.1 Comparison of terminal quantities

Flux decay test simulations are performed on two machines, the Eggborough machine and the Uskmouth machine. Both of these machines are of similar design topology but differ in detail and are of different overall size. This enables a single equivalent circuit topology to be used to simulate the test for both machines.

The terminal quantities presented for comparison in figures 6.1 and 6.2 are for the flux decay test simulation on the Eggborough machine. Figures 6.3 and 6.4 refer to the Uskmouth machine. The D axis terminal quantities presented for comparison are the decay of the stator voltage envelope and the decay of the field current for the duration of the transient. The Q axis terminal quantity presented is the decay of stator voltage only. This is because the field winding does not effectively link the stator during the Q axis transient.

It is acknowledged that Haydock (16) has presented flux decay simulation results for both the Eggborough and Uskmouth machines using a similar equivalent circuit technique. However, there are two significant differences between the results presented in this thesis and those presented by Haydock.

The results presented by Haydock are limited to an envelope of stator voltage. The results presented in this thesis include the stator voltage envelope, the field winding current and a eddy current quantities from the wedge, damper and iron eddy current paths within the rotor. Further, the wide range of results presented throughout this chapter clearly demonstrate the wide range of additional electrical and magnetic quantities which can be obtained from test simulations using the generalised equivalent circuit technique developed in chapters three and four of this thesis.

The results presented by Haydock are for the initial four seconds of the flux decay test. The results presented in this thesis demonstrate a good correlation with actual test data for the full duration of the test, up to twelve seconds after $t = 0$.

These differences between the work presented by Haydock and the work presented in this thesis centre around the equivalent circuit representation of mutual dampance between flux paths within a machine. It is clearly demonstrated in earlier chapters that Haydock assumes no mutual dampance between linked magnetic circuits. The implications of this assumption for the simulation results presented by Haydock are discussed fully later in this chapter.

The results throughout this chapter are therefore presented as results which have been obtained from original equivalent circuit models developed in the earlier chapters of this thesis.

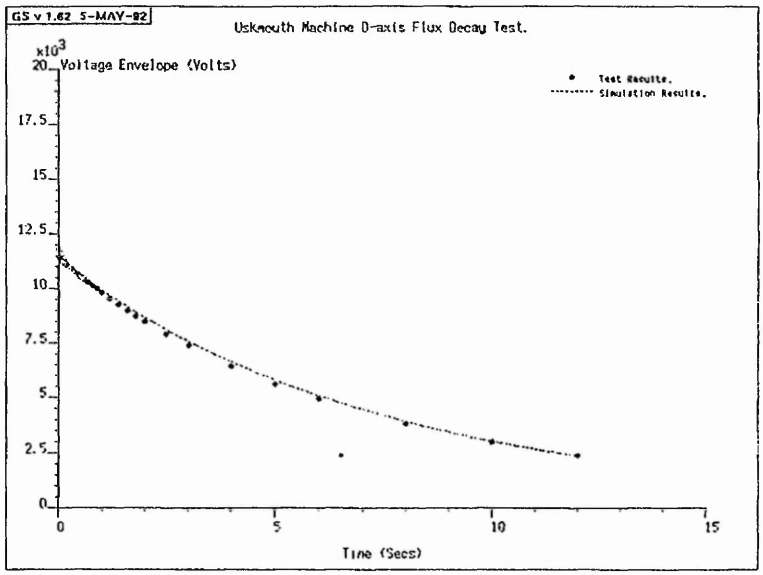

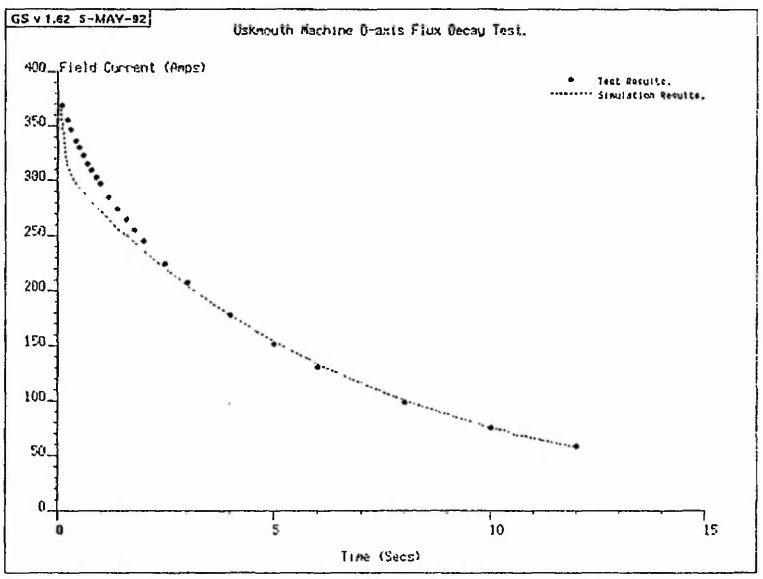

Figure 6.3, Uskmouth machine D axis flux decay test results

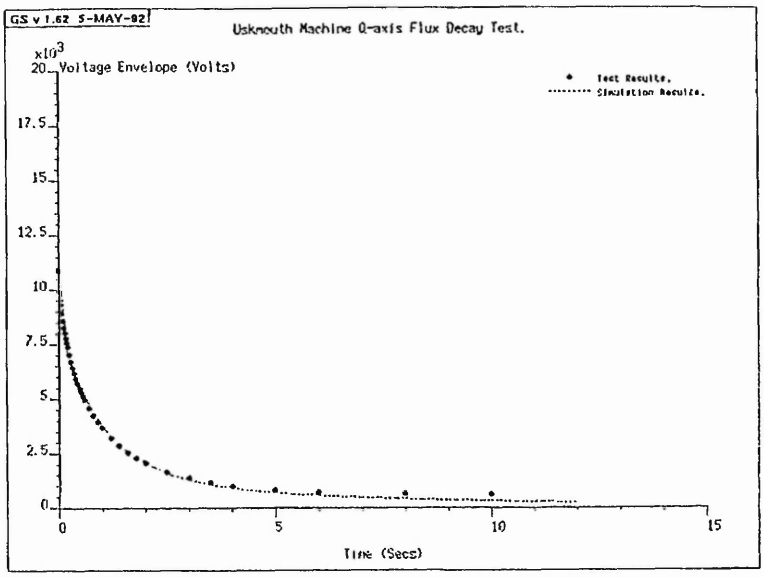

Figure 6.4, Uskmouth machine Q axis flux decay test results

6.2.2 The behaviour of the equivalent circuit model during the flux decay test

During the flux decay test simulation the magnetic flux stored within the machine's air gap is allowed to decay. This decaying flux induces an electric potential in any electric circuit linking it, in such a way that the resulting electric current will attempt to support the decaying flux. As the level of flux decays the rate of change of flux also decays as energy is dissipated from the system. Within the less well defined damper circuit of a solid iron pole, a reducing rate of change of flux will cause an increasing cross-sectional area of the iron to be used by the eddy currents. This has the effect of continually reducing the amount of resistance in the damper circuit. The damping effect of the damper circuits will, therefore, be continually increased as the transient progresses. This effect becomes apparent at the stator terminals because the time constant of the stator voltage decay envelope is continually increasing as the

transient develops. Early workers (5,23,24,33) have attempted to describe this continual changing time constant using a number of discrete parameters. Whereas this is certainly feasible if the rotor damper circuits are made up of discrete well defined windings, it is only an approximation if the damper circuits are less well defined, as is the case for the solid iron pole of a synchronous machine.

This process is very similar to the behaviour of the equivalent circuit model. Consider the equivalent circuit representing a single slot pitch presented in figure 4.7. Electric flux stored in the magnetic capacitors representing the air gap permeance is allowed to decay. The rate of decay of electric flux will be controlled by the network representing the rotor topology. Within this network potentials are induced into the circuits representing the eddy current paths by the magnetic current (defined as rate of change of flux) flowing in the circuit representing the magnetic paths. The resulting currents in the eddy current paths are fed back into the magnetic equivalent circuit so as to oppose the changing flux. This arrangement is usually simplified by referring the network representing the eddy current paths into the magnetic equivalent circuit as a combination of purely resistive devices. Although this simplification tends to mask the traceability that may exist between the magnetic circuit and its equivalent, it does provide a useful insight into the passive nature of eddy current circuits within the rotor magnetic circuit of a machine. The individual time constant of each of the layers within the model allow the equivalent circuit to represent the effect of the penetration of the eddy currents into the rotor.

Although the operation of the equivalent circuit is similar to that of the flux within the machine, the rate of change of flux in the equivalent circuit model is represented as a conduction current in magnetic conductors whereas in the rotor of a machine the rate of change of flux is equivalent to a displacement current. This conceptual difference is more fully discussed in chapter three of this thesis.

6.2.3 The effect of the mutual dampance terms on flux decay test results

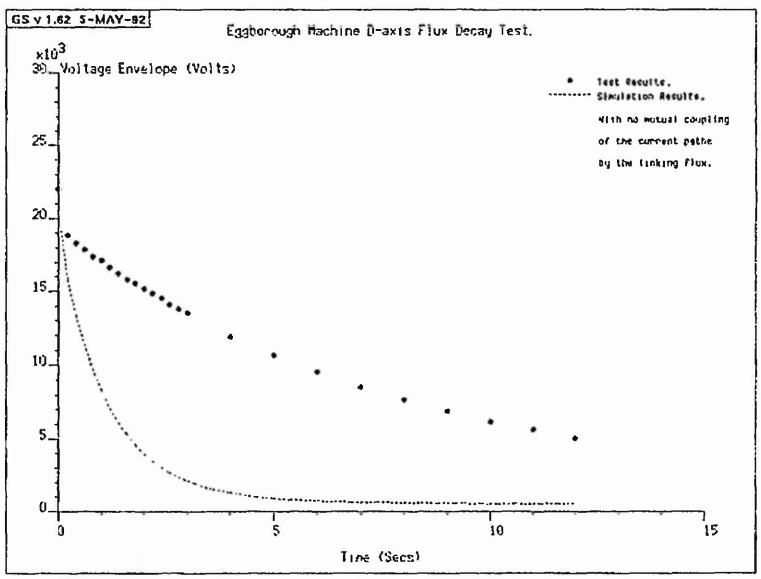

Figure 6.5, Eggborough machine D axis flux decay test results ignoring mutual dampance

The equivalent circuit models, derived by Haydock (16) for the purpose of simulating the flux decay test, were based on the assumption that the linking effect of damper and

eddy current circuits within a machine's rotor can be ignored. This assumption is implied when electric circuits linking more than one flux path are referred into the magnetic circuit solely as resistive elements. Equivalent circuit models would, therefore, only represent the self dampance terms of the dampance matrix presented in chapter three and ignore mutual terms. This assumption is made throughout the equivalent circuit simulations presented by both Haydock (16) and Carpenter M.J. (29).

Figure 6.5 shows a comparison between the results obtained for a D axis flux decay test simulation in which mutual dampance terms are ignored and actual test data. The agreement with the actual test data is clearly very poor. This is consistent with the work presented in chapter three of this thesis. In chapter three it is demonstrated that the mutual terms in the dampance matrix are responsible for a significant part of the overall damping effect. If these terms are ignored the damping effect of the rotor is greatly reduced causing the flux to decay more quickly. This is clearly demonstrated in figure 6.5.

A Q axis flux decay test simulation in which mutual terms in the dampance matrix are ignored was also performed. The simulation results more closely matched actual test data when compared to the equivalent D axis simulation. This suggests that the mutual linking of electric circuits within the rotor is less important for a Q axis simulation. It is thought that there may be two reasons for this. Firstly, the field winding, which dominates the D axis transient, links a number of permeance paths in the rotor. Any reduction in the damping effect of the field winding will therefore

severely affect the decay of the flux within the machine as a whole. This effect of the field winding is not present in a Q axis flux decay test. Secondly, the topology of the equivalent circuit is based on layers of increasing depth to represent layers of eddy current paths within the pole region. As a result the damping effect of each of the layers closer to the rotor surface is reduced as the number of linked permeance paths is increased. This technique of layering the defined permeance paths within the pole region of the rotor has also been used by Carpenter M.J. (29).

The effect of the mutual terms within the dampance matrix clearly suggests a possible explanation for Haydock's limited simulation results (16). Clearly the inclusion of these mutual dampance terms are fundamental to a successful flux decay test simulation. This is particularly so for the D axis simulation.

The solution of the equivalent circuits configured for a flux decay test varies between approximately 10 minutes CPU time for a Q axis simulation and approximately 30 minutes CPU time for a D axis simulation. These times are for a solution using SPICE ver 2G6 running on a VAX 8700 at Nottingham Trent University.

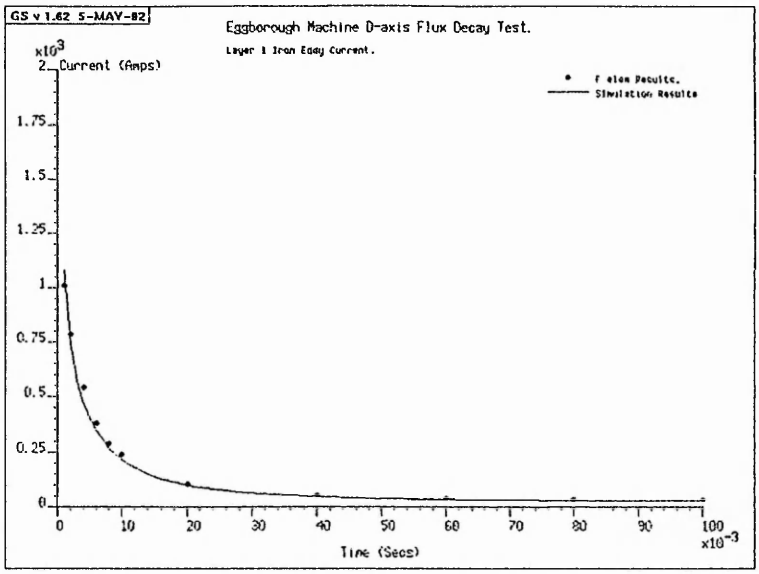

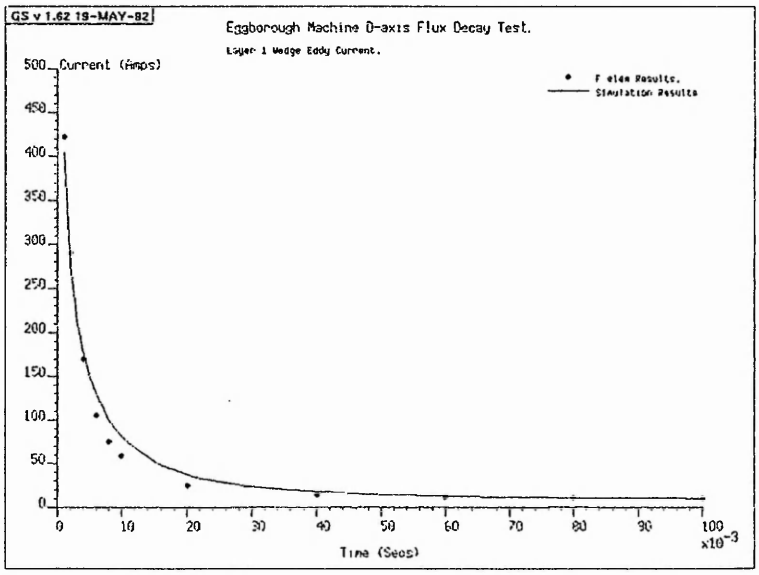

Figure 6.6a, Eggborough machine D axis flux decay test. Current in layer 1 iron (upper) and current in layer 1 wedge (lower)

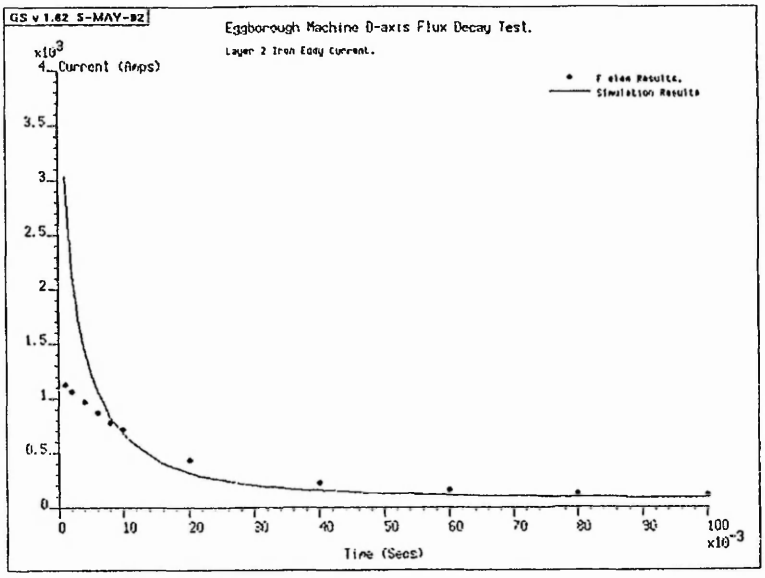

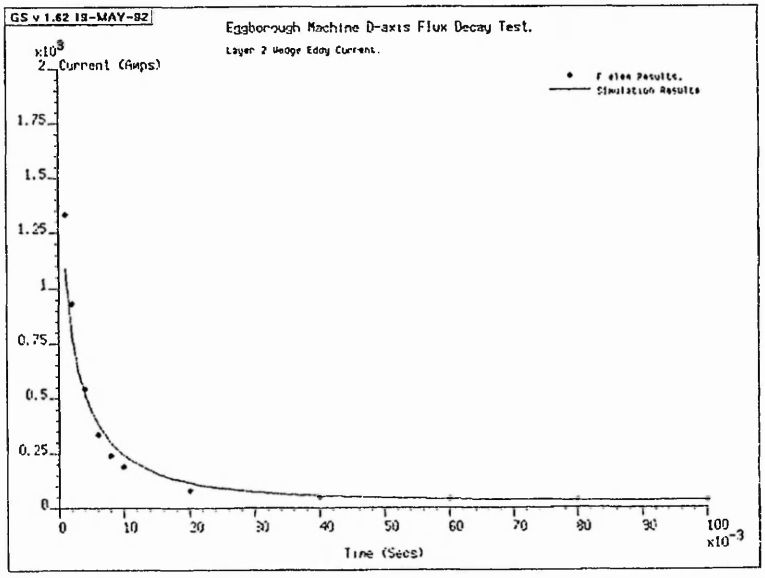

Figure 6.6b, Eggborough machine D axis flux decay test. Current in layer 2 iron (upper) and current in layer 2 wedge (lower)

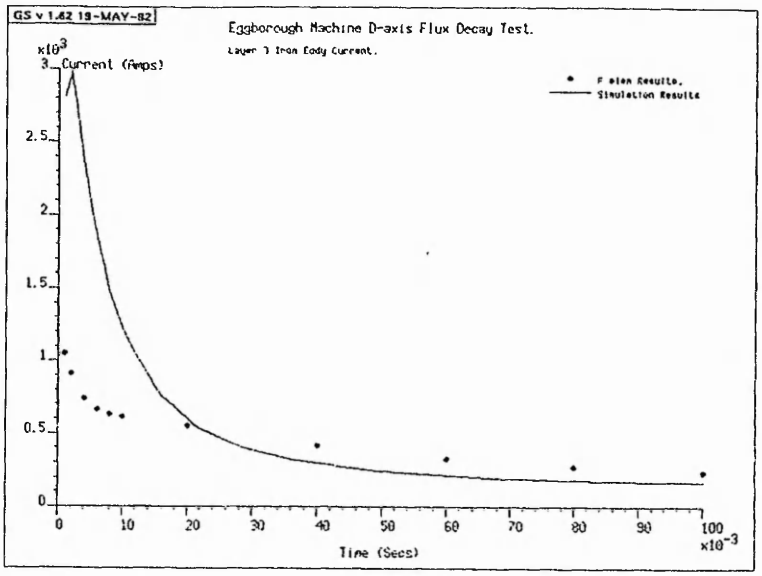

Figure 6.6c, Eggborough machine D axis flux decay test. Current in layer 3 iron

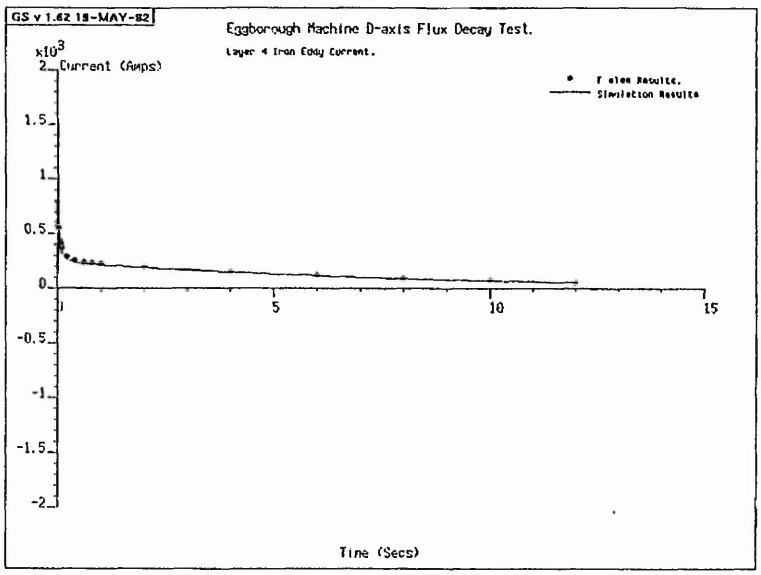

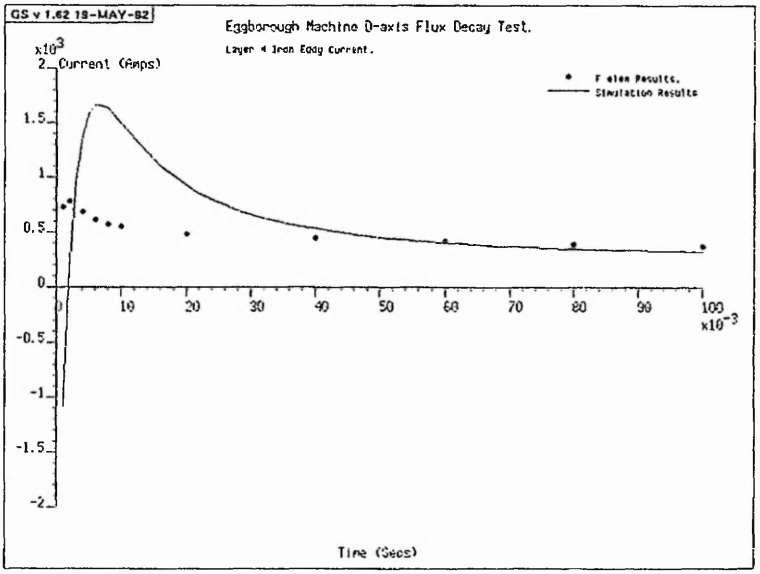

Figure 6.7a, Eggborough machine D axis flux decay test. Current in layer 4 iron

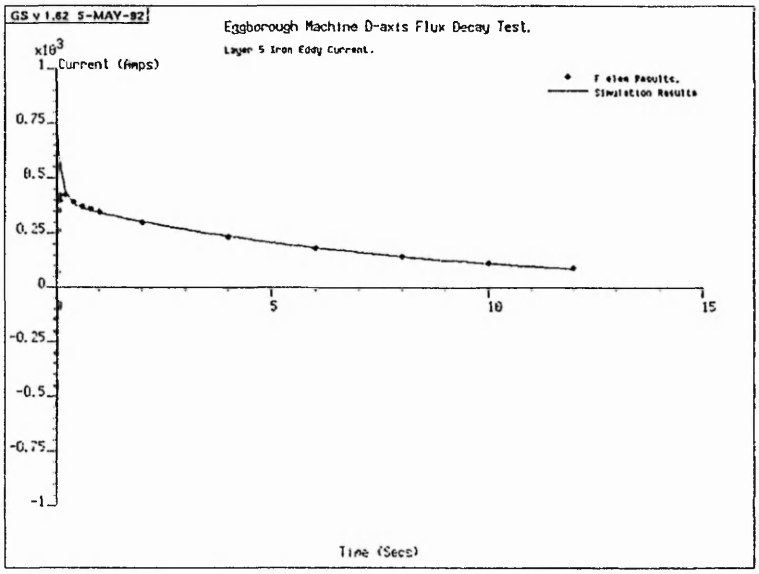

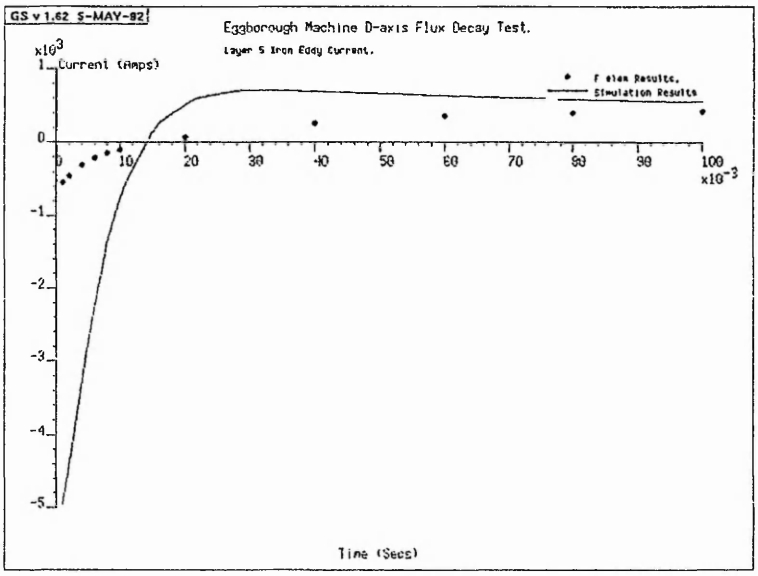

Figure 6.7b, Eggborough machine D axis flux decay test. Current in layer 5 iron

6.2.4 Comparison of internal rotor quantities

The flux decay test typically yields results in the form of the stator and field winding terminal quantities presented earlier in this chapter. However, it is demonstrated in chapters four and five that the behaviour of eddy currents in the machine's rotor damper circuits can also be investigated using the generalised equivalent circuit technique developed in this thesis. The prediction of both terminal and internal rotor quantities during transient conditions is particularly important because large forces can be exerted on current carrying conductors within a machine's magnetic field. Whereas the current in a winding may be physically measured, it is more difficult to measure a current that exists within the damper circuits made up of the wedges, damper bars, iron and end bell. Within this section, therefore, eddy currents in different parts of the machine are investigated.

A parallel finite element simulation of a flux decay test is described in the chapter five of this thesis. The results from this simulation are compared with the results obtained from the equivalent circuit simulation. The material constants used throughout the equivalent circuit model have been used in the finite element model in an identical manner so that any difference between the results from the two simulations may be attributed to the modelling methodology.

The basis for the equivalent circuit topology used throughout this thesis is the subdivision of the rotor's topology in two dimensions. Figure 4.5 shows how each segment is sub divided into a number of layers. The outer most layer is typically 1.5mm thick and the thickness of each layer is doubled with increasing depth. Eddy

currents are assumed to flow axially within the boundaries of the different materials and defined concentric segments. Although the eddy currents within the finite element model are also assumed to run axially, the level of discretisation is many times that adopted by the equivalent circuit model. This effect of the increase in discretisation is discussed later on in this chapter.

Figures 6.6 and 6.7 demonstrate how the eddy currents in the third slot pitch from the Q axis vary with both position and time in an approximate slot depth during a typical D axis flux decay test simulation.

In general terms there is a close agreement between the results obtained from the equivalent circuit and finite element simulations. This is particularly evident for times in excess of 0.1 second after the start of the transient. The level of agreement prior to 0.1 second varies depending on the depth of the layer being considered. There appears to be an improved agreement for layers closest to the surface of the rotor. This is thought to be due to the differing levels of discretisation. The ability of the equivalent circuit to represent the penetration of eddy currents perpendicular to the slot wall is limited because of the lack of radial discretisation. The finite element mesh, however, provides a high level of discretisation in this area and is therefore more capable of representing these eddy currents.

The results obtained from both simulations show a very sharp peak in the value of these eddy currents immediately after the transient has started. This large peak only lasts for a very short period typically a few tens of micro seconds and depends on the

depth of the eddy current. A summing of the values of the currents which are shown to exist within the wedge immediately after the switch has been opened indicates a peak current in excess of 3000A. The presence of this relatively large current in the wedge will cause an additional force to be exerted on the wedge and teeth due to the presence of the resulting magnetic field.

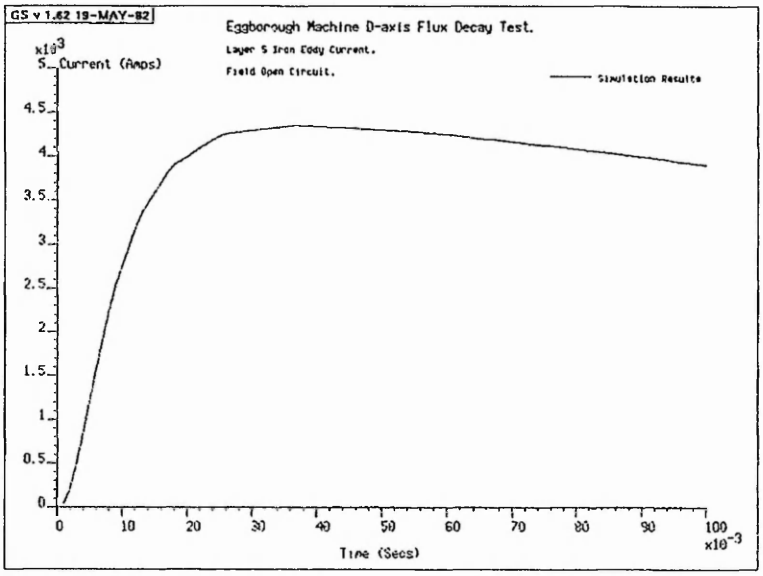

Figure 6.8, Eggborough machine D axis flux decay test. Current in layer 5 iron with field open circuit

The eddy currents induced in the iron teeth at a depth which corresponds to layers four and five are shown in figure 6.7. Immediately after the start of the transient the eddy current is shown to be induced in opposition to the flow of eddy currents in layers 1, 2 and 3. This phenomenon is present in both the equivalent circuit and finite element simulations. To assist with the following discussion it has been assumed that a decaying magnetic field will induce a positive current flow in the rotor damper circuits. The depth of the layers which experience a negative eddy current flow correspond to

the depth of the copper conductors of the field winding. The negative direction of the eddy currents within the area defined by these layers would suggest that there is a magnetic field which is increasing in magnitude. It is thought that this phenomenon is caused by the multiple turns of the field winding transporting the electric current induced close to the surface of the rotor down into the rotor body (58). The current in the field winding would, therefore, be responsible for the increasing magnitude of the magnetic field in this area. The initial negative eddy current in the tooth iron would therefore be induced in an attempt to oppose the locally changing magnetic field. This hypothesis is supported by an equivalent circuit simulation of a flux decay test with the field open circuit. The flux decay test simulation is identical in every other respect to that used to obtain the results shown in figures 6.6 and 6.7. Figure 6.8 shows the eddy currents present in layer five during this simulation. It is evident from figure 6.8 that there are no negative eddy currents within the tooth iron, which would suggest that the flux within a tooth is decaying for the whole of its depth.

6.3 The frequency response test simulation results

6.3.1 Comparison of terminal quantities

Frequency response test simulations are performed for two machines, the 500MW Eggborough machine and the 660MW Torness machine. The equivalent circuits used to represent the machine for the simulation are identical in every respect to the equivalent circuits used for the flux decay test simulations with the exception of the representation of the stator. The representation of the stator is modified to include the relevant stator winding and stator slot leakage permeance. These modifications are fully described in the previous chapter. Test results available for comparison with the

simulation results were limited to the Torness machine (58). However the results from the simulation for the Eggborough machine are compared to the three circuit mathematical model described by Adkins (42). This approach has also been adopted by Turner (6) to enable a validation of the results obtained from a finite element study. It is, therefore, demonstrated that the results presented here are also in close agreement with those presented by Turner.

The results usually associated with frequency response tests are in the form of an operational impedance or inductance and field current transfer function depending on the quantity of interest. These are obtained from actual test data using the three axis to two axis transformations described by Adkins (42). This transformation is also performed within the equivalent circuit model to ensure that the results obtained from the models are in a comparable format. The implementation of the two axis winding is fully described in chapter five of this thesis. The simulation results are presented and compared in graphical form as operational inductance and field current transfer function versus frequency.

The frequency response test is often criticised because the physical conditions which prevail during a typical test are not consistent with normal operating conditions. The two most common criticisms are that the contact resistances within the damper circuits are likely to be increased because the machine is at standstill and the level of flux within the machine is also greatly reduced because of the reduced level of excitation. This will obviously affect the level of saturation within the machine. Although these are some typical comments criticising the frequency response test, the test conditions

are in fact more compatible with the assumptions made for a typical frequency response simulation.

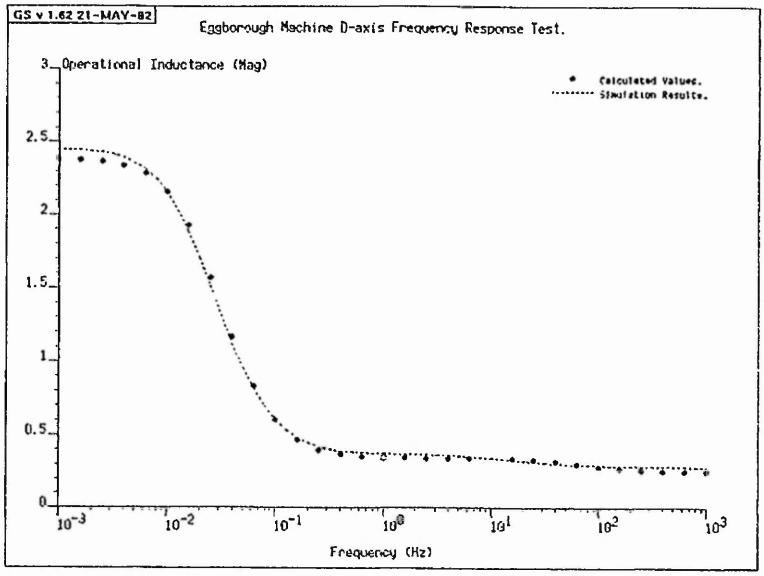

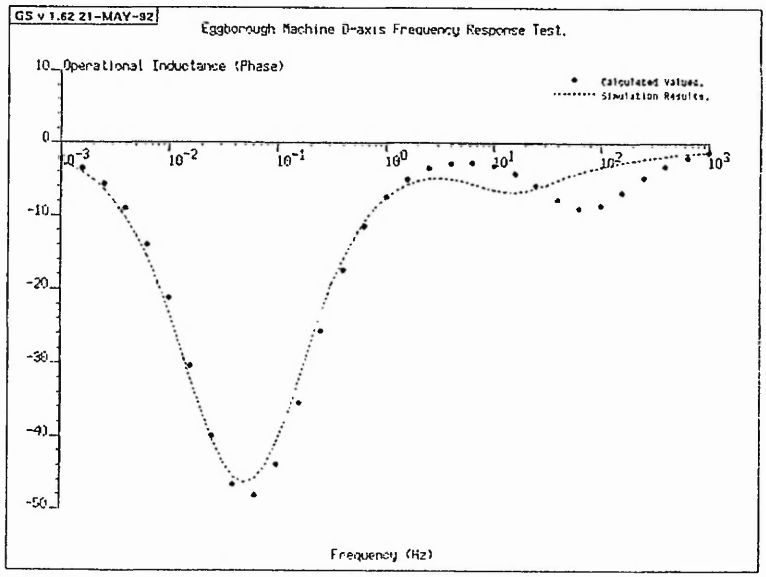

Figure 6.9, Eggborough machine D axis frequency response test. Operational inductance, magnitude (upper) and phase (lower)

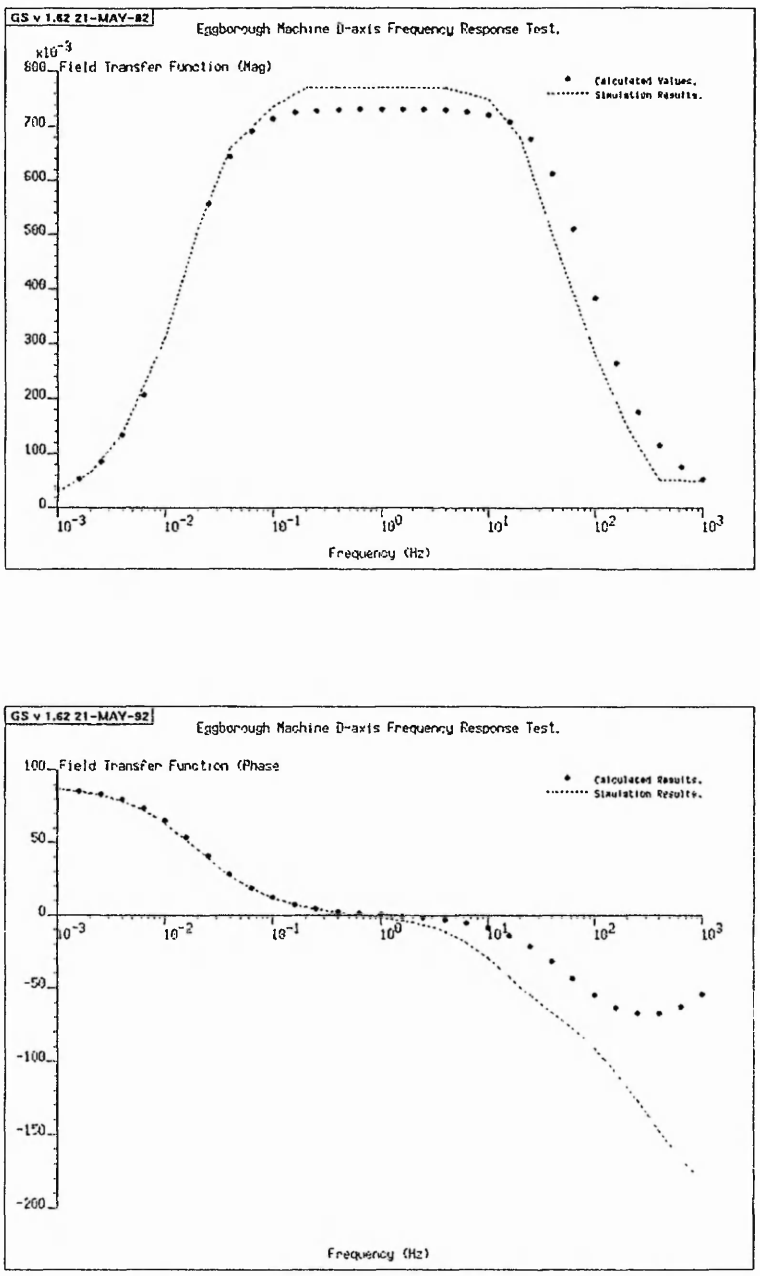

Figure 6.10, Eggborough machine D axis frequency response test. Field transfer function, magnitude (upper) and phase (lower)

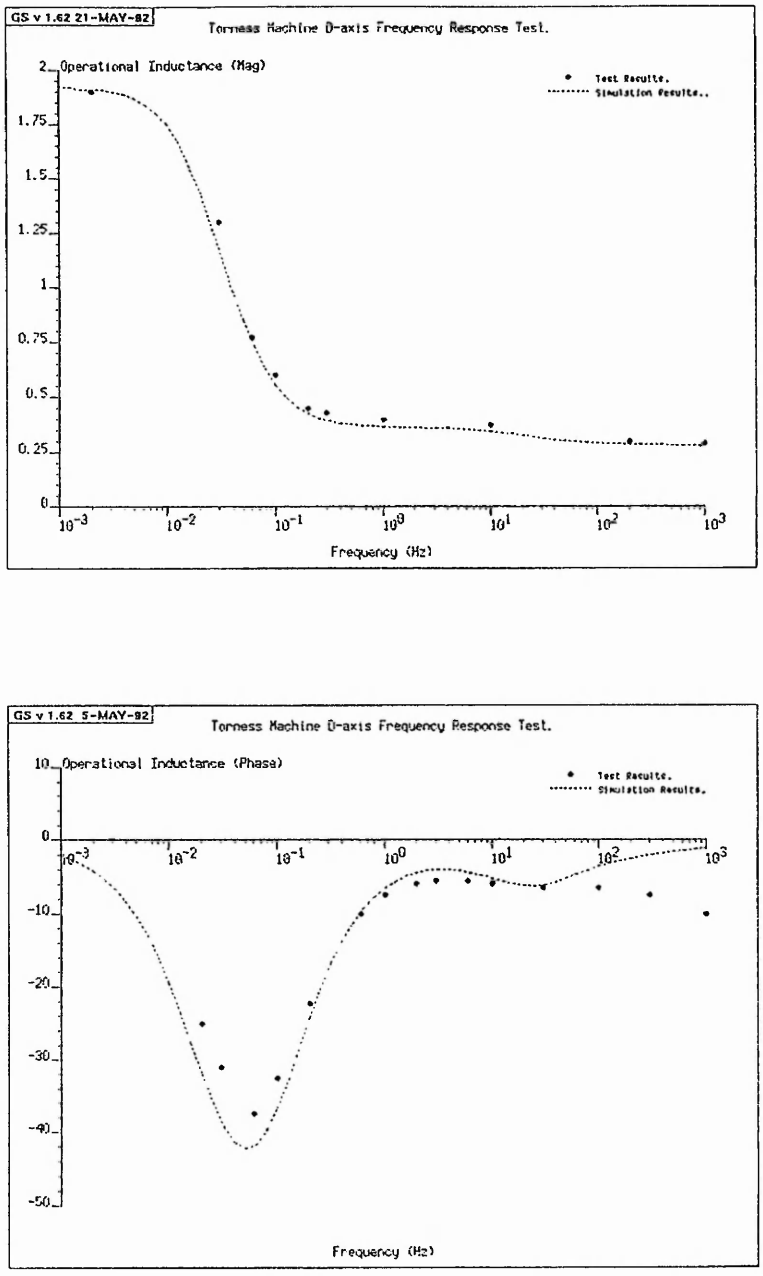

Figure 6.11, Torness machine D axis frequency response test. Operational inductance, magnitude (upper) and phase (lower)

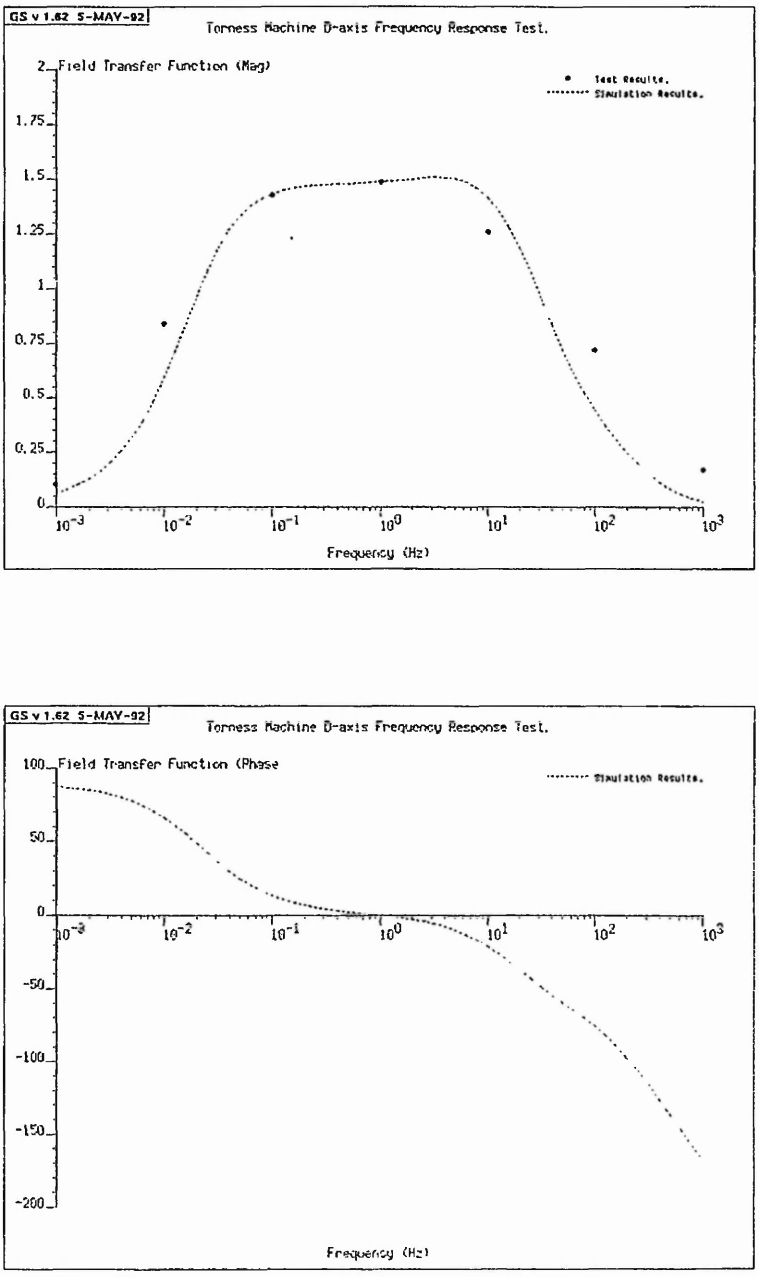

Figure 6.12, Torness machine D axis frequency response test. Field transfer function, magnitude (upper) and phase (lower)

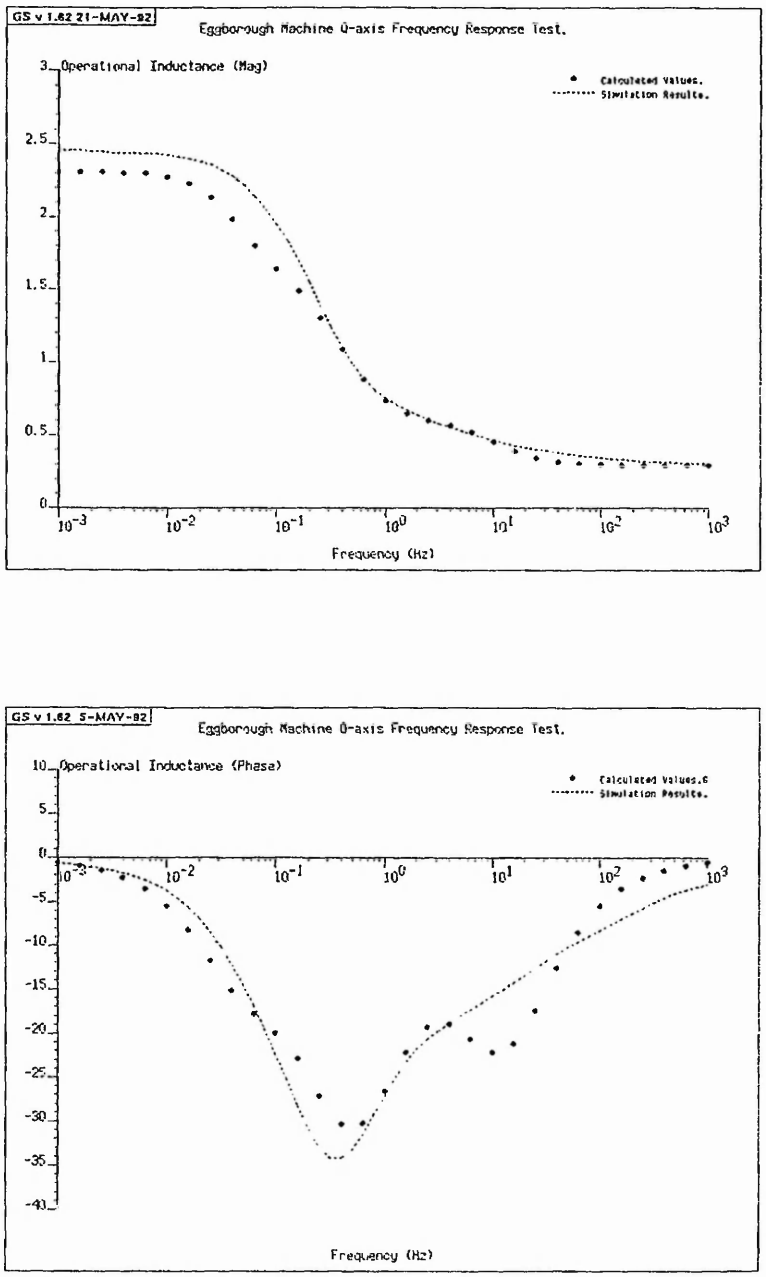

Figure 6.13, Eggborough machine Q axis frequency response test. Operational inductance, magnitude (upper) and phase (lower)

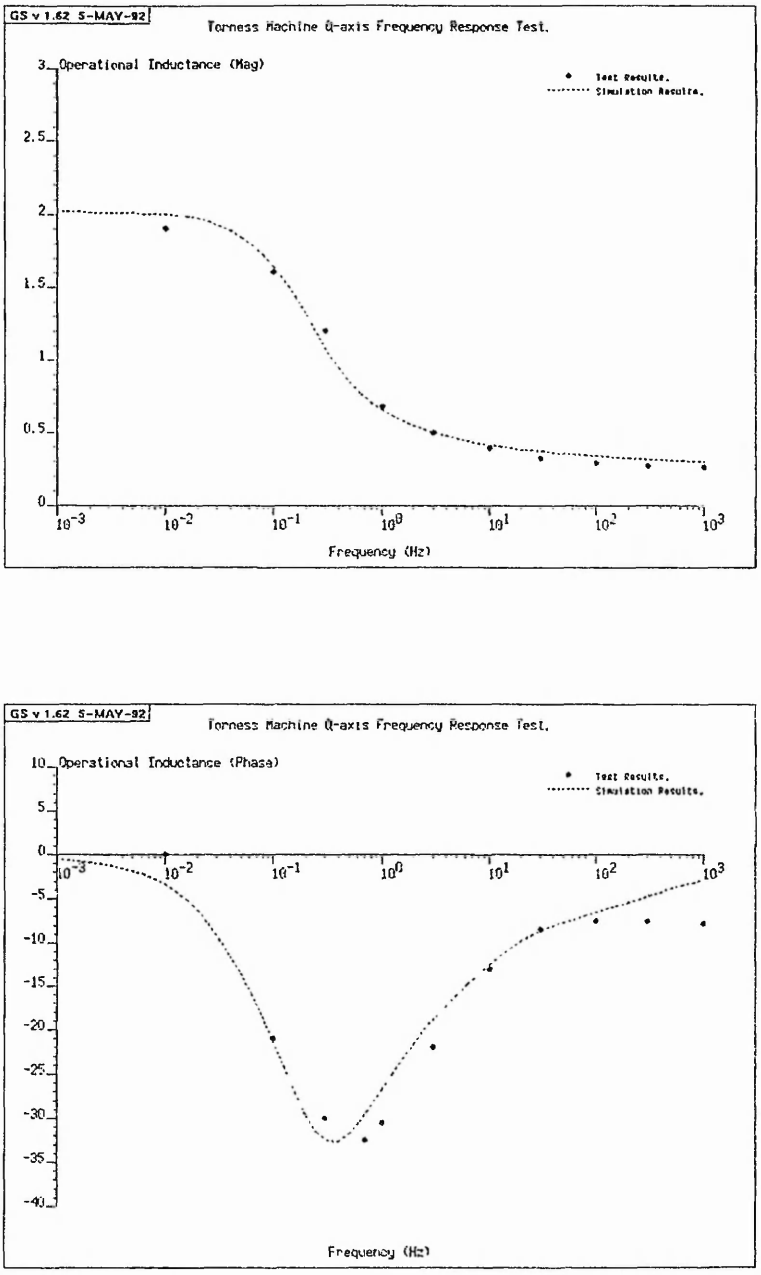

Figure 6.14, Torness machine Q axis frequency response test. Operational inductance, magnitude (upper) and phase (lower)

Figures 6.9, 6.10 and 6.13 show a comparison between the results obtained from the Eggborough machine frequency response test simulation and the two or three circuit mathematical model described by Adkins (42) and presented here as equations 6.1, 6.2 and 6.3. In these equations the D axis and Q axis operational inductances $L_d(s)$ and $L_q(s)$ respectively and the field current transfer function $sG(s)$ are given by:

$$L_d(s) = L_d\frac{(1+sT_d')(1+sT_d'')}{(1+sT_{do}')(1+sT_{do}'')} \quad \text{.... 6.1}$$

$$L_q(s) = L_q\frac{(1+sT_q')(1+sT_q'')(1+sT_q''')}{(1+sT_{qo}')(1+sT_{qo}'')(1+sT_{qo}''')} \quad \text{.... 6.2}$$

$$sG(s) = G_0\frac{(1+T_{kd})}{(1+sT_{do}')(1+sT_{do}'')} \quad \text{.... 6.3}$$

Where T_d' and T_d'' are the D axis short circuit time constants,
T_q', T_q'' and T_q''' are the Q axis short circuit time constants,
T_{do}' and T_{do}'' are the D axis open circuit time constants,
T_{qo}', T_{qo}'' and T_{qo}''' are the Q axis open circuit time constants,
T_{kd} is the time constant of the damper circuit, (i.e. $T_{kd} = X_{kd}/\omega_0 R_{kd}$),
L_d and L_q are the stator input inductance at zero frequency,
and G_0 is the ratio of the direct axis magnetising reactance and the field resistance, (i.e. $G_0 = X_{md}/R_f$).

It was found that the two circuit model was in closest agreement with the simulation results for the D axis test whilst the three circuit fit gave the closest agreement for the Q axis case. Although it is acknowledged that verification of the frequency response

simulation results using this approach is not ideal, it was found to be necessary because no frequency response test data is available for the Eggborough machine. Turner (6) has also used this technique to verify results obtained from a finite element simulation of the frequency response test on the Eggborough machine. The finite element simulation results were also in close agreement with the two and three circuit mathematical model.

Figures 6.11, 6.12 and 6.14 show a comparison between the frequency response test simulation and actual test data for the 660 MW Torness machine (58). The actual test results have been corrected for winding resistance. The effect of winding resistance has, therefore, been eliminated from the simulation results by measuring only the potential induced in the stator winding by the magnetic circuit. The equivalent circuit model topology used to represent the Torness machine for the frequency response test is identical to that used for the Eggborough machine. The values of the equivalent circuit devices have been calculated from the physical machine dimensions and modified material bulk constants of the Torness machine.

6.3.2 The behaviour of the equivalent circuit model during the frequency response test

The equivalent circuit model used to represent the rotor of the Eggborough machine during the frequency response test is identical in every respect to that used to represent the flux decay test. However, the behaviour of the magnetic field within the rotor is subtly different under these test conditions. This is demonstrated within the equivalent circuit model.

$$\text{skin depth, } \delta = \frac{1}{\sqrt{\omega\sigma\mu}} \qquad \ldots. 6.4$$

The behaviour of the magnetic field within a synchronous machine during a frequency response test has been investigated using finite element techniques (6,54,58). It has been demonstrated that the flux within the machine is prevented from penetrating into the rotor by eddy currents flowing in the rotor. These eddy currents are induced by the changing field, and their magnitude is dependent on the per unit rate of change of the flux or frequency. The depth to which the flux penetrates is described by the equation for skin depth shown here as equation 6.4. By considering this equation it is apparent that the depth to which the field will penetrate is dependent on frequency, conductivity and permeability. The following paragraphs will attempt to describe the mechanism by which this phenomenon takes place within the equivalent circuit analogy.

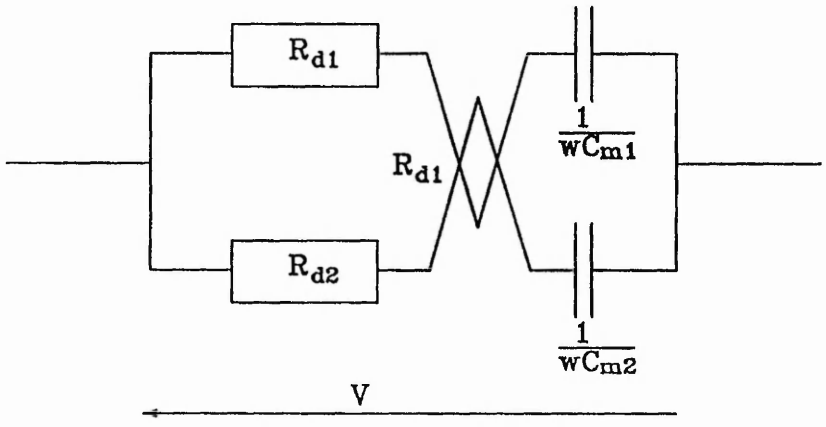

Figure 6.15 Parallel RC branches

Within the equivalent circuit model the conductivity and permeability are represented by lumping volumes of material or space to form discrete components. Dampance may therefore be described as a lumped form of conductivity, and permeance may be described as a lumped form of permeability. This is further demonstrated by equations 3.2, 3.4 and 4.2. These discrete devices are then linked by magnetic conductors. Within these conductors the magnetic current is proportional to the frequency of the supply and the charge held by the capacitive elements is a representation of the flux. Consider figure 4.7, in which the values of the electric resistances present in the damper circuits are fixed by the physical dimensions of the machine in the same way as the conductivity of the rotor is fixed. However, the value of impedance associated with the capacitive elements will vary depending on the frequency of the induced m.m.f.. The mechanism which prevents the penetration of flux within the equivalent circuit may therefore by described as a function of the permeance with respect to the dampance for each layer within the equivalent circuit.

Figure 6.15 shows a very much simplified representation of a ladder network typical of those shown in the equivalent circuit described in chapters four and five of this thesis. R_{d1} and R_{d2} represent the dampance of two different layers within the equivalent circuit and C_{m1} and C_{m2} represent two leakage permeances associated with those layers. Typically if R_{d1} is closer to the rotor surface than R_{d2} the value of R_{d1} would be very much smaller than R_{d2}. At low frequencies the reactances of C_{m1} and C_{m2} would be relatively high thus causing a larger quantity of charge to be stored, due to an increased proportion of the m.m.f. being dropped across them. At increased frequency the reactances of C_{m1} and C_{m2} would be reduced and the potential would therefore be

redistributed in favour of the dampances R_{d1} and R_{d2}. This has the effect of reducing the amount of stored charge within permeances at a greater depth. To demonstrate how flux is effectively prevented from penetrating into the rotor some typical values have been introduced into figure 6.15. The value of C_{m1} is made equal to that of C_{m2}. This is because the typical values within the equivalent circuit models are a function of the discretisation and not the physical properties associated with the machine. They can, therefore, be chosen in an arbitrary manner.

The following table shows how the distribution of flux varies for two frequencies and has been constructed using the following values, $R_{d1} = 20\Omega$, $R_{d2} = 200\Omega$, $C_{m1} = C_{m2} = 20\mu F$. The table below compares the potential drop across C_{m1} and C_{m2} as a percentage of the overall potential V.

Frequency	1Hz	100Hz
C_{m1}	99%	99%
C_{m2}	88%	35%

Clearly the distribution of magnetic charge within the equivalent circuit model during the frequency response test will be such that, at high frequencies, the flux will tend to be distributed away from the centre of the deeper layers because they have larger damping effects associated with them. This explanation, although it describes the same effect, is subtly different from their more traditional explanation which describes the penetration of flux and eddy currents.

6.4 The sustained short circuit test simulation results

A sustained short circuit test simulation is attempted for the Eggborough machine using an equivalent circuit model derived from that presented in figure 5.5. Within this model the representation of the rotor is less descretised than that used for the flux decay and frequency response test although the concept of segments and layers is maintained. The representation of the stator is similar to that used in the frequency response test simulation although the three phase windings are represented explicitly using time variant linkages. These aspects of the equivalent circuit model are fully described in the previous chapter.

The sustained short circuit test requires that the phase windings be shorted and connected to the neutral point. However, the circuit solver SPICE failed to converge to a solution under these conditions. A simulation was, therefore, performed with the phase windings open and the field winding excited with a current of one amp. The resultant open circuit waveforms are presented in figure 6.16.

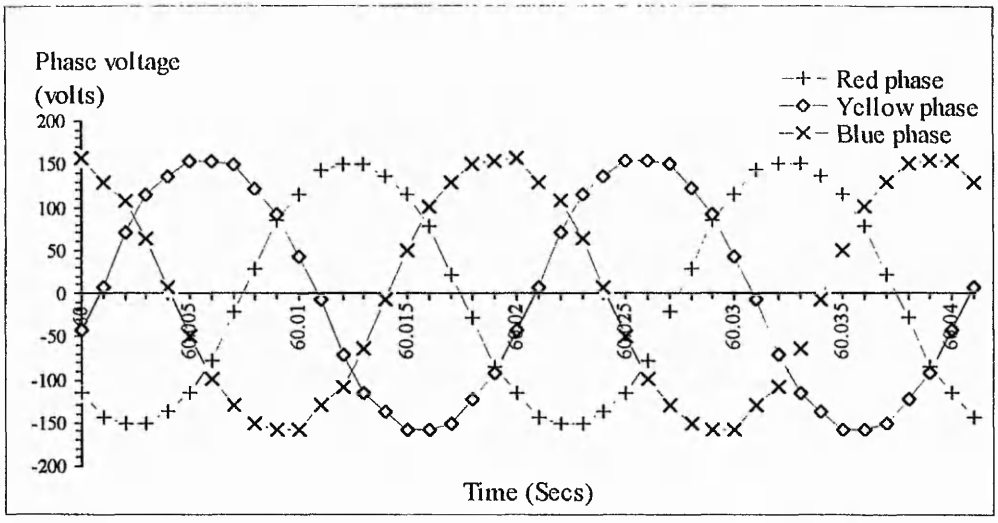

Figure 6.16, Eggborough machine D axis open circuit waveform

Clearly visible in figure 6.16 are the three sinusoidal phase voltages with a time period of 20mS and 120° displaced. The results from this simulation clearly improve the credibility of the equivalent circuit model, particularly in terms of the operation of the stator winding linkages and the representation of the rotationally induced e.m.f..

Harmonic	Frequency (Hz)	Normalised component	Normalised phase (°)
1	50	1.000	0.000
2	100	0.000	-0.329
3	150	0.051	84.103
4	200	0.000	65.137
5	250	0.002	35.728
6	300	0.000	149.089
7	350	0.004	235.764
8	400	0.000	23.739
9	450	0.022	193.991

Figure 6.17 Fourier components of red phase open circuit voltage for the Eggborough machine simulation

A fourier analysis of the waveform obtained from the red phase winding, presented in figure 6.17, indicates the presence of two harmonic voltages. These are the 3rd and 9th harmonic with normalised components of 5% and 2% respectively. Further, these harmonic voltages have a normalised phase displacement of 84° and 193° respectively. The existence of these harmonic voltages in the simulated waveform is thought to be due to the topology of the equivalent circuit model. Within the model the phase windings and rotationally induced e.m.f. sources are crudely lumped into six segments per pole and the phase winding linkages assumed to be based on triangular waveforms. Clearly these simplifications and assumptions will have an effect on the quality of the open circuit waveforms.

6.5 Conclusion

In general terms the results obtained from the equivalent circuit models developed in the previous chapters are in close agreement with actual test data. The agreement is also consistent with the finite element simulations which have been performed for similar transient conditions (6,58,54). However, the level of detail which is obtainable from the finite element models is far in excess of a realistic equivalent circuit model. This is reflected in the computation requirements required for the different methods.

There is a very close agreement between the simulation and test results for the flux decay test simulation, however a similar level of agreement is not apparent for the frequency response test simulation results. Initially this would appear to be the

converse to the discussion presented earlier in this chapter. This was to suggest that it is more appropriate to model the frequency response test because the representation of the machine is more consistent with the physical test conditions.

It is thought likely that the very close agreement between the simulation and test results for the flux decay test simulation, and in particular the envelope of stator voltage, indicate that the overall level of flux present in the machine is being represented accurately. However, the distribution of the flux within the machine is determined by the equivalent circuit topology, discretisation and material bulk constants. The topology and discretisation of the equivalent circuit has been reduced in order to reduce unnecessary complexity and computation time. This process of development for the equivalent circuits is fully described in chapter four of this thesis. The bulk constants of the materials present within the machine have also been modified to reduce the complexity of the model. This is an attempt to include the effects of inertia gashes and the end bells within a two dimensional model. The penetration and/or distribution of flux within the machine is therefore likely to vary slightly from the actual distribution present along the length of the machine. The results presented in this chapter indicate that the frequency response test results may depend more heavily on the distribution of flux. This is demonstrated by the comparison of the results for the field transfer function.

The sudden short circuit test simulation failed to converge to a solution. However, the equivalent circuit model did yield a solution when the phase windings were opened. The resulting open circuit waveforms, therefore, are presented to demonstrate the

functionality of the equivalent circuit model topology.

There is always a trade off between accuracy and computation requirements. However, in this particular case, the level of complexity of the equivalent circuit was also limited by the electric circuit solver SPICE. It is considered that the reduction in the equivalent circuit complexity using the methods described previously is more than justified by the quality of the results obtained from the simulations.

The simulation results presented in this chapter are believed to be a significant improvement on those presented by previous authors (16,29) for two reasons. Firstly the scope for potential simulations has been widened to include the frequency response test. Secondly, and perhaps more importantly, the potential to use this equivalent circuit technique to evaluate a wide variety of electric and magnetic quantities within the machine is established. For example, the models developed in this thesis have been used to evaluate a machine's terminal voltages and currents, eddy current values and the winding transfer functions associated with a machine's frequency response test.

The original work which has facilitated these improvements to the scope and quality of simulation results centres around the development and implementation of the dampance matrix developed in chapter three of this thesis.

Chapter Seven
Introducing dynamic dampance

7.1 Introduction

The equivalent circuit models developed in the earlier chapters of this thesis have been used successfully to represent a synchronous machine under two transient conditions. Although it is now possible to develop these models to enable an increasingly detailed representation of a machine there would be a corresponding increase in the computational demands made by such models. It is, therefore, thought by the author that applications for such work are likely to be limited because sophisticated finite element packages (28) are now widely accepted as the tool for the detailed analysis of machine behaviour.

The contents of this chapter describe the initial work undertaken with the intention of simplifying the topology of the equivalent circuit models developed in the earlier chapters of this thesis. A particular advantage of the approach adopted here is that it utilises standard computer software which is universally available. This would make such models attractive to engineers requiring a relatively accurate representation of a synchronous machine for inclusion in wider simulations. A typical application may be the simulation of a power system or a simultaneous representation of a power electronic controller and machine (29). Unfortunately, the time restrictions associated with this project are limited and therefore it is impossible to develop this approach beyond the stage of initial trials.

A particular characteristic of the equivalent circuit approach developed in the earlier

chapters for representing the magnetic circuit within any rotating machine is the relatively large and cumbersome nature of the models required. This characteristic has also been exhibited by models developed by a number of other authors (11,29,30,48). This is because the magnetic field within a synchronous machine exists within a complex topology and cannot, therefore, be represented using a simple linear equivalent circuit model, particularly if a wide range of transient conditions are to be represented.

A key area which is considered to significantly affect the accuracy of a machine model is the representation of the damping effect of the damper circuits within the rotor. It is acknowledged that improving the accuracy of an equivalent circuit model in this area alone by no means eliminates all the simplifying assumptions typically associated with synchronous machine models. However, it is believed by the author that a significant improvement in the accuracy of simple equivalent circuits could be achieved if this effect could be incorporated in a simple synchronous machine model.

7.2 An introduction to dynamic dampance

It has been demonstrated using finite element and equivalent circuit techniques both here and elsewhere (6,39,48) that the damping effect of a synchronous machine rotor is a factor which has a significant influence on the behaviour of the synchronous machine under transient conditions. The damping effect of the rotor is due to a number of closed electrical circuits consisting of the wedges, damper bars, and rotor iron in association with the end bells. All these rotor circuits have a significant effect on the transient behaviour, but the most difficult of these to represent is the solid iron of the

rotor. This is because the rate at which eddy currents penetrate into the solid iron is relatively slow when compared to the corresponding penetration of eddy currents into the non iron damper circuits of the wedges or field winding.

The following work describes how the damping effect of a solid iron pole region is represented using a single dynamic damping device. The dynamic damping device is implemented in SPICE in the form of a voltage dependent resistive component which is included in a simple equivalent circuit model. This representation is initially tested within a simple Q axis equivalent circuit model, the topology of which is derived from a very simple representation of the magnetic circuit that exists within a machine.

The Q axis flux decay test provides an ideal example to demonstrate this representation for two reasons. Firstly it has been demonstrated that the relative permeability of the rotor iron can be frozen at its pre test value (6) and secondly, the Q axis of this machine has no well defined damper circuits in the pole region. This allows the effect of a varying skin depth in the pole region to be modelled in relative isolation. The effects of magnetic saturation and additional well defined damper circuits may be added at a later stage in the development of the model.

The equivalent circuits developed in the earlier chapters of this thesis represent a typical solid pole region as parallel layers of leakage permeance. These enable the penetration of the eddy currents into the slotted and pole region to be represented with a reasonable degree of accuracy. The topological complexity of this equivalent circuit model is now effectively transferred into a single voltage dependent resistive device

present within a simplified equivalent circuit model.

7.3 The derivation of the equivalent circuit model topology

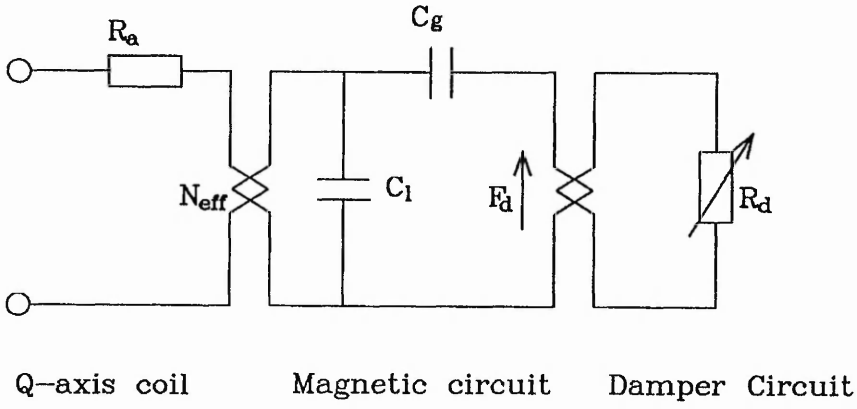

Figure 7.1 Experimental equivalent circuit model used in the initial trials for the dynamic damping model

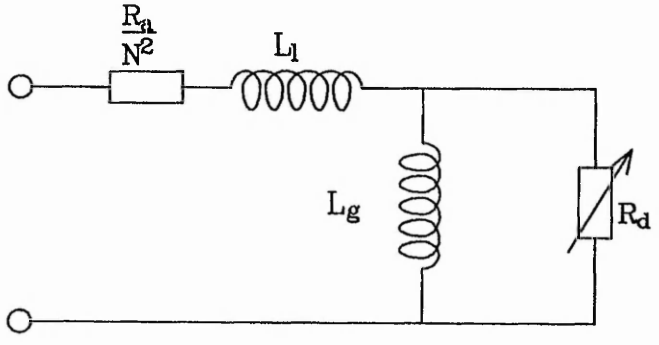

Figure 7.2 Dual of experimental equivalent circuit model presented in figure 7.1

Figure 7.1 shows the topology of the magnetic equivalent circuit model into which the dynamic dampance device will be incorporated. This magnetic equivalent circuit model is derived from a very simple assumed flux distribution within the machine. It is

assumed that the flux exists within a single ellipsoidal flux tube linking the pole region damper circuits and the stator winding. The stator winding is represented as a Q axis equivalent winding similar to that used in the frequency response test simulation described in chapter five.

All the electrical circuits are torn away from the centre of the machine and the appropriate linkages positioned to represent their effect on the magnetic circuit.

It is assumed that the permeance of the defined flux tube may be represented using a single capacitive device, the value of which is determined from the modified dimensions of the air gap. The value for the permeance is therefore assumed to be constant for the duration of the transient.

The rotor damper circuit is represented as a single lumped resistance representing the electrical resistance of the pole region. This is shown diagramatically in figures 7.1 and 7.2 as the variable resistive device R_d. Its value is determined from the air gap m.m.f. using the parameters obtained from the machine test data. This lumped damper circuit is linked to the main magnetic circuit using a simple single turn half transformer linkage.

The magnetic dual of the magnetic equivalent circuit shown in figure 7.1 is presented in figure 7.2. The lumped damper circuit and stator winding are referred into the magnetic circuit prior to its inversion. The resulting electric equivalent circuit model has similarities with the traditional two axis equivalent circuit model presented in figure

2.2. However, the traditional two axis model includes a device for representing the self inductance of the damper circuit in series with its resistance. This device is not included in this model because of the very much simplified assumed flux distribution.

$$\text{Average air gap flux} = (2/\pi)\int_0^{\pi/2} \sin\theta.d\theta \quad \ldots. 7.1$$

$$= \frac{2}{\pi} \quad \ldots. 7.2$$

$$C_{air} = \frac{2.\mu_0\mu_r A}{\pi \; l} \quad \ldots. 7.3$$

The permeance representing the air gap within the magnetic equivalent circuit is denoted by C_{air}, the value of which is calculated using equation 7.3. This is assumed to be constant for the duration of the transient. The value of the permeance representing the air gap is calculated assuming a sinusoidal distribution of flux in the air gap. The air gap dimensions are initially modified to allow for fringing and stator slotting in an identical manner to that described in chapter four. The value for the air gap permeance is then further modified by a factor of $2/\pi$. This is required because the magnetic charge stored in the air gap permeance is evenly distributed throughout its cross-section. Within the air gap of a typical machine however, the magnetic flux is sinusoidally distributed. The calculation for the average value of air gap flux is presented as equations 7.1 and 7.2. The topological position of the permeance

representing the air gap (C_{air}) is such that it is equivalent to the steady state reactance within the dual of the equivalent circuit shown in figure 7.2. The effect of rotor slot leakage permeance has been ignored for this Q axis flux decay test simulation because there are no slots within the pole region.

The representation of the stator is similar although simplified to that used during the frequency response test simulation described in chapter five of this thesis. The stator winding may therefore be described as the equivalent to a Q axis winding described by Adkins (42). The potential quantity present at the stator terminals, therefore, represents the envelope of the stator voltage decay during the transient. The stator leakage permeance corresponds to a summation of the stator leakage permeances within the stator representation described in figure 5.3. The dual equivalent circuit of figure 7.2 shows the dual of the stator leakage permeance consistently placed in the position of the leakage reactance.

7.4 The derivation of the representation for dynamic dampance

The damping effect of any damper circuit is dependent on its electrical resistance. For a typical round rotor synchronous machine without pole face dampers the solid iron pole region is almost exclusively responsible for the decay of the stator voltage during the flux decay test. The electrical resistance of the pole region is dependent on the depth to which the eddy currents have penetrated into the pole iron, and therefore, the rate of change of flux linking the rotor. If the rate of change of flux linking the rotor is large the damping effect of the rotor will be small. This is because the eddy currents induced in the rotor iron are restricted to an outer layer of the iron with a relatively

small cross-sectional area and therefore a high electrical resistance. If the rate of change of flux is very much smaller, the eddy currents will penetrate further into the rotor iron, and consequently the larger cross-sectional area available for the eddy currents will have a very much smaller electrical resistance.

It should, therefore, be possible to create a resistive equivalent circuit component to represent the variable damping effect of the rotor, the value of which is dependent on the rate of change of flux linking the air gap. Such a method of representing the damping effect of the rotor would effectively transfer the complex nature of the damping circuits from a network of static permeances, self and mutual dampances of the type shown in figure 4.7 to a mathematical form within a single equivalent circuit device.

$$i_m = \frac{d\Phi}{dt} \qquad \text{.... 7.4a}$$

For an exponential decay...

$$\frac{d\Phi}{dt} \propto -\Phi \qquad \text{.... 7.4b}$$

$$i_m \propto \text{m.m.f.} \qquad \text{.... 7.4c}$$

The method adopted to determine a mathematical function linking the damping effect of the rotor and air gap m.m.f. is predominantly graphical. The Q axis time constant variation in relation to the p.u. air gap m.m.f. can be determined from the rate of change of the stator voltage envelope during the flux decay test. The air gap m.m.f.

can be assumed to be approximately proportional to the rate of change of magnetic flux because the decay of the air gap m.m.f. is approximately exponential. This link between air gap m.m.f. and rate of change of magnetic flux is presented mathematically by equations 7.4a, 7.4b and 7.4c. Although a m.m.f. controlled dampance is relatively straightforward to implement in SPICE ver. 2G6, a particular weakness of using this approach more generally is that it is dependent on an exponentially decaying air gap flux.

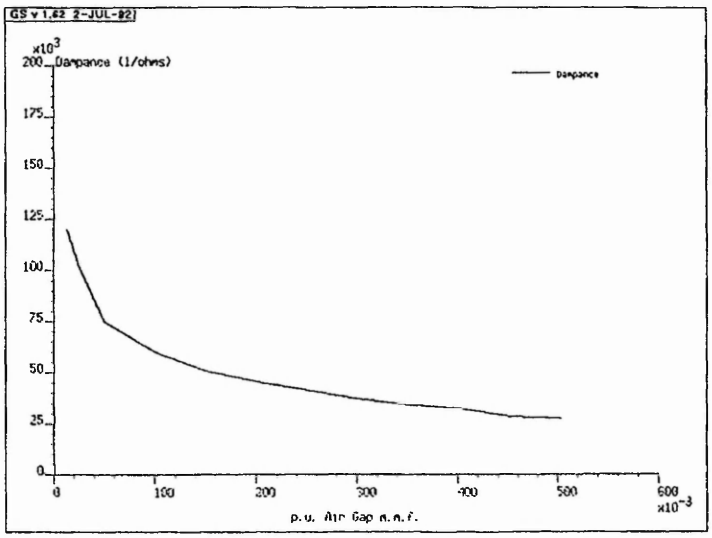

Figure 7.3 Variation of dampance with air gap m.m.f. for a Q axis flux decay test

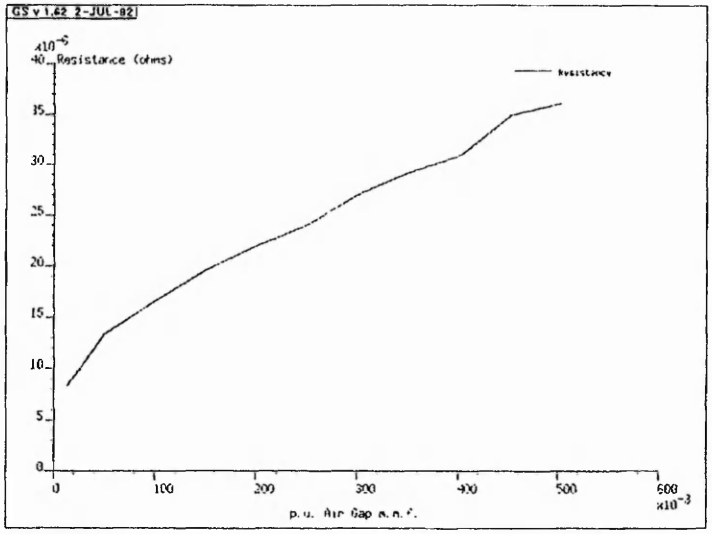

Figure 7.4 Variation of damper circuit resistance with air gap m.m.f. for a Q axis flux decay test

An initial plot of damping resistance versus air gap m.m.f. is determined from the actual flux decay test data. This is presented in figure 7.3. The damping resistance is evaluated by analysing the changing time constant present in the decay of the envelope of stator voltage for the duration of the transient. This is done by assuming that the equivalent circuit model is a simple RC network with a constant capacitance. The air gap m.m.f. can be derived directly from the magnitude of the stator voltage. The variation of the electrical resistance of the machine's damper circuits with the air gap m.m.f. during the flux decay test, is then obtained by plotting a graph of the reciprocal of the dampance against the air gap m.m.f.. This graph is presented in figure 7.4. For the purposes of the initial trials and the relative ease with which it can be incorporated into a SPICE circuit simulation, a straight line approximation to the graph shown in figure 7.4 has been used to represent the damping effect of the rotor's pole region.

7.5 Implementation using SPICE ver 2G6

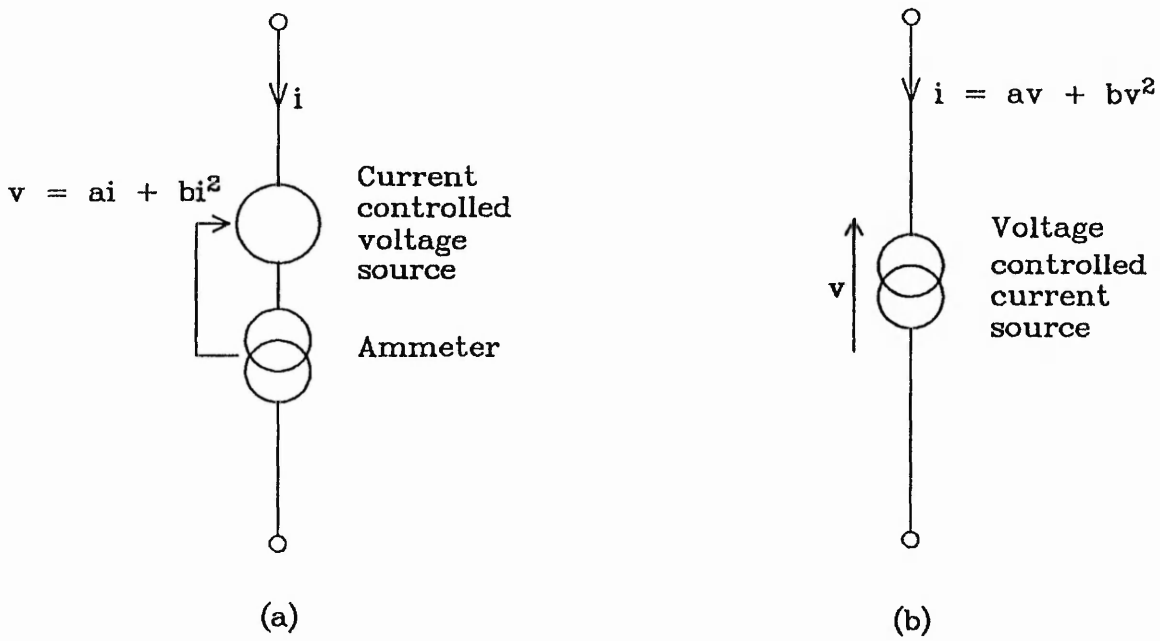

Figure 7.5 Dependent potential and current source configurations to implement dynamic resistance and dampance

The relationship between the electrical resistance of the machine's damper circuits and the electric current flowing in them is relatively straightforward in this example. Consider figure 7.1. The air gap m.m.f. is assumed to be equal to the m.m.f. induced by the current flowing in the damper circuits because these components are considered to be connected in parallel. Although this is not strictly true, the effect of the leakage permeance is considered to be negligible because its value is only a fraction of the value for the large permeance of the air gap.

$$R_e = \frac{v_e}{i_e} = a + bi \quad \text{.... 7.5}$$

$$v_e = ai + bi^2 \quad \text{.... 7.6}$$

$$i_m = av + bv^2 \quad \text{.... 7.7}$$

$$R_d = \frac{1}{(a+bF_d)} \quad \text{.... 7.8}$$

The linear relationship between the electrical resistance of the rotor damping circuits and the air gap m.m.f. may therefore be incorporated in a current dependent electrical resistance described by equation 7.5. This may be implemented using a current controlled voltage source described by equation 7.6. Such a source exists within SPICE and is presented in figure 7.5a.

In order to simplify the equivalent circuit model still further, the current dependent resistance may be transferred across the linkage linking the damper and magnetic circuits, and represented as a m.m.f. dependent dampance within the magnetic circuit. This is implemented using SPICE as a voltage controlled current source described by equation 7.7. This type of dependent source is presented in figure 7.5b. If multiple turn damper circuits are to be represented a multiplying factor of N^2 must be incorporated into the calculations for dampance when they are transferred across the linkage. The damping effect of a single turn damper circuit is therefore being represented in the magnetic circuit as a dampance, the value of which is derived from equation 7.8.

7.6 Conclusion

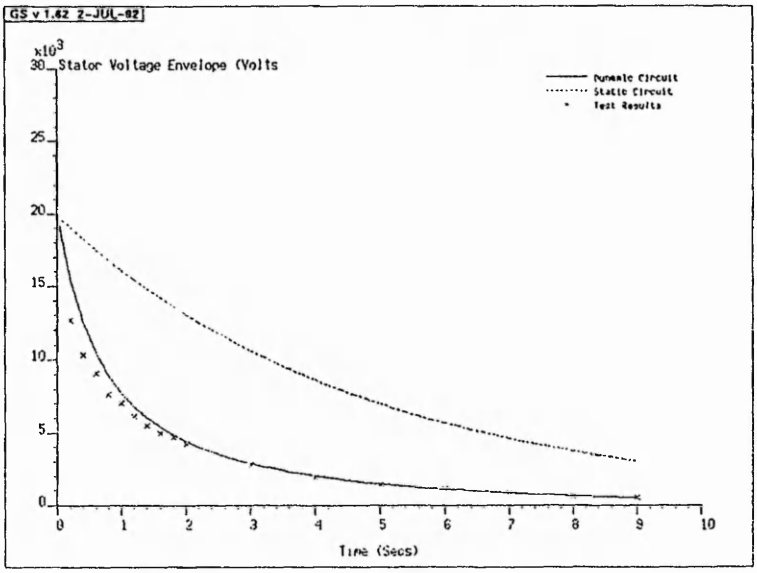

Figure 7.6 Comparison between the improved simulation results, results from a simulation using a static dampance and actual test results

A comparison of the results obtained from a simulation using this improved model, a fixed time constant model and actual test results for the Q axis flux decay test is presented in figure 7.6.

The value of the static dampance used within the equivalent circuit with a fixed time constant is equivalent to a value calculated from the physical dimensions and material bulk constants of the machine's rotor. This is represented in equations 7.5, 7.6, 7.7 and 7.8 as the constant 'a', the R_e-axis intercept on the electrical resistance versus air gap m.m.f. plot of figure 7.4.

It is acknowledged that the results presented here do not compare as well with the

actual test results as those which are obtained from the simulations described in chapter six. However, the equivalent circuits presented earlier in this thesis have employed a relatively large number of circuit devices and require between 5 and 30 minutes of computer time to solve. By comparing the equivalent circuit used to generate the results presented in figure 7.6 is a wholly magnetic form of figure 7.1. This circuit consisted of three components, the air gap permeance, the leakage permeance and the voltage controlled current source representing the dynamic dampance, and required only a fraction of a second of computer time to provide a solution.

It is also acknowledged that a considerable number of assumptions have been made during the construction of the equivalent circuit presented in figure 7.1. Perhaps the most significant of these is the assumption that the air gap m.m.f. is assumed to decay exponentially during the transient. However, a significant improvement in the results obtained from the Q axis flux decay test simulation has been achieved. The improved simple two axis equivalent circuit model presented in this chapter is intended to demonstrate a possible approach that could be developed further rather than a simple equivalent circuit model for immediate application. It is hoped, therefore, that this work will be developed by future workers in their endeavours to design a simpler and more accurate representation of the synchronous machine.

7.7 Summary

The work contained within this chapter represents a starting point from which simple reasonably accurate equivalent circuit models may be developed. The example

presented here has been developed specifically to represent the dynamic nature of dampance within the solid iron regions of a machine's rotor by linking dampance to rate of change of magnetic flux. In more general terms, however, this type of equivalent circuit model is intended to provide power system and power electronic engineers with a model which is less computationally demanding but still maintains an adequate degree of accuracy.

The equivalent circuit model described in this chapter is specifically designed to be solved using the general circuit solver SPICE ver 2G6 (17). Although this has limited the choice of mathematical functions to describe the variable damping resistance, it enables the effect to be represented using standard computer software which is universally available. An approach to describe the variable nature of the damper circuits is also described by Canay (25) in the form of a frequency dependent complex resistance to represent the rotor surface. However this requires more specialised computer software which is not widely available.

It is thought by the author that this approach to representing the variable nature of the damper circuits may be developed to incorporate the work by Shackshaft (26) which describes an equivalent circuit approach to represent saturation. The resulting equivalent circuit model would thus provide an improved model for power systems and power electronic engineers, because an improved level of accuracy could be achieved with a relatively small increase in the computational demands compared to the traditional two axis equivalent circuit models.

Chapter Eight
Conclusions

8.1 Introduction

The representation of the magnetic circuit within a synchronous machine using an equivalent circuit approach has been investigated in detail. New and original techniques have been developed to represent electric circuits linking multiple flux tubes. These techniques have enabled a more discretised representation of a machine's rotor by enabling a complete representation of the effects of multiple damper circuits. The simulation results obtained from the equivalent circuit models were found to be in close agreement with actual test data. The only exception to this relates to the sudden short circuit test simulation where results were limited to an open circuit steady state simulation. The work described in this thesis is presented in three clearly defined sections. These are: An appraisal of existing equivalent circuit modelling techniques; The development of an improved modelling technique for use with synchronous machines; The evaluation of the newly developed technique using other simulation methods and actual machine test data.

The work presented in chapter two investigates the development of equivalent circuit methods both in general and, in particular, their application to synchronous machine modelling throughout this century.

The equivalent circuit approach using the flux versus charge analogy described by Haydock (16) and Carpenter M.J. (29) is discussed in detail in chapter three. A detailed investigation of the equivalent circuit analogy exposes the fundamental

analogous quantities as electric and magnetic flux. Further, it is suggested that the phenomenon of duality, presented by Cherry (44), is due to the differing relationships between field quantities and electrical networks. For example, within an electric field electric flux is proportional to electric potential whereas within a magnetic field magnetic flux is proportional to electric current.

Also developed in chapter three is the concept of magnetic linkages presented by Haydock (16). The equivalent circuit representation for magnetic linkages used by Haydock is demonstrated to be incapable of supporting a multiple flux tube topology. Simulation results consistent with those presented by Haydock (16) could not, therefore, be obtained. An equivalent circuit representation for magnetic linkages is developed to enable a complete representation of mutually linking electric and magnetic circuits in a wholly magnetic equivalent circuit form.

The improved and more flexible equivalent circuit approach developed by the author (32) and presented in chapter three is applied to the modelling of three transient tests on three synchronous machines. The flux decay test, the frequency response test and the sudden short circuit test. This work has been presented in chapters four, five and six. A significant feature of the work presented in these chapters is the identical topological framework which has been used to generate all the equivalent circuit models. The results presented in chapter six demonstrate a significant degree of success with the new models. The variety of the results obtained from these models also highlights the level of flexibility which can now be achieved using these techniques.

The equivalent circuit models presented in chapters four, five and six are believed to represent original work in this field. The reasons for this are three fold. Firstly, the models incorporate, what is believed to be, an original representation for a multiple flux tube topology. Secondly, the models utilise a single standard topology for multiple test simulations. Finally, it is demonstrated that a wide variety of simulation quantities can be readily obtained from a single simulation run. These techniques, therefore, represent a significant advance on previous equivalent circuit models presented in work by Haydock (16) and Carpenter M.J. (29) where both the test simulations and range of results are limited.

8.2 The equivalent circuit approach to modelling

An equivalent circuit representation of any system is effectively an analogue model. Analogue quantities that exist within the model directly correspond to quantities which exist in the system under investigation. The analogue model which has been adopted throughout this thesis is an approach in which the magnetic field within a magnetic circuit is represented by analogous quantities within an electric circuit. The fundamental analogous quantities are described by Carpenter C.J. (15) and Haydock (16) as electric charge and magnetic flux. This conceptual view has been discussed in chapter three and it is suggested that a more consistent description of the analogy could be achieved if electric flux and magnetic flux were presented as the analogous quantities. It is acknowledged that this modification to the conceptual view of the modelling approach has little or no effect on the application of the technique.

However, it is intended to provide an increased level of understanding of the reasons for the analogy being appropriate.

An important part of the original work presented in chapter three concerns the representation of closed electric circuits linking multiple flux paths. A requirement to represent such a system may arise if there is a need to increase the level of discretisation or it may arise directly from the topology of the magnetic circuit. The technique is demonstrated in this thesis using layers of leakage permeance within a single slot pitch of a synchronous machine, to enable an increased level of discretisation to be achieved. The terms mutual and self dampance are introduced to describe the effect of mutually linked closed electric circuits. The term dampance used by Haydock (16) and Carpenter M.J. (29) is equivalent to the concept of self dampance described in chapter three. Further, it is demonstrated that the relative contribution to the overall damping effect made by the self and mutual dampance terms are equal for a single coil linking two flux tubes. This challenges the assumption made by Haydock (16) and Carpenter M.J. (29) that mutual dampance terms can be ignored when developing equivalent circuit models.

A dampance matrix is developed to represent the effects of self and mutual dampance in a network of closed electric circuits and mutually linking flux tubes. The matrix format is particularly useful because the existence of a pattern within the matrix structure simplifies the implementation of the technique within the equivalent circuit model.

The technique presented in chapter three for representing mutually linked flux tubes has enabled a theoretically limitless level of complexity to be achieved using this approach. Although this additional ability may be used to achieve an increased level of discretisation within a particular model it is felt by the author that the equivalent circuit approach in general is not suited to high levels of discretisation in more than one dimension.

The developed equivalent circuit models rely heavily on the availability of standard computer software to provide a solution to them. The computer's CPU requirements for equivalent circuits with an increased level of discretisation rises considerably. This is due to the rapid increase in the number of interdependencies between linked branches within the equivalent circuit model. It is felt by the author that a special purpose computer program could be written with the aim of increasing the efficiency of circuit solution. However, it is also felt that enthusiasm for such an undertaking is likely to be limited because of the advances in finite element computer software which are targeted at a very similar application.

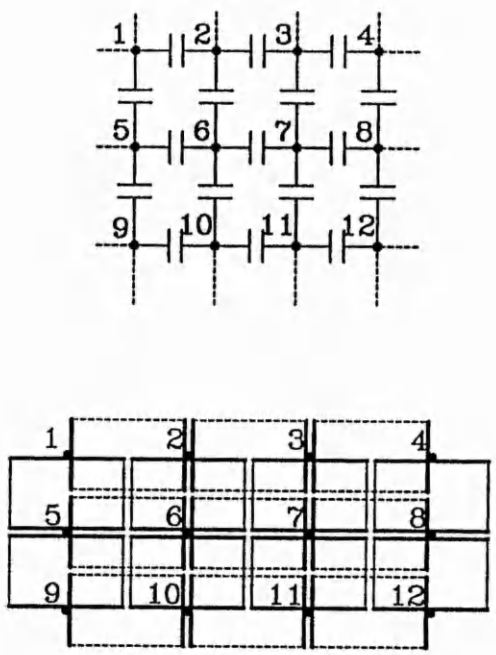

Figure 8.1 A physical interpretation of a two dimensional permeance network

The fundamental component used within an equivalent circuit model is the permeance, which is essentially one dimensional. That is to say, the distribution of magnetic flux is assumed to be fixed in space and be perpendicular to a permeance's defining pair of parallel surfaces. This is analogous to the two surfaces of a parallel plate capacitor within which an electric field exists perpendicular to the plate surfaces. The permeance is, therefore, described as one dimensional because it can only represent magnetic flux in one direction, that is, perpendicular to its defining surfaces.

Carpenter M.J. (29) has constructed a two dimensional network of permeances to represent the solid pole region of a synchronous. However, a closer investigation of the topology reveals that each area of the rotor's cross-section is being represented by

two perpendicular overlapping cuboids. Consider figure 8.1, this shows a two dimensional permeance network similar to that used by Carpenter M.J. The permeances within the network are interconnected using magnetic conductors. The purpose of these conductors is to join magnetic terminals of equal magnetic potential. The topology of the network is such that the depth of the network is equivalent to the effective length of the rotor, and is perpendicular to the plane of the paper. The two dimensions which are represented may be described as a horizontal direction which is equivalent to a direction parallel to the rotor surface and the vertical direction which is equivalent to the radial direction within the rotor.

The effect of using this topology is to superimpose into a single model an equivalent circuit model designed to represent the radial field and a model designed to represent the field parallel to the circumference. Although this approach has been demonstrated to work successfully for steady state conditions (29) it is believed that further investigation of this topology would be required to determine the ability of such an arrangement to represent the effects of a changing flux under transient conditions and the effects of saturation.

A more suitable approach to representing the magnetic field within an electrical machine is clearly the finite element approach (6,28). This approach is, in principle, a two or three dimensional numerical approximation technique. It is felt that this approach is more suitable for representing less well defined magnetic circuits, because it is based on a concept which divides the space in which the field is present independently of any assumed flux distribution that may or may not be present. The

equivalent circuit method technique, however, relies on the concept of magnetic terminals (15). This implies that the topology of the equivalent circuit is of paramount importance because the flux is assumed to exist perpendicular to the plane of the magnetic terminals of the permeance.

8.3 Implementation of the equivalent circuit approach

The equivalent circuit approach for representing a magnetic field is particularly suited to physical topologies consisting of well defined magnetic and electric circuits. This has been described as a one dimensional system in earlier paragraphs because magnetic permeance has two magnetic terminals, thus implying a one dimensional flow of magnetic current. A definition of magnetic terminals is presented by Carpenter C.J. (15) and described briefly in chapter two of this thesis. This approach is therefore consistent with a magnetic circuit which has been constructed from a number of regularly shaped blocks. A good example of this type of magnetic circuit is that which exists within a transformer.

The rotating machine is more difficult to represent using an equivalent circuit model for two reasons. Firstly, the magnetic field within the machine is not constrained within a well defined regular magnetic circuit. The magnetic circuit within any rotating machine exists within a complex topology of the rotor and stator. Distributed throughout this topology are electric circuits which form part of a winding or damper circuits. Secondly, the distribution of flux within the machine is continually changing when the machine is experiencing transient conditions. Under transient conditions the

changing magnetic field will induce abnormal currents in any linking electric circuit. This has the effect of further facilitating the redistribution of flux within the machine.

The equivalent circuit models developed and presented in chapters four and five have been developed with the aim of producing a general purpose equivalent circuit approach to represent a synchronous machine experiencing transient conditions. The fundamental approach adopted throughout these chapters is to identify the principal flux distribution using a steady state finite element simulation, and attempt to represent this topology using an equivalent circuit. Superimposed onto this fundamental topology are a number of, what have been termed, layers of leakage permeance. These have been incorporated at increasing distances from the surface of the rotor. This is to represent the ability of the machine's rotor to respond to rates of change of flux.

The layering of the leakage permeance has proved to be the most significant feature of the equivalent circuit models during both the flux decay test and the frequency response test. The work presented in chapter three of this thesis has been incorporated into these models to enable the model to represent the mutually linking effect of the field winding and rotor damper circuits. A dampance matrix has been developed to simplify the representation the damping effect of the damper circuits in a typical slot pitch. It has been demonstrated that it is necessary to represent the mutually linking electric circuits within the model for transient studies. This is particularly true for the frequency response test and for the representation of the field winding during the flux decay test.

The method of representing the damper circuits of the rotor in a wholly magnetic form is a useful tool, enabling the size and complexity of an equivalent circuit model to be considerably reduced. However, to demonstrate the flexibility of the approach, the damper circuits of the rotor have also been represented in the linked electric form. This has enabled an investigation of the electric current within the damper circuits. To demonstrate this the magnitude of the eddy currents present within a number of layers in a typical rotor tooth are presented in chapter six. These compare well with a comparable finite element study. However, it must be remembered that both the equivalent circuit and finite element method of representing the rotor assume that the eddy currents flow axially along the full length of the machine and that the effects of end bells and inertia slits have been incorporated by modifying the values for the material bulk constants.

An attempt is also made in chapter six to provide an explanation of the behaviour of a magnetic field within a synchronous machine using the equivalent circuit analogy. It has been made clear from the discussion in chapter six that the terms and phrases traditionally used to describe the behaviour of flux and eddy currents within the rotor are inappropriate. The traditional description of flux being prevented from penetrating into the rotor by eddy currents implies an active current source within the damper circuits. Whereas, the magnitude of the eddy currents are dependent on the rate of change of magnetic flux. Essentially, therefore, a changing magnetic field is inherently prevented from penetrating into the rotor. It is considered, therefore, more

appropriate to describe the behaviour of flux and eddy currents within the rotor in terms of distributions or redistribution's.

The fundamental approach to the development of a single topological form for the equivalent circuit models has been adopted throughout this thesis. The general purpose topology has been used successfully to represent three different synchronous machines for the flux decay test and frequency response test. A significant component of this topology is the layers of leakage permeance used to represent the rotor of a machine. The modular form of this topology is ideally suited to incorporation into computer software to allow the automatic generation of equivalent circuit models from machine dimensional and material data. This would be the equivalent to the present pre processors used to prepare data for finite element simulations (28).

A solution to the sudden short circuit test simulation proved to be beyond the capabilities of SPICE ver. 2G6 because of problems with the solution optimisation routine within the software. However, a steady state simulation is completed and the results presented. The effects of saturation have initially been ignored during this test simulation to reduce the complexity of the model. It is acknowledged, therefore, that the effects of saturation have proved to be significant during this test (6) and it would therefore be necessary to include this effect at a later stage in the development of such a model should sufficient computing resources become available.

The equivalent circuit models developed in chapters four and five of this thesis represent a compromise between sufficient complexity to obtain a reasonably accurate representation of the machine, and sufficient simplicity to enable the simulation software to provide a solution within a realistic time. It is acknowledged that a number of assumptions have been made so that the equivalent circuit may be presented in a manageable form. These assumptions may be considered in two categories.

The first type of assumptions are those which have traditionally been used in both equivalent circuit and finite element simulations. These may be described as the assumptions which allow a machine to be represented in two dimensions. Typical assumptions which fall into this category are the assumption that eddy currents will flow axially, there is a consistent field along the full length of the machine and the effects of the end bells and inertia gashes are included by modifying the appropriate material bulk constants. These assumptions have been consistently justified by a number of authors (6,16,29).

The second type of assumptions are those which concern the development of the topology for the equivalent circuit model. The assumptions concerning the distribution of flux within the machine is a necessary part of the equivalent circuit approach because of the one dimensional characteristic of magnetic permeance and its associated magnetic terminals. The topology of the equivalent circuit models developed in this thesis assumes that the rotor leakage permeance is the most significant feature affecting the transient behaviour of a machine. This assumption

was initially made after investigation of previous work (6,16) and the initial finite element studies described in chapters four and six of this thesis. The results presented in chapter six of this thesis go some way to justifying these assumptions concerning the distribution of flux for the frequency response and flux decay tests.

8.4 Recommendations for further work

The principal aim of the work described in this thesis is to design improved equivalent circuit models for synchronous machines. This work, therefore, follows on from the work presented by Haydock (16) and Carpenter M.J. (29). The aim has been interpreted as a requirement to produce a general purpose equivalent circuit model with the capability of representing the machine for a number of transient conditions. Although this objective has, to a large extent, been achieved for the flux decay, frequency response and sudden short circuit tests, the work has high lighted a number of areas which the author would like to discuss in terms of pursuing this work further.

8.4.1 Improved simulation facilities

Although an original advantage of this approach has been the availability of standard computer software in the form of SPICE (17) which has enabled a solution to equivalent circuit models to be obtained, the limitations of such software are now becoming evident. These difficulties may be categorised into two areas. Firstly, the large and cumbersome nature of the equivalent circuit models developed in chapters five and six have proved to be expensive in terms of computer CPU time requirements. Secondly, the range and characteristics of the equivalent circuit devices which are available from standard software is not consistent with those required for this

application. For example, models to represent dynamic dampance or saturation must be represented within the scope of existing standard circuit devices. This has the effect of unnecessarily increasing the complexity of the equivalent circuit models because a number of standard devices are required to model some magnetic effects.

A dedicated simulation software package incorporating a limited selection of relevant devices would certainly eliminate a lot of the problems discussed in the previous paragraph. Dedicated equivalent circuit devices could be used to represent permeance and include saturation effects, dampance, and linkages, possibly using a form of the dampance matrix developed in chapter three. However, the equivalent circuit models developed in chapters four and five are large and complex with complex inter branch interactions and, although it is believed that dedicated computer software may improve the efficiency of a particular solution, the CPU requirements are effectively proportional to the complexity of the developed equivalent circuit model.

8.4.2 Developments to the equivalent circuit analogy

It is believed that the equivalent circuit analogy described and developed throughout this thesis has been developed to its full potential in its present form. However, it has also been demonstrated that the fundamental equivalent circuit component is essentially one dimensional. This has proved to be a significant limitation to this equivalent circuit approach. It is proposed, therefore, that a distributed magnetic field that exists within a complex topology can be represented more consistently using a two dimensional permeance with four magnetic terminals, each pair being mutually perpendicular. Linkages with electrical conductors could be constructed in a similar

manner to the method described in chapter three because the topology is such that rate of change of flux between magnetic terminals would be represented by current as it is now. As a further extension it may also be possible to develop a three dimensional permeance with six magnetic terminals for use in three dimensional simulations.

8.4.3 Simplification of the equivalent circuit topology

The work presented in chapter seven of this thesis describes some initial work carried out with the intention of developing a topologically simple equivalent circuit model. It is suggested in chapter seven that the topological complexity of the equivalent circuits developed in chapters four and five could be transferred to the equivalent circuit devices themselves. It is proposed that this work be continued so as to enable the complex behavioural characteristics of a synchronous machine to be incorporated into a limited number of dedicated equivalent circuit devices. For example, the effects of saturation may be included in a single permeance component. Some preliminary work has been carried out in this area (8) using the ability within SPICE to represent a voltage dependent capacitor. However, the limitation of a polynomial function for capacitance limited the use of such an approach. The dependence of dampance on frequency or per unit rate of change of flux could also be represented within a single equivalent circuit component. Using this approach it would, therefore, be possible to develop equivalent circuit models with a comparable topology to the traditional two axis models (5), but using dynamic circuit components to represent the true characteristics of the machine.

The continued development of computer technology could enable a considerable level

of automation to be introduced into this area. This would enable simple equivalent circuit models to be determined directly from test results in seconds using up to date statistical analysis software to determine parameters for the new equivalent circuit devices.

8.5 Conclusion

A considerable amount of work has been carried out investigating the subject of equivalent circuit modelling and, in particular, its application to representing the synchronous machine. Although it has been implied that finite element methods may be more suitable for machine design engineers, the simplified equivalent circuit model using dedicated computer software incorporating specialised or dedicated devices would represent a significant advance on the traditional two axis equivalent circuit models. Such an advance is both necessary and inevitable if the development of the equivalent circuit model is to be consistent with the ongoing development of the synchronous machine.

References

1. Armstrong R.L. and King J.D., "The Electromagnetic Interaction", Book, Prentice Hall, 1973.

2. Bowers B., "A History of Electric Light and Power", Book, Peter Peregrinus Ltd, 1982.

3. Faraday M., "Historical Sketch of Electromagnetism", Annals of Philosophy, 1822, 3, pp107-121.

4. Park R.H. and Robertson B.L., "The Reactances of Synchronous Machines", Trans. AIEE, 1928, pp 514-536.

5. Park R.H., "Definition of An Ideal Synchronous Machine and Formula for the Armature Flux Linkages", General Electric Review, Vol 31, N° 6, Jun 1928, pp 332-334.

6. Turner P.J., "Finite Element Electromagnetic Analysis of Turbine Generator Performance", PhD Thesis, Imperial College, London University, 1981.

7. Haydock L. and Sutton R., "The Modelling of Electrical Machines by Equivalent Magnetic Circuits", Proc UPEC, Sunderland Polytechnic, 1987.

8. Haydock L., Cooper A.W. and Wilson J.W., "The Modelling of Electro- magnetic Device Behaviour by Distributed Magnetic and Linked Electric Equivalent Circuits", Proc UPEC Nottingham (formely Trent) Polytechnic, 1988.

9. Hendry J., "James Clerk Maxwell and the Theory of the Electromagnetic Field", Book, Adam Hilger, 1986.

10. Karaptoff V., "The Magnetic Circuit", Book, McGraw Hill, 1911.

11. Slemon G.R., "Equivalent Circuits for Transformers and Machines Including Non-linear Effects", Proc IEE, Vol 100, Part IV, N° 5, Oct 1953, pp 129-143.

12. Laithwaite E.R., "Magnetic Equivalent Circuits for Electrical Machines", Proc IEE, Vol 114, N° 11, Nov 1967, pp 1805-1809.

13. Ostovic V., "Magnetic Equivalent Circuit Presentation of Electric Machines", Electric Machines and Power Systems, 1987, pp 407-432.

14. Ostovic V., "Dynamics of Saturated Electric Machines", Book, Springer Verlag, 1990.

15. Carpenter C.J., "Magnetic Equivalent Circuits", Proc IEE, Vol 115, N° 10, Oct 1968, pp 1503-1511.

16. Haydock L., "Systematic Development of Equivalent Circuits for Synchronous Machines", PhD Thesis, Imperial College, London University, 1986.

17. Vladimirescu A., Newton, A.R. and Pederson D.O., SPICE Ver. 2G0, Users Guide, IBID 94720, 1980.

18. Vickers V.J., "Recent Trends in Turbogenerators", Proc. IEE, Vol. 121, No 11R, November 1974, IEE Review.

19. Frankel A., "Large Turbine Generators: Survey of Progress", Proc. IEE, Vol. 117, N° 4, April 1970.

20. Doherty R.E. and Nickle C.A., "Synchronous Machines Parts I and II", Trans. AIEE, 1926, pp 912-947.

21. Alger P.L., "The Calculation of the Armature Reactance of Synchronous Machines", Trans AIEE, Feb 1928, pp 493-512.

22. Concordia C., "Two Reaction Theory of Synchronous Machines With Any Balanced Terminal Impedance", Trans AIEE, Sept 1937, pp 1124-1127.

23. Shackshaft G., "General Purpose Turbo-alternator Model", Proc IEE, Vol 110, N° 4, Apr 1963, pp 703-712.

24. Canay I.M., "Equivalent Circuits of Synchronous Machines for Calculating Quantities of the Rotor during Transient Processes and Asynchronous Starting, Part 1, Turbo-generators", Brown Bovervi Review, Vol 56, 1969, pp 60-71.

25. Canay I.M., "Causes of Discrepancies on Calculation of Rotor Quantities and Exact Equivalent Diagrams of the Synchronous Machine", IEEE Trans PAS, Vol PAS-88, N° 7, July 1969, pp 1114-1120.

26. Shackshaft G., "Model of Generator Saturation for Use in Power System Studies", Proc IEE, Vol 126, N° 8, Aug 1979, pp 759-763.

27. Silvester P.P. and Ferrari R.L., "Finite Elements for Electrical Engineers", Book, Cambridge, 1982.

28. Davies A.J., Preston T.W. and Smith P., "An Integrated Approach to the Solution of 3D Engineering Problems in a Workstation Environment", IEE Colloquium, "Visualisation of Fields in 3-D", Digest N° 1983/66, pp7/1-7/4, May 1988.

29. Carpenter M.J. and MacDonald D.C., "Circuit Representation of Inverter Fed Synchronous Motors", IEEE Trans on Energy Conversion, Vol 4, N° 3, Sept 1989, pp 531-537.

30. Slemon G.R., "An Equivalent Circuit Approach to Analysis of Synchronous Machines with Saliency and Saturation", IEEE Trans Energy Conversion, Vol 5, N° 3, Sept 1990, pp 538-544.

31. Haydock L., Holland S. and Hudson W.J., " A Hybrid Finite Element and Distributed Magnetic Equivalent Circuit Modelling Methodology for Electromagnetic Devices", Proc 1st Conference on Electrical Engineering Analysis and Design, Lowell, Mass, USA, Aug 1990.

32. Hudson W.J., "New Equivalent Circuits Applied to Industrial Machines", Interim report describing the PhD research undertaken by the author between May 1989 and October 1990, Department of Electrical and Electronic Engineering, Nottingham Trent University (formerly Nottingham Polytechnic), October 1990.

33. Rankin A.W., "The Direct and Quadrature Axis Equivalent Circuits of the Synchronous Machine", Trans AIEE, Vol 64, Dec 1945, pp 861-868.

34. Jackson W.B. and Winchester R.L., "Direct and Quadrature Axis Equivalent Circuits for Solid Rotor Turbine Generators", IEEE Trans PAS, Vol PAS-88, N° 7, July 1969, pp 1121-1136.

35. Haydock L., "Integrative Equivalent Circuit Models For Electrical Machines, Their Power Electronic Controllers And Power System Studies", Proc 27th UPEC, Bath University, Bath, UK, September 1992.

36. Schultz R.P., Jones W.D. and Ewart D.N., "Dynamic Models for Synchronous Machines Derived From Solid Rotor Equivalent Circuits", IEEE Trans PAS, Vol PAS-92, 1973, pp 926-933.

37. Levy W., Landy C.F. and McCulloch M.D., "Improved Models for the Simulation of Deep Bar Induction Motors", IEEE Trans on Energy Conversion, Vol 5, N° 2, pp 393-400.

38. Babb D.S. and Williams J.E., "Circuit Analysis Method for Determination of AC Impedances of Machine Conductors", Trans AIEE, Jan 1951, pp 661-665.

39. Hudson W.J. and Haydock L., "Parametric Sources for Improved Models of Electrical Machines", Proc UPEC Robert Gordons Institute of Technology, Sept 1990.

40. Shi S. and Li N., "A General Model of a Synchronous Machine for its Steady State Performance Analysis", IEEE Trans on Energy Conversion, Vol 5, N° 3, Sept 1990, pp 531-537.

41. Kron G., "Equivalent Circuits for Electric Machinery", Book, Dover, 1967.

42. Adkins B., "The General Theory of Electrical Machines", Book, Wiley, 1957.

43. Rankin A.W., "Per unit Impedances of Synchronous Machines", Trans AIEE, Vol 64, Aug 1945, pp 569-573.

44. Cherry E.C., "The Duality Between Interlinked Electric and Magnetic Circuits and the Formation of Transformer Equivalent Circuits", Proc Phys Soc, 1949, [B], pp 101.

45. Takeda Y. and Adkins B., "Determination of Synchronous Machine Parameters allowing for Unequal Mutual Inductances", Proc IEE, Vol 121, N° 12, Dec 1974, pp 1501-1504.

46. Fiennes J., "New Approach to General Theory of Electrical Machines Using Magnetic Equivalent Circuits", Proc IEE, Vol 120, N° 1, Jan 1973, pp 95-104.

47. Kron G., "Tensor Analysis of Networks", Book, Wiley 1939

48. Haydock L., "Magnetic Models for Synchronous Machines", Proc UPEC Imperial College, 1986.

49. Levy W., Landy C.F. and McCulloch M.D., "Improved Models for the Simulation of Deep Bar Induction Motors", IEEE Trans on Energy Conversion, Vol 5 N° 2, June 1990, pp 393-400.

50. Barber M.D., Humphreys P., Poray A.T. and Shackshaft G.S., "Report on Generator Parameter Tests at Eggborough Power Station, August 1975", CEGB 1976.

51. Turner P.J. and MacDonald D.C., "Electromagnetic Simulation of the Flux Decay Test for Determining Turbine Generator Parameters", Proc IEE, Elect Machines Design and Applications Conference, July 1982, pp 90-93.

52. Turner P.J., "Finite Element Simulation of Turbine Generator Terminal Faults and Application to Machine Parameter Prediction", Proc. IEEE/PES Winter Meeting, February 1986.

53. Hannalla A.Y. and MacDonald D.C., "Numerical Analysis of Transient Field Problems in Electrical Machines", Proc. IEE, Vol 123, N° 9, Sept 1976.

54. Reece A.B.J., Khan G.K.M. and Chant M.J., "Generator Parameter Prediction, Finite Element Simulation of the Variable Frequency Response Test", GEC Journal of Science and Technology, Vol 49, N° 1, 1983.

55. BS4296, "Determination of Synchronous Machine Quantities", British Standards Institute, 1968.

56. BS4999, "General Requirements for Rotating Machines", British Standards Institute, 1987.

57. Hannalla A.Y. and MacDonald D.C., "Sudden Three Phase Short Circuit Characteristics of Turbine Generators From Design Data Using Electromagnetic Field Calculations", Proc. IEE, Vol 127, N° 4, July 1980.

58. Private Communications with GECAlsthom Engineering Research Centre, Lichfield Road, Stafford (Jan 1990 - March 1992).

59. Yee H., and Wilson T., "Open Circuit Decay of a Turbogenerator", Proc IEE, Vol 120, N° 2, Feb 1973, pp 228-232.

Appendix One

Key to the equivalent circuit developed by Rankin (43) presented in figure 2.2

a	armature	b	bar
f	field	n	damper winding
g	air gap	e	end ring
d/q	direct/quadrature		

To interchange the equivalent circuit between a representation of the D or Q axis interchange the subscripts d and q. Damper bars are numbered from the direct/quadrature axis outwards.

$X_1 = X_d - X_{afd}$ $\quad X_2 = X_{afd} - X_{a3d}$

$X_3 = X_{a3d} - X_{a2d}$ $\quad X_4 = X_{a2d} - X_{a1d}$

$X_5 = X_{a1d} - X_{a2d}$

$X_6 = (X_{f3d} - X_{a3d}) - (X_{f2d} - X_{a2d})$

$X_7 = (X_{f2d} - X_{a2d}) - (X_{f1d} - X_{a1d})$

$X_8 = (X_{f1d} - X_{a1d})$

$X_9 = \underline{R_{b33d}} + X_{b33d}$ $\quad X_{10} = \underline{R_{b22d}} + X_{b22d}$

jmv $\qquad$ jmv

$X_{11} = \underline{R_{b11d}} + X_{b11d}$

jmv

$X_{12} = \underline{R_{e33d} + X_{b22d}}$ $\quad X_{14} = \underline{R_{e22d} + X_{e11d}}$

jmv $\qquad$ jmv

$X_{16} = \underline{R_{e11d}}$ $\quad X_{18} = \underline{R_{ffd}}$

jmv $\qquad$ jmv

$X_{13} = (X_{g33d} + X_{e33d} - X_{f3d}) - (X_{g22d} + X_{e22d} - X_{f2d\psi})$

$X_{15} = (X_{g22d} + X_{e22d} - X_{f2d}) - (X_{g11d} + X_{e11d} - X_{f1d})$

$X_{17} = (X_{g11d} + X_{e11d} - X_{f1d})$

$X_{19} = (X_{ffd} - X_{afd}) - (X_{f3d} - X_{a3d})$

Equations used by Rankin (43) to develop the equivalent circuit presented in figure 2.2

$$\psi_d = X_{afd}I_{fd} + X_{a1d}I_{1d} + X_{a2d}I_{2d} + \ldots - x_d i_d \quad \ldots. \text{A1.1a}$$

$$\psi_{fd} = X_{ffd}I_{fd} + X_{f1d}I_{1d} + X_{f2d}I_{2d} + \ldots - x_{fad} i_d \quad \ldots. \text{A1.1b}$$

$$\psi_{1d} = X_{1fd}I_{fd} + X_{11d}I_{1d} + X_{12d}I_{2d} + \ldots - x_{1ad} i_d \quad \ldots. \text{A1.1c}$$

$$\psi_{2d} = X_{2fd}I_{fd} + X_{21d}I_{1d} + X_{22d}I_{2d} + \ldots - x_{2ad} i_d \quad \ldots. \text{A1.1d}$$

$$E_{fd} = p\psi_{fd} + R_{ffd}I_{fd} + R_{f1d}I_{1d} + R_{f2d}I_{2d} + \ldots \quad \ldots. \text{A1.2a}$$

$$E_{1d} = p\psi_{1d} + R_{1fd}I_{fd} + R_{11d}I_{1d} + R_{12d}I_{2d} + \ldots \quad \ldots. \text{A1.2b}$$

$$E_{2d} = p\psi_{2d} + R_{2fd}I_{fd} + R_{21d}I_{1d} + R_{22d}I_{2d} + \ldots \quad \ldots. \text{A1.2c}$$

$$\psi_d = X_{afd}I_{fd} + X_{a1d}I_{1d} + X_{a2d}I_{2d} + \ldots - x_d i_d \quad \ldots. \text{A1.3a}$$

$$0 = \left[X_{ffd} + \frac{R_{ffd}}{p}\right] I_{fd} + \left[X_{f1d} + \frac{R_{f1d}}{p}\right] I_{1d} + \left[X_{f2d} + \frac{R_{f2d}}{p}\right] I_{2d} + \ldots - X_{fad}\, I_d \quad \ldots. \text{A1.3b}$$

$$0 = \left[X_{1fd} + \frac{R_{1fd}}{p}\right] I_{fd} + \left[X_{11d} + \frac{R_{11d}}{p}\right] I_{1d} + \left[X_{12d} + \frac{R_{12d}}{p}\right] I_{2d} + \ldots - X_{1ad}\, I_d \quad \ldots. \text{A1.3c}$$

$$0 = \left[X_{2fd} + \frac{R_{2fd}}{p}\right] I_{fd} + \left[X_{21d} + \frac{R_{21d}}{p}\right] I_{1d} + \left[X_{22d} + \frac{R_{22d}}{p}\right] I_{2d} + \ldots - X_{2ad}\, I_d \quad \ldots. \text{A1.3d}$$

Appendix Two

The calculation of typical equivalent circuit component values used within the models presented in this thesis

The following examples are based on a typical slot pitch as defined by figure 4.5 in chapter four of this thesis. This is reproduced here as figure A2.1

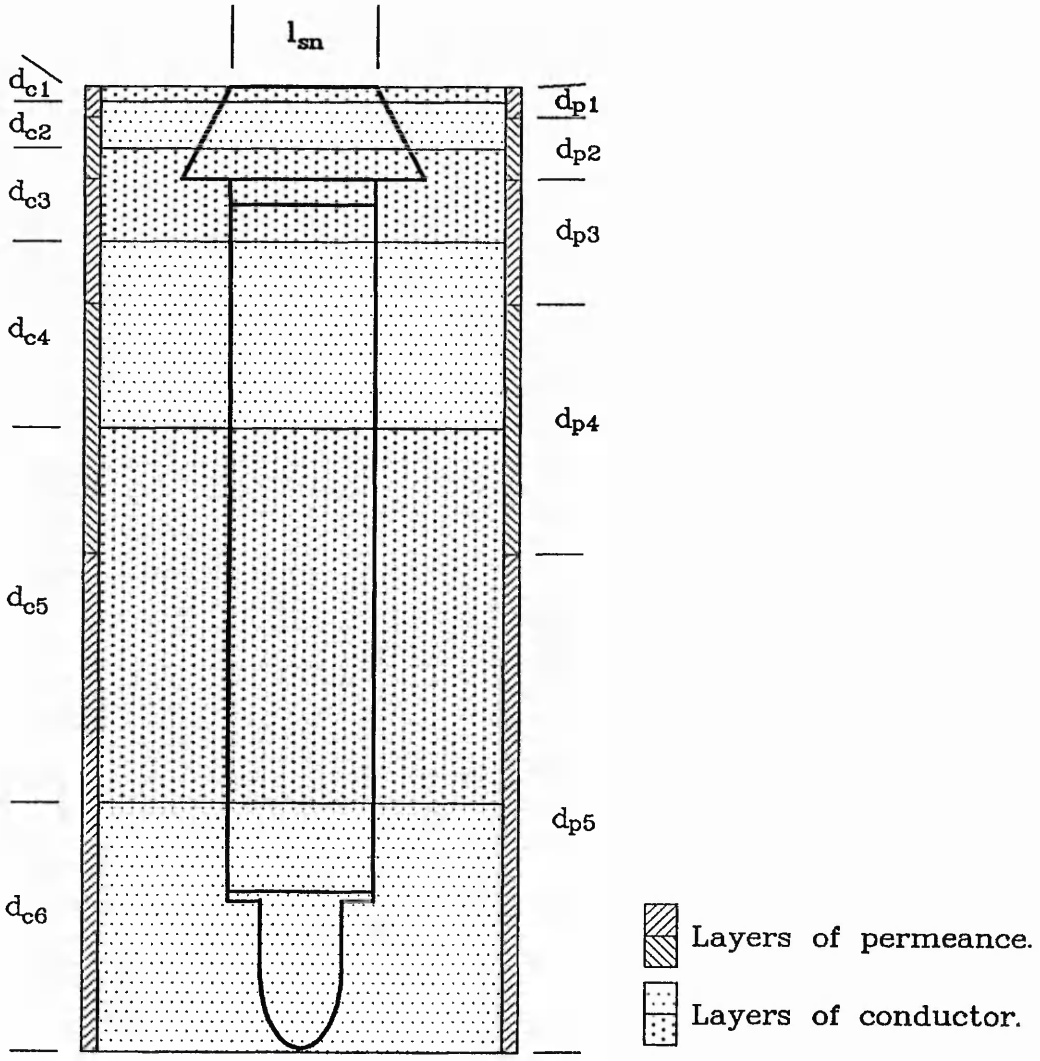

Figure A2.1, Defined dimensions within a typical slot pitch

Calculation method for slot leakage permeances within a typical slot pitch

If the overall depth of the slot is d_{sd} and the depth of the outermost leakage permeance as defined as d_{p1} then the corresponding depths of the deeper leakage permeances are

$$d_{p2} = 2.d_{p1} \quad \text{.... A2.1}$$

$$d_{p3} = 2.d_{p2} \quad \text{.... A2.2}$$

$$d_{p4} = 2.d_{p3} \quad \text{.... A2.3}$$

$$d_{p5} = 2.d_{p4} \quad \text{.... A2.4}$$

This implies

$$31.d_{p1} = d_{sd} \quad \text{.... A2.5}$$

The cross sectional area A_{sn} for each layer n of leakage permeance is therefore given by.

$$A_{s1} = d_{p1}.w_s \quad \text{.... A2.6}$$

$$A_{s2} = d_{p2}.w_s \quad \text{.... A2.7}$$

$$A_{s3} = dp_3.w_s \quad \text{.... A2.8}$$

$$A_{s4} = d_{p4}.w_s \quad \text{.... A2.9}$$

$$A_{s5} = d_{p5}.w_s \quad \text{.... A2.10}$$

Where w_s is the width of the leakage permeance and, in this example, is equivalent to the effective length of the machine.

The values for leakage permeance C_{mn} for each layer n are then calculated using the standard equation for permeance in air.

$$C_{mn} = \frac{\mu_0 A_{sn}}{l_{sn}} \quad \text{.... A2.11}$$

Where l_{sn} is the slot width appropriate to the permeance C_{mn}. The effects of the iron tooth on the value of permeance is considered to be negligible.

Calculation method for the electrical resistance values of the layers of conducting material defined within a slot pitch

If the depth of the slot leakage permeances are defined by equations A2.1 ... A2.4 as d_{p1} ... d_{p5} respectively then the depth of the conducting material layers are defined as.

$$d_{c1} = 1/2.d_{p1} \quad \text{.... A2.12}$$

$$d_{c2} = 1/2.d_{p1} + 1/2.d_{p2} \quad \text{.... A2.13}$$

$$d_{c3} = 1/2.d_{p2} + 1/2.d_{p3} \quad \text{.... A2.14}$$

$$d_{c4} = 1/2.d_{p3} + 1/2.d_{p4} \quad \text{.... A2.15}$$

$$d_{c5} = 1/2.d_{p4} + 1/2.d_{p5} \quad \text{.... A2.16}$$

$$d_{c6} = 1/2.d_{p5} \quad \text{.... A2.17}$$

The conductor layer depths d_{c1} ... d_{c6} are used within the calculations for the cross sectional area of the individual conducting materials using the geometrical information made available to the author (58).

The value of electrical resistance for each conducting material within layer n is calculated using the standard equation for resistance.

$$R_n = \frac{l}{\sigma A_{cn}} \quad \text{.... A2.18}$$

Where, l is the effective length of the machine, σ is the unmodified material bulk conductivity and A_{cn} is the cross sectional area of the conducting material. For the corresponding calculations of resistance within the pole region the conductivity of the rotor iron is doubled (6) to allow for inertia gashes and end effects.

By using the effective length of the machine in equation A2.18 the resistance of the conducting path is effectively halved. The reason for this is discussed in section 4.3.3.1, of chapter four of this thesis.

Where two or more conducting materials are present within a defined layer the values for their electrical resistance are combined as if they were connected in parallel. This method is used to form a single electrical resistance for each conduction layer of the model. For example, the total electrical resistance of the outermost layer of this example is the parallel combination of the resistance for the two half tooth tops and the wedge to a depth defined as d_{c1}.

Appendix Three

Spice program and results listing for a typical D axis flux decay test on the Uskmouth machine

```
*******18-FEB-91*******SPICE 2G.6(10AUG81)  *******09:25:07***********
Uskmouth flux decay test. (D-axis)
INPUT LISTING                    TEMPERATURE =   27.000 DEG C
LATEST SPICE UPDATE 17/5/85,FOR INFORMATION TYPE DRB2:[FPS]SPICE.NEW
**********************************************************************
* This circuit is used to model the D-axis
* flux decay test, assuming iron is saturated
* on the main flux paths and Ur = 100 on any
* leakage paths.
*
* W J Hudson.
*
.WIDTH IN=80 OUT=80
.OPTIONS ITL4=1000 ITL5=0
*
* Dummy resistors to ground.
*
RD1      1    0    20MEG
RD2      2    0    20MEG
RD3      3    0    20MEG
RD4      4    0    20MEG
RD5      5    0    20MEG
RD6      6    0    20MEG
RD7      7    0    20MEG
RD8      8    0    20MEG
RD9      9    0    20MEG
RDA     10    0    20MEG
RDB     11    0    20MEG
RDC     12    0    20MEG
*
* Air gap permeances.
*
C1       1    0    6.27UFM     IC=000.0
C2       2    0    6.27UFM     IC=5004.40
C3       3    0    6.27UFM     IC=9919.50
C4       4    0    6.27UFM     IC=14657.6
C5       5    0    6.27UFM     IC=19134.1
C6       6    0    6.27UFM     IC=23269.1
C7       7    0    6.27UFM     IC=26988.8
C8       8    0    6.27UFM     IC=30226.9
C9       9    0    6.82UFM     IC=33000.7
CA      10    0    6.82UFM     IC=35203.2
CB      11    0    6.82UFM     IC=36694.9
CC      12    0    6.82UFM     IC=37449.5
*
* Air gap m.m.f generators.
*
V1      13    1
V2      14    2
V3      15    3
V4      16    4
V5      17    5
V6      18    6
V7      19    7
V8      20    8
V9      21    9
VA      22   10
VB      23   11
VC      24   12
*
* Neuman Boundary.
RN      13    0    1
* Layer by layer permeances and dampances.
*
* Subckts for each layer combining
* permeance with a small resistance.
* For the slotted region only.
```

```
*
* Subckt for layer 1.
.SUBCKT LAY1 1 3
C1      1    2   1.03UFM
R1      2    3   138.5
.ENDS
* Subckt for layer 2.
.SUBCKT LAY2 1 3
C2      1    2   2.06UFM
R2      2    3   550.8
.ENDS
* Subckt for layer 3.
.SUBCKT LAY3 1 3
C3      1    2   4.11UFM
R3      2    3   2434.0
.ENDS
* Subckt for layer 4.
.SUBCKT LAY4 1 3
C4      1    2   8.22UFM
R4      2    3   3453.7
.ENDS
* Subckt for layer 5.
.SUBCKT LAY5 1 3
C5      1    2   16.45UFM
R5      2    3   5073.1
.ENDS
*
* Subckts for each layer combining
* permeance with a small resistance.
* For the pole region only.
*
* Subckt for layer 1.
.SUBCKT PLAY1 1 3
C1      1    2   41.9UFM
R1      2    3   1
.ENDS
* Subckt for layer 2.
.SUBCKT PLAY2 1 3
C2      1    2   84.9UFM
R2      2    3   1
.ENDS
* Subckt for layer 3.
.SUBCKT PLAY3 1 3
C3      1    2   177.4UFM
R3      2    3   1
.ENDS
* Subckt for layer 4.
.SUBCKT PLAY4 1 3
C4      1    2   380.9UFM
R4      2    3   1
.ENDS
* Subckt for layer 5.
.SUBCKT PLAY5 1 3
C5      1    2   900.6UFM
R5      2    3   1
.ENDS
*
* Slotted region layer by layer.
*
* Slot 1.
*
* Layer 1.
X11    14    13      LAY1
* Layer 2.
X12    14    13      LAY2
* Layer 3.
X13    14    13      LAY3
* Layer 4.
X14    14   142      LAY4
HM14  142   141      VMF 1.99
VM14  141    13
* Layer 5.
X15    14   152      LAY5
HM15  152   151      VMF 7.09
```

```
VM15  151    13
* Layer 8.
R18    14   182       5905.7
HM18  182   181       VMF 10
VM18  181    13
*
* Slot 2.
*
* Layer 1.
X21    15    14       LAY1
* Layer 2.
X22    15    14       LAY2
* Layer 3.
X23    15    14       LAY3
* Layer 4.
X24    15   242       LAY4
HM24  242   241       VMF 1.99
VM24  241    14
* Layer 5.
X25    15   252       LAY5
HM25  252   251       VMF 7.09
VM25  251    14
* Layer 6.
R26    15   263       5984.8
C26   263   262       2059.2UFM
HM26  262   261       VMF 10
VM26  261    14
* Layer 7.
R27    15   273       6271.8
C27   273   272       2059.2UFM
HM27  272   271       VMF 10
VM27  271    14
* Layer 8.
R28    15   282       6415.3
HM28  282   281       VMF 10
VM28  281    14
*
* Slot 3.
*
* Layer 1.
X31    16    15       LAY1
* Layer 2.
X32    16    15       LAY2
* Layer 3.
X33    16    15       LAY3
* Layer 4.
X34    16   342       LAY4
HM34  342   341       VMF 1.99
VM34  341    15
* Layer 5.
X35    16   352       LAY5
HM35  352   351       VMF 7.09
VM35  351    15
* Layer 6.
R36    16   363       6227.5
C36   363   362       2059.2UFM
HM36  362   361       VMF 10
VM36  361    15
* Layer 7.
R37    16   373       6999.8
C37   373   372       2059.2UFM
HM37  372   371       VMF 10
VM37  371    15
* Layer 8.
R38    16   382       7386.0
HM38  382   381       VMF 10
VM38  381    15
*
* Slot 4.
*
* Layer 1.
X41    17    16       LAY1
* Layer 2.
X42    17    16       LAY2
```

```
* Layer 3.
X43    17    16       LAY3
* Layer 4.
X44    17   442       LAY4
HM44  442   441       VMF 1.99
VM44  441    16
* Layer 5.
X45    17   452       LAY5
HM45  452   451       VMF 7.09
VM45  451    16
* Layer 6.
R46    17   463       6574.3
C46   463   462       2059.2UFM
HM46  462   461       VMF 10
VM46  461    16
* Layer 7.
R47    17   473       8041.1
C47   473   472       2059.2UFM
HM47  472   471       VMF 10
VM47  471    16
* Layer 8.
R48    17   482       8774.4
HM48  482   481       VMF 10
VM48  481    16
*
* Slot 5.
*
* Layer 1.
X51    18    17       LAY1
* Layer 2.
X52    18    17       LAY2
* Layer 3.
X53    18    17       LAY3
* Layer 4.
X54    18   542       LAY4
HM54  542   541       VMF 1.99
VM54  541    17
* Layer 5.
X55    18   552       LAY5
HM55  552   551       VMF 7.09
VM55  551    17
* Layer 6.
R56    18   563       6992.7
C56   563   562       2059.2UFM
HM56  562   561       VMF 10
VM56  561    17
* Layer 7.
R57    18   573       9295.5
C57   573   572       2059.2UFM
HM57  572   571       VMF 10
VM57  571    17
* Layer 8.
R58    18   582       10446.9
HM58  582   581       VMF 10
VM58  581    17
*
* Slot 6.
*
* Layer 1.
X61    19    18       LAY1
* Layer 2.
X62    19    18       LAY2
* Layer 3.
X63    19    18       LAY3
* Layer 4.
X64    19   642       LAY4
HM64  642   641       VMF 1.99
VM64  641    18
* Layer 5.
X65    19   652       LAY5
HM65  652   651       VMF 7.09
VM65  651    18
* Layer 6.
R66    19   663       7464.0
```

```
C66   663   662       2059.2UFM
HM66  662   661       VMF 10
VM66  661    18
* Layer 7.
R67    19   673       10709.3
C67   673   672       2059.2UFM
HM67  672   671       VMF 10
VM67  671    18
* Layer 8.
R68    19   682       12332.0
HM68  682   681       VMF 10
VM68  681    18
*
* Slot 7.
*
* Layer 1.
X71    20    19       LAY1
* Layer 2.
X72    20    19       LAY2
* Layer 3.
X73    20    19       LAY3
* Layer 4.
X74    20   742       LAY4
HM74  742   741       VMF 1.99
VM74  741    19
* Layer 5.
X75    20   752       LAY5
HM75  752   751       VMF 7.09
VM75  751    19
* Layer 6.
R76    20   763       7938.9
C76   763   762       2059.2UFM
HM76  762   761       VMF 10
VM76  761    19
* Layer 7.
R77    20   773       12134.1
C77   773   772       2059.2UFM
HM77  772   771       VMF 10
VM77  771    19
* Layer 8.
R78    20   782       14231.7
HM78  782   781       VMF 10
VM78  781    19
*
* Slot 8.
*
* Layer 1.
C81    21   813       1.03UFM
R81   813    20       143.9
* Layer 2.
C82    21   823       2.06UFM
R82   823    20       572.0
* Layer 3.
C83    21   833       4.11UFM
R83   833    20       2428.4
* Layer 4.
C84    21   843       8.22UFM
R84   843   842       3582.6
HM84  842   841       VMF 1.79
VM84  841    20
* Layer 5.
C85    21   853       16.45UFM
R85   853   852       5444.4
HM85  852   851       VMF 6.38
VM85  851    20
* Layer 6.
R86    21   863       8994.3
C86   863   862       1996.0UFM
HM86  862   861       VMF 9
VM86  861    20
* Layer 7.
R87    21   873       14273.3
C87   873   872       1996.0UFM
HM87  872   871       VMF 9
```

```
VM87  871    20
* Layer 8.
R88    21   882       16912.8
HM88  882   881       VMF 9
VM88  881    20
*
*
* Slot 9.
*
* Layer 1.
X91    22   913       PLAY1
R91   913    21       89.86
* Layer 2.
X92    22   923       PLAY2
R92   923    21       316.2
* Layer 3.
X93    22   933       PLAY3
R93   933    21       835.2
* Layer 4.
X94    22   943       PLAY4
R94   943    21       1820.4
* Layer 5.
X95    22   953       PLAY5
R95   953    21       3579.5
* Layer 6.
R96    22   963       7768.3
C96   963    21       1938.8UFM
* Layer 7.
R97    22   973       14113.4
C97   973    21       1938.8UFM
* Layer 8.
R98    22    21       17286.0
*
* Slot 10.
*
* Layer 1.
X101   23  1013       PLAY1
R101 1013    22       74.5
* Layer 2.
X102   23  1023       PLAY2
R102 1023    22       295.2
* Layer 3.
X103   23  1033       PLAY3
R103 1033    22       725.3
* Layer 4.
X104   23  1043       PLAY4
R104 1043    22       1541.7
* Layer 5.
X105   23  1053       PLAY5
R105 1053    22       3300.8
* Layer 6.
R106   23  1063       7838.2
C106 1063    22       1938.8UFM
* Layer 7.
R107   23  1073       14880.6
C107 1073    22       1938.8UFM
* Layer 8.
R108   23    22       18401.8
*
* Slot 11.
*
* Layer 1.
X111   24  1113       PLAY1
R111 1113    23       57.4
* Layer 2.
X112   24  1123       PLAY2
R112 1123    23       227.6
* Layer 3.
X113   24  1133       PLAY3
R113 1133    23       657.7
* Layer 4.
X114   24  1143       PLAY4
R114 1143    23       1474.1
* Layer 5.
```

```
X115   24  1153      PLAY5
R115 1153    23      2931.9
* Layer 6.
R116   24  1163      7698.3
C116 1163    23      1938.8UFM
* Layer 7.
R117   24  1173      15198.7
C117 1173    23      1938.8UFM
* Layer 8.
R118   24    23      18948.9
*
*
* Field electric circuit.
*
Vfield   0   70
Rfield  71   70  0.04141
HF8     72   71  POLY(8) VM18 VM28 VM38 VM48 VM58 VM68 VM78
+ VM88
+ 0 10 10 10 10 10 10 10 9
HF7     73   72  POLY(7) VM27 VM37 VM47 VM57 VM67 VM77 VM87
+ 0 10 10 10 10 10 10 9
HF6     74   73  POLY(7) VM26 VM36 VM46 VM56 VM66 VM76 VM86
+ 0 10 10 10 10 10 10 9
HF5     75   74  POLY(8) VM15 VM25 VM35 VM45 VM55 VM65 VM75
+ VM85
+ 0 7.09 7.09 7.09 7.09 7.09 7.09 7.09 6.38
HF4     76   75  POLY(8) VM14 VM24 VM34 VM44 VM54 VM64 VM74
+ VM84
+ 0 1.99 1.99 1.99 1.99 1.99 1.99 1.99 1.79
VMF     76    0
*
* Fourier analysis circuit.
*
EF      0    50   POLY(12) (1,0) (2,0) (3,0) (4,0) (5,0) (6,0) (7,0)
+ (8,0) (9,0) (10,0) (11,0) (12,0)
+ 0,3.83,7.66,7.66,7.66,7.66,7.66,7.66,7.66,7.90,8.14,8.14,8.14
VM      51   50
RF      51    0    178.43
*
* Analysis.
*
*.TRAN .0002 0.01 UIC
.TRAN .2 12 UIC
.PRINT TRAN I(Vfield)
.PRINT TRAN I(VM)
.END
```

```
*******18-FEB-91*******SPICE2G.6(10AUG81)  *******09:25:07************
Uskmouth flux decay test. (D-axis)
TRANSIENT ANALYSIS       TEMPERATURE =   27.000 DEG C
LATEST SPICE UPDATE 17/5/85,FOR INFORMATION TYPE DRB2:[FPS]SPICE.NEW
******************************************************************************
TIME             I(Vfield)
0.000E+00     4.531E+02
2.000E-01     3.644E+02
4.000E-01     3.458E+02
6.000E-01     3.347E+02
8.000E-01     3.249E+02
1.000E+00     3.157E+02
1.200E+00     3.068E+02
1.400E+00     2.982E+02
1.600E+00     2.898E+02
1.800E+00     2.816E+02
2.000E+00     2.737E+02
2.200E+00     2.660E+02
2.400E+00     2.586E+02
2.600E+00     2.514E+02
2.800E+00     2.443E+02
3.000E+00     2.374E+02
3.200E+00     2.308E+02
3.400E+00     2.243E+02
3.600E+00     2.181E+02
3.800E+00     2.120E+02
4.000E+00     2.060E+02
4.200E+00     2.002E+02
4.400E+00     1.946E+02
4.600E+00     1.892E+02
4.800E+00     1.839E+02
5.000E+00     1.788E+02
5.200E+00     1.738E+02
5.400E+00     1.689E+02
5.600E+00     1.642E+02
5.800E+00     1.596E+02
6.000E+00     1.552E+02
6.200E+00     1.508E+02
6.400E+00     1.466E+02
6.600E+00     1.425E+02
6.800E+00     1.386E+02
7.000E+00     1.347E+02
7.200E+00     1.309E+02
7.400E+00     1.273E+02
7.600E+00     1.237E+02
7.800E+00     1.203E+02
8.000E+00     1.169E+02
8.200E+00     1.137E+02
8.400E+00     1.105E+02
8.600E+00     1.075E+02
8.800E+00     1.045E+02
9.000E+00     1.016E+02
9.200E+00     9.874E+01
9.400E+00     9.600E+01
9.600E+00     9.334E+01
9.800E+00     9.075E+01
1.000E+01     8.823E+01
1.020E+01     8.578E+01
1.040E+01     8.339E+01
1.060E+01     8.109E+01
1.080E+01     7.884E+01
1.100E+01     7.666E+01
1.120E+01     7.454E+01
1.140E+01     7.247E+01
1.160E+01     7.047E+01
1.180E+01     6.851E+01
1.200E+01     6.663E+01
```

```
*******18-FEB-91*******SPICE2G.6(10AUG81)  *******09:25:07***********
Uskmouth flux decay test. (D-axis)
TRANSIENT ANALYSIS        TEMPERATURE =   27.000 DEG C
LATEST SPICE UPDATE 17/5/85,FOR INFORMATION TYPE DRB2:[FPS]SPICE.NEW
******************************************************************************
TIME             I(VM)
0.000E+00     1.198E+04
2.000E-01      1.113E+04
4.000E-01      1.081E+04
6.000E-01      1.051E+04
8.000E-01      1.023E+04
1.000E+00     9.954E+03
1.200E+00     9.686E+03
1.400E+00     9.425E+03
1.600E+00     9.172E+03
1.800E+00     8.925E+03
2.000E+00     8.686E+03
2.200E+00     8.454E+03
2.400E+00     8.228E+03
2.600E+00     8.008E+03
2.800E+00     7.795E+03
3.000E+00     7.587E+03
3.200E+00     7.385E+03
3.400E+00     7.189E+03
3.600E+00     6.999E+03
3.800E+00     6.813E+03
4.000E+00     6.633E+03
4.200E+00     6.458E+03
4.400E+00     6.287E+03
4.600E+00     6.122E+03
4.800E+00     5.961E+03
5.000E+00     5.805E+03
5.200E+00     5.653E+03
5.400E+00     5.505E+03
5.600E+00     5.361E+03
5.800E+00     5.222E+03
6.000E+00     5.086E+03
6.200E+00     4.954E+03
6.400E+00     4.826E+03
6.600E+00     4.701E+03
6.800E+00     4.579E+03
7.000E+00     4.462E+03
7.200E+00     4.347E+03
7.400E+00     4.236E+03
7.600E+00     4.127E+03
7.800E+00     4.022E+03
8.000E+00     3.919E+03
8.200E+00     3.820E+03
8.400E+00     3.723E+03
8.600E+00     3.629E+03
8.800E+00     3.537E+03
9.000E+00     3.448E+03
9.200E+00     3.361E+03
9.400E+00     3.277E+03
9.600E+00     3.196E+03
9.800E+00     3.116E+03
1.000E+01     3.039E+03
1.020E+01     2.963E+03
1.040E+01     2.890E+03
1.060E+01     2.819E+03
1.080E+01     2.750E+03
1.100E+01     2.683E+03
1.120E+01     2.617E+03
1.140E+01     2.554E+03
1.160E+01     2.491E+03
1.180E+01     2.431E+03
1.200E+01     2.373E+03 YY
JOB CONCLUDED
TIME                 PAGE     DIRECT    BUFFERED
CPU          ELAPSED   FAULTS     I/O        I/O
0: 1:19.21    0: 1:41.60     332         7          3
TOTAL JOB TIME           79.21
```

Spice program and results listing for a typical Q axis flux decay test on the Uskmouth machine

```
*******7-APR-92*******SPICE 2G.6(10AUG81)  *******16:20:45************
Uskmouth flux decay test. (Q-axis)
INPUT LISTING            TEMPERATURE =   27.000 DEG C
LATEST SPICE UPDATE 17/5/85,FOR INFORMATION TYPE DRB2:[FPS]SPICE.NEW
**********************************************************************
* Assuming rotor and stator iron
* is infinitely permeable.
*
* This circuit is used to model the Q-axis
* flux decay test, assuming iron is saturated
* on the main flux paths and Ur = 100 on any
* leakage paths.
*
* W J Hudson.
*
.WIDTH IN=80 OUT=80
.OPTIONS ITL4=1000 ITL5=0
*
* Air gap permeances.
*
C1      1    0    6.27UFM     IC=37460
C2      2    0    6.27UFM     IC=36791
C3      3    0    6.27UFM     IC=35466
C4      4    0    6.27UFM     IC=33508
C5      5    0    6.27UFM     IC=30952
C6      6    0    6.27UFM     IC=27844
C7      7    0    6.27UFM     IC=24238
C8      8    0    6.27UFM     IC=20200
C9      9    0    27.5UFM     IC=10498
*
* Air gap m.m.f generators.
*
V1      13    1
V2      14    2
V3      15    3
V4      16    4
V5      17    5
V6      18    6
V7      19    7
V8      20    8
*
* Layer by layer permeances and dampances.
*
* Subckts for each layer combining
* permeance with a small resistance.
* For the slotted region only.
*
* Subckt for layer 0.
.SUBCKT LAY0 1 3
C0      1    2   0.347UFM
R0      2    3   46.1
.ENDS
* Subckt for layer 1.
.SUBCKT LAY1 1 3
C1      1    2   0.691UFM
R1      2    3   184.0
.ENDS
* Subckt for layer 2.
.SUBCKT LAY2 1 3
C2      1    2   2.06UFM
R2      2    3   550.8
.ENDS
* Subckt for layer 3.
.SUBCKT LAY3 1 3
C3      1    2   4.11UFM
R3      2    3   2434.0
.ENDS
* Subckt for layer 4.
.SUBCKT LAY4 1 3
C4      1    2   8.22UFM
```

```
R4      2    3   3453.7
.ENDS
* Subckt for layer 5.
.SUBCKT LAY5 1 3
C5      1    2   16.45UFM
R5      2    3   5073.1
.ENDS
*
* Slotted region layer by layer.
*
* Slot 1.
*
* Layer 0.
X10    14    13      LAY0
* Layer 1.
X11    14    13      LAY1
* Layer 2.
X12    14    13      LAY2
* Layer 3.
X13    14    13      LAY3
* Layer 4.
X14    14    13      LAY4
* Layer 5.
X15    14    13      LAY5
* Layer 6.
C16    14   161      2059UFM
R16   161    13      10631
* Layer 7.
C17    14   171      2059UFM
R17   171    13      15421
* Layer 8.
R18    14    13      20211
*
* Slot 2.
*
* Layer 0.
X20    15    14      LAY0
* Layer 1.
X21    15    14      LAY1
* Layer 2.
X22    15    14      LAY2
* Layer 3.
X23    15    14      LAY3
* Layer 4.
X24    15    14      LAY4
* Layer 5.
X25    15    14      LAY5
* Layer 6.
R26    15   263      10441
C26   263    14      2059UFM
* Layer 7.
R27    15   273      15041
C27   273    14      2059UFM
* Layer 8.
R28    15    14      19641
*
* Slot 3.
*
* Layer 0.
X30    16    15      LAY0
* Layer 1.
X31    16    15      LAY1
* Layer 2.
X32    16    15      LAY2
* Layer 3.
X33    16    15      LAY3
* Layer 4.
X34    16    15      LAY4
* Layer 5.
X35    16    15      LAY5
* Layer 6.
R36    16   363      10121
C36   363    15      2059UFM
* Layer 7.
```

```
R37     16   373       14401
C37    373    15       2059UFM
* Layer 8.
R38     16    15       18681
*
* Slot 4.
*
* Layer 0.
X40     17    16       LAY0
* Layer 1.
X41     17    16       LAY1
* Layer 2.
X42     17    16       LAY2
* Layer 3.
X43     17    16       LAY3
* Layer 4.
X44     17    16       LAY4
* Layer 5.
X45     17    16       LAY5
* Layer 6.
R46     17   463       9651
C46    463    16       2059UFM
* Layer 7.
R47     17   473       13461
C47    473    16       2059UFM
* Layer 8.
R48     17    16       17271
*
* Slot 5.
*
* Layer 0.
X50     18    17       LAY0
* Layer 1.
X51     18    17       LAY1
* Layer 2.
X52     18    17       LAY2
* Layer 3.
X53     18    17       LAY3
* Layer 4.
X54     18    17       LAY4
* Layer 5.
X55     18    17       LAY5
* Layer 6.
R56     18   563       9141
C56    563    17       2059UFM
* Layer 7.
R57     18   573       12441
C57    573    17       2059UFM
* Layer 8.
R58     18    17       15741
*
* Slot 6.
*
* Layer 0.
X60     19    18       LAY0
* Layer 1.
X61     19    18       LAY1
* Layer 2.
X62     19    18       LAY2
* Layer 3.
X63     19    18       LAY3
* Layer 4.
X64     19    18       LAY4
* Layer 5.
X65     19    18       LAY5
* Layer 6.
R66     19   663       8471
C66    663    18       2059UFM
* Layer 7.
R67     19   673       11101
C67    673    18       2059UFM
* Layer 8.
R68     19    18       13731
*
```

```
* Slot 7.
*
* Layer 0.
X70    20    19      LAY0
* Layer 1.
X71    20    19      LAY1
* Layer 2.
X72    20    19      LAY2
* Layer 3.
X73    20    19      LAY3
* Layer 4.
X74    20    19      LAY4
* Layer 5.
X75    20    19      LAY5
* Layer 6.
R76    20   763      7841
C76   763    19      2059UFM
* Layer 7.
R77    20   773      9841
C77   773    19      2059UFM
* Layer 8.
R78    20    19      11841
*
* Slot 8. ( Pole Area)
*
* Layer 0.
RM80   30     9      93.0
* Layer 1.
RM81   29    30      277.6
* Layer 2.
RM82   27    29      734.7
* Layer 3.
RM83   25    27      5181.4
* Layer 4.
RM84   23    25      5530.0
* Layer 5.
RM85   21    23      3702.8
* Layer 5a.
RM85A  31    21      4838.2
* Layer 6.
RM86   32    31      2230.5
*
* Slot 9. (Pole Area)
*
* Layer 0.
C90    20    30      0.347UFM
RM90   30     0      149.7
* Layer 1.
C91    20    29      0.691UFM
RM91   29    30      447.0
* Layer 2.
C92    20    27      2.06UFM
RM92   27    29      1182.5
* Layer 3.
C93    20    25      4.11UFM
RM93   25    27      7247.5
* Layer 4.
C94    20    23      8.22UFM
RM94   23    25      9158.3
* Layer 5.
C95    20    21      16.45UFM
RM95   21    23      7000.8
* Layer 5a.
C95A   20    31      209UFM
RM95A  31    21      8819.3
* Layer 6.
C96    20    32      1089UFM
RM96   32    31      3647.6
* Layer 7.
C97    20    33      500UFM
RM97   33    32      4251.2
* Layer 8.
R98    20    33      4251.2
*
```

```
* Fourier analysis circuit.
*
EF      0    50   POLY(9) (1,0) (2,0) (3,0) (4,0) (5,0) (6,0) (7,0)
+ (8,0) (9,0)
+ 0,3.83,7.66,7.66,7.66,7.66,7.66,7.66,7.66,32.55
VM      51   50
RF      51    0    192
*
* Analysis.
*
*.TRAN .0002 0.01 UIC
.TRAN .2 12 UIC
.PRINT TRAN I(VM)
.PLOT TRAN I(VM)
.END
```

```
*******7-APR-92*******SPICE 2G.6(10AUG81)  *******16:20:45************
Uskmouth flux decay test. (Q-axis)
TRANSIENT ANALYSIS     TEMPERATURE =   27.000 DEG C
LATEST SPICE UPDATE 17/5/85,FOR INFORMATION TYPE DRB2:[FPS]SPICE.NEW
******************************************************************************
TIME             I(VM)
0.000E+00     1.085E+04
2.000E-01     6.984E+03
4.000E-01     5.917E+03
6.000E-01     5.071E+03
8.000E-01     4.349E+03
1.000E+00     3.742E+03
1.200E+00     3.240E+03
1.400E+00     2.818E+03
1.600E+00     2.457E+03
1.800E+00     2.148E+03
2.000E+00     1.885E+03
2.200E+00     1.660E+03
2.400E+00     1.473E+03
2.600E+00     1.314E+03
2.800E+00     1.178E+03
3.000E+00     1.061E+03
3.200E+00     9.608E+02
3.400E+00     8.747E+02
3.600E+00     8.025E+02
3.800E+00     7.409E+02
4.000E+00     6.877E+02
4.200E+00     6.416E+02
4.400E+00     6.016E+02
4.600E+00     5.671E+02
4.800E+00     5.375E+02
5.000E+00     5.122E+02
5.200E+00     4.898E+02
5.400E+00     4.701E+02
5.600E+00     4.529E+02
5.800E+00     4.374E+02
6.000E+00     4.242E+02
6.200E+00     4.123E+02
6.400E+00     4.017E+02
6.600E+00     3.921E+02
6.800E+00     3.833E+02
7.000E+00     3.755E+02
7.200E+00     3.682E+02
7.400E+00     3.617E+02
7.600E+00     3.556E+02
7.800E+00     3.499E+02
8.000E+00     3.446E+02
8.200E+00     3.395E+02
8.400E+00     3.350E+02
8.600E+00     3.305E+02
8.800E+00     3.263E+02
9.000E+00     3.222E+02
9.200E+00     3.183E+02
9.400E+00     3.147E+02
9.600E+00     3.110E+02
9.800E+00     3.076E+02
1.000E+01     3.042E+02
1.020E+01     3.009E+02
1.040E+01     2.978E+02
1.060E+01     2.946E+02
1.080E+01     2.917E+02
1.100E+01     2.886E+02
1.120E+01     2.858E+02
1.140E+01     2.830E+02
1.160E+01     2.801E+02
1.180E+01     2.775E+02
1.200E+01     2.747E+02
JOB CONCLUDED
TIME                PAGE     DIRECT    BUFFERED
CPU          ELAPSED   FAULTS     I/O        I/O
0: 1:37.42    0: 1:46.74     179         7          3
TOTAL JOB TIME           97.41
```

Spice program and results listing for a typical D axis frequency response test on the Torness machine

```
*******23-APR-92*******SPICE 2G.6(10AUG81)  *******12:06:08***********
Torness frequency response test. (D-axis)
INPUT LISTING                TEMPERATURE =   27.000 DEG C
LATEST SPICE UPDATE 17/5/85,FOR INFORMATION TYPE DRB2:[FPS]SPICE.NEW
**********************************************************************
* D-axis coil to field winding.
* Assuming rotor and stator iron
* is infinately permeable.
*
* This circuit is identical to circuit used
* for the D-axis flux decay test except
* for the D-axis coil which is now
* linking the stator across the air gap.
*
* W J Hudson.
*
.WIDTH IN=80 OUT=80
.OPTIONS NUMDGT=6 ITL4=1000 ITL5=0
*
* Subckt definition for the air gap.
*
.SUBCKT AIRGAP 1 2 3 4 5 6 7 8 9 10 11 12
+37 38 39 40 41 42 43 44 45 46 47 48
C11   48    12   4.59UFM
C12   47    11   4.59UFM
C13   46    10   4.59UFM
C14   45     9   4.59UFM
C15   44     8   4.59UFM
C16   43     7   4.59UFM
C17   42     6   4.59UFM
C18   41     5   4.59UFM
C19   40     4   4.26UFM
C1A   39     3   4.26UFM
C1B   38     2   4.26UFM
C1C   37     1   4.26UFM
.ENDS
*
* Dummy Resistors to ground.
*
RDD1      13   0    100MEG
RDD2      14   0    100MEG
RDD3      15   0    100MEG
RDD4      16   0    100MEG
RDD5      17   0    100MEG
RDD6      18   0    100MEG
RDD7      19   0    100MEG
RDD8      20   0    100MEG
RDD9      21   0    100MEG
RDD10     22   0    100MEG
RDD11     23   0    100MEG
RDD12     24   0    100MEG
*
* Stator D-axis Coil.
*
ISUP   300   0    AC 1 0
RDAX   300 301    0.001222
HDAX   301 302    POLY(11) VS1 VS2 VS3 VS4 VS5 VS6 VS7 VS8 VS9
+ VSA VSB
+ 0 35.3 34.6 33.2 31.1 28.5 25.0 21.5 17.3 13.3 9.0 4.5
VDAX   302   0
*
* Air Gap Subckt
XAIR  24 23 22 21 20 19 18 17 16 15 14 13
+ 2112 2102 2292 2282 2272 2262 2252 2242 2232 2222 2212 0
+ AIRGAP
*
* Stator permeances.
*
CL1     0 2212    67.0UFM
VS1     0 2211
```

```
HS1  2212 2211    VDAX   35.3
*
CL2  2212 2222    33.5UFM
VS2  2212 2221
HS2  2222 2221    VDAX   34.6
*
CL3  2222 2232    33.5UFM
VS3  2222 2231
HS3  2232 2231    VDAX   33.2
*
CL4  2232 2242    33.5UFM
VS4  2232 2241
HS4  2242 2241    VDAX   31.1
*
CL5  2242 2252    33.5UFM
VS5  2242 2251
HS5  2252 2251    VDAX   28.5
*
CL6  2252 2262    33.5UFM
VS6  2252 2261
HS6  2262 2261    VDAX   25.0
*
CL7  2262 2272    33.5UFM
VS7  2262 2271
HS7  2272 2271    VDAX   21.5
*
CL8  2272 2282    33.5UFM
VS8  2272 2281
HS8  2282 2281    VDAX   17.3
*
CL9  2282 2292    33.5UFM
VS9  2282 2291
HS9  2292 2291    VDAX   13.3
*
CLA  2292 2102    33.5UFM
VSA  2292 2101
HSA  2102 2101    VDAX   9.0
*
CLB  2102 2112    33.5UFM
VSB  2102 2111
HSB  2112 2111    VDAX   4.5
*
*
* Neuman Boundary.
RN      13    0    1E-9
* Layer by layer permeances and dampances.
*
* Subckts for each layer combining
* permeance with a small resistance.
* For the slotted region only.
*
* Subckt for layer 1.
.SUBCKT LAY1 1 3
C1      1    2   1.19UFM
R1      2    3   1
.ENDS
* Subckt for layer 2.
.SUBCKT LAY2 1 3
C2      1    2   2.38UFM
R2      2    3   1
.ENDS
* Subckt for layer 3.
.SUBCKT LAY3 1 3
C3      1    2   4.77UFM
R3      2    3   1
.ENDS
* Subckt for layer 4.
.SUBCKT LAY4 1 3
C4      1    2   9.54UFM
R4      2    3   1
.ENDS
* Subckt for layer 5.
.SUBCKT LAY5 1 3
C5      1    2   26.6UFM
```

```
R5      2    3   1
.ENDS
* Subckt for layer 6.
.SUBCKT LAY6 1 3
C6      1    2   3040UFM
R6      2    3   1
.ENDS
* Subckt for layer 7.
.SUBCKT LAY7 1 3
C7      1    2   3040UFM
R7      2    3   1
.ENDS
*
* Subckts for each layer combining
* permeance with a small resistance.
* For the pole region only.
*
* Subckt for layer 1.
.SUBCKT PLAY1 1 3
C1      1    2   1.60UFM
R1      2    3   1
.ENDS
* Subckt for layer 2.
.SUBCKT PLAY2 1 3
C2      1    2   3.21UFM
R2      2    3   1
.ENDS
* Subckt for layer 3.
.SUBCKT PLAY3 1 3
C3      1    2   120UFM
R3      2    3   1
.ENDS
* Subckt for layer 4.
.SUBCKT PLAY4 1 3
C4      1    2   742UFM
R4      2    3   1
.ENDS
* Subckt for layer 5.
.SUBCKT PLAY5 1 3
C5      1    2   1777UFM
R5      2    3   1
.ENDS
* Subckt for layer 6.
.SUBCKT PLAY6 1 3
C6      1    2   3135UFM
R6      2    3   1
.ENDS
* Subckt for layer 7.
.SUBCKT PLAY7 1 3
C7      1    2   3135UFM
R7      2    3   1
.ENDS
*
* Slotted region layer by layer.
* Including Mutual coupling effect.
*
* Slot 1.
*
* Layer 1.
X11    14   112      LAY1
HM11  112   111      POLY(6) VM11 VM12 VM13 VM14 VM15 VM18
+ 0 77.4 77.4 77.4 77.4 77.4 77.4
VM11  111    13
* Layer 2.
X12    14   122      LAY2
HM12  122   121      POLY(6) VM11 VM12 VM13 VM14 VM15 VM18
+ 0 77.4 299.4 299.4 299.4 299.4 299.4
VM12  121    13
* Layer 3.
X13    14   132      LAY3
HM13  132   131      POLY(6) VM11 VM12 VM13 VM14 VM15 VM18
+ 0 77.4 299.4 635.6 635.6 635.6 635.6
VM13  131    13
* Layer 4.
```

```
X14    14   142      LAY4
HM14  142   141      POLY(7) VM11 VM12 VM13 VM14 VM15 VM18
+ VMF
+ 0 77.4 299.4 635.6 1052.0 1052.0 1052.0 6.0
VM14  141    13
* Layer 5.
X15    14   152      LAY5
HM15  152   151      POLY(7) VM11 VM12 VM13 VM14 VM15 VM18
+ VMF
+ 0 77.4 299.4 635.6 1052.0 1714.1 1714.1 18.0
VM15  151    13
* Layer 8.
R18    14   182      1
HM18  182   181      POLY(7) VM11 VM12 VM13 VM14 VM15 VM18
+ VMF
+ 0 77.4 299.4 635.6 1052.0 1714.1 2373.8 18.0
VM18  181    13
*
* Slot 2.
*
* Layer 1.
X21    15   212      LAY1
HM21  212   211      POLY(8) VM21 VM22 VM23 VM24 VM25 VM26
+ VM27 VM28
+ 0 77.4 77.4 77.4 77.4 77.4 77.4 77.4 77.4
VM21  211    14
* Layer 2.
X22    15   222      LAY2
HM22  222   221      POLY(8) VM21 VM22 VM23 VM24 VM25 VM26
+ VM27 VM28
+ 0 77.4 299.4 299.4 299.4 299.4 299.4 299.4 299.4
VM22  221    14
* Layer 3.
X23    15   232      LAY3
HM23  232   231      POLY(8) VM21 VM22 VM23 VM24 VM25 VM26
+ VM27 VM28
+ 0 77.4 299.4 635.6 635.6 635.6 635.6 635.6 635.6
VM23  231    14
* Layer 4.
X24    15   242      LAY4
HM24  242   241      POLY(9) VM21 VM22 VM23 VM24 VM25 VM26
+ VM27 VM28 VMF
+ 0 77.4 299.4 635.6 1052.0 1052.0 1052.0 1052.0 1052.0 6.0
VM24  241    14
* Layer 5.
X25    15   252      LAY5
HM25  252   251      POLY(9) VM21 VM22 VM23 VM24 VM25 VM26
+ VM27 VM28 VMF
+ 0 77.4 299.4 635.6 1052.0 1714.1 1714.1 1714.1 1714.1 18.0
VM25  251    14
* Layer 6.
X26    15   262      LAY6
HM26  262   261      POLY(9) VM21 VM22 VM23 VM24 VM25 VM26
+ VM27 VM28 VMF
+ 0 77.4 299.4 635.6 1052.0 1714.1 2478.7  2478.7  2478.7 18.0
VM26  261    14
* Layer 7.
X27    15   272     LAY7
HM27  272   271      POLY(9) VM21 VM22 VM23 VM24 VM25 VM26
+ VM27 VM28 VMF
+ 0 77.4 299.4 635.6 1052.0 1714.1 2478.7  2596.8 2596.8 18.0
VM27  271    14
* Layer 8.
R28    15   282      1
HM28  282   281     POLY(9) VM21 VM22 VM23 VM24 VM25 VM26
+ VM27 VM28 VMF
+ 0 77.4 299.4 635.6 1052.0 1714.1 2478.7  2596.8 2714.9 18.0
VM28  281    14
*
* Slot 3.
*
* Layer 1.
X31    16   312      LAY1
HM31  312   311      POLY(8) VM31 VM32 VM33 VM34 VM35 VM36
```

```
+ VM37 VM38
+ 0 77.4 77.4 77.4 77.4 77.4 77.4 77.4 77.4
VM31  311    15
* Layer 2.
X32    16   322       LAY2
HM32  322   321       POLY(8) VM31 VM32 VM33 VM34 VM35 VM36
+ VM37 VM38
+ 0 77.4 299.4 299.4 299.4 299.4 299.4 299.4 299.4
VM32  321    15
* Layer 3.
X33    16   332       LAY3
HM33  332   331       POLY(8) VM31 VM32 VM33 VM34 VM35 VM36
+ VM37 VM38
+ 0 77.4 299.4 635.6 635.6 635.6 635.6 635.6 635.6
VM33  331    15
* Layer 4.
X34    16   342       LAY4
HM34  342   341       POLY(9) VM31 VM32 VM33 VM34 VM35 VM36
+ VM37 VM38 VMF
+ 0 77.4 299.4 635.6 1052.0 1052.0 1052.0 1052.0 1052.0 6.0
VM34  341    15
* Layer 5.
X35    16   352       LAY5
HM35  352   351       POLY(9) VM31 VM32 VM33 VM34 VM35 VM36
+ VM37 VM38 VMF
+ 0 77.4 299.4 635.6 1052.0 1714.1 1714.1 1714.1 1714.1 18.0
VM35  351    15
* Layer 6.
X36    16   362       LAY6
HM36  362   361       POLY(9) VM31 VM32 VM33 VM34 VM35 VM36
+ VM37 VM38 VMF
+ 0 77.4 299.4 635.6 1052.0 1714.1 2682.4  2682.4  2682.4 18.0
VM36  361    15
* Layer 7.
X37    16   372       LAY7
HM37  372   371       POLY(9) VM31 VM32 VM33 VM34 VM35 VM36
+ VM37 VM38 VMF
+ 0 77.4 299.4 635.6 1052.0 1714.1 2682.4  3004.2 3004.2 18.0
VM37  371    15
* Layer 8.
R38    16   382       1
HM38  382   381       POLY(9) VM31 VM32 VM33 VM34 VM35 VM36
+ VM37 VM38 VMF
+ 0 77.4 299.4 635.6 1052.0 1714.1 2682.4  3004.2 3326.0 18.0
VM38  381    15
*
* Slot 4.
*
* Layer 1.
X41    17   412       LAY1
HM41  412   411       POLY(8) VM41 VM42 VM43 VM44 VM45 VM46
+ VM47 VM48
+ 0 77.4 77.4 77.4 77.4 77.4 77.4 77.4 77.4
VM41  411    16
* Layer 2.
X42    17   422       LAY2
HM42  422   421       POLY(8) VM41 VM42 VM43 VM44 VM45 VM46
+ VM47 VM48
+ 0 77.4 299.4 299.4 299.4 299.4 299.4 299.4 299.4
VM42  421    16
* Layer 3.
X43    17   432       LAY3
HM43  432   431       POLY(8) VM41 VM42 VM43 VM44 VM45 VM46
+ VM47 VM48
+ 0 77.4 299.4 635.6 635.6 635.6 635.6 635.6 635.6
VM43  431    16
* Layer 4.
X44    17   442       LAY4
HM44  442   441       POLY(9) VM41 VM42 VM43 VM44 VM45 VM46
+ VM47 VM48 VMF
+ 0 77.4 299.4 635.6 1052.0 1052.0 1052.0 1052.0 1052.0 6.0
VM44  441    16
* Layer 5.
X45    17   452       LAY5
```

```
HM45  452   451       POLY(9) VM41 VM42 VM43 VM44 VM45 VM46
+ VM47 VM48 VMF
+ 0 77.4 299.4 635.6 1052.0 1714.1 1714.1 1714.1 1714.1 18.0
VM45  451     16
* Layer 6.
X46     17   462       LAY6
HM46  462   461       POLY(9) VM41 VM42 VM43 VM44 VM45 VM46
+ VM47 VM48 VMF
+ 0 77.4 299.4 635.6 1052.0 1714.1 2964.6  2964.6  2964.6 18.0
VM46  461     16
* Layer 7.
X47     17   472       LAY7
HM47  472   471       POLY(9) VM41 VM42 VM43 VM44 VM45 VM46
+ VM47 VM48 VMF
+ 0 77.4 299.4 635.6 1052.0 1714.1 2964.6  3568.6 3568.6 18.0
VM47  471     16
* Layer 8.
R48     17   482       1
HM48  482   481       POLY(9) VM41 VM42 VM43 VM44 VM45 VM46
+ VM47 VM48 VMF
+ 0 77.4 299.4 635.6 1052.0 1714.1 2964.6  3568.6 4172.6 18.0
VM48  481     16
*
* Slot 5.
*
* Layer 1.
X51     18   512       LAY1
HM51  512   511       POLY(8) VM51 VM52 VM53 VM54 VM55 VM56
+ VM57 VM58
+ 0 77.4 77.4 77.4 77.4 77.4 77.4 77.4 77.4
VM51  511     17
* Layer 2.
X52     18   522       LAY2
HM52  522   521       POLY(8) VM51 VM52 VM53 VM54 VM55 VM56
+ VM57 VM58
+ 0 77.4 299.4 299.4 299.4 299.4 299.4 299.4 299.4
VM52  521     17
* Layer 3.
X53     18   532       LAY3
HM53  532   531       POLY(8) VM51 VM52 VM53 VM54 VM55 VM56
+ VM57 VM58
+ 0 77.4 299.4 635.6 635.6 635.6 635.6 635.6 635.6
VM53  531     17
* Layer 4.
X54     18   542       LAY4
HM54  542   541       POLY(9) VM51 VM52 VM53 VM54 VM55 VM56
+ VM57 VM58 VMF
+ 0 77.4 299.4 635.6 1052.0 1052.0 1052.0 1052.0 1052.0 6.0
VM54  541     17
* Layer 5.
X55     18   552       LAY5
HM55  552   551       POLY(9) VM51 VM52 VM53 VM54 VM55 VM56
+ VM57 VM58 VMF
+ 0 77.4 299.4 635.6 1052.0 1714.1 1714.1 1714.1 1714.1 18.0
VM55  551     17
* Layer 6.
X56     18   562       LAY6
HM56  562   561       POLY(9) VM51 VM52 VM53 VM54 VM55 VM56
+ VM57 VM58 VMF
+ 0 77.4 299.4 635.6 1052.0 1714.1 3294.8  3294.8  3294.8 18.0
VM56  561     17
* Layer 7.
X57     18   572       LAY7
HM57  572   571       POLY(9) VM51 VM52 VM53 VM54 VM55 VM56
+ VM57 VM58 VMF
+ 0 77.4 299.4 635.6 1052.0 1714.1 3294.8  4229.0 4229.0 18.0
VM57  571     17
* Layer 8.
R58     18   582       1
HM58  582   581       POLY(9) VM51 VM52 VM53 VM54 VM55 VM56
+ VM57 VM58 VMF
+ 0 77.4 299.4 635.6 1052.0 1714.1 3294.8  4229.0 5163.2 18.0
VM58  581     17
*
```

```
* Slot 6.
*
* Layer 1.
X61    19   612      LAY1
HM61  612   611      POLY(8) VM61 VM62 VM63 VM64 VM65 VM66
+ VM67 VM68
+ 0 77.4 77.4 77.4 77.4 77.4 77.4 77.4 77.4
VM61  611    18
* Layer 2.
X62    19   622      LAY2
HM62  622   621      POLY(8) VM61 VM62 VM63 VM64 VM65 VM66
+ VM67 VM68
+ 0 77.4 299.4 299.4 299.4 299.4 299.4 299.4 299.4
VM62  621    18
* Layer 3.
X63    19   632      LAY3
HM63  632   631      POLY(8) VM61 VM62 VM63 VM64 VM65 VM66
+ VM67 VM68
+ 0 77.4 299.4 635.6 635.6 635.6 635.6 635.6 635.6
VM63  631    18
* Layer 4.
X64    19   642      LAY4
HM64  642   641      POLY(9) VM61 VM62 VM63 VM64 VM65 VM66
+ VM67 VM68 VMF
+ 0 77.4 299.4 635.6 1052.0 1052.0 1052.0 1052.0 1052.0 6.0
VM64  641    18
* Layer 5.
X65    19   652      LAY5
HM65  652   651      POLY(9) VM61 VM62 VM63 VM64 VM65 VM66
+ VM67 VM68 VMF
+ 0 77.4 299.4 635.6 1052.0 1714.1 1714.1 1714.1 1714.1 18.0
VM65  651    18
* Layer 6.
X66    19   662      LAY6
HM66  662   661      POLY(9) VM61 VM62 VM63 VM64 VM65 VM66
+ VM67 VM68 VMF
+ 0 77.4 299.4 635.6 1052.0 1714.1 3666.5  3666.5  3666.5 18.0
VM66  661    18
* Layer 7.
X67    19   672      LAY7
HM67  672   671      POLY(9) VM61 VM62 VM63 VM64 VM65 VM66
+ VM67 VM68 VMF
+ 0 77.4 299.4 635.6 1052.0 1714.1 3666.5  4972.4 4972.4 18.0
VM67  671    18
* Layer 8.
R68    19   682      1
HM68  682   681      POLY(9) VM61 VM62 VM63 VM64 VM65 VM66
+ VM67 VM68 VMF
+ 0 77.4 299.4 635.6 1052.0 1714.1 3666.5  4972.4  6278.3 18.0
VM68  681    18
*
* Slot 7.
*
* Layer 1.
X71    20   712      LAY1
HM71  712   711      POLY(8) VM71 VM72 VM73 VM74 VM75 VM76
+ VM77 VM78
+ 0 77.4 77.4 77.4 77.4 77.4 77.4 77.4 77.4
VM71  711    19
* Layer 2.
X72    20   722      LAY2
HM72  722   721      POLY(8) VM71 VM72 VM73 VM74 VM75 VM76
+ VM77 VM78
+ 0 77.4 299.4 299.4 299.4 299.4 299.4 299.4 299.4
VM72  721    19
* Layer 3.
X73    20   732      LAY3
HM73  732   731      POLY(8) VM71 VM72 VM73 VM74 VM75 VM76
+ VM77 VM78
+ 0 77.4 299.4 635.6 635.6 635.6 635.6 635.6 635.6
VM73  731    19
* Layer 4.
X74    20   742      LAY4
HM74  742   741      POLY(9) VM71 VM72 VM73 VM74 VM75 VM76
```

```
+ VM77 VM78 VMF
+ 0 77.4 299.4 635.6 1052.0 1052.0 1052.0 1052.0 1052.0 6.0
VM74  741    19
* Layer 5.
X75    20   752       LAY5
HM75  752   751       POLY(9) VM71 VM72 VM73 VM74 VM75 VM76
+ VM77 VM78 VMF
+ 0 77.4 299.4 635.6 1052.0 1714.1 1714.1 1714.1 1714.1 18.0
VM75  751    19
* Layer 6.
X76    20   762       LAY6
HM76  762   761       POLY(9) VM71 VM72 VM73 VM74 VM75 VM76
+ VM77 VM78 VMF
+ 0 77.4 299.4 635.6 1052.0 1714.1 4054.6  4054.6  4054.6 18.0
VM76  761    19
* Layer 7.
X77    20   772       LAY7
HM77  772   771       POLY(9) VM71 VM72 VM73 VM74 VM75 VM76
+ VM77 VM78 VMF
+ 0 77.4 299.4 635.6 1052.0 1714.1 4054.6  5748.6 5748.6 18.0
VM77  771    19
* Layer 8.
R78    20   782       1
HM78  782   781       POLY(9) VM71 VM72 VM73 VM74 VM75 VM76
+ VM77 VM78 VMF
+ 0 77.4 299.4 635.6 1052.0 1714.1 4054.6  5748.6 7442.6 18.0
VM78  781    19
*
* Slot 8.
*
* Layer 1.
X81    21   812       LAY1
HM81  812   811       POLY(8) VM81 VM82 VM83 VM84 VM85 VM86
+ VM87 VM88
+ 0 61.5 61.5 61.5 61.5 61.5 61.5 61.5 61.5
VM81  811    20
* Layer 2.
X82    21   822       LAY2
HM82  822   821       POLY(8) VM81 VM82 VM83 VM84 VM85 VM86
+ VM87 VM88
+ 0 61.5 240.0 240.0 240.0 240.0 240.0 240.0 240.0
VM82  821    20
* Layer 3.
X83    21   832       LAY3
HM83  832   831       POLY(8) VM81 VM82 VM83 VM84 VM85 VM86
+ VM87 VM88
+ 0 61.5 240.0 482.9 482.9 482.9 482.9 482.9 482.9
VM83  831    20
* Layer 4.
X84    21   842       LAY4
HM84  842   841       POLY(9) VM81 VM82 VM83 VM84 VM85 VM86
+ VM87 VM88 VMF
+ 0 61.5 240.0 482.9 762.8 762.8 762.8 762.8 762.8 4.7
VM84  841    20
* Layer 5.
X85    21   852       LAY5
HM85  852   851       POLY(9) VM81 VM82 VM83 VM84 VM85 VM86
+ VM87 VM88 VMF
+ 0 61.5 240.0 482.9 762.8 1304.1 1304.1 1304.1 1304.1 14.0
VM85  851    20
* Layer 6.
X86    21   862       LAY6
HM86  862   861       POLY(9) VM81 VM82 VM83 VM84 VM85 VM86
+ VM87 VM88 VMF
+ 0 61.5 240.0 482.9 762.8 1304.1 3740.9  3740.9  3740.9 14.0
VM86  861    20
* Layer 7.
X87    21   872       LAY7
HM87  872   871       POLY(9) VM81 VM82 VM83 VM84 VM85 VM86
+ VM87 VM88 VMF
+ 0 61.5 240.0 482.9 762.8 1304.1 3740.9  5729.5 5729.5 14.0
VM87  871    20
* Layer 8.
R88    21   882       1
```

```
HM88  882   881       POLY(9) VM81 VM82 VM83 VM84 VM85 VM86
+ VM87 VM88 VMF
+ 0 61.5 240.0 482.9 762.8 1304.1 3740.9  5729.5 7718.1 14.0
VM88  881    20
*
* Slot 9.
*
* Layer 1.
X91    22   912       PLAY1
HM91  912   911       POLY(8) VM91 VM92 VM93 VM94 VM95 VM96
+ VM97 VM98
+ 0 76.2 76.2 76.2 76.2 76.2 76.2 76.2
VM91  911    21
* Layer 2.
X92    22   922       PLAY2
HM92  922   921       POLY(8) VM91 VM92 VM93 VM94 VM95 VM96
+ VM97 VM98
+ 0 76.2 300.4 300.4 300.4 300.4 300.4 300.4
VM92  921    21
* Layer 3.
X93    22   932       PLAY3
HM93  932   931       POLY(8) VM91 VM92 VM93 VM94 VM95 VM96
+ VM97 VM98
+ 0 76.2 300.4 1594.6 1594.6 1594.6 1594.6 1594.6
VM93  931    21
* Layer 4.
X94    22   942       PLAY4
HM94  942   941       POLY(8) VM91 VM92 VM93 VM94 VM95 VM96
+ VM97 VM98
+ 0 76.2 300.4 1594.6 3725.3 3725.3 3725.3 3725.3
VM94  941    21
* Layer 5.
X95    22   952       PLAY5
HM95  952   951       POLY(8) VM91 VM92 VM93 VM94 VM95 VM96
+ VM97 VM98
+ 0 76.2 300.4 1594.6 3725.3 5794.1 5794.1 5794.1
VM95  951    21
* Layer 6.
X96    22   962       PLAY6
HM96  962   961       POLY(8) VM91 VM92 VM93 VM94 VM95 VM96
+ VM97 VM98
+ 0 76.2 300.4 1594.6 3725.3 5794.1 9055.2  9055.2  9055.2
VM96  961    21
* Layer 7.
X97    22   972       PLAY7
HM97  972   971       POLY(8) VM91 VM92 VM93 VM94 VM95 VM96
+ VM97 VM98
+ 0 76.2 300.4 1594.6 3725.3 5794.1 9055.2  111141.3 111141.3
VM97  971    21
* Layer 8.
R98    22   982       1
HM98  982   981       POLY(8) VM91 VM92 VM93 VM94 VM95 VM96
+ VM97 VM98
+ 0 76.2 300.4 1594.6 3725.3 5794.1 9055.2  111141.3 13227.4
VM98  981    21
*
* Slot 10.
*
* Layer 1.
X101    23   1012      PLAY1
HM101 1012   1011      POLY(8) VM101 VM102 VM103 VM104
+ VM105 VM106 VM107 VM108
+ 0 86.4 86.4 86.4 86.4 86.4 86.4 86.4
VM101 1011     22
* Layer 2.
X102    23   1022      PLAY2
HM102 1022   1021      POLY(8) VM101 VM102 VM103 VM104
+ VM105 VM106 VM107 VM108
+ 0 86.4 340.4 340.4 340.4 340.4 340.4 340.4
VM102 1021     22
* Layer 3.
X103    23   1032      PLAY3
HM103 1032   1031      POLY(8) VM101 VM102 VM103 VM104
+ VM105 VM106 VM107 VM108
```

```
+ 0 86.4 340.4 1450.4 1450.4 1450.4 1450.4 1450.4 1450.4
VM103 1031     22
* Layer 4.
X104    23   1042      PLAY4
HM104 1042   1041      POLY(8) VM101 VM102 VM103 VM104
+ VM105 VM106 VM107 VM108
+ 0 86.4 340.4 1450.4 3127.4 3127.4 3127.4 3127.4 3127.4
VM104 1041     22
* Layer 5.
X105    23   1052      PLAY5
HM105 1052   1051      POLY(8) VM101 VM102 VM103 VM104
+ VM105 VM106 VM107 VM108
+ 0 86.4 340.4 1450.4 3127.4 5196.2 5196.2 5196.2 5196.2
VM105 1051     22
* Layer 6.
X106    23   1062      PLAY6
HM106 1062   1061      POLY(8) VM101 VM102 VM103 VM104
+ VM105 VM106 VM107 VM108
+ 0 86.4 340.4 1450.4 3127.4 5196.2 8638.7  8638.7  8638.7
VM106 1061     22
* Layer 7.
X107    23   1072      PLAY7
HM107 1072   1071      POLY(8) VM101 VM102 VM103 VM104
+ VM105 VM106 VM107 VM108
+ 0 86.4 340.4 1450.4 3127.4 5196.2 8638.7  10906.2 10906.2
VM107 1071     22
* Layer 8.
R108    23   1082      1
HM108 1082   1081      POLY(8) VM101 VM102 VM103 VM104
+ VM105 VM106 VM107 VM108
+ 0 86.4 340.4 1450.4 3127.4 5196.2 8638.7  10906.2 13173.7
VM108 1081     22
*
* Slot 11.
*
* Layer 1.
X111    24   1112      PLAY1
HM111 1112   1111      POLY(8) VM111 VM112 VM113 VM114
+ VM115 VM116 VM117 VM118
+ 0 76.2 76.2 76.2 76.2 76.2 76.2 76.2 76.2
VM111 1111     23
* Layer 2.
X112    24   1122      PLAY2
HM112 1122   1121      POLY(8) VM111 VM112 VM113 VM114
+ VM115 VM116 VM117 VM118
+ 0 76.2 300.4 300.4 300.4 300.4 300.4 300.4 300.4
VM112 1121     23
* Layer 3.
X113    24   1132      PLAY3
HM113 1132   1131      POLY(8) VM111 VM112 VM113 VM114
+ VM115 VM116 VM117 VM118
+ 0 76.2 300.4 1594.6 1594.6 1594.6 1594.6 1594.6 1594.6
VM113 1131     23
* Layer 4.
X114    24   1142      PLAY4
HM114 1142   1141      POLY(8) VM111 VM112 VM113 VM114
+ VM115 VM116 VM117 VM118
+ 0 76.2 300.4 1594.6 3725.3 3725.3 3725.3 3725.3 3725.3
VM114 1141     23
* Layer 5.
X115    24   1152      PLAY5
HM115 1152   1151      POLY(8) VM111 VM112 VM113 VM114
+ VM115 VM116 VM117 VM118
+ 0 76.2 300.4 1594.6 3725.3 5794.1 5794.1 5794.1 5794.1
VM115 1151     23
* Layer 6.
X116    24   1162      PLAY6
HM116 1162   1161      POLY(8) VM111 VM112 VM113 VM114
+ VM115 VM116 VM117 VM118
+ 0 76.2 300.4 1594.6 3725.3 5794.1 9351.1  9351.1  9351.1
VM116 1161     23
* Layer 7.
X117    24   1172      PLAY7
HM117 1172   1171      POLY(8) VM111 VM112 VM113 VM114
```

```
+ VM115 VM116 VM117 VM118
+ 0 76.2 300.4 1594.6 3725.3 5794.1 9351.1  11437.2 11437.2
VM117 1171     23
* Layer 8.
R118    24   1182      1
HM118 1182   1181      POLY(8) VM111 VM112 VM113 VM114
+ VM115 VM116 VM117 VM118
+ 0 76.2 300.4 1594.6 3725.3 5794.1 9351.1  11437.2 13523.3
VM118 1181     23
*
*
* Field electric circuit.
*
Vfield  70    0
Rfield  71   70  0.0902
HF8     72   71  POLY(8) VM18 VM28 VM38 VM48 VM58 VM68 VM78
+ VM88
+ 0 18.0 18.0 18.0 18.0 18.0 18.0 18.0 14.0
HF7     73   72  POLY(7) VM27 VM37 VM47 VM57 VM67 VM77 VM87
+ 0 18.0 18.0 18.0 18.0 18.0 18.0 18.0 14.0
HF6     74   73  POLY(7) VM26 VM36 VM46 VM56 VM66 VM76 VM86
+ 0 18.0 18.0 18.0 18.0 18.0 18.0 18.0 14.0
HF5     75   74  POLY(8) VM15 VM25 VM35 VM45 VM55 VM65 VM75
+ VM85
+ 0 18.0 18.0 18.0 18.0 18.0 18.0 18.0 14.0
HF4     76   75  POLY(8) VM14 VM24 VM34 VM44 VM54 VM64 VM74
+ VM84
+ 0 6.0 6.0 6.0 6.0 6.0 6.0 6.0 4.7
VMF     76    0
*
*
* Analysis.
*
.AC DEC 10 0.001 1000
.PRINT AC VM(0,301) VP(0,301)
.PLOT  AC VM(301) VP(301)
.PRINT AC IM(Vfield) IP(Vfield)
.PLOT  AC IM(Vfield) IP(Vfield)
.PLOT  AC IM(VM31) IM(VM32) IM(VM33) IM(VM34)
.PLOT  AC IM(VM35) IM(VM36) IM(VM37) IM(VM38)
.END
```

```
*******23-APR-92 *******SPICE 2G.6(10AUG81)  *******12:06:08**********
Torness frequency response test. (D-axis)
AC ANALYSIS                 TEMPERATURE =   27.000 DEG C
LATEST SPICE UPDATE 17/5/85,FOR INFORMATION TYPE DRB2:[FPS]SPICE.NEW
******************************************************************************
FREQ              VM(0,301)     VP(0,301)
1.00000E-03     1.20426E-02   8.78642E+01
1.25893E-03     1.51506E-02   8.73172E+01
1.58489E-03     1.90541E-02   8.66299E+01
1.99526E-03     2.39500E-02   8.57674E+01
2.51189E-03     3.00775E-02   8.46873E+01
3.16228E-03     3.77206E-02   8.33390E+01
3.98107E-03     4.72048E-02   8.16639E+01
5.01187E-03     5.88797E-02   7.95981E+01
6.30957E-03     7.30773E-02   7.70787E+01
7.94328E-03     9.00338E-02   7.40583E+01
1.00000E-02     1.09769E-01   7.05273E+01
1.25893E-02     1.31948E-01   6.65442E+01
1.58489E-02     1.55791E-01   6.22653E+01
1.99526E-02     1.80151E-01   5.79580E+01
2.51189E-02     2.03821E-01   5.39820E+01
3.16228E-02     2.26006E-01   5.07330E+01
3.98107E-02     2.46730E-01   4.85657E+01
5.01187E-02     2.66991E-01   4.77276E+01
6.30957E-02     2.88689E-01   4.83189E+01
7.94328E-02     3.14481E-01   5.02771E+01
1.00000E-01     3.47660E-01   5.33807E+01
1.25893E-01     3.92076E-01   5.72800E+01
1.58489E-01     4.52094E-01   6.15625E+01
1.99526E-01     5.32602E-01   6.58398E+01
2.51189E-01     6.39152E-01   6.98185E+01
3.16228E-01     7.78235E-01   7.33263E+01
3.98107E-01     9.57673E-01   7.62981E+01
5.01187E-01     1.18710E+00   7.87422E+01
6.30957E-01     1.47851E+00   8.07080E+01
7.94328E-01     1.84697E+00   8.22619E+01
1.00000E+00     2.31146E+00   8.34717E+01
1.25893E+00     2.89595E+00   8.43968E+01
1.58489E+00     3.63067E+00   8.50833E+01
1.99526E+00     4.55341E+00   8.55633E+01
2.51189E+00     5.71095E+00   8.58592E+01
3.16228E+00     7.16054E+00   8.59878E+01
3.98107E+00     8.97171E+00   8.59650E+01
5.01187E+00     1.12281E+01   8.58075E+01
6.30957E+00     1.40291E+01   8.55357E+01
7.94328E+00     1.74923E+01   8.51766E+01
1.00000E+01     2.17551E+01   8.47668E+01
1.25893E+01     2.69802E+01   8.43552E+01
1.58489E+01     3.33646E+01   8.40024E+01
1.99526E+01     4.11591E+01   8.37752E+01
2.51189E+01     5.07011E+01   8.37322E+01
3.16228E+01     6.24586E+01   8.39015E+01
3.98107E+01     7.70700E+01   8.42639E+01
5.01187E+01     9.53665E+01   8.47580E+01
6.30957E+01     1.18383E+02   8.53065E+01
7.94328E+01     1.47377E+02   8.58451E+01
1.00000E+02     1.83886E+02   8.63367E+01
1.25893E+02     2.29808E+02   8.67691E+01
1.58489E+02     2.87525E+02   8.71450E+01
1.99526E+02     3.60048E+02   8.74713E+01
2.51189E+02     4.51167E+02   8.77541E+01
3.16228E+02     5.65644E+02   8.79990E+01
3.98107E+02     7.09462E+02   8.82125E+01
5.01187E+02     8.90167E+02   8.84010E+01
6.30957E+02     1.11729E+03   8.85685E+01
7.94328E+02     1.40284E+03   8.87157E+01
1.00000E+03     1.76187E+03   8.88418E+01
```

```
*******23-APR-92 *******SPICE 2G.6(10AUG81)  *******12:06:08**********
Torness frequency response test. (D-axis)
AC ANALYSIS                     TEMPERATURE =   27.000 DEG C
LATEST SPICE UPDATE 17/5/85,FOR INFORMATION TYPE DRB2:[FPS]SPICE.NEW
******************************************************************************
FREQ                IM(Vfield)     IP(Vfield)
1.00000E-03     6.45413E-02   8.74918E+01
1.25893E-03     8.12071E-02   8.68404E+01
1.58489E-03     1.02146E-01   8.60218E+01
1.99526E-03     1.28421E-01   8.49933E+01
2.51189E-03     1.61331E-01   8.37022E+01
3.16228E-03     2.02426E-01   8.20836E+01
3.98107E-03     2.53495E-01   8.00592E+01
5.01187E-03     3.16471E-01   7.75383E+01
6.30957E-03     3.93191E-01   7.44232E+01
7.94328E-03     4.84915E-01   7.06230E+01
1.00000E-02     5.91572E-01   6.60792E+01
1.25893E-02     7.10875E-01   6.07980E+01
1.58489E-02     8.37720E-01   5.48805E+01
1.99526E-02     9.64499E-01   4.85328E+01
2.51189E-02     1.08269E+00   4.20429E+01
3.16228E-02     1.18521E+00   3.57252E+01
3.98107E-02     1.26830E+00   2.98521E+01
5.01187E-02     1.33178E+00   2.46061E+01
6.30957E-02     1.37809E+00   2.00677E+01
7.94328E-02     1.41076E+00   1.62341E+01
1.00000E-01     1.43330E+00   1.30491E+01
1.25893E-01     1.44866E+00   1.04309E+01
1.58489E-01     1.45908E+00   8.29092E+00
1.99526E-01     1.46619E+00   6.54458E+00
2.51189E-01     1.47111E+00   5.11609E+00
3.16228E-01     1.47465E+00   3.93942E+00
3.98107E-01     1.47742E+00   2.95705E+00
5.01187E-01     1.47986E+00   2.11747E+00
6.30957E-01     1.48235E+00   1.37242E+00
7.94328E-01     1.48519E+00   6.73965E-01
1.00000E+00     1.48857E+00  -2.76163E-02
1.25893E+00     1.49255E+00  -7.85158E-01
1.58489E+00     1.49702E+00  -1.65575E+00
1.99526E+00     1.50172E+00  -2.70313E+00
2.51189E+00     1.50610E+00  -4.00100E+00
3.16228E+00     1.50909E+00  -5.63379E+00
3.98107E+00     1.50885E+00  -7.68991E+00
5.01187E+00     1.50274E+00  -1.02468E+01
6.30957E+00     1.48754E+00  -1.33564E+01
7.94328E+00     1.46008E+00  -1.70414E+01
1.00000E+01     1.41764E+00  -2.13013E+01
1.25893E+01     1.35811E+00  -2.61130E+01
1.58489E+01     1.28032E+00  -3.14157E+01
1.99526E+01     1.18476E+00  -3.70882E+01
2.51189E+01     1.07446E+00  -4.29411E+01
3.16228E+01     9.55254E-01  -4.87479E+01
3.98107E+01     8.34764E-01  -5.43168E+01
5.01187E+01     7.20202E-01  -5.95787E+01
6.30957E+01     6.16374E-01  -6.46415E+01
7.94328E+01     5.24885E-01  -6.97787E+01
1.00000E+02     4.44718E-01  -7.53462E+01
1.25893E+02     3.73612E-01  -8.16626E+01
1.58489E+02     3.09485E-01  -8.89142E+01
1.99526E+02     2.51253E-01  -9.71319E+01
2.51189E+02     1.98863E-01  -1.06230E+02
3.16228E+02     1.52814E-01  -1.16053E+02
3.98107E+02     1.13664E-01  -1.26400E+02
5.01187E+02     8.16913E-02  -1.37037E+02
6.30957E+02     5.67184E-02  -1.47726E+02
7.94328E+02     3.80845E-02  -1.58271E+02
1.00000E+03     2.47714E-02  -1.68545E+02
JOB CONCLUDED
TIME                  PAGE      DIRECT    BUFFERED
CPU          ELAPSED    FAULTS      I/O         I/O
0:37: 3.66    0:38:31.39    1021         21           7
TOTAL JOB TIME          2223.64
```

Spice program and results listing for a typical D axis frequency response test on the Torness machine

```
*******28-APR-92*******SPICE 2G.6(10AUG81)  *******14:06:49***********
Torness frequency response test. (Q-axis)
INPUT LISTING                TEMPERATURE =   27.000 DEG C
LATEST SPICE UPDATE 17/5/85,FOR INFORMATION TYPE DRB2:[FPS]SPICE.NEW
**********************************************************************
* Assuming rotor and stator iron
* is infinately permeable.
*
* This circuit is used to model the Q-axis
* flux decay test, assuming iron is saturated
* on the main flux paths and Ur = 100 on any
* leakage paths.  The circuit also enables the
* eddy currents from within the pole area to be viewed,
* however it must be remembered that this is only
* a model of an infinataly long machine, the edyy
* current values may not therefore be correct
* along the complete length of the machine.
*
* W J Hudson.
*
.WIDTH IN=80 OUT=80
.OPTIONS ITL4=1000 ITL5=0
*
* Stator Q-axis Coil.
ISUP   300   0    AC 1 0
RQAX   301 300    0.00044
HQAX   302 301    POLY(8) VS1 VS2 VS3 VS4 VS5 VS6 VS7 VS8
+ 0 2.25 7.44 12.28 16.84 21.04 24.88 28.16 140.0
VQAX   302   0
*
* Air gap permeances.
*
C1      1 2211    4.8UFM
CL1  2211 2221    33.5UFM
VS1  2211 2212
HS1  2212 2221    VQAX  2.25
C2      2 2221    4.8UFM
CL2  2221 2231    33.5UFM
VS2  2221 2222
HS2  2222 2231    VQAX  7.44
C3      3 2231    4.8UFM
CL3  2231 2241    33.5UFM
VS3  2231 2232
HS3  2232 2241    VQAX  12.28
C4      4 2241    4.8UFM
CL4  2241 2251    33.5UFM
VS4  2241 2242
HS4  2242 2251    VQAX  16.84
C5      5 2251    4.8UFM
CL5  2251 2261    33.5UFM
VS5  2251 2252
HS5  2252 2261    VQAX  21.04
C6      6 2261    4.8UFM
CL6  2261 2271    33.5UFM
VS6  2261 2262
HS6  2262 2271    VQAX  24.88
C7      7 2271    4.8UFM
CL7  2271 2281    33.5UFM
VS7  2271 2272
HS7  2272 2281    VQAX  28.16
C8      8 2281    4.8UFM
CL8  2281    0    8.38UFM
VS8  2281 2282
HS8  2282    0    VQAX  140.0
*
* Air gap m.m.f gemerators.
*
V1      13    1
V2      14    2
V3      15    3
```

```
V4      16    4
V5      17    5
V6      18    6
V7      19    7
V8      20    8
*
* Layer by layer permeances and dampances.
*
* Subckts for each layer combining
* permeance with a the relevent dampance.
* For the slotted region only.
*
* Subckt for layer 1.
.SUBCKT LAY1 1 3
C1      1     2    1.19UFM
R1      2     3    77.4
.ENDS
* Subckt for layer 2.
.SUBCKT LAY2 1 3
C2      1     2    2.38UFM
R2      2     3    299.4
.ENDS
* Subckt for layer 3.
.SUBCKT LAY3 1 3
C3      1     2    4.77UFM
R3      2     3    635.6
.ENDS
* Subckt for layer 4.
.SUBCKT LAY4 1 3
C4      1     2    9.54UFM
R4      2     3    1052.0
.ENDS
* Subckt for layer 5.
.SUBCKT LAY5 1 3
C5      1     2    26.6UFM
R5      2     3    1714.1
.ENDS
*
*
* Slotted region layer by layer.
*
* Slot 1.
*
* Layer 1.
X11     14    13      LAY1
* Layer 2.
X12     14    13      LAY2
* Layer 3.
X13     14    13      LAY3
* Layer 4.
X14     14    13      LAY4
* Layer 5.
X15     14    13      LAY5
* Layer 6.
R16     14   161      5028.6
C16    161    13      3056UFM
* Layer 7.
R17     14   171      7696.6
C17    171    13      3056UFM
* Layer 8.
R18     14    13     10364.6
*
* Slot 2.
*
* Layer 1.
X21     15    14      LAY1
* Layer 2.
X22     15    14      LAY2
* Layer 3.
X23     15    14      LAY3
* Layer 4.
X24     15    14      LAY4
* Layer 5.
X25     15    14      LAY5
```

```
* Layer 6.
R26     15    261       4926.6
C26    261     14       3056UFM
* Layer 7.
R27     15    271       7492.6
C27    271     14       3056UFM
* Layer 8.
R28     15     14      10058.6
*
* Slot 3.
*
* Layer 1.
X31     16     15       LAY1
* Layer 2.
X32     16     15       LAY2
* Layer 3.
X33     16     15       LAY3
* Layer 4.
X34     16     15       LAY4
* Layer 5.
X35     16     15       LAY5
* Layer 6.
R36     16    361       4722.6
C36    361     15       3056UFM
* Layer 7.
R37     16    371       7084.6
C37    371     15       3056UFM
* Layer 8.
R38     16     15       9446.6
*
* Slot 4.
*
* Layer 1.
X41     17     16       LAY1
* Layer 2.
X42     17     16       LAY2
* Layer 3.
X43     17     16       LAY3
* Layer 4.
X44     17     16       LAY4
* Layer 5.
X45     17     16       LAY5
* Layer 6.
R46     17    461       4445.6
C46    461     16       3056UFM
* Layer 7.
R47     17    471       6530.6
C47    471     16       3056UFM
* Layer 8.
R48     17     16       8615.6
*
* Slot 5.
*
* Layer 1.
X51     18     17       LAY1
* Layer 2.
X52     18     17       LAY2
* Layer 3.
X53     18     17       LAY3
* Layer 4.
X54     18     17       LAY4
* Layer 5.
X55     18     17       LAY5
* Layer 6.
R56     18    561       4080.6
C56    561     17       3056UFM
* Layer 7.
R57     18    571       5800.6
C57    571     17       3056UFM
* Layer 8.
R58     18     17       7520.6
*
* Slot 6.
*
```

```
* Layer 1.
X61     19     18       LAY1
* Layer 2.
X62     19     18       LAY2
* Layer 3.
X63     19     18       LAY3
* Layer 4.
X64     19     18       LAY4
* Layer 5.
X65     19     18       LAY5
* Layer 6.
R66     19    661       3730.6
C66    661     18       3056UFM
* Layer 7.
R67     19    671       5100.6
C67    671     18       3056UFM
* Layer 8.
R68     19     18       6470.6
*
* Slot 7.
*
* Layer 1.
X71     20     19       LAY1
* Layer 2.
X72     20     19       LAY2
* Layer 3.
X73     20     19       LAY3
* Layer 4.
X74     20     19       LAY4
* Layer 5.
X75     20     19       LAY5
* Layer 6.
R76     20    761       3352.0
C76    761     19       3056UFM
* Layer 7.
R77     20    771       4343.4
C77    771     19       3056UFM
* Layer 8.
R78     20     19       5334.8
*
* Slot 8. (Pole Area)
*
* Layer 1.
R81     20    811       1
C81    811     29       0.40UFM
VM81    30      0
HM81    29     30       VE81    1
* Layer 2.
R82     20    821       1
C82    821     27       0.79UFM
VM82    28     29
HM82    27     28       VE82    1
* Layer 3.
R83     20    831       1
C83    831     25       4.42UFM
VM83    26     27
HM83    25     26       VE83    1
* Layer 4.
R84     20    841       1
C84    841     23       9.53UFM
VM84    24     25
HM84    23     24       VE84    1
* Layer 5.
R85     20    851       1
C85    851     21       26.58UFM
VM85    22     23
HM85    21     22       VE85    1
* Layer 6.
C86     20     31       400UFM
R86     31     21       5.4E3
* Layer 8.
R88     20     31       5.4E3
*
* Eddy Current path for the pole area.
```

```
*
* End Bell Resistance.
*
REND   25     0      1E-12
*
* Pole Layer 1.
VE81  812    25
HE81  812   813      VM81    1
RP81  813     0      3.33E-3
*
* Pole Layer 2.
VE82  822    25
HE82  822   823      VM82    1
RP82  823     0      1.13E-3
*
* Pole Layer 3.
VE83  832    25
HE83  832   833      VM83    1
RP83  833     0      0.254E-3
*
* Pole Layer 4.
VE84  842    25
HE84  842   843      VM84    1
RP84  843     0      0.161E-3
*
* Pole Layer 5.
VE85  852    25
HE85  852   853      VM85    1
RP85  853     0      0.148E-3
*
* Analysis.
*
.AC DEC 10 0.001 1000
.PRINT AC VM(0,301) VP(0,301)
.PLOT  AC VM(0,301) VP(0,301)
.END
```

```
*******28-APR-92*******SPICE 2G.6(10AUG81)  *******14:06:49***********
Torness frequency response test. (Q-axis)
AC ANALYSIS                  TEMPERATURE =   27.000 DEG C
LATEST SPICE UPDATE 17/5/85,FOR INFORMATION TYPE DRB2:[FPS]SPICE.NEW
**********************************************************************
FREQ            VM(0,301)   VP(0,301)
1.000E-03     1.268E-02   8.952E+01
1.259E-03     1.595E-02   8.941E+01
1.585E-03     2.007E-02   8.928E+01
1.995E-03     2.525E-02   8.913E+01
2.512E-03     3.176E-02   8.895E+01
3.162E-03     3.994E-02   8.873E+01
3.981E-03     5.022E-02   8.847E+01
5.012E-03     6.315E-02   8.815E+01
6.310E-03     7.940E-02   8.775E+01
7.943E-03     9.980E-02   8.725E+01
1.000E-02     1.254E-01   8.662E+01
1.259E-02     1.574E-01   8.582E+01
1.585E-02     1.973E-01   8.483E+01
1.995E-02     2.468E-01   8.363E+01
2.512E-02     3.077E-01   8.218E+01
3.162E-02     3.823E-01   8.049E+01
3.981E-02     4.724E-01   7.854E+01
5.012E-02     5.803E-01   7.637E+01
6.310E-02     7.080E-01   7.399E+01
7.943E-02     8.571E-01   7.139E+01
1.000E-01     1.028E+00   6.859E+01
1.259E-01     1.218E+00   6.567E+01
1.585E-01     1.422E+00   6.279E+01
1.995E-01     1.637E+00   6.025E+01
2.512E-01     1.859E+00   5.836E+01
3.162E-01     2.096E+00   5.736E+01
3.981E-01     2.360E+00   5.734E+01
5.012E-01     2.672E+00   5.816E+01
6.310E-01     3.055E+00   5.957E+01
7.943E-01     3.529E+00   6.131E+01
1.000E+00     4.118E+00   6.315E+01
1.259E+00     4.844E+00   6.497E+01
1.585E+00     5.737E+00   6.674E+01
1.995E+00     6.835E+00   6.840E+01
2.512E+00     8.184E+00   6.996E+01
3.162E+00     9.840E+00   7.139E+01
3.981E+00     1.187E+01   7.271E+01
5.012E+00     1.435E+01   7.395E+01
6.310E+00     1.740E+01   7.516E+01
7.943E+00     2.118E+01   7.635E+01
1.000E+01     2.586E+01   7.748E+01
1.259E+01     3.170E+01   7.852E+01
1.585E+01     3.896E+01   7.942E+01
1.995E+01     4.799E+01   8.019E+01
2.512E+01     5.918E+01   8.085E+01
3.162E+01     7.307E+01   8.141E+01
3.981E+01     9.029E+01   8.190E+01
5.012E+01     1.116E+02   8.232E+01
6.310E+01     1.380E+02   8.271E+01
7.943E+01     1.708E+02   8.309E+01
1.000E+02     2.114E+02   8.345E+01
1.259E+02     2.620E+02   8.381E+01
1.585E+02     3.248E+02   8.417E+01
1.995E+02     4.030E+02   8.453E+01
2.512E+02     5.003E+02   8.491E+01
3.162E+02     6.220E+02   8.532E+01
3.981E+02     7.744E+02   8.574E+01
5.012E+02     9.658E+02   8.614E+01
6.310E+02     1.206E+03   8.650E+01
7.943E+02     1.509E+03   8.680E+01
1.000E+03     1.888E+03   8.703E+01
JOB CONCLUDED
TIME                 PAGE     DIRECT    BUFFERED
CPU          ELAPSED   FAULTS     I/O        I/O
0: 0:14.23    0: 1: 9.64     363         8          3
TOTAL JOB TIME           14.22
```

Appendix Four
Supporting publications

Hudson W.J., "New Equivalent Circuits Applied to Industrial Machines", Interim report describing the PhD research undertaken by the author between May 1989 and October 1990, Department of Electrical and Electronic Engineering, Nottingham Trent University (formerly Nottingham Polytechnic), October 1990.

Haydock L., Holland S. and Hudson W.J., "A Hybrid Finite Element and Distributed Magnetic Equivalent Circuit Modelling Methodology for Electromagnetic Devices", Proc 1st Conference on Electrical Enginerring Analysis and Design, Lowell, Mass, USA, Aug 1990.

Hudson W.J. and Haydock L., "Parametric Sources for Improved Models of Electrical Machines", Proc UPEC, Robert Gordons Institute of Technology, Sept 1990.

Hudson W.J. and Haydock L., "Equivalent Circuits for Synchronous Machines", International Conference on the Evolution and Modern Aspects of Synchronous Machines, Zurich, Aug 1991.

Hudson W.J. and Haydock L., "A Dynamic Equivalent Circuit for Electrical Machines", Proc UPEC Brighton Polytechnic, Sept 1991.

Haydock L. and Hudson W.J., "Extended Linked Magnetic and Electric Equivalent Circuit Models for Electrical Machines", Internanional Conference on Electrical Machines, Manchester, Sept 1992.